UCRL--15617

DE84 012685

GDC REPORT NO. MFTF-7200-R-911-RWB

Final report
for the

HIGH FIELD Nb_3Sn AXICELL INSERT COILS

for the

MIRROR FUSION TEST FACILITY-B (MFTF-B) AXICELL CONFIGURATION

March 1984

R.W. Baldi, R.E. Tatro, et al.

Prepared for:
Lawrence Livermore National Laboratory
P.O. Box 5511
Livermore, California 94550

Prepared by:
General Dynamics Convair Division
P.O. Box 85377
San Diego, California 92138

This document prepared by
General Dynamics Convair
and approved by

R. W. Baldi
Chief Engineer, MFTF-B

R. E. Tatro
Program Manager, MFTF-B

FOREWORD

This report documents the design of the High Field Nb_3Sn Axicell Insert coil for the Mirror Fusion Test Facility-B (MFTF-B). This work was sponsored by the Department of Energy under University of California Lawrence Livermore National Laboratory subcontract 9590309. This work was performed from September 1982 to March 1984.

ACKNOWLEDGEMENTS

LLNL personnel who made significant contributions to this program are:

T. A. Kozman, MFTF-B Associate Project Manager
*R. M. Scanlan, Magnet Development & Technology
S. T. Wang, MFTF-B Deputy Associate Project Manager

General Dynamics Convair Division personnel who made significant contributions to this program are:

*K. L. Agarwal, Materials & Processes
*R. E. Bailey, Test Integration
*R. W. Baldi, Chief Engineer
W. F. Baxter, Structural Analysis
*J. E. Burgeson, Design
E. H. Christensen, Thermodynamics Analysis
T. L. Cross, Manufacturing & Producibility
*I. K. Kim, Thermodynamic Analysis
*G. D. Magnuson, Electromagnetic Analysis
*B. D. Mallett, Instrumentation
*J. L. Pickering, Structural Analysis
D. S. Ring, Structural Analysis
*A. J. Ritschel, Manufacturing & Producibility
R. E. Tatro, Program Manager
W. L. White, Manufacturing & Producibility

The Furukawa Corporation personnel who made significant contributions in the area of conductor development are:

Dr. Yoshio Futuro, Deputy Manager SC Development Dept., and his staff

*Denotes contributing author to this report.

TABLE OF CONTENTS

TABLE OF CONTENTS (continued)

LIST OF FIGURES

TABLE OF CONTENTS (continued)

LIST OF TABLES

APPENDICES PAGE

SUMMARY

Two 12-tesla superconducting insert coils are being designed by General Dynamics Convair Division for the axicell regions of MFTF-B for Lawrence Livermore National Laboratory. A major challenge of this project is to ensure that combined fabrication and operational strains induced in the conductor are within stringent limitations of the relatively brittle Nb_3Sn superconductor filaments. These coils are located in the axicell region of MFTF-B, as shown in Figure 1-1. They have a clear-bore diameter of 36.195cm (14.25 inches) and consist of 27 double pancakes (i.e., 54 pancakes per coil) wound on an electrically insulated 304LN stainless steel/bobbin helium vessel. Each pancake has 57 turns separated by G-10CR insulation. The complete winding bundle has 4.6 million ampere-turns and uniform current density of 2007 A/cm^2. In conjunction with the other magnets in the system, they produce a 12-tesla central field and a 12.52-tesla peak field. A multifilamentary Nb_3Sn conductor was selected to meet these requirements. The conductor consists of a monolithic insert soldered into a copper stabilizer. Sufficient cross-sectional area and work-hardening of the copper stabilizer has been provided for the conductor to self-react the electromagnetic Lorentz force induced hoop stresses with normal operational tensile strains less than 0.07 percent. This conductor configuration also provides adequate stabilizer area for unconditional cryostability in pool boiling liquid helium. The monolithic insert has a geometric aspect ratio of 3.2:1 that was selected to minimize the strain induced during winding without excessive critical current anisotropic degradation. The resulting cross sectional area of the insert has a 1,517-ampere operational current. In addition, layer winding of the insert for Nb_3Sn reaction further reduced manufacturing induced strains. The combined fabrication and operation induced strains are within the design goals of -0.6 to +0.4 percent (extrinsic strain in the fibers). Detailed analysis of the proposed design indicates that it will meet all performance requirements and can be economically built with today's technology.

1.0

INTRODUCTION

1.1 Technical Requirements

The high field coil design described herein fully meets the design requirements defined in Reference 1-1. The essential design parameters are summarized in Table 1-1. Also included in Table 1-1 are comments relating design conformity to the requirements. Table 1-2 further defines the breakdown of considerations which justifies the requirement of 100 percent margin on critical current. The calculation for this requirement is illustrated below.

15% peaking current		+5% test accuracy		+10% current enhancement due to operational tensile strain		+20% Nb_3Sn cross section uniformity along length	
(.85)	X	(.95)	X	(1.1)	X	(.67)	= 0.595

This calculated value was rounded down to 0.500 to account for other unknowns. The 0.500 factor results in the need for 100 percent margin in the critical current. As shown, the +20% in the uniformity of Nb_3Sn cross-sectional area is the major contributor to the relatively high margin requirement. The 0.67 factor developed from this potential variation represents a worst case condition. That is, it is assumed that the critical current tests were performed using an oversized conductor (+20%, thus .8/1.2). Actual experience on prototype conductor development for this project showed samples taken from each end of a 370-meter-long conductor length were relatively uniform in critical current performance. The results of the verification tests performed on the prototype conductor are presented in Section 8.0 of this report. Consequently, future projects involving Nb_3Sn conductor could consider reducing the allowable variation in cross-sectional area and thereby reduce material cost and produce a more compact conductor. The location of the high field insert coil (A21) in the Mirror Fusion Test Facility-B for the axicell configuration is shown in Figure 1-1.

1.2 Conductor Design Options

To meet the requirements for the high field coil, the design parameters in Table 1-3 were selected. The primary rationale for the selection of these parameters was the similarity of this coil to LLNL's High Field Test Facility (HFTF) coil. Although a larger conductor was initially preferred, the relatively small 1517A conductor proved to be necessary to permit winding without overstraining. Details of the strain history induced in the conductor from reaction of the Nb_3Sn during fabrication through winding and operation is presented in Section 4.0 of this report.

MIRROR FUSION TEST FACILITY - B
AXICELL CONFIGURATION

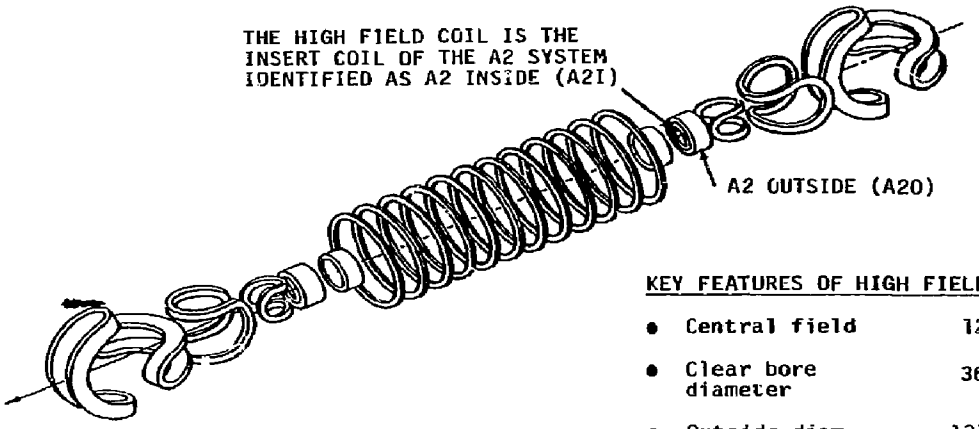

KEY FEATURES OF HIGH FIELD Nb_3Sn COIL

• Central field	12.0T (w/background)
• Clear bore diameter	36.195 cm (14.25 in)
• Outside diam.	131.57 cm (51.80 in)
• Width	80.0 cm (31.50 in)
• Stored energy	4.25MJ (alone) 11.6 MF (w/outer)
• Weight (per coil)	6,248 kg (13,776 lb)

Figure 1-1. High Field Insert Coils are Located Within the Bore of the Barrier Coils.

Table 1-1. Summary of High Field Coil Requirements/Key Features

	PARAMETER	REQUIREMENT	KEY FEATURE/COMMENT
o	Electromagnetic field.	12.0T (central).	12.0T (central) provided with 12.7T (peak) capability. Present configuration has 12.52T (peak field).
o	Clear bore.	36.60-cm diameter* (14.25-inch bore).	21.11-cm radius inside radius of first turn.
o	Operating conditions.	4.6305 MA turns @ 12.7T and 4.5K (Kelley/TDF Mode).	1517 current @ 12.52T. Current density (unit cell) = 2007 A/cm^2.
o	Operating margin.	≥ 7.5% field) ≥15.0% cryostability)	Approximately 40 percent margin provided.
		≥100% current.	See Table 2.
o	Operating life.	10 years.	G-10CR proven by neutron test at LANL.
o	Cyclic performance.	100 cool-down/ warm-up cycles.	Acceptable stress for 120-hour time limit.
		490 normal charge/ discharge cycles.	Cyclically tested splice joint.
		10 fault conditions.	
o	Rate of charge/ discharge.	4 hours charge time ≤ 1000V discharge voltage across terminals.	750 maximum terminal voltage for 7.5-second fast dump.
o	Design stress.	2/3 yield (normal) yield (fault)	15% current peaking strength capacity provided. 3.3% current peaking presently anticipated.
o	Design strain. for Nb_3Sn filaments.	+0.4% to -0.6%.	Highest tensile strains in bobbin region <0.4%.

Table 1-2. Factors Leading to Choice of 100 Percent Current Margin

	CONDITION	INFLUENCE ON CRITICAL CURRENT SELECTION
o	Peaking Current.	+15%
o	Anisotropy	±10% (field orientation included in specification)
o	Soldering	-33% to -40% (insert only)
o	Test Accuracy	±5%
o	Operational Strains	±10%
o	Nb_3Sn Cross-Sectional Area Uniformity	±20%

Compensation for the difference between test temperature (4.2K) and operating (4.4K) was also provided.

Table 1-3. Key Features of Candidate Conductor Concepts.

- Multifilamentary Nb_3Sn stabilized with OFE copper.
- LHe pool-boiling, cryostable.
- 2007 A/cm^2 (nominal unit cell).
- 1517 amperes rated operating current at 12.7T and 4.5K.
- 3200 amperes critical current at 12.7T and 4.2K.
- Double-pancake winding (295-meter lengths, not including lengths required for test.

Three multifilamentary Nb_3Sn conductor options considered are shown with their relative advantages and disadvantages in Table 1-4. All three of these options were included as potential candidates in a procurement request for proposals. Of these three options, the proposals for the cable soldered into the copper stabilizer and the monolith soldered into the copper stabilizer technically ranked the highest. Ultimately, the monolith soldered in the copper stabilizer was selected since the selected vendor, Furukawa Electric Company of Japan, had the most experience with this type of conductor. The Furukawa proposed conductor is presented in Section 2.0 of this report.

The superconducting insert is fabricated by the triple extrusion internal bronze process. The composition of bronze is Cu-14.3 w/o Sn content, including 0.23 w/o Ti additive. The Ti doping was added to enhance the critical current density. This enhancement was intended to compensate for the critical current degradation expected in the soldering of the copper stabilizer to the insert. The critical current of the insert alone shall be 3,560 amperes at 4.2K and 12.7T (parallel to the broad face of the conductor).

For reference, the technical specification for the Nb_3Sn conductor is provided in Appendix A.

In addition to multifilamentary Nb_3Sn conductors, tin-tape conductor was also considered. The main technical disadvantage was that the hoop strength of tin-tape conductor was lower than the multifilamentary conductor. This is a key technical parameter because the conductor pack is designed to self-react the electromagnetic forces without relying on the case for support. Also, a programmatic concern was that the lack of qualified producers of Nb_3Sn tape precluded the opportunity for a competitive procurement. Ultimately, this option was dropped from consideration, since the sole domestic vendor withdrew his proposal in favor of other business opportunities.

1.3 Conductor Pack Design

The overall conductor pack design is shown in Figure 1-2. As shown, the winding consists of 27 double pancakes (i.e., 54 pancakes total) with 57 turns per pancake (i.e., 3,078 total turns). For analysis, the number of turns is reduced to 3,052 to account for the partial loss of 26 turns in the pancake-to-pancake joggle region.

The electrical insulation consists of G-10CR fiberglass epoxy and multilayer kapton. A slotted G-10CR 1.19mm (0.047-inch-thick) fiberglass/epoxy is used between pancakes. A fishbone configuration of G-10CR 1mm (0.039-inch-thick) fiberglass/epoxy is used between conductor turns. Ground plane insulation consists of six layers of 0.127mm (0.005-inch-thick) kapton film laminated between sheets of G-10CR fiberglass/epoxy.

The structural case is fabricated by Chicago Bridge and Iron. It is made from 304LN stainless steel. All weldments are 100 percent penetration using E316L weldrod per Reference 1-2.

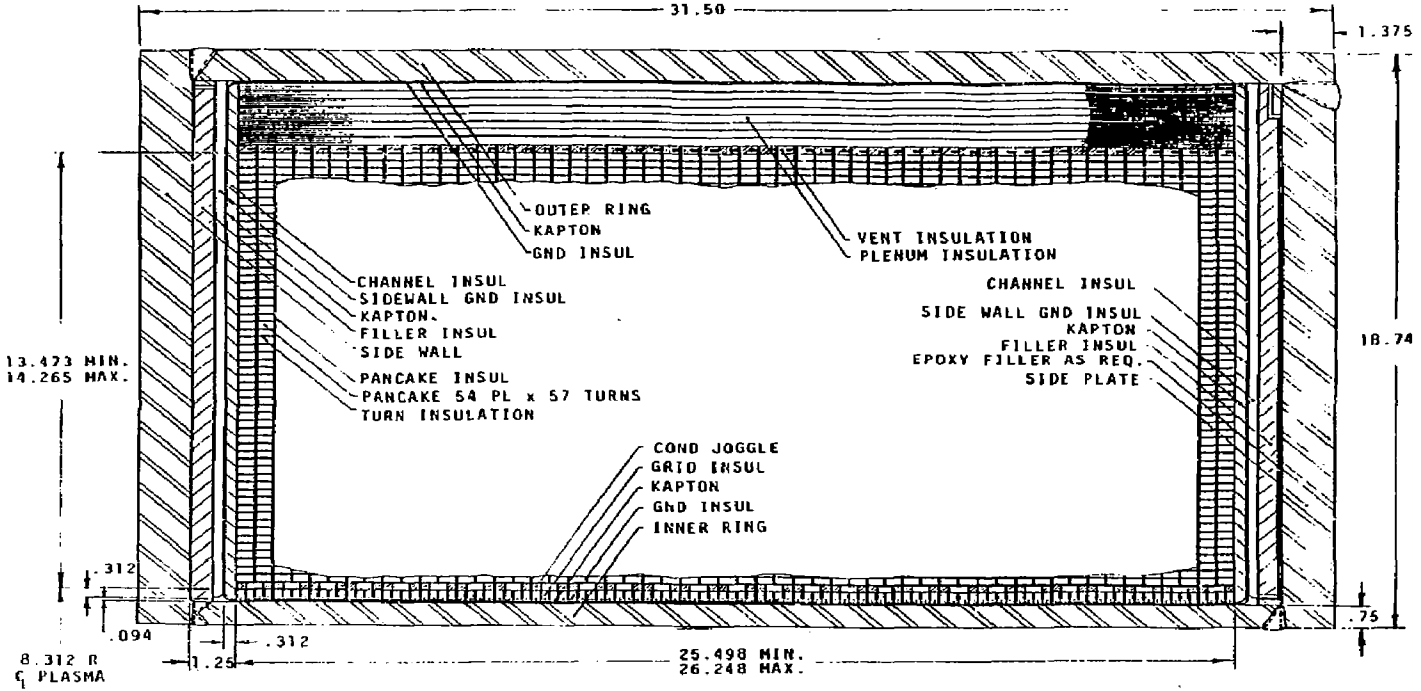

Figure 1-2. High Field Insert Coil Cross Section.

1.4 References

1-1 "MFTF Design Requirements Document" published by Lawrence Livermore National Laboratory, dated 17 August 1982 (revised 20 May 1983).

1-2 "Specification for Magnet Structures" General Dynamics Convair Specification 71E0002, dated 15 October 1982.

2.0

DESIGN

2.1 Design Requirements

Design parameters have been selected to ensure reliable operation of the A21 high field insert coils. Critical current specification for the conductor is a minimum of 3200 amperes at 12.7 tesla and 4.2K, for a zero applied strain condition. This design provides approximately 100 percent critical current margin since the operating current is 1517 amperes. The coils are designed for 490 normal electrical charge-discharge and 10 fault mode cycles. Fault modes include conditions such as a coil quench. The time required for charging is four hours. The design discharge voltage is ≤1000, and a fast dump of 7.5 seconds produces a maximum of 750 volts across the coil terminals. The cool-down and warm-up time for the coil is 120 hours. The design operating life is 10 years, considering irradiation degradation effects.

2.2 Case Structure

2.2.1 Case Material

The entire case structure is fabricated from 304LN annealed stainless steel plate. The only exception is the weld back-up bars which are 304L annealed stainless steel. All joints in the structure are full penetration 316L weldments.

2.2.2 Coil Winding Form

The coil winding form consists of a two-piece inner ring, one single-piece side plate, the tunnel bottom and sides, and the helium fill pipe. Figures 2-1, 2-2, and 2-3 show the coil winding form assembly and details. The inner ring and side plate are machined, which will provide a true base for the conductor winding. Both the outside surface and the inside surface of the inner ring are machined. The inside of the inner ring is machined to provide accurate space provisions for the liquid nitrogen shields. Available space is at a premium and close dimensional control is required. After machining, the thickness of the side plate is 35 mm (1.38 in) and the inner ring is 19.8 mm (0.780 in). The tunnel is fabricated from 25.4-mm (1.00-in) plate and is attached to the winding form so the current leads can be installed during coil winding.

2.2.3 Closeout Side Plate

The closeout side plate is machined after the weld back-up bar is welded in place. Only the coil inside surface of the plate is machined. The side plate thickness is 35 mm (1.38 in) after machining. Figure 2-4 shows the closeout side plate. The closeout weld to the winding form is at the inner ring.

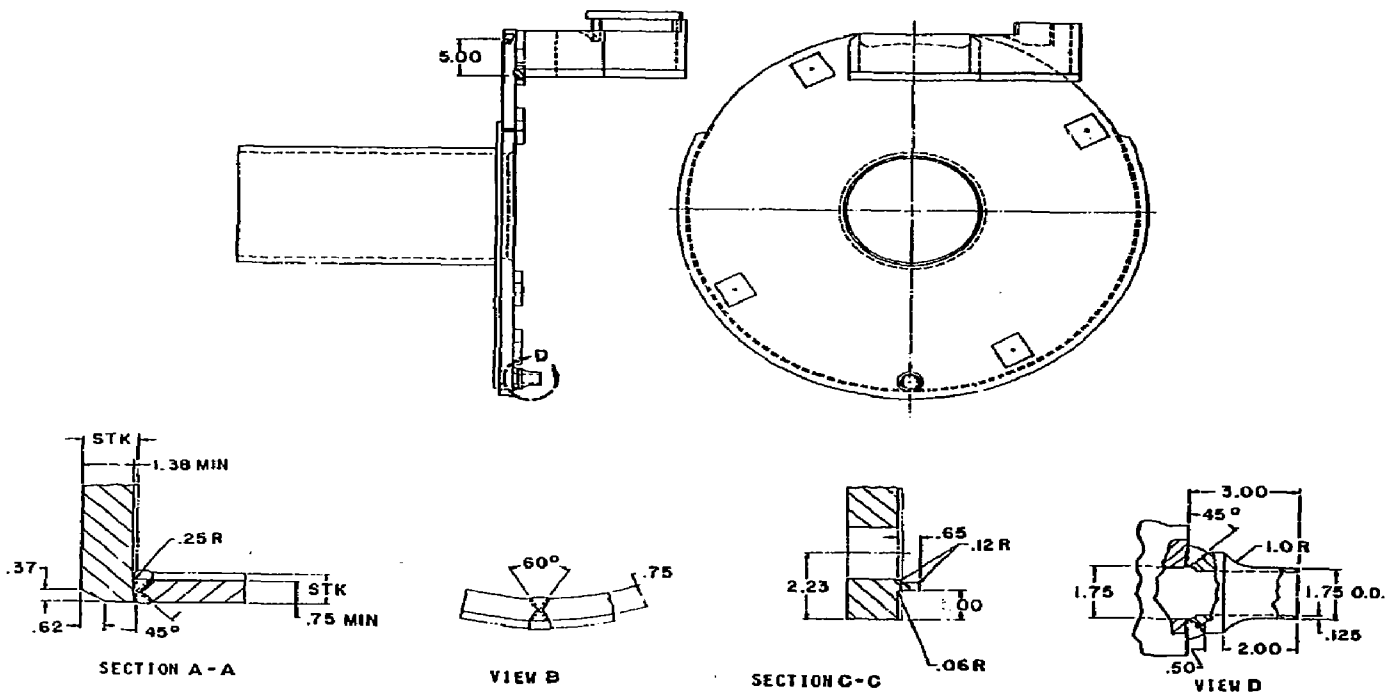

Figure 2-1. Coil Winding Form Assembly

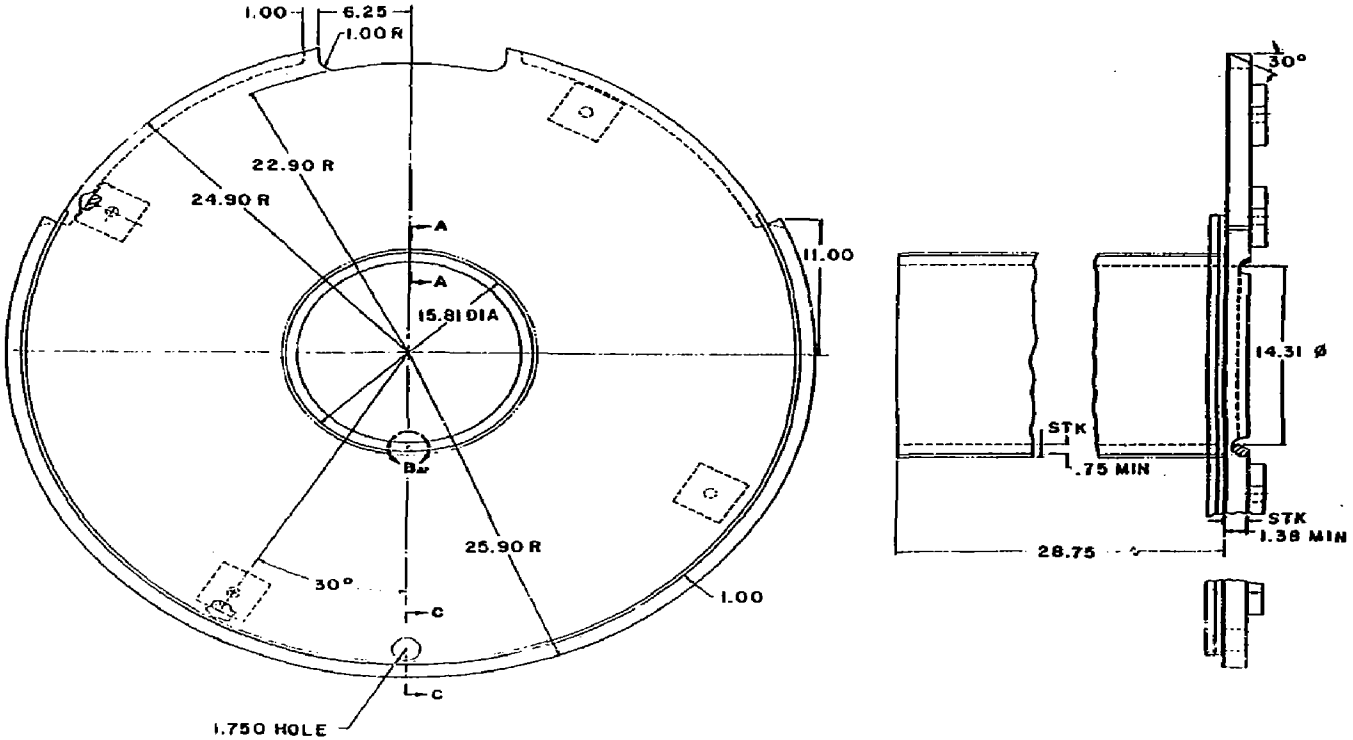

Figure 2-2. Coil Winding Form

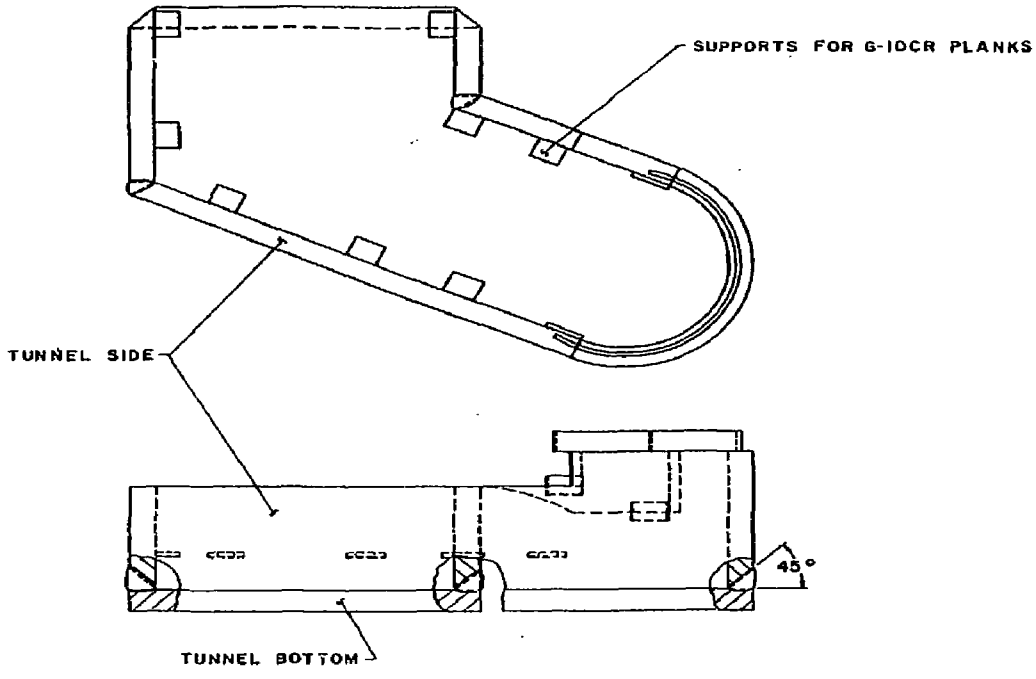

Figure 2-3. Tunnel Structure

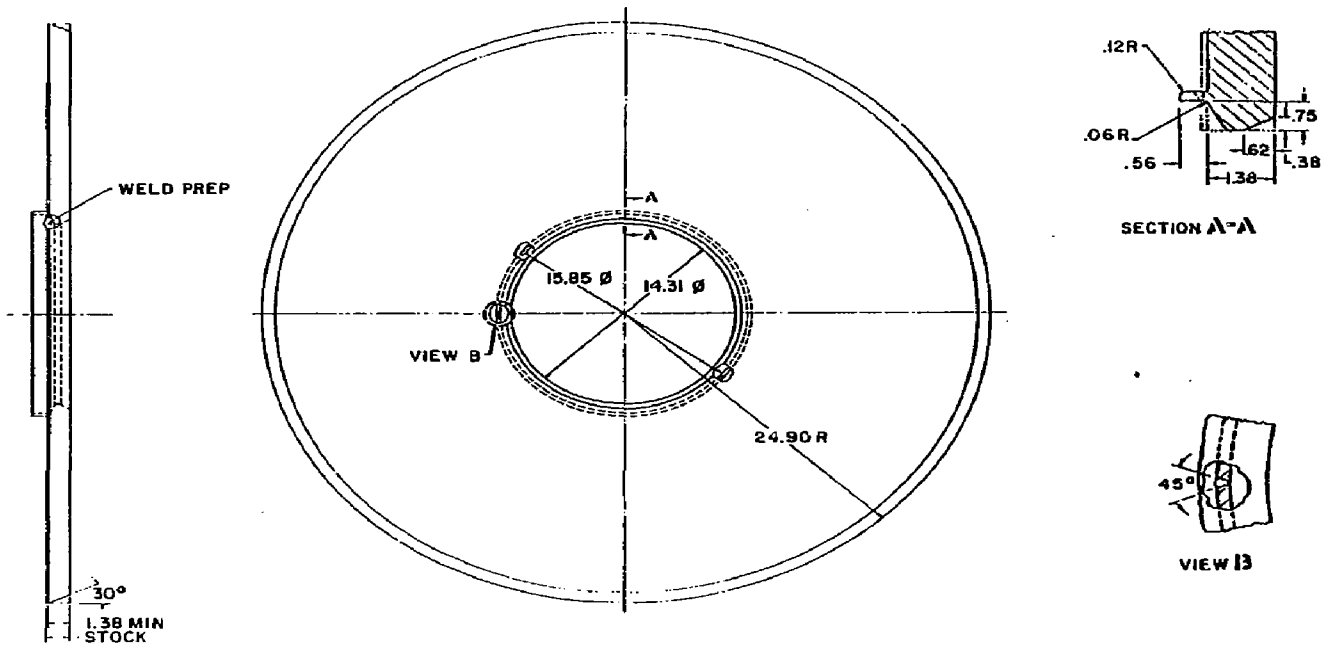

Figure 2-4. Side Plate

2.2.4 Outer Ring

The outer ring is in two halves and is fabricated from 25.4-mm (1.0-in) plate. The upper half outer ring has the tunnel cover attached. Figures 2-5, 2-6, and 2-7 show the outer ring and tunnel cover assembly and details. Attaching the tunnel cover to the outer ring eliminates a weld back-up bar. A weld back-up bar going across the tunnel opening would trap helium bubbles, since this is the high point on the coil.

2.2.5 Case Structural Assembly

The coil case structue assembly is shown in Figure 2-8. The closeout welding for the case structure is shown in Figure 2-9. View B shows the longitudinal closeout weld between outer ring halves. View C shows the closeout weld between the side plate and outer ring. View D, View E, and Section G-G show the outer-ring-to-side-plate closeout welding. View H shows the closeout weld between the tunnel cover and tunnel side wall.

2.3 Conductor

The conductor is manufactured by the Furukawa Electric Company, Ltd. of Japan. The conductor consists of an Nb_3Sn monolith superconductor soldered into a copper stabilizer housing. The conductor has a rectangular cross-section 5.21 mm by 11.00 mm (0.205 inch by 0.433 in). Figure 2-10 shows the composite conductor. The conductor is supplied in 295-meter (968-ft) lengths which is sufficient to wind one double pancake. The total conductor length in a completed coil is 7520 meters (24,692 feet). A summary of the conductor's design characteristics is listed in Appendix B.

2.3.1 Superconductor

The superconducting insert is a multifilmentary Nb/Cu-Sn composite monolith with a single pure Nb barrier and a stabilizing copper sheath. The superconducting insert is rectangular in cross-section and is 2.11 mm by 6.91 mm (0.083 inch by 0.272 in) in size. There are 145,000 Nb filaments, 3 microns in diameter, in a bronze matrix and with a twist pitch of 250 mm (9.8 in). Titanium additive of 0.23 percent has been added to the matrix to enhance critical current density.

2.3.2 Copper Housing

A two-piece copper stabilizer housing is used to contain the superconductor. The superconductor insert is soldered into the copper housing using 60 Sn/40 Pb solder. The stabilizer material is C10100 oxygen-free electronic (OFE) copper which is cold worked to a minimum tension yield stress of 31 ksi at room temperature. The residual resistivity ratio (RRR) of the stabilizer is a

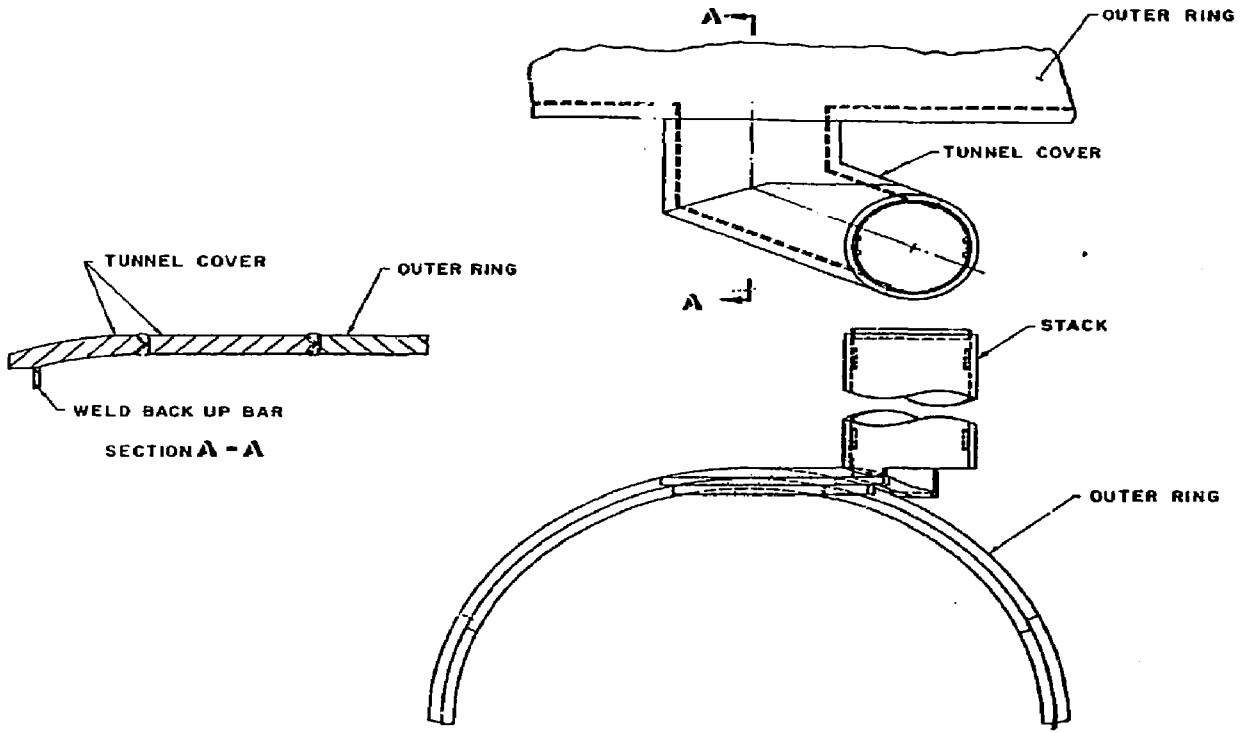

Figure 2-5. Outer Ring and Tunnel Cover

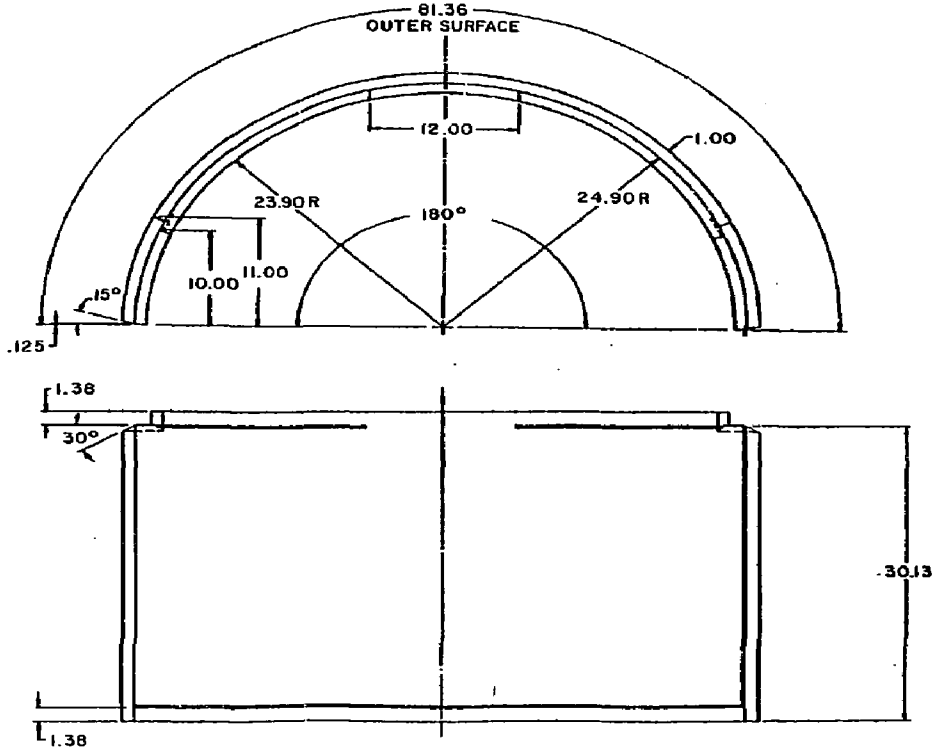

Figure 2-6. Outer Ring

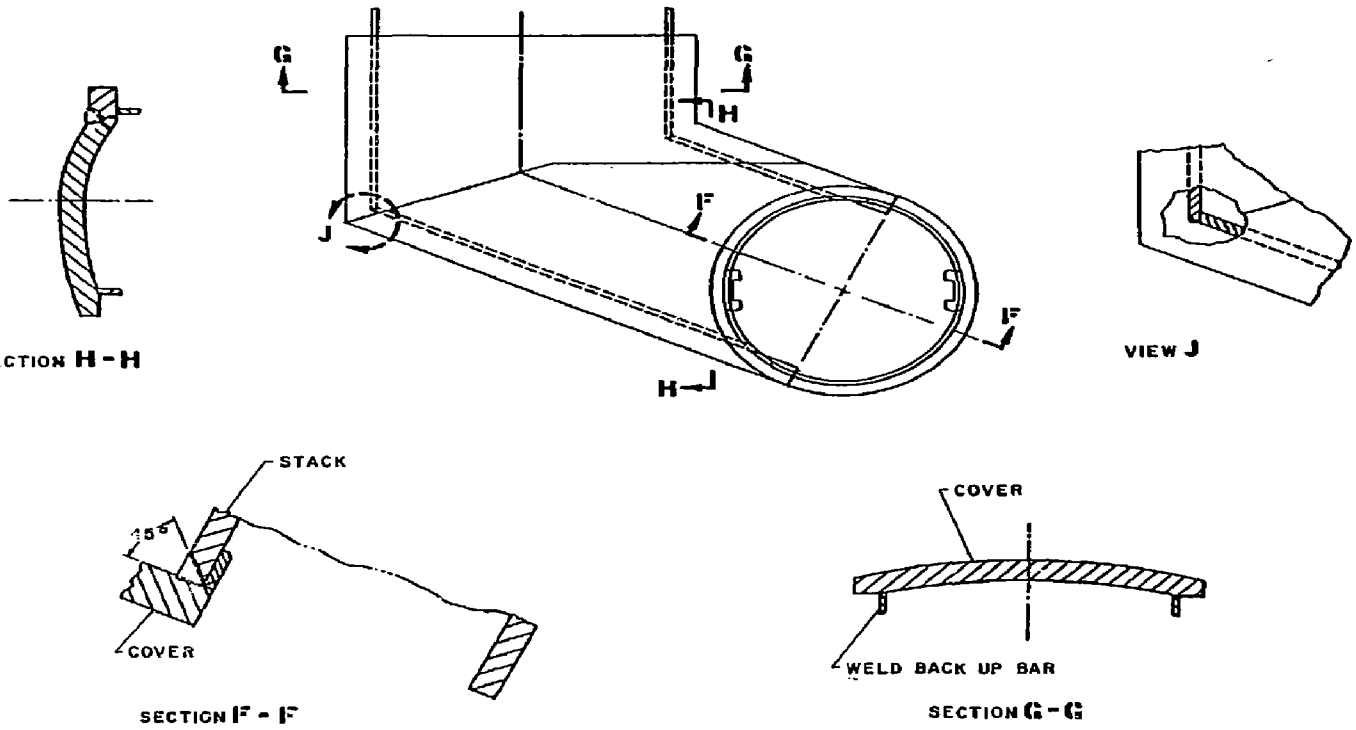

Figure 2-7. Tunnel Cover

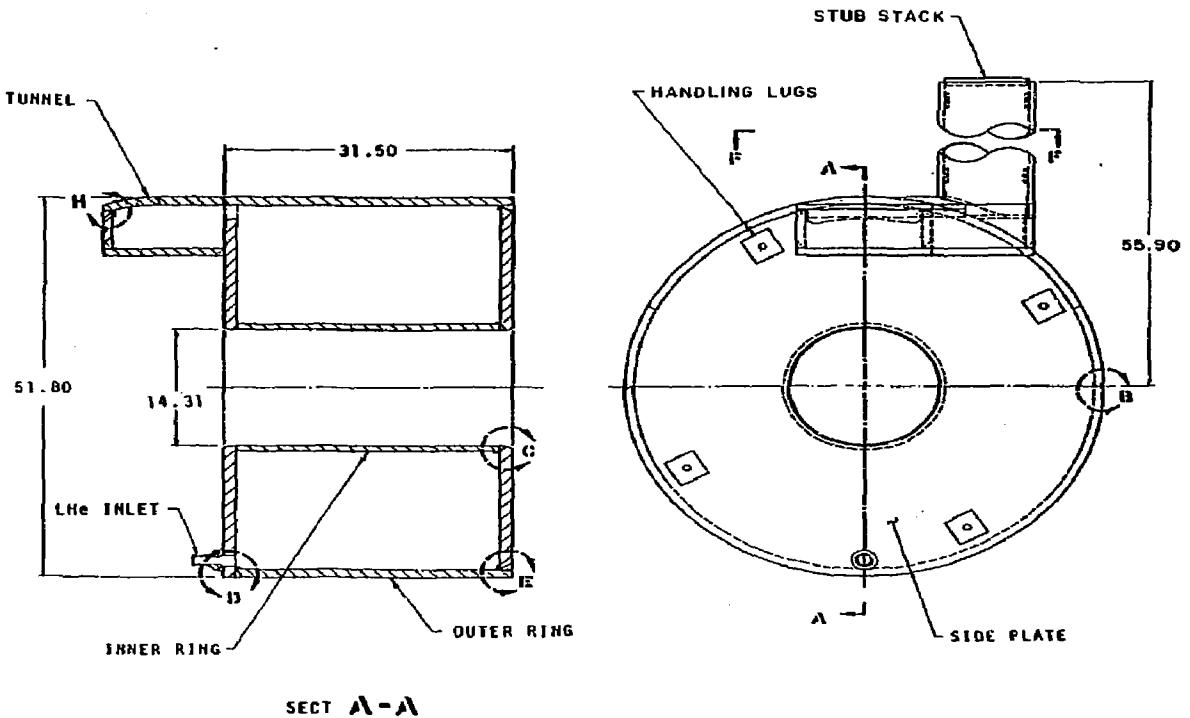

Figure 2-8. Coil Case Structure Assembly

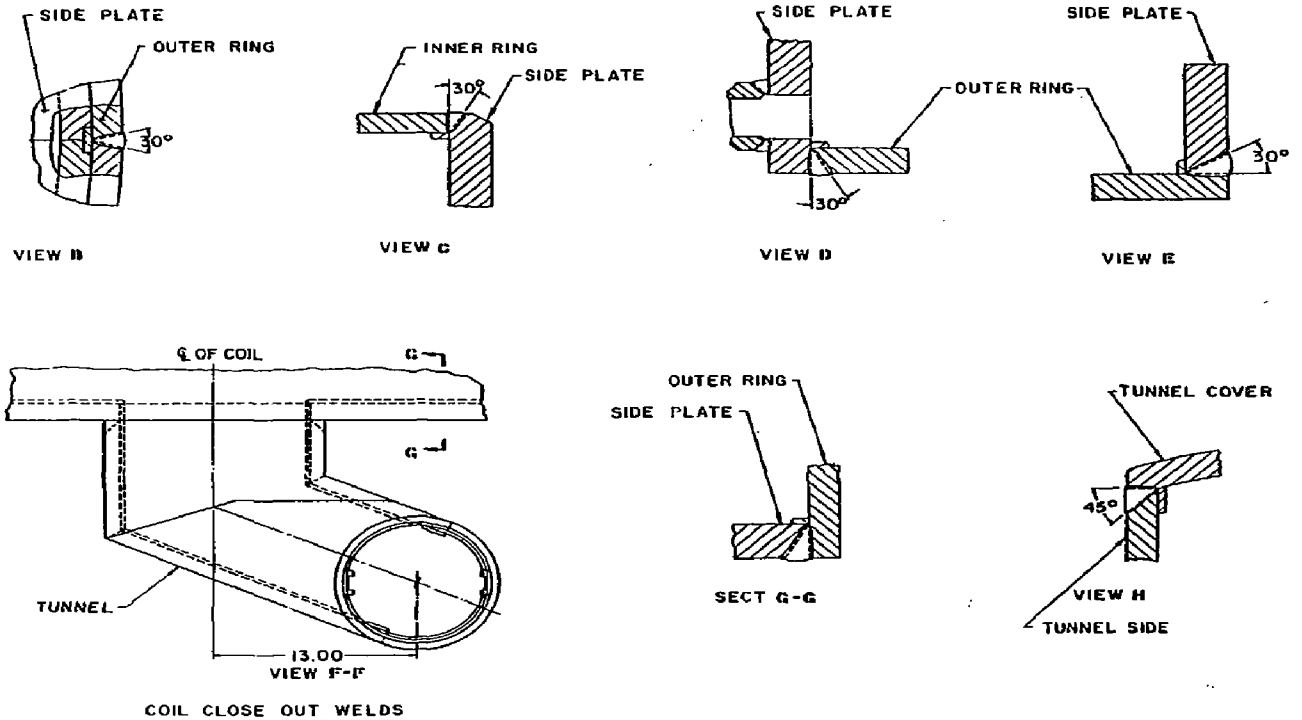

Figure 2-9. Coil Case Structure Assembly

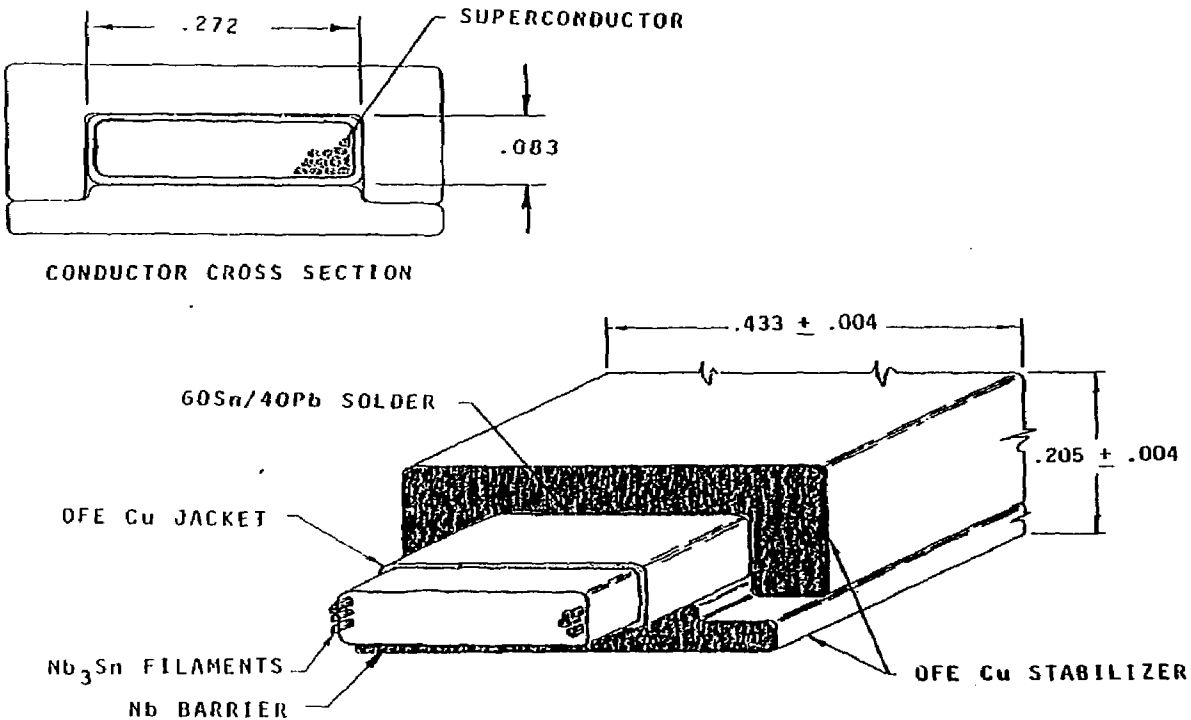

Figure 2-10. Conductor for High Field Insert Coil

minimum of 100 for a zero field condition. The exterior of the copper housing is covered with anodic-oxidized film. Solder will not adhere to the coating, and the exterior surface of the copper is free of any visible solder. Also, the oxide coating enhances conductor cooling in the liquid helium.

2.3.3 Conductor Processing

Processing the Nb_3Sn insert monolith consists of three stages of fabrication, including triple hot extrusions. The first is fabrication of multifilamentary composite of Nb and bronze. The second is fabrication of the multifilamentary composite of 380 Nb cores and in a bronze matrix. The third is fabrication of final composite of 145,000 Nb filaments and bronze matrix with Nb barrier and copper housing.

The reacting temperature for the formation of Nb_3Sn is carried out at approximately 700C and requires several days.[3] The insert is reacted in a controlled atmosphere furnace on a steel mandrel. Concentric mandrels having winding diameters of 60, 70, and 80 cm (23.6, 27.6 and 31.5 in) are used.

The prereacted Nb_3Sn monolith insert and the copper stabilizer housing are continuously assembled and soldered to each other in a single line. Ultrasonic vibration is employed during the soldering operation, which produces a high quality solder bond between the superconducting insert and the copper stabilizer. The conductor size and solder bond quality are inspected along the entire length on the assembly line.

During assemblying, handling, and spooling for shipment, the reacted conductor when rebent is bent in the same direction the conductor was bent on the reacting spool. Throughout the processing, a maximum applied strain of no greater than +0.4 to -0.6 percent shall be exerted on the Nb_3Sn filaments.

The delivered, spooled conductor is marked with a serial number. This provides traceability over the whole conductor process, from raw materials, all the various manufacturing processes, insert reacting spool diameter, and conductor assembly.

2.4 Insulation System

2.4.1 Coil Ground Wall Insulation

Prior to start of winding the coil, the winding form is covered with ground wall insulation. The inner ring ground wall insulation consists of two thicknesses of solid G-10CR epoxy/glass fabric laminate sheet and six layers of Kapton film. Each G-10CR is 0.79-mm (0.031-inch) thick and the Kapton is between the G-10CR sheets. Figure 2-11 shows the ground wall insulation for the

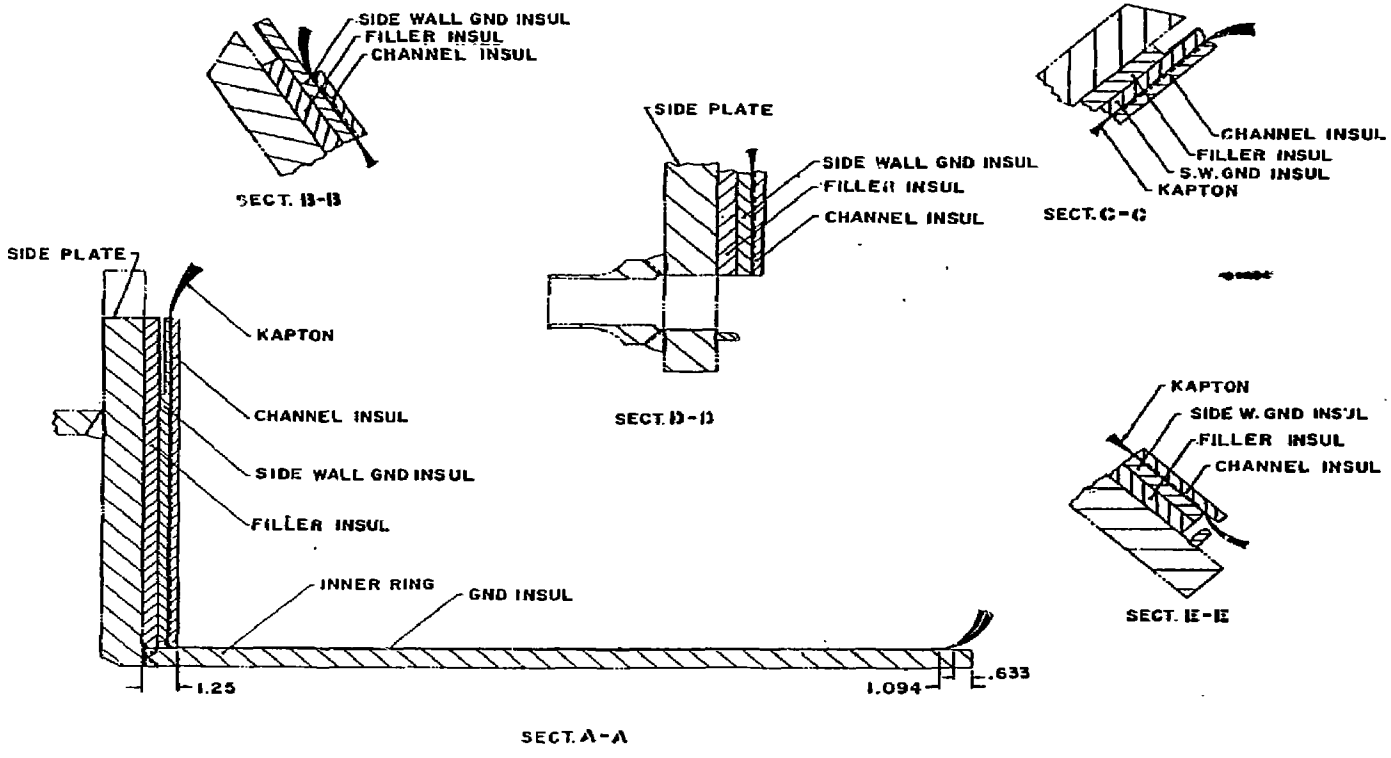

Figure 2-11. Coil Winding Insulation Installation

inner ring and coil side plate. The Kapton film is 0.13-mm (0.005-inch) thick and is in strip form and looks similar to a "bow tie," with the narrow portion at the inner ring and the wide area at the outer ring. The Kapton strips are installed so each layer overlaps the previous layer by 50 percent. The Kapton strips come in lengths long enough to cover the inner ring, both side plates, and part of the outer ring.

The coil side plate ground insulation consists of three layers of G-10CR sheet insulation and the six layer of Kapton strip insulation. There is a 13.5-mm (0.533-inch) thick G-10CR filler insulation next to the stainless steel side plate. The insulation is solid sheet and butts on the coil vertical centerline. Figure 2-12 shows the G-10CR filler insulation and the G-10CR ground insulation. The 9.5-mm (0.375-in) thick G-10CR ground insulation is next to the filler insulation. The ground insulation is in two pieces and butts on the coil horizontal centerline. The Kapton strips from the inner ring are installed on the G-10CR ground insulation. The 7.9-mm (0.312-in) thick G-10CR channel insulation is placed on the Kapton insulation. Figure 2-13 shows the channel insulation. The insulation is installed with the slots orientated as shown in Figure 2-13. The insulation provides 50 percent wetted area to the edge of the conductor next to the channel insulation. The channels provide a large liquid helium volume at the coil side wall and direct bubble flow towards the outer ring.

The insulation on the closeout side plate is installed upon completion of winding all of the pancakes. The insulation is the same as used on the coil winding form except that the order of installation is reversed.

The ground insulation at the outer ring is installed after the coil is wound; the closeout side plate is welded in place and the plenum insulation is installed. The ground insulation is located between the plenum insulation and the stainless outer ring. The outer ring ground insulation consists of two sheets of .79-mm (0.031-in) G-10CR with Kapton insulation between the G-10CR sheets. The Kapton strip pigtails at the outer edge of the side plates are folded over the first G-10CR sheet insulation. The pigtails overlap the G-10CR sheet by three inches. Four layers of .127-mm (0.005-in) thick Kapton sheet estending from pancake 1 to pancake 54 and the length is the circumference of the coil, goes over the Kapton pigtails and the first G-10CR sheet insulation. The second sheet of G-10CR is then put over the Kapton sheet insulation.

The thick side plate insulation of G-10CR was selected for two primarily reasons: (1) the entering and exiting current lead, where it splices into the Nb_3Sn conductor, can be bolted to the G-10CR insulation to react conductor loads and (2) it provides a greater distance from conductor to ground.

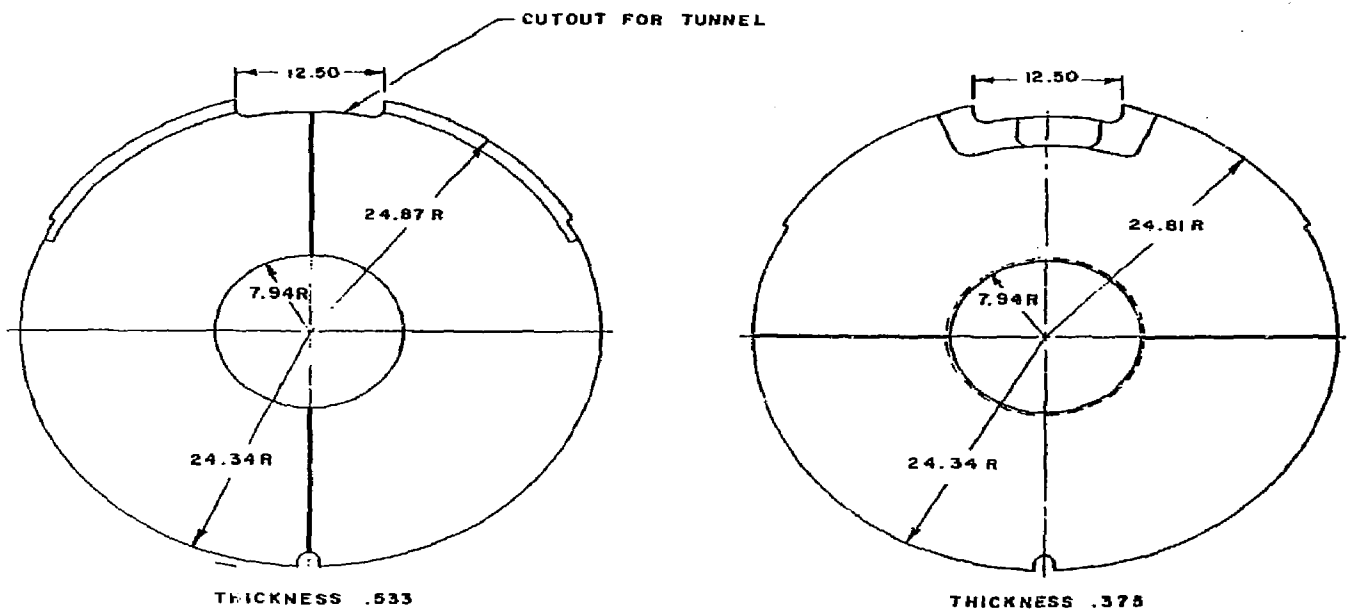

Figure 2-12. Side Wall Insulation

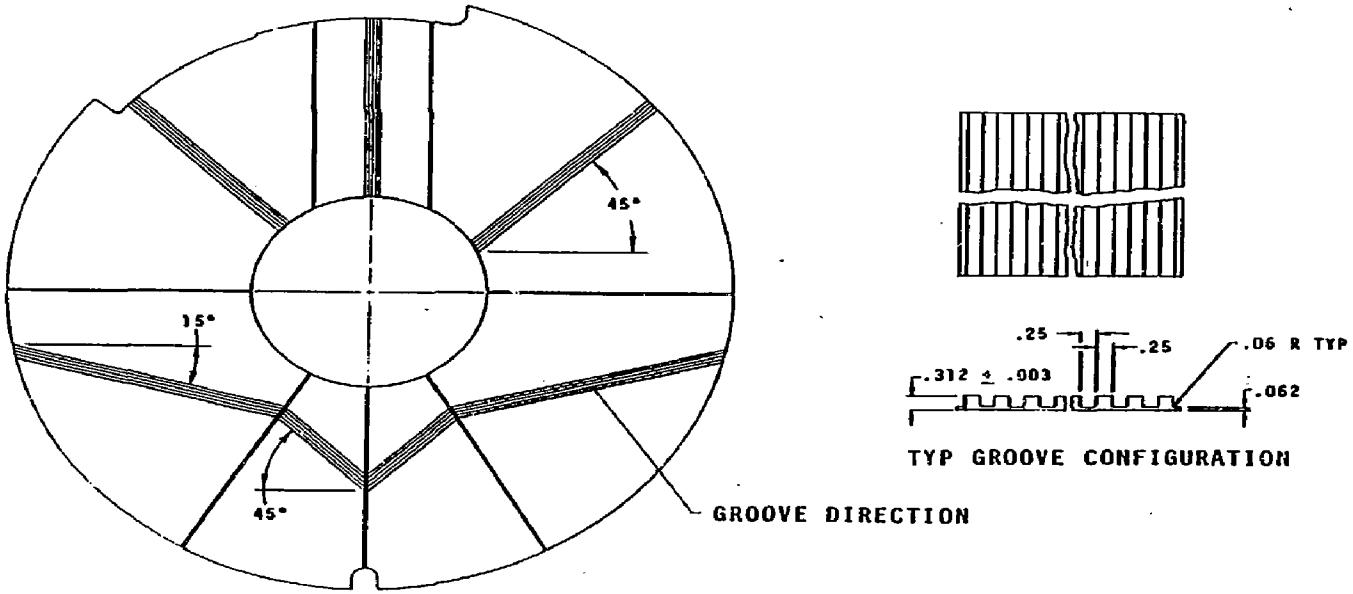

Figure 2-13. Side Wall Channel Insulation

2.4.2 Helium Inlet Insulation

The helium fill inlet requires special insulation locally to provide a 7.6-cm (3-in) conductor-to-ground arc length. A layed-up epoxy glass fabric shoulder bushing is used in the helium fill hole. The shoulder portion of the bushing fits into a machined pocket in the channel insulation. The bushing wall thickness is 2.3 mm (0.090 in) thick. Figure 2-14 shows the epoxy glass fabric shoulder bushing. A .25-mm (0.010-in) thick vacuum formed polyurethane shoulder bushing goes on the outside of the fiberglass shoulder bushing. This provides a second insulation barrier. The polyurethane bushing is bonded to the fiberglass bushing, and this captivates the polyurethane bushing between the case structure and the fiberglass bushing.

2.4.3 Current Lead Splice Insulation

Locally, additional Kapton strip insulation is used where the entering and exiting current leads splice to the Nb_3Sn conductor. The additional insulation goes between the side wall G-10CR filler insulation and the G-10CR ground insulation. The insulation is required due to the fasteners that anchor the conductor splice fitting to the G-10CR ground insulation which, in turn, is bolted to the case structure.

2.4.4 Tunnel Entrance Insulation

A layed-up epoxy glass fabric shoulder bushing is installed at the entrance to the current lead tunnel. A vacuum-formed polyurethane shoulder bushing is installed over the outside of the fiberglass shoulder bushing. This provides a double insulation barrier at the tunnel entrance. This insulation is installed in conjunction with the coil side wall ground insulation.

2.4.5 Grid and Joggle Insulation

The grid insulation is installed on the ground insulation at the inner ring and the length extends the lower 180° of the inner ring. Figure 2-15 shows the grid insulation and Figure 2-16 shows the joggle insulation. Conductor turn one joggles from one winding pancake to the other pancake on the grid insulation and it is used in conjunction with two joggle insulation pieces. The grid insulation is machined from G-10CR epoxy-glass fabric laminate and is the width of two pancakes, with 27 required per coil. The grid insulation provides a large liquid helium volume and 75 percent wetted area to the conductor in the high field region. The joggle insulation is machined from G-10CR and is located on the top of the grid insulation. A large, 902-cm (355-in) radius is used for the joggle. This radius puts an additional strain on the superconductor of only 0.04 percent. The joggle insulation provides 75 percent wetted area to the edge of the conductor. A total of 54 pieces are required per coil.

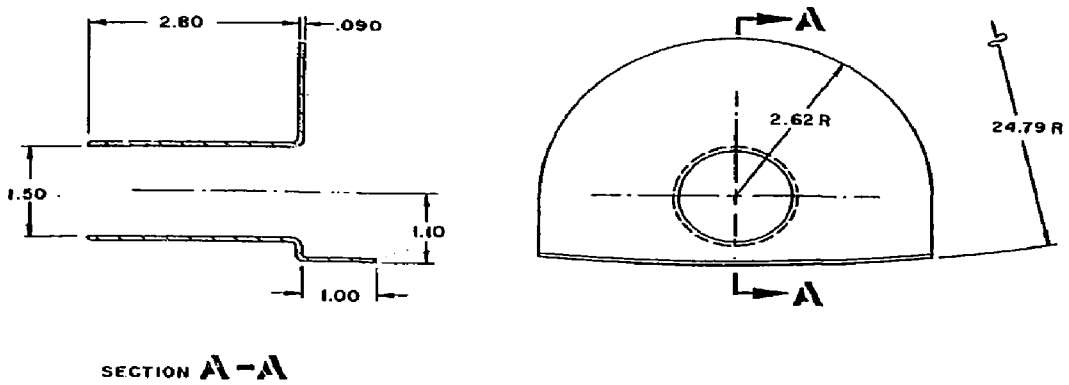

Figure 2-14. Helium Inlet Bushing Insulation

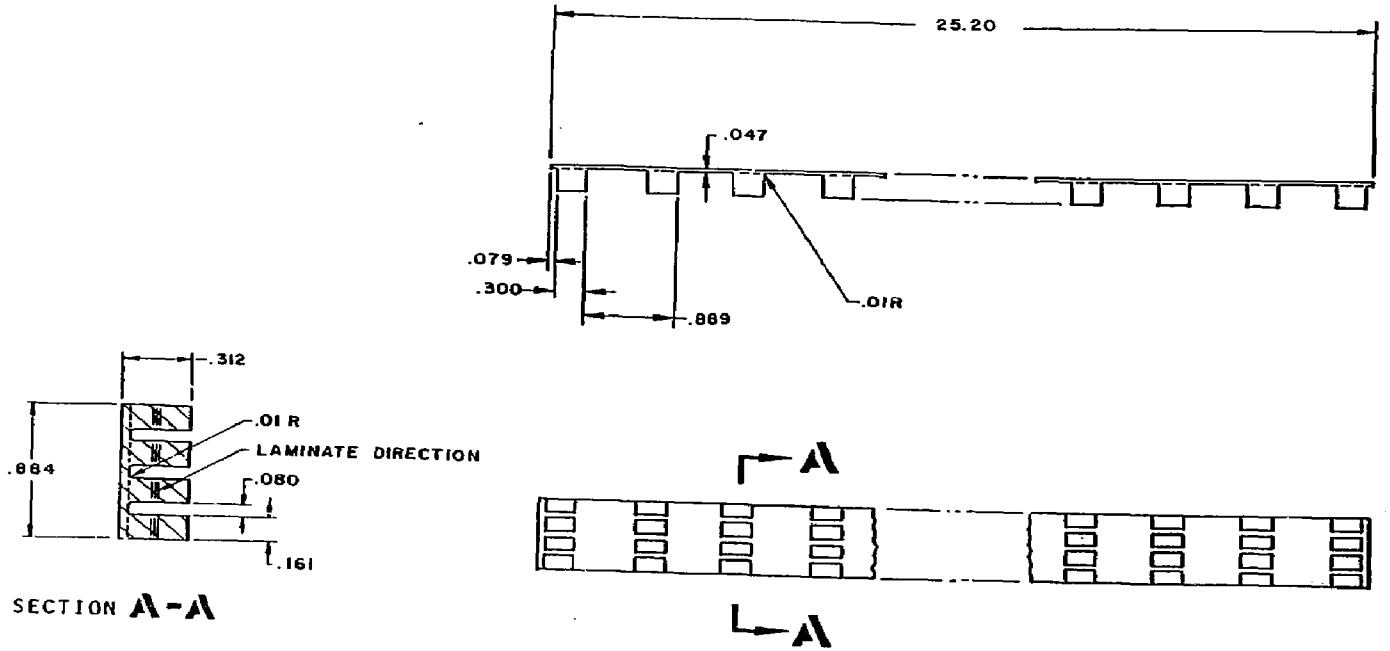

Figure 2-15. Grid Insulation

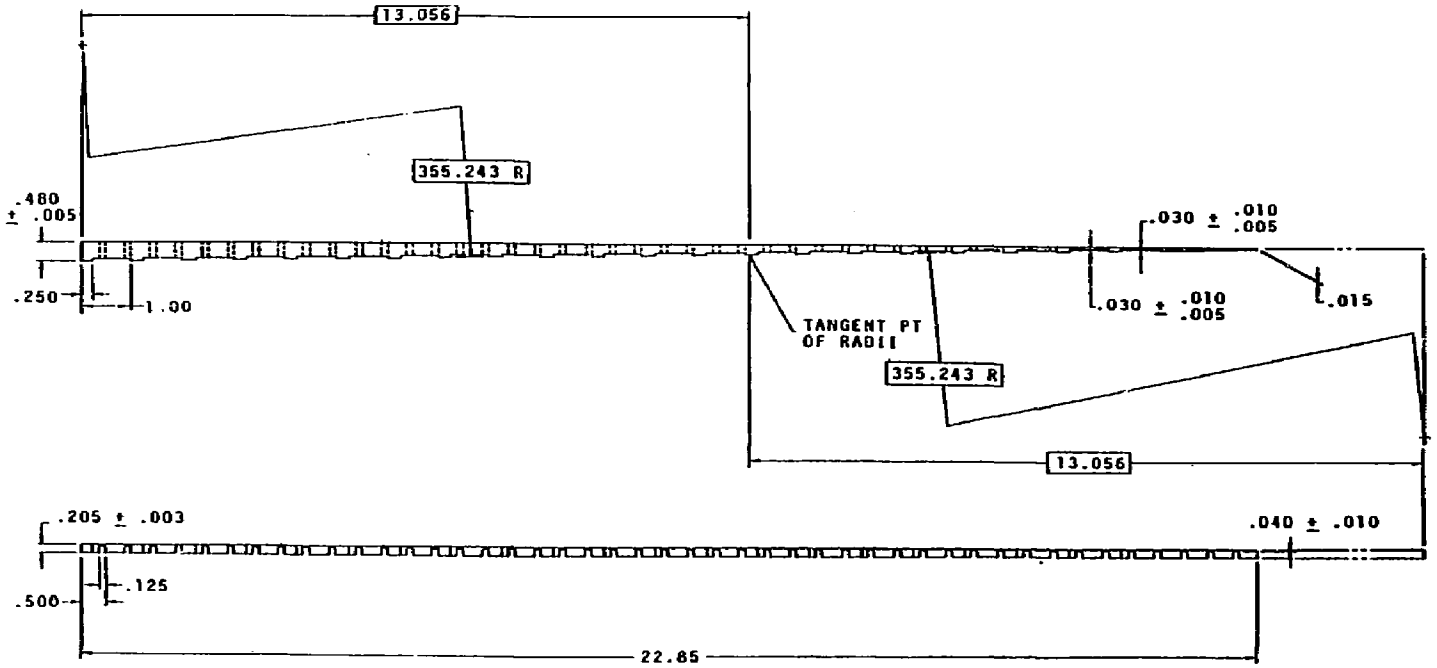

Figure 2-16. Joggle Insulation

2.4.6 Riser Grid Insulation

The riser grid insulation is installed on the inner ring ground insulation. The length extends the upper 180° of the inner ring. Figure 2-17 shows the riser grid insulation details. The riser grid insulation is machined from G-10CR with 54 pieces required per coil. Conductor turn one rises to become turn two at the end of the insulation. The insulation provides 67 percent wetted area to the conductor in the high field region.

2.4.7 Conductor Turn Insulation

The turn insulation is fabricated from 1-mm (0.039-in) thick G-10CR epoxy-glass fabric laminate. The insulation is a fishbone-type design and provides circumferential and lateral helium flow at the conductor. Figure 2-18 shows the turn insulation. The insulation provides 27.5 percent bearing area on the conductor. The insulation is used between each conductor turn when winding a pancake. A total of 7,965 m (26,132 ft) of turn insulation is required per coil. A turn insulation twice the width of that shown in Figure 2-18 is used in the conductor joggle area. The insulation goes between turn one and turn two. This provides positive protection against turn one shorting out to turn two. The insulation is the same thickness as the other turn insulation.

2.4.8 Conductor Pancake Insulation

The pancake insulation is fabricated from 1.2-mm (0.047-in) thick G-10CR epoxy glass fabric laminate. The insulation has punched slots 4.7 mm (0.187 in) wide by 38 mm (1.50 in) long and provides 50 percent open pattern. The slots are orientated as shown in Figure 2-19 for all of the pancakes. The slot orientation directs the energy laden helium flow out of the conductor winding pack, towards the outer ring. There are seven types of pancake insulation used in the coil, however, they are all similar. The differences occur due to the conductor splice fittings and the entering and exiting current leads. The insulation at the conductor splice fittings will either have a notch for the splice or no notch as it goes between the splice fittings. Where the insulation is between the splices, the thickness is increased locally to 3.6 mm (0.141 in) to prevent pancake shorting.

2.4.9 Ventilated Post Insulation

The ventilated post-insulation is made from G-10CR epoxy glass fabric laminate and the width matches the conductor pancake width. Figure 2-20 shows a typical ventilated post-insulation width. There are several versions used in the coil for conductor turn 57, outboard of turn 57, and for the entering and exiting leads.

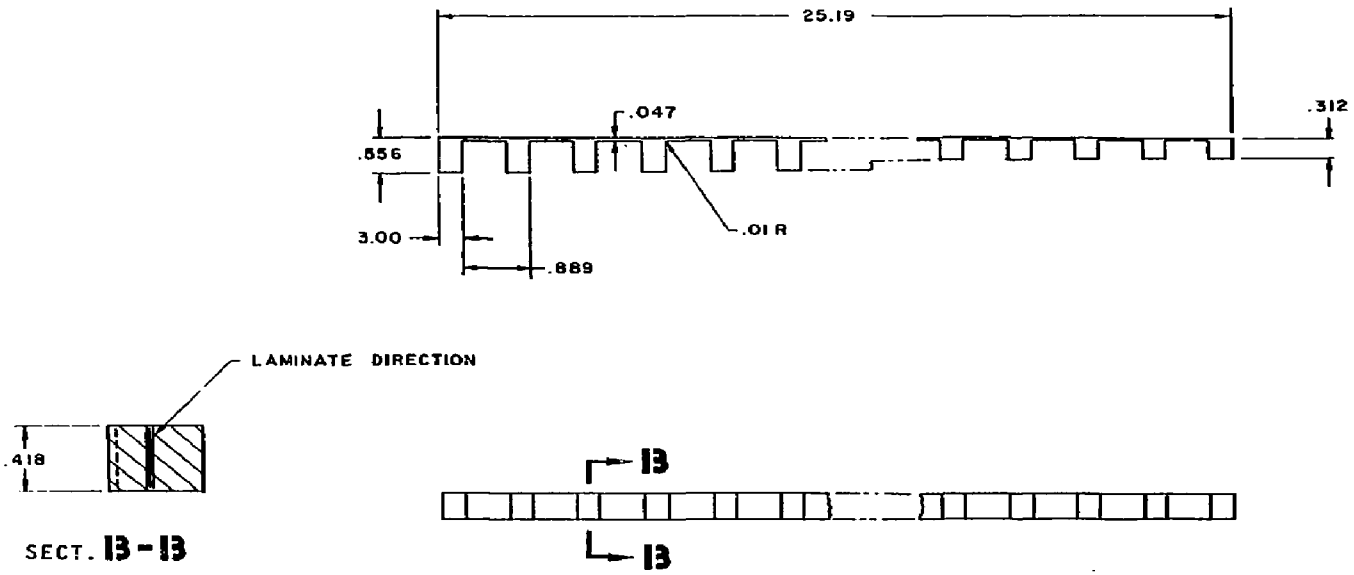

Figure 2-17. Riser Grid Insulation

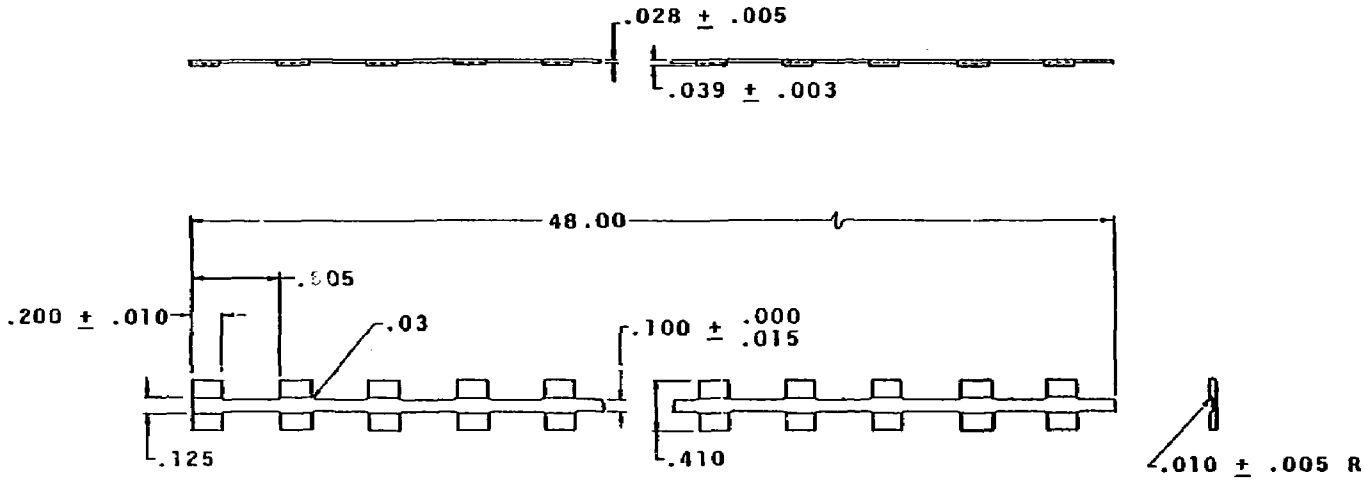

Figure 2-18 Turn Insulation

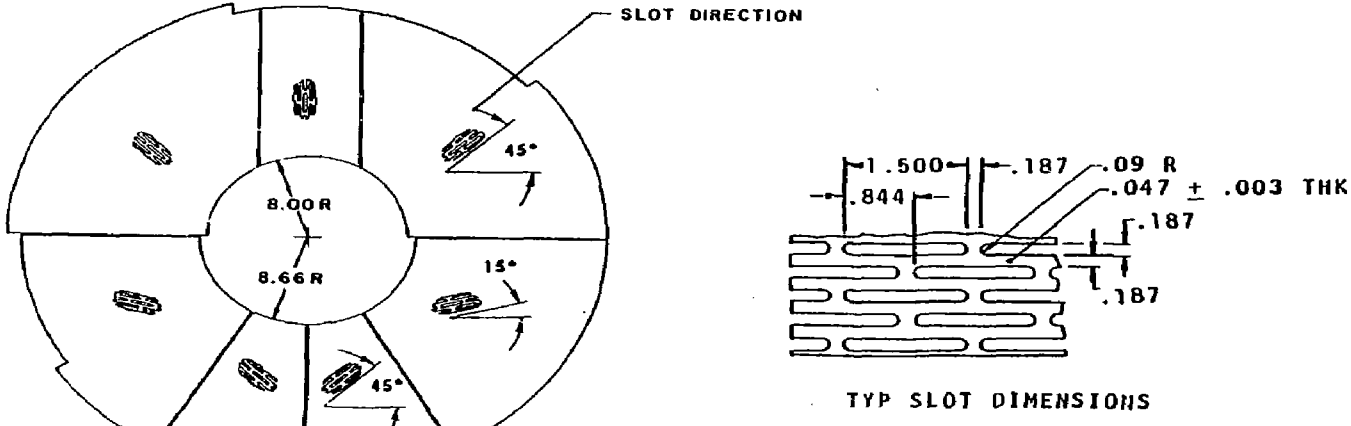

Figure 2-19. Pancake Insulation

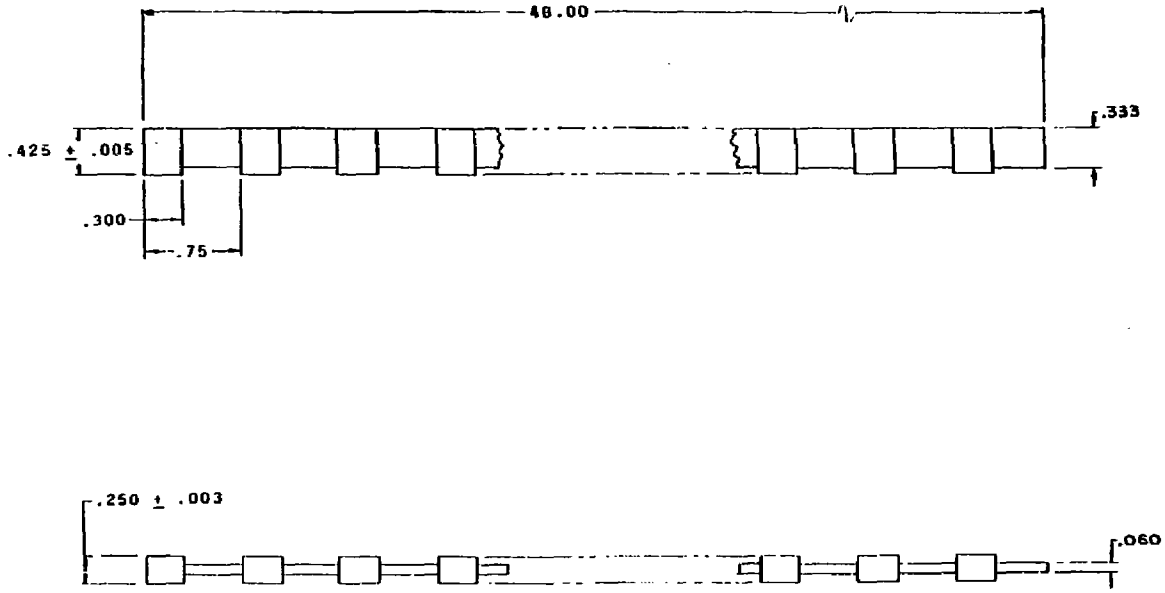

Figure 2-20. Ventilated Insulation

Tapered post-insulation is used inboard and outboard of conductor turn 57 where it rises to the conductor splice fitting. Outboard of conductor turn 57, post-insulation is installed between the conductor and plenum insulation. The post-insulation is bonded on one face only to the adjacent pancake insulation. This holds both the post-insulation and the pancake insulation in relation to the conductor.

2.4.10 Plenum Insulation

The plenum insulation is fabricated from 1.51-mm (0.062-in) thick G-10CR sheet. The insulation has punched slots 4.7 mm (0.187 in) wide by 38 mm (1.50 in) long, and the lands are 3.2 mm (0.126 in) wide. The pattern is identical to that used on the solenoid coils. The plenum insulation panels consist of four punched sheets bonded together to the radius of the coil. The slots are aligned for helium flow in the four-ply panel and the adhesive is 3M 3549 A/B urethane. Figure 2-21 shows a typical plenum insulation panel. The panels are installed in the coil between the ventilated post-insulation and the outer ring ground insulation. There is space for four panels. Panels are installed in the coil with the adjacent panel flip-flopping the 48° angle slots.

2.4.11 Tunnel Insulation

The insulations that support the current leads are 38 mm (1.50-in) thick and 12.7-mm (0.50 in) G-10CR planks. Figures 2-22 and 2-23 show the tunnel insulation, current lead, and structure. The 12.7-mm (0.50- in) thick G-10CR plank is bolted to the tunnel structure with eight bolts and the 38-mm (1.50-in) G-10CR plank is bolted to the 12.7-mm (0.50-in) plank. Kapton sheet insulation is used between the G-10CR planks. Two epoxy-glass fabric layed-up housings are used for insulation along the top and sides of the tunnel. Kapton insulation is used between the two fiberglass housings. Vacuum-formed polyurethane insulation is used at the corners of the tunnel where Kapton insulation cannot be used.

At the junction of the tunnel to the stub stack there are two layed-up epoxy glass fabric insulation housings. Both of the fiberglass parts are 1.5 mm (0.060 in) in thickness. A vacuum-formed polyurethane insulation .25 mm (0.010 in) thick is used in the area of the tunnel to the stub stack intersection. The polyurethane insulation is between two fiberglass housings.

The stub stack has two 12.7-mm (0.50-in) thick planks back to back inside the stack to support the current leads. The G-10CR planks run the length of the stub stack along with two tapered stack planks. Kapton insulation is installed between the G-10CR planks which insulates the bolts that support the conductor.

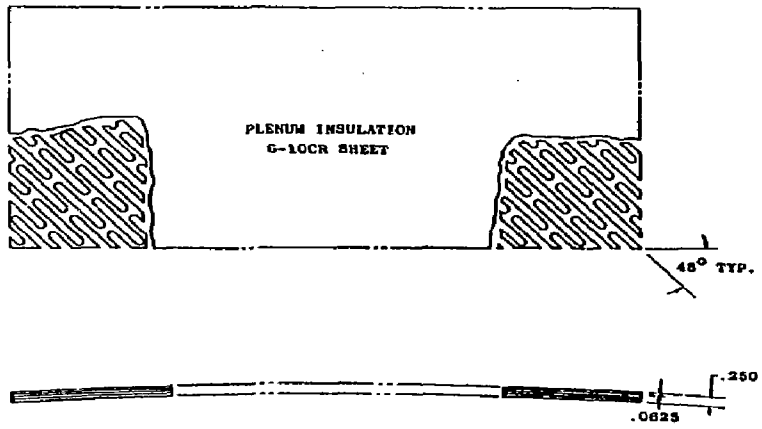

Figure 2-21. Plenum Insulation

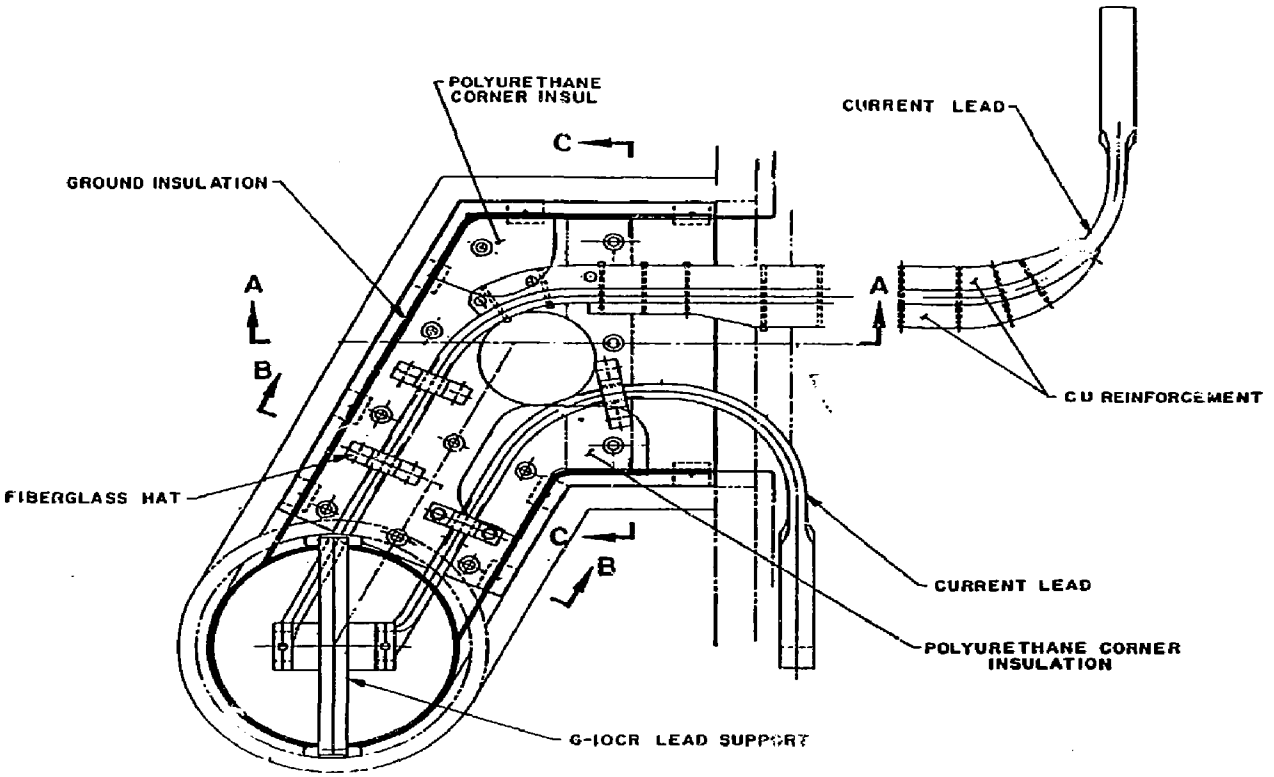

Figure 2-22. Tunnel Insulation

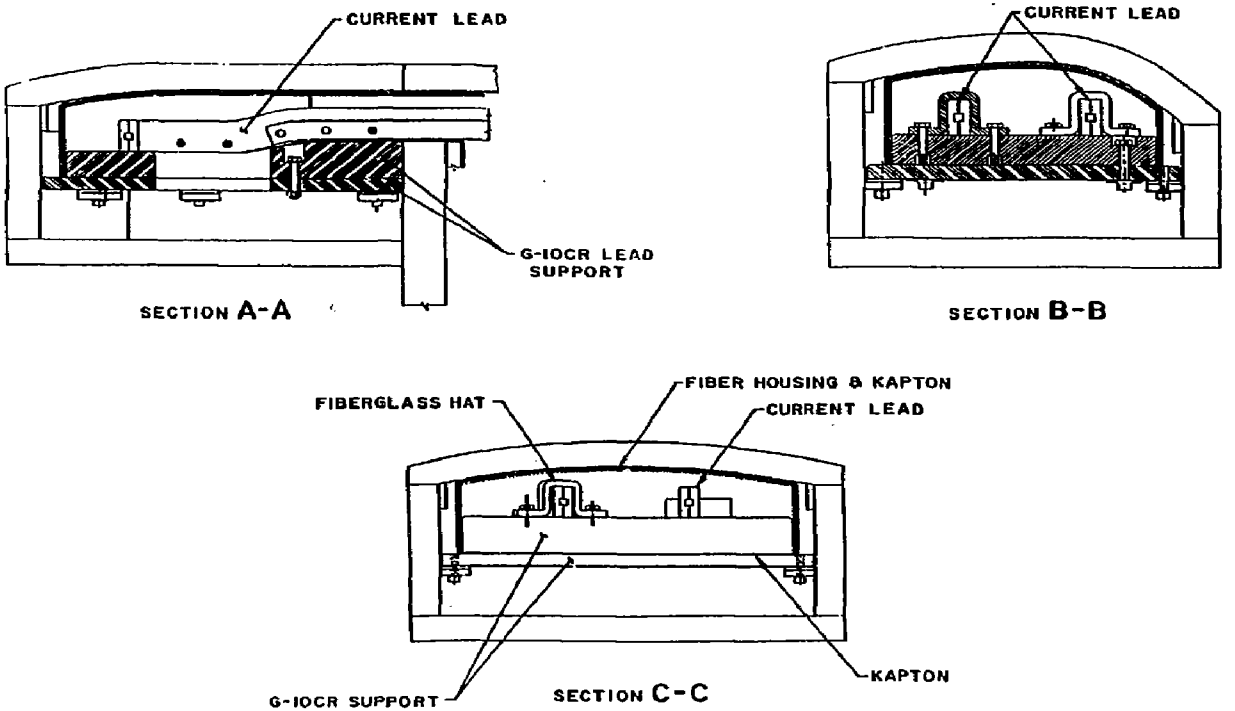

Figure 2-23. Tunnel Insulation

2.5 Coil Winding

The coil is pancake-wound, winding the conductor on its face (easy way). The bending strains on the conductor are minimized when bending about the smaller dimension. The conductor comes in 295-m (968-ft) lengths which will wind one double pancake. A double pancake has the advantage of eliminating a conductor splice at the inner ring, which is the highest field region in the coil. All of the conductor splices are on the outside of the coil winding, where access is good and the field is lowest. Figure 2-24 shows the left and right hand sides of the coil winding, conductors being spliced, and the conductor splice fittings.

2.5.1 Winding Pancake One

Upon completion of installation of the ground insulation on the coil form, it is ready for winding. Figure 2-25 shows the winding for pancake one. The grid insulation and joggle insulation for pancakes one and two are installed in the lower 180° of the coil. The conductor joggle length is the full 180° between pancake one and pancake two. The conductor rise insulation is installed in the upper 180° of the coil, which produces a very gradual rise from turn one to turn two. The middle of the 295 m (968 ft) length of conductor is installed in the joggle area and the conductor for pancake two is clamped down. Then pancake one is wound with the fishbone turn insulation installed. Locally, at the conductor joggle area, a two-pancake-wide fishbone turn insulation is installed between turn one and turn two. This provides positive protection against turn one shorting to turn two due to conductor movement when the coil is energized. The pancake is wound completing 56 turns. A riser post-insulation is installed on the outboard side of turn 56. The insulation starts at the bottom centerline of the coil and runs up to the entering current lead splice. Turn 57 is wound on the riser post-insulation and the splice is made to the current lead. Install the post-insulation outboard of turn 57. The pancake insulation is installed covering pancake one winding. The pancake insulation is bonded to the post-insulation outboard of turn 57 with 3M 3549 A/B urethane adhesive. The post-insulation is bonded on one side only to the pancake insulation.

2.5.2 Winding Pancake Two

After the conductor has been installed in the tensioner, the conductor is unclamped from the winding form. The riser post-insulation is installed in the uppper 180° of the coil, over the ground insulation at the inner ring. Turn one is wound on the riser post insulation and becomes turn two. The fishbone turn insulation is installed on the conductor and the winding continues through turn 56. Figure 2-26 shows the winding of pancake two (the figure also applies to pancakes 6, 10, 14, 18, 22, 26, 30, 34, 38, 42, 46, and 50). The riser post-insulation is installed outboard of turn 56. The riser post-insulation starts at the bottom centerline of the coil and extends to the conductor splice fitting. Turn 57 is wound on the riser post-insulation and

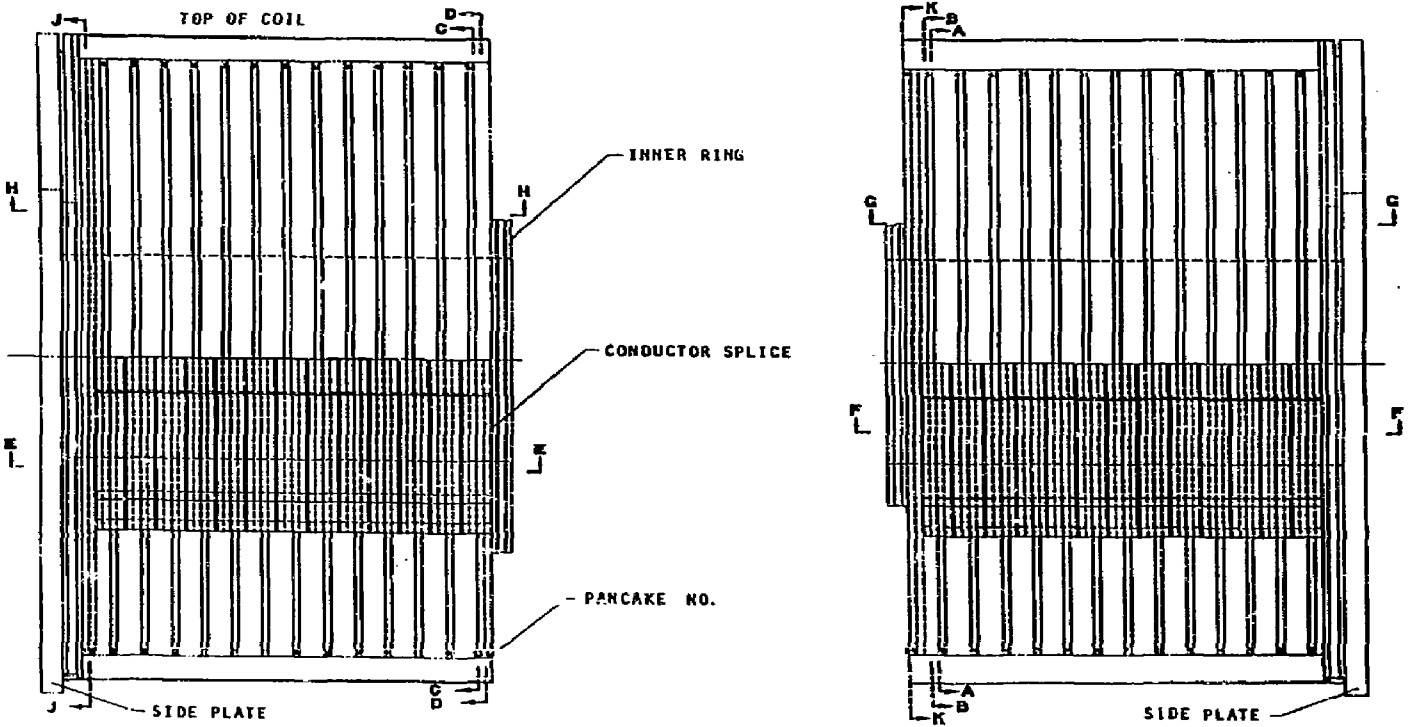

Figure 2-24. Coil Winding

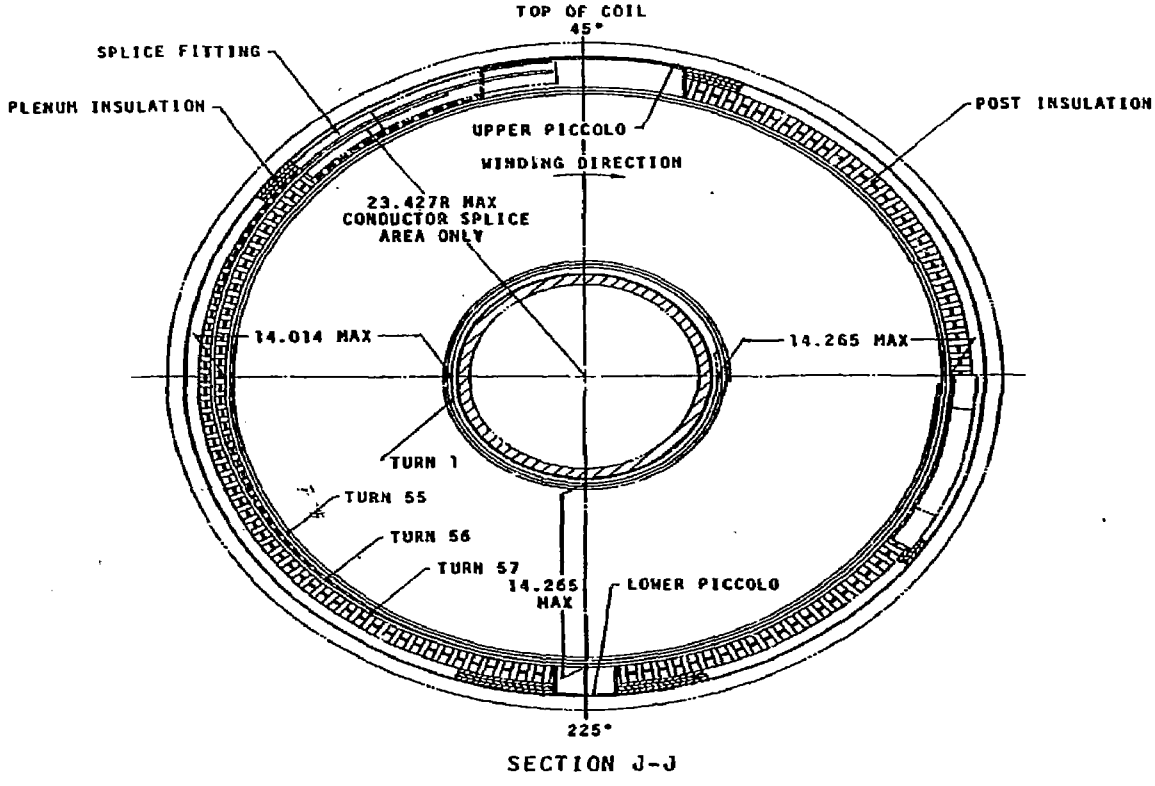

Figure 2-25. Coil Winding

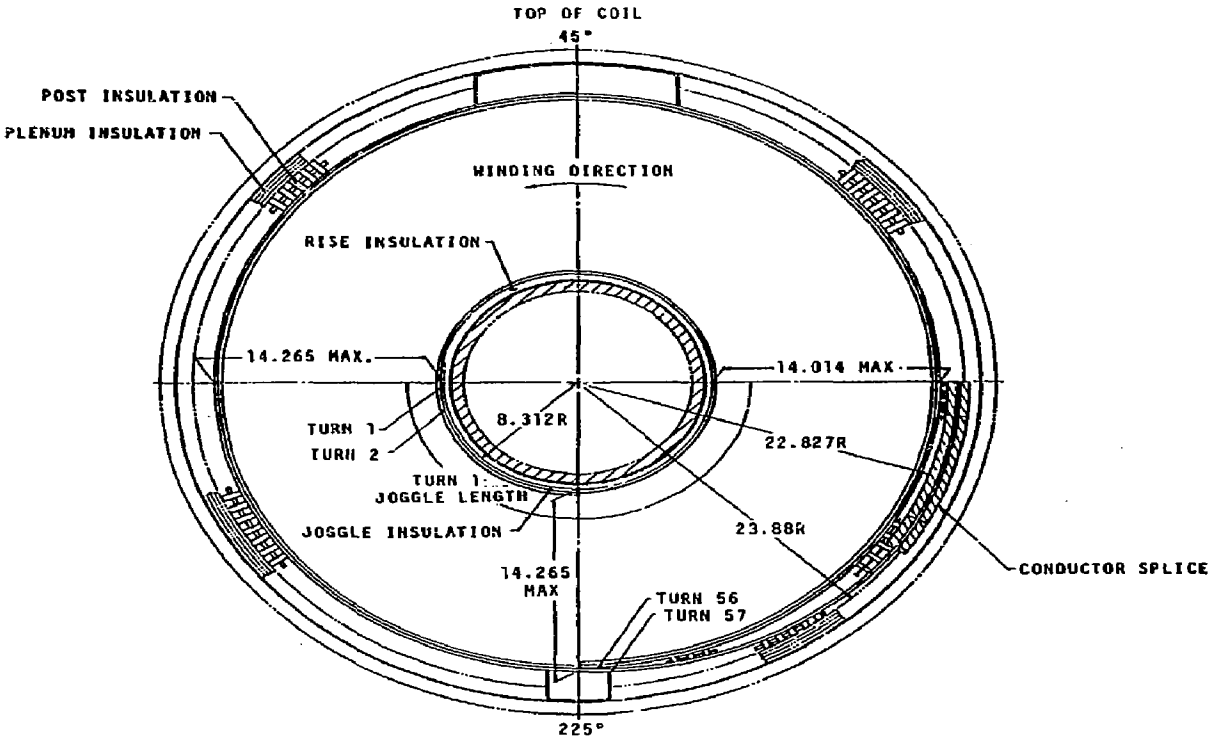

Figure 2-26. Coil Winding

clamped down. The splice will be made after winding pancake three. The post-insulation is installed outboard of turn 57. The pancake insulation is installed covering pancake two winding. The pancake insulation is bonded to the post-insulation outboard of turn 57. Note: bond one side only of the post-insulation.

2.5.3 Winding Pancake Three

The grid insulation and joggle insulation for pancakes three and four are installed on the ground insulation at the inner ring. The insulation extends 180° over the lower portion of the coil. The riser post-insulation for pancake three is installed in the upper 180° of the coil, on the inner ring ground insulation. Figure 2-27 shows the winding for pancake three (the figure also applies to pancakes 7, 11, 15, 19, 23, 27, 31, 35, 39, 43, 47, and 51). The middle of the 295 m (968 ft) length of conductor is installed in the joggle area, and the conductor for pancake four is clamped down. Then pancake three is wound installing turn insulation as described for pancake one. After winding 56 turns, a riser post-insulation is installed. The insulation is installed on the outboard side of turn 56, starting at the top centerline of the coil and extending to the conductor splice fitting. Turn 57 is then wound on the rise insulation. The conductor splice of pancake two to pancake three is made. The post-insulation outboard of turn 57 is installed. The pancake insulation is installed covering pancake three. The post-insulation is bonded on one side to the pancake insulation.

2.5.4 Winding Pancake Four

The winding of pancake four is similar to the winding of pancake two. Figure 2-28 shows the winding for pancake four (the figure also applies to pancakes 8, 12, 16, 20, 24, 28, 32, 36, 40, 44, 48, and 52). The main difference is that the conductor splice is on the opposite side of the coil.

2.5.5 Winding Pancake Five

The winding of pancake five is similar to the winding of pancake three. Figure 2-29 shows the winding for pancake five (The figure also applies to pancakes 9, 13, 17, 21, 25, 29, 33, 37, 41, 45, 49, and 53). The main difference from pancake three is that the conductor splice is on the opposite side of the coil.

2.5.6 Winding Pancake 54

Winding pancake 54 is similar to winding pancake two. Figure 2-30 shows the winding for pancake 54. After winding turn 56, a riser post-insulation is installed on the outboard side of turn 56. The riser post-insulation starts at the bottom centerline of the coil

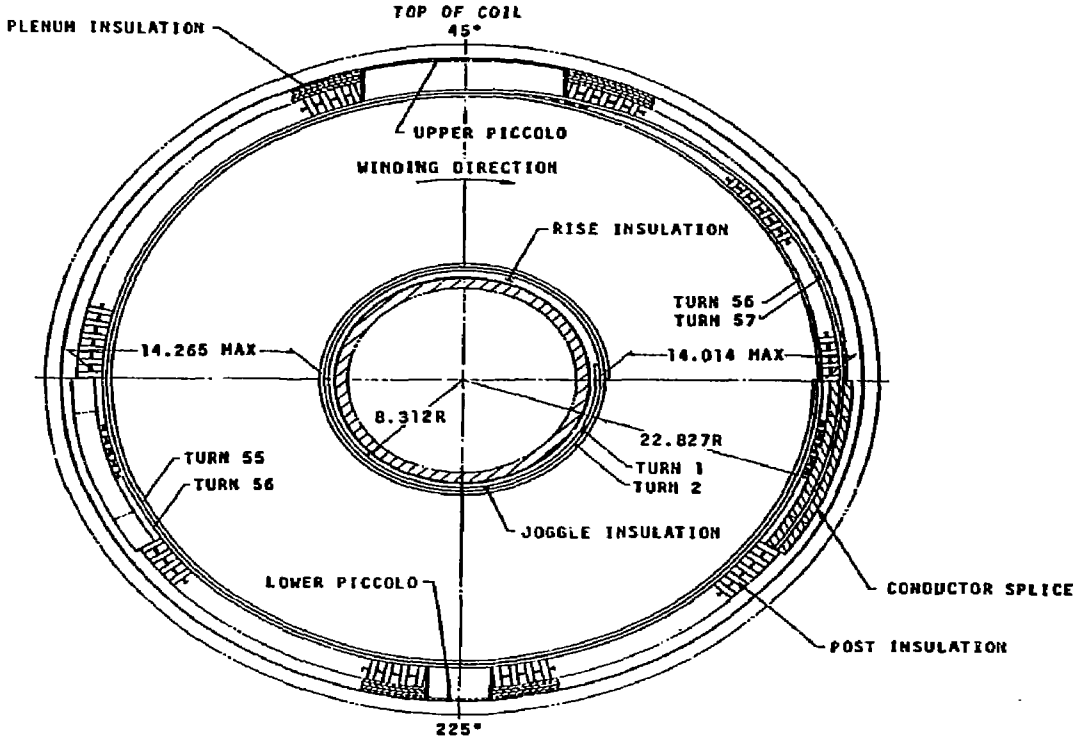

SECTION B-B

Figure 2-27. Coil Winding

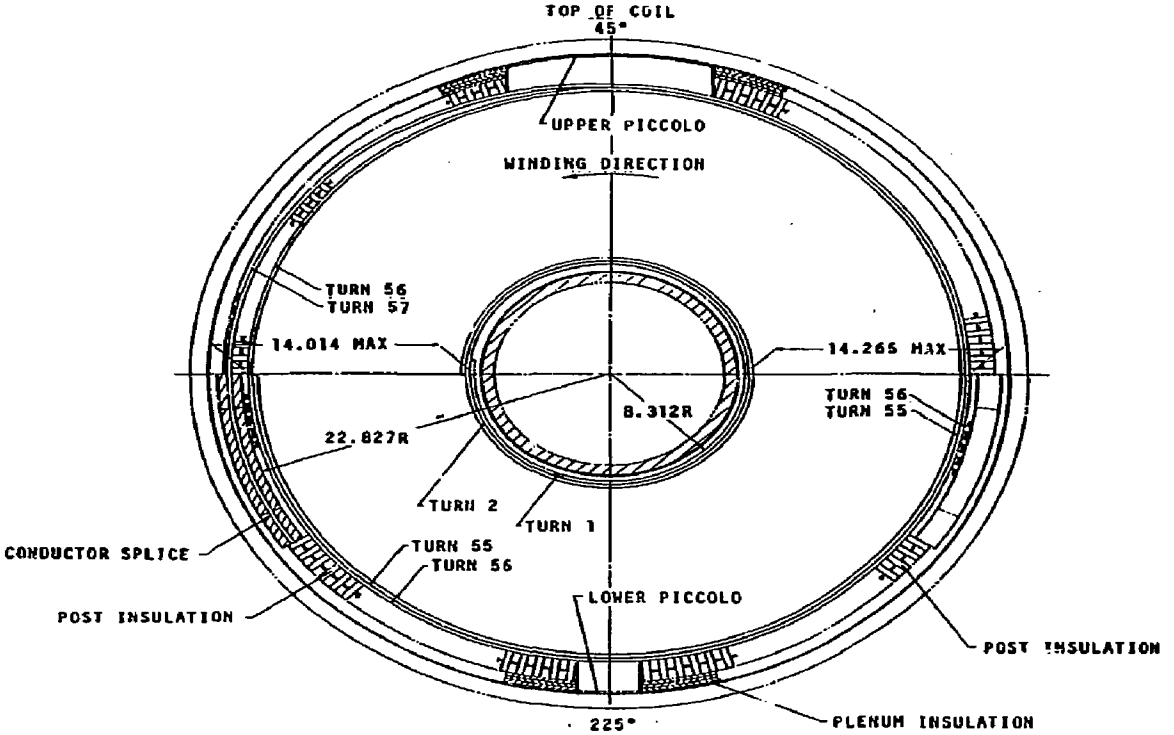

SECTION C-C

Figure 2-28. Coil Winding

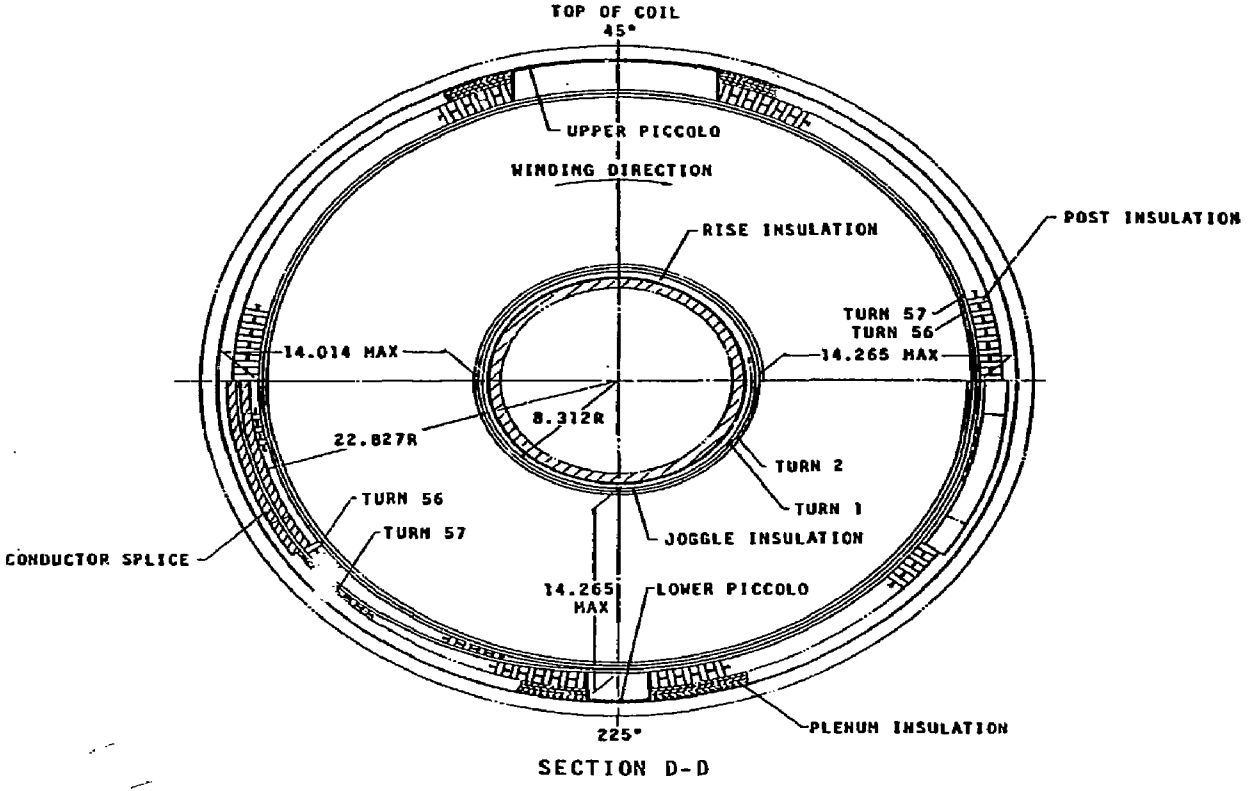

Figure 2-29. Coil Winding

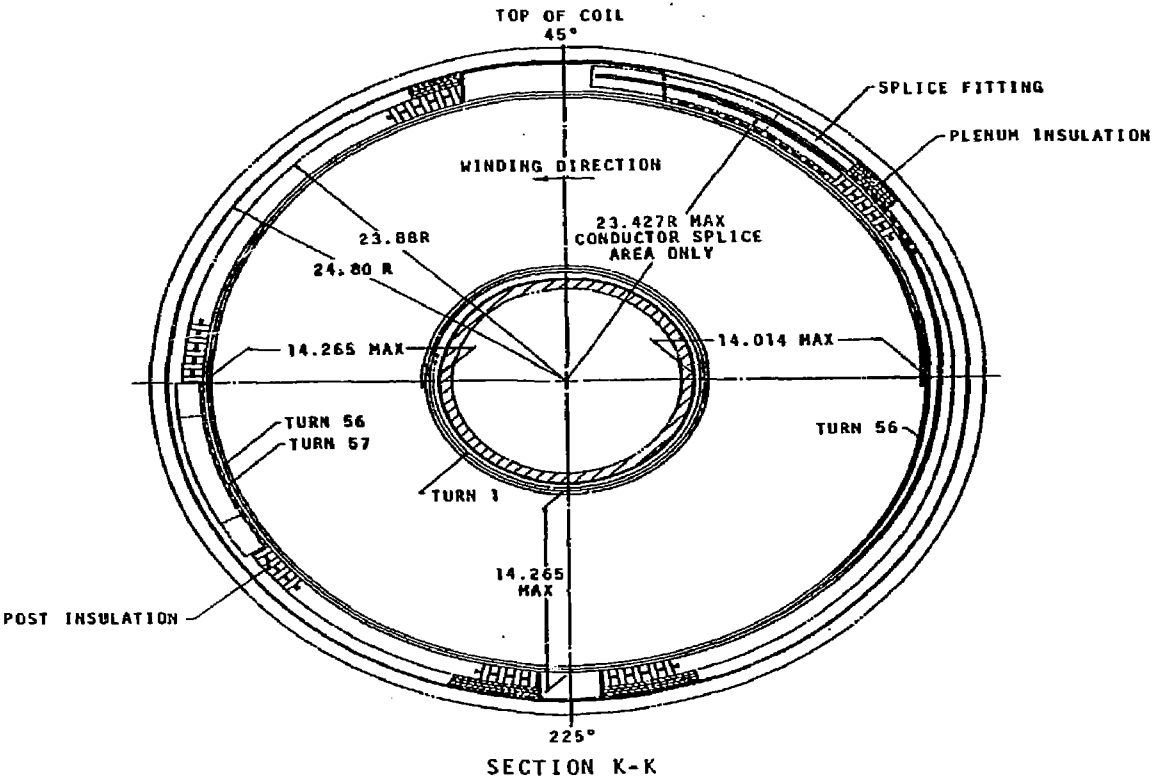

Figure 2-30. Coil Winding

and extends to the exiting current lead splice. Turn 57 is installed on the tapered post-insulation and spliced to the exiting current lead. The post-insulation is installed on the ouboard face of turn 57. The post-insulation on pancake 54 is not bonded to the pancake insulation or the side wall insulation.

2.5.7 Winding Details

Figure 2-31 shows section cuts of the coil winding. Section E-E is a cut below the horizontal centerline of the coil. Note that turn one does not line up with the pancakes since the conductor is joggling from one pancake to the other pancake. Below the coil's horizontal center, turns of the same number are in a straight line from pancake one through pancake fifty-four.

Section H-H is a section cut above the coil's horizontal centerline. Note that turn one is at a different radial position than the adjacent pancake turn. This is due to the conductor rising to the next turn level, however, at the top centerline of the coil, the turns are aligned since each conductor has risen the same amount.

2.6 Conductor Splices

There are 26 conductor splice assemblies per coil. The splices are on the left-hand and right-hand sides of the coil, and are below the coil's horizontal centerline. Alternating the splices provides four pancake widths for the splices. Figure 2-32 shows the conductor splice assembly. A splice assembly consists of one electrical splice and two structural splices.

2.6.1 Electrical Splice

The electrical splice consists of two 1/2-hard C10100 OFE copper clamping bars. The clamping bars are 17.3 mm (0.68 in) thick, 45.2 mm (1.779 in) wide, and 21.3 cm (8.4 in) long. Each copper bar has a slot 2 mm (0.080 in) deep by 23.2 mm (0.913 in) wide running the length of the clamping bar. Figure 2-33 shows one half of an electrical splice and a structural splice. The conductors being spliced are placed side by side in the groove in the clamping bar. Solder (60 Sn/40 Pb) is applied to all faying surfaces of the conductors and clamping bars. The assembly is bolted together and heated to 193°C (380°F) to 204°C (400°F). The solder bond is ultrasonically inspected for voids after soldering. Bolts are torqued while the solder is liquid and after the joint has returned to room temperature. Self-locking helical coil inserts are used in the copper clamp bar to insure the bolts do not relax and maintain torque.

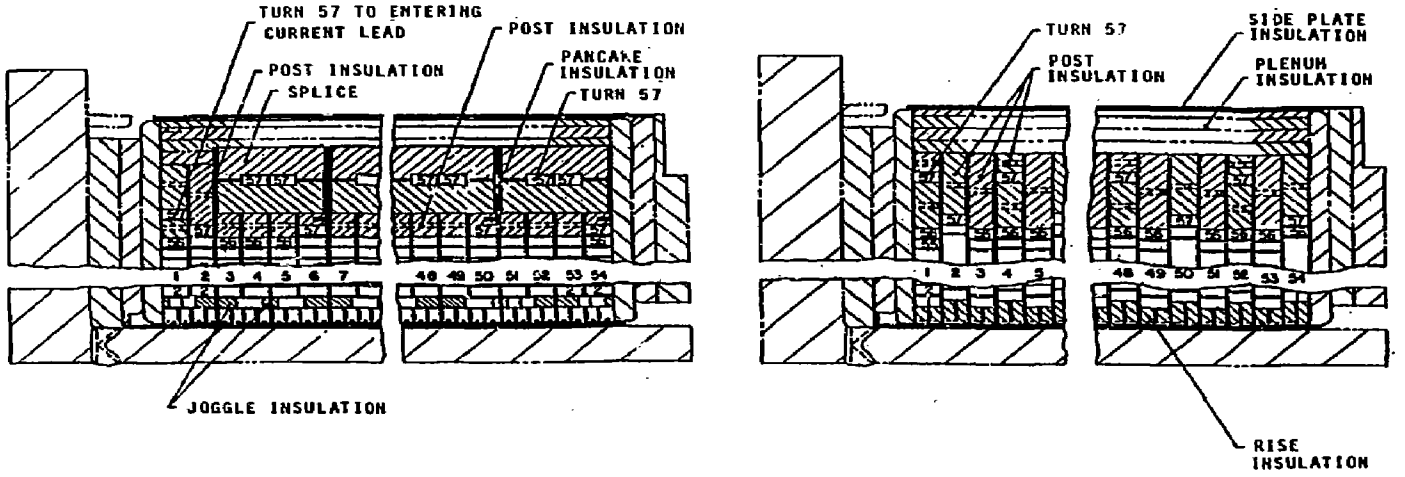

SECTION E-E

SECTION H-H

Figure 2-31. Coil Winding

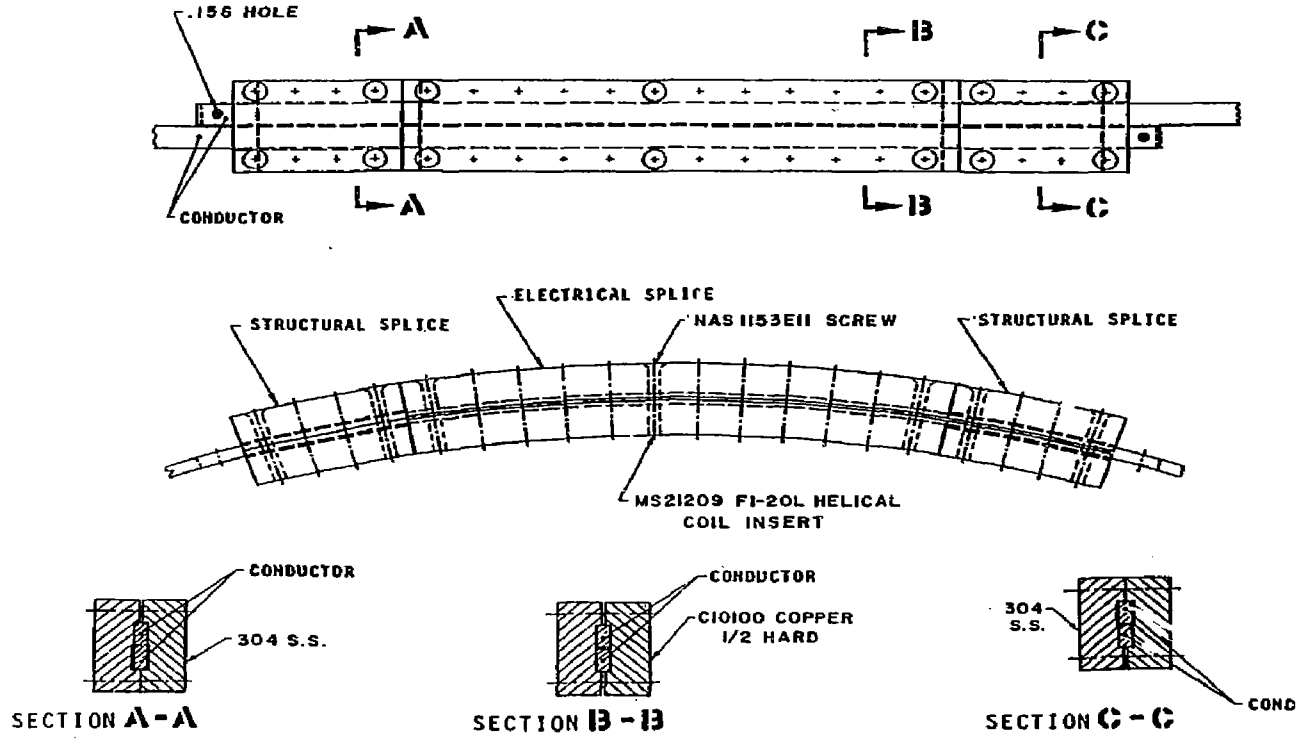

Figure 2-32. Conductor Splice Assembly

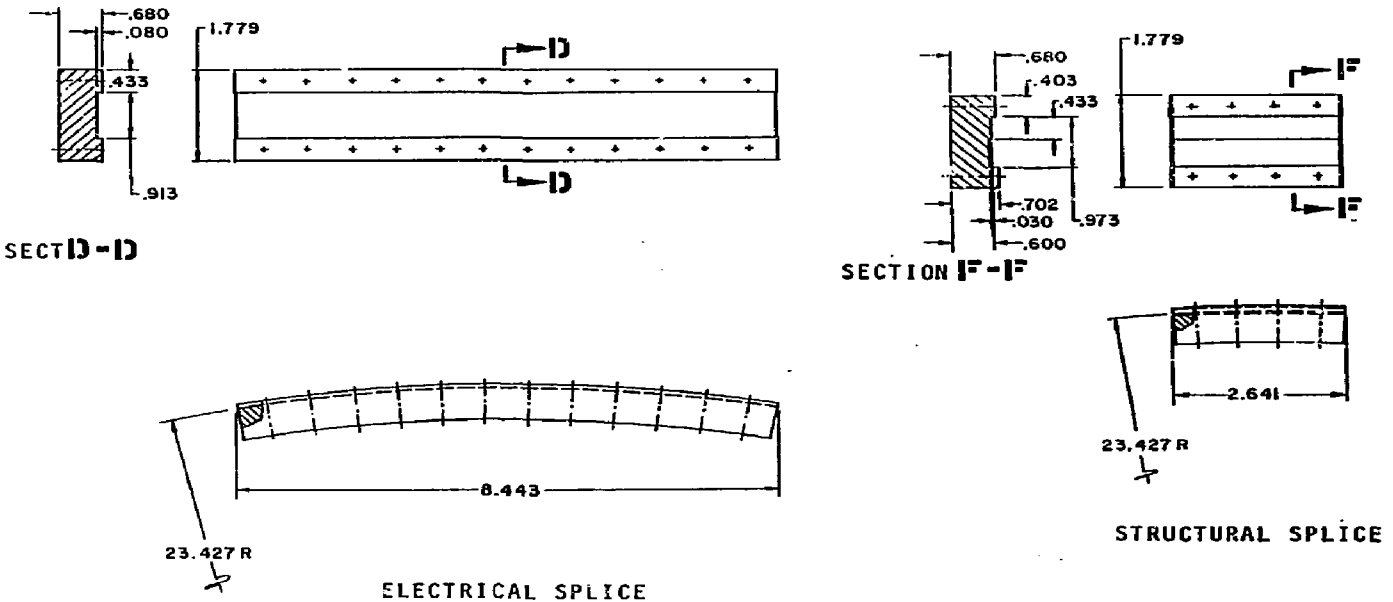

Figure 2-33. Conductor Splice Fittings

2.6.2 Structural Splice

Each structural splice consists of two 304-annealed stainless steel clamping bars 17.3 mm (0.68 in) thick by 45.2 mm (1.779 in) wide and 6.6 cm (2.6 in) long. Each clamping bar has slots for the conductors. One conductor slot is oversize, so the clamping bars hold one conductor. The structural splice on the other end of the electrical splice holds the other conductor. The structural splices are positioned against the electrical splice with no gap to minimize electrical splice load transfer. The fasteners are torqued to 50-55 inch-pounds.

2.7 Current Leads

The current leads consist of a two-piece machined copper stabilizer and an "A"-Cell, Grade I, NbTi superconductor. The two-piece copper stabilizer and superconductor are soldered together with 60 Sn/40 Pb solder. Figure 2-22 and 2-32 shows the current lead installation in the tunnel and in the coil. The copper stabilizer is C10100 OFE 1/8-hard copper and is machined in the flat. During installation in the tunnel and coil, the current lead is bent to the required shape.

2.7.1 Current Lead Splice to Coil

The current lead splice to the coil Nb_3Sn conductor is made outside of the coil winding pack. The splice consists of two parts, a structural splice and an electrical splice. Figures 2-34 and 2-35 show the splice installation of the current lead to the coil Nb_3Sn conductor. Both the entering and exiting lead splices are identical. The structural splice is made from 304 annealed stainless steel and consists of an inner and outer clamping bar. There is a slot in each clamping bar the width of the Nb_3Sn conductor. The conductor is placed between the clamping bars and the bolts are installed. The inner clamping bar, in turn, is bolted to the 9.53-mm (0.375-in) thick G-10CR side plate insulation which reacts the conductor tension load. The 9.53-mm (0.375-in) thick G-10CR side plate insulation is bolted to the case structure.

The electrical splice is incorporated in the end of the current lead copper stabilizer. The last 13.97 cm (5.5 in) of the copper has a machined slot to accept the Nb_3Sn conductor. There is a 13.97-cm (5.5-in) overlap of conductors and the joint is soldered. The end of the current lead is bolted to the 9.53-mm (0.375-in) thick G-10CR side plate insulation.

2.7.2 Current Lead Installation

The entering current lead is bent to shape and fit up before the start of coil winding. The holes in the side plate G-10CR and case are made and inserts are installed. The entering lead has two fiberglass hat sections in the tunnel area to hold the lead in

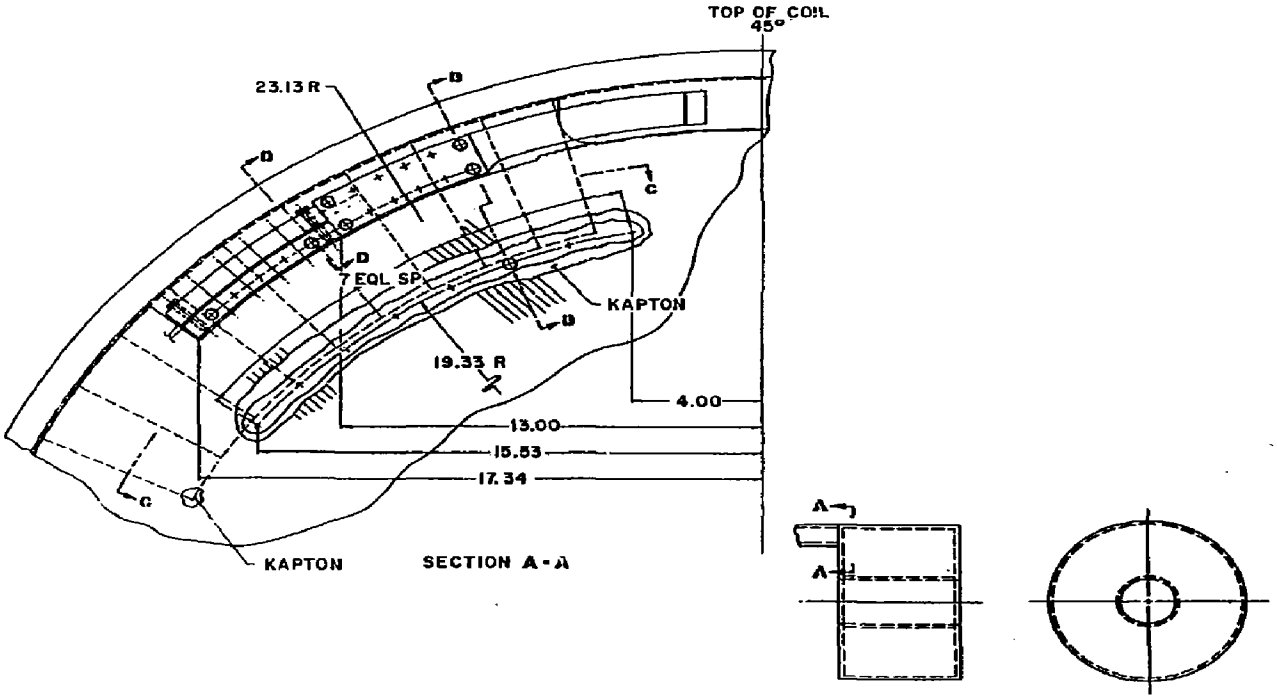

Figure 2-34. Splice Fitting Installation

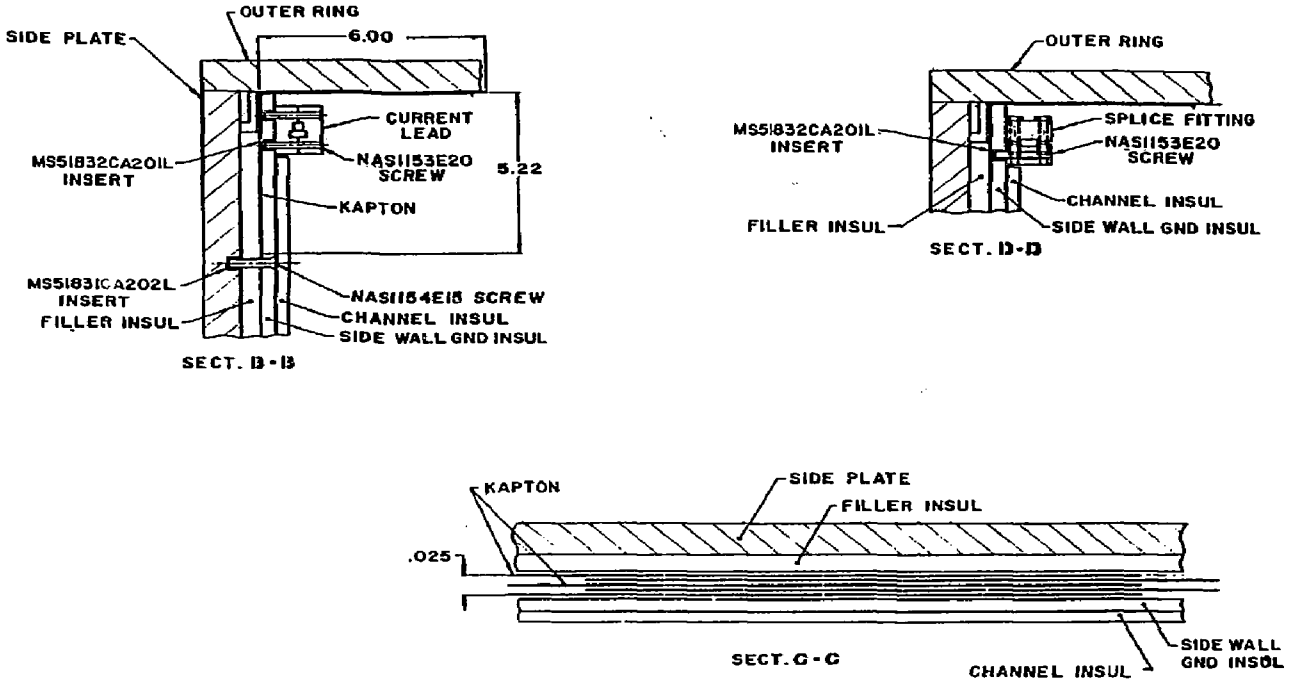

Figure 2-35. Splice Fitting Installation

place. There is a splice in the entering current lead at the stub stack to tunnel area. This splice is required since the current lead in the stub stack would get in the way when winding the coil. The exiting current lead is bent to shape and fit up after the coil is wound. The holes in the side plate G-10CR insulation and the case are drilled before the closeout side plate is welded to the coil winding form. Copper reinforcement bars are bolted to the current lead where it crosses the top of the coil and enters the tunnel. This reinforcement is required due to the tangential loads imposed on the current lead. The current lead sits inside a fiberglass channel which is lined with Kapton and polyurethane insulation. Two fiberglass hat sections support the lead in the tunnel area.

Each entering and exiting lead extends 15.24 cm (6 in) above the stub stack. The leads are supported in the stub stack by two 12.7-mm (0.50-in) thick G-10CR planks.

2.8 Voltage Tap Wire Runs

There is a voltage tap at each conductor splice in the coil and there are 26 pancake splices. The voltage tap is attached with a screw in to the copper splice bar portion of the splice. Figure 2-36 shows the voltage tap wire run assembly on the coil. There are voltage taps on both the left hand and right hand sides of the coil. Section A-A shows the voltage tap anchored at a screw in the splice. Section B-B shows the G-10CR housing which protects the voltage tap wire being secured by two screws. The voltage tap wires run in G-10CR fiberglass tunnels from the conductor splice up to the top of the coil. At the top of the coil, the tunnel, and the stub stack the wires run in a polyurethane tube which is covered with epoxy glass fabric sleeving.

2.8.1 Fiberglass Wire Runs

G-10CR sheets .79 or 1.57 mm (0.031 or 0.062 in) thick are bonded together to form tunnels to protect the voltage tap wires. Figure 2-37 shows the tunnel for a single wire and is located in the conductor splice area. The G-10CR sheets are bonded with 3M 3549 A/B urethane adhesive. The base or channel portion is attached with two screws to the conductor splice fitting, then the voltage tap wire is installed in the base. After the wire is installed, the tunnel cover is bonded to the base channel, forming a tunnel. There are 26 wire runs required at the conductor pancake splices.

The thirteen single voltage tap wires are joined into two wire bundles on each side of the coil. The wires are placed in the G-10CR channels, then routed to the top of the coil. Figure 2-38 shows the channels that run the wires to the top of the coil (upper piccolo area). The channels are made from sheets of G-10CR and are bonded together. A G-10CR cover is bonded to the channels after the wires are installed. This provides positive protection to the voltage tap wires.

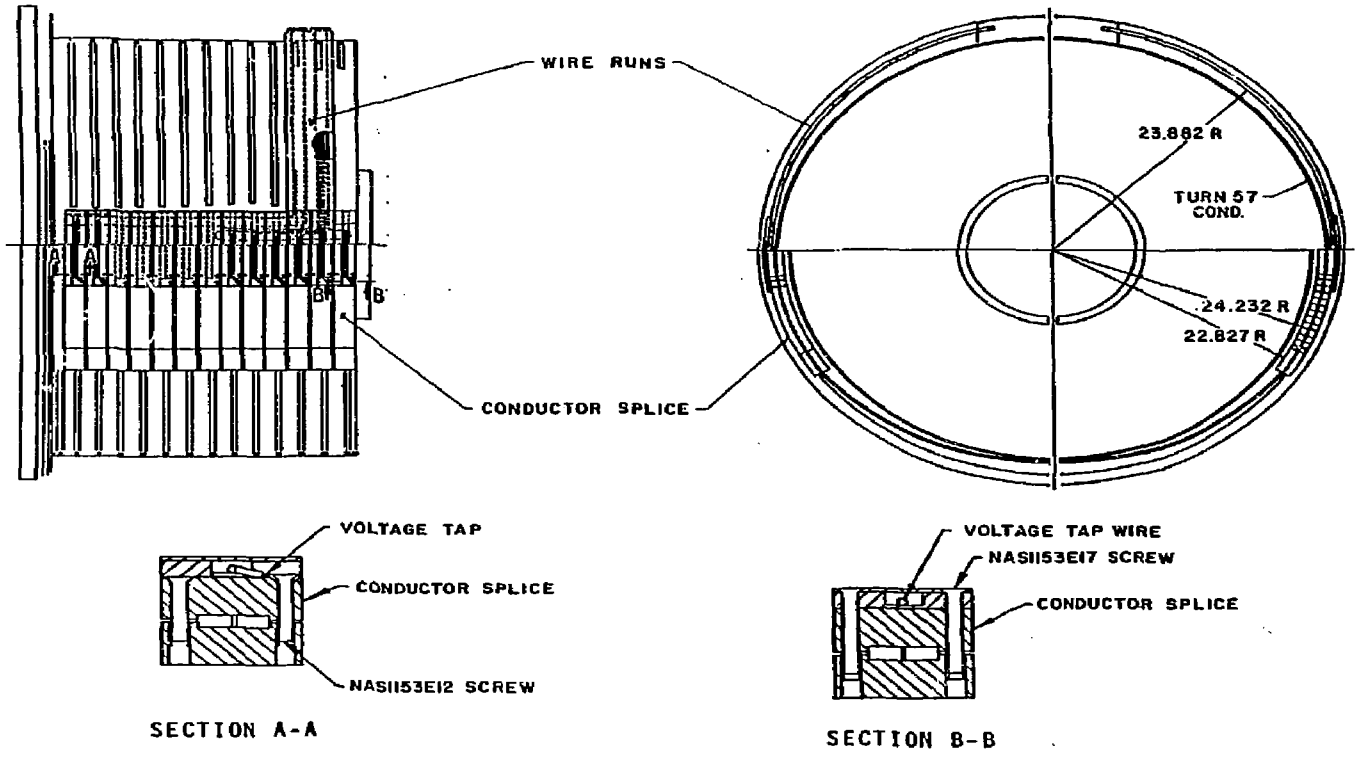

Figure 2-36. Voltage Tap Wire Assembly

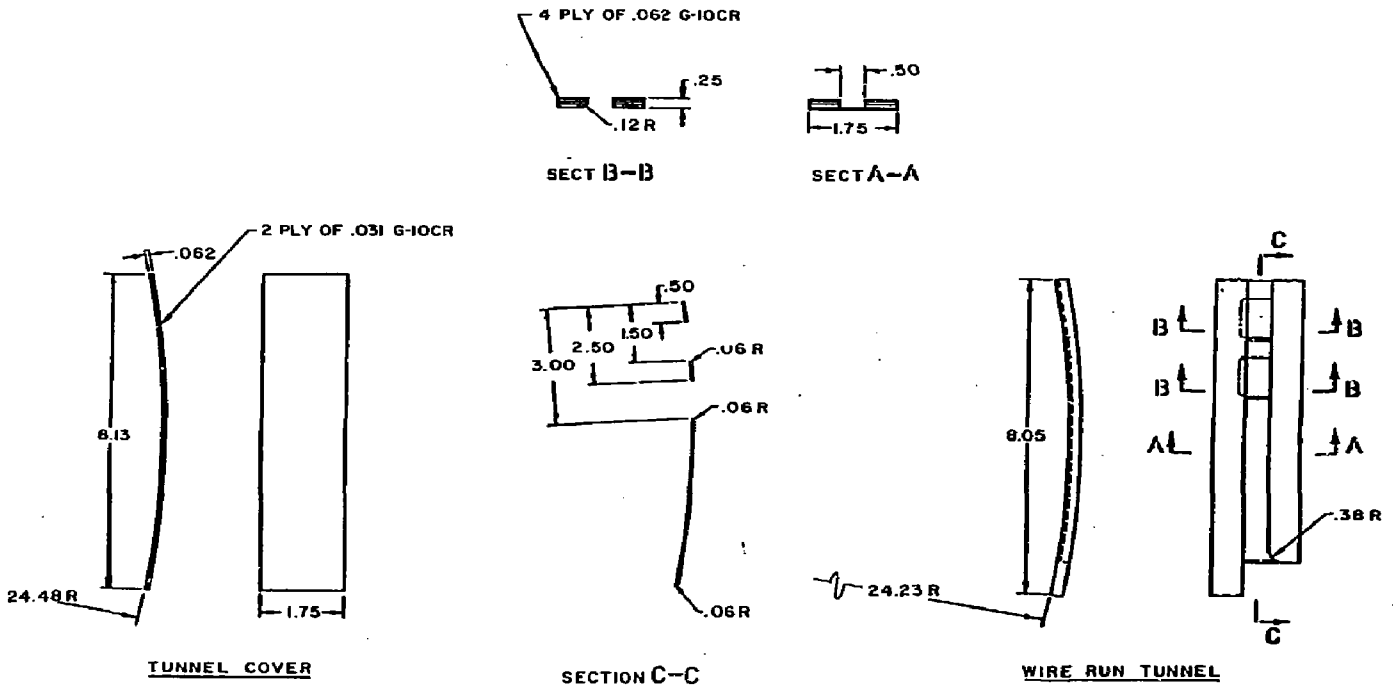

Figure 2-37. Voltage Tap Runs

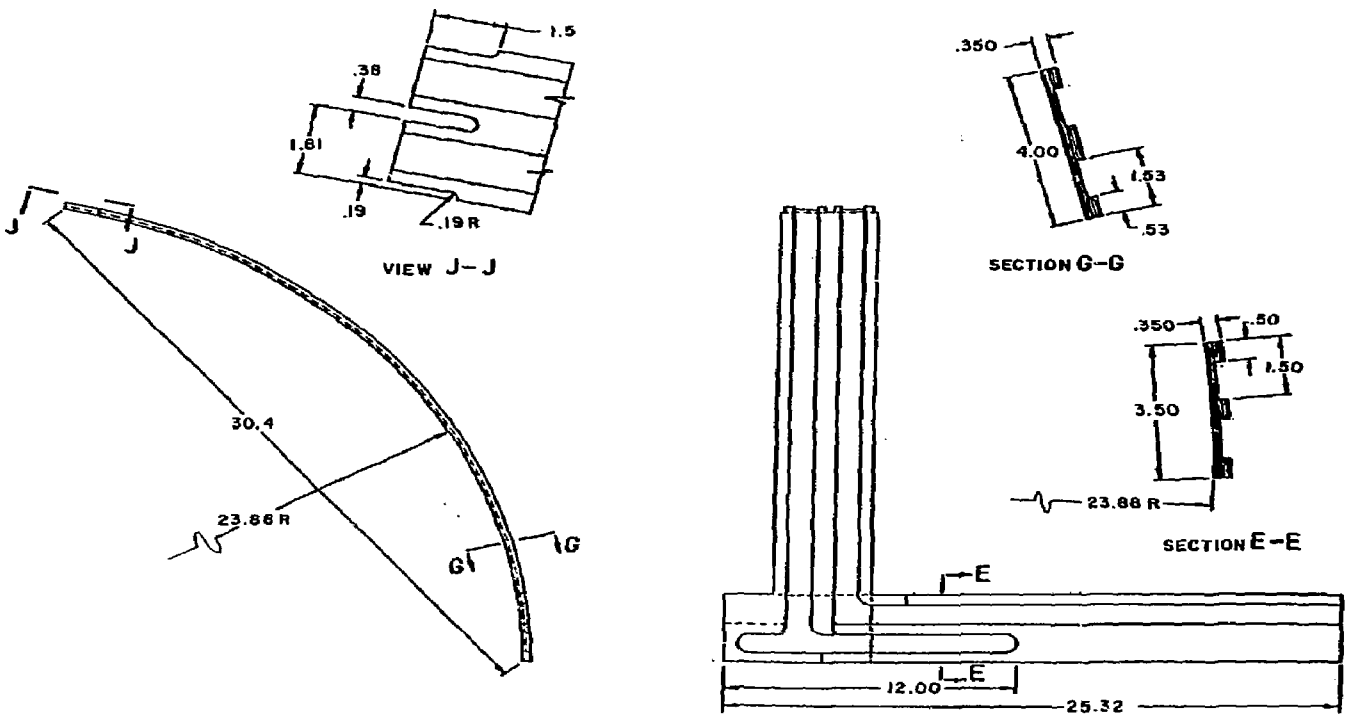

Figure 2-38. Voltage Tap Wire Runs

2.8.2 Tunnel Area Wire Runs

In the upper piccolo, tunnel, and stub stack area, the voltage tap wire bundles run in polyurethane tubing that is covered with glass fabric sleeving. The wire runs cannot go straight and have several bends. Figure 2-39 and 2-40 show the voltage tap wire runs and section cuts in the above area.

The braided glass fabric sleeving is installed over the polyurethane tubing. This sleeving has a 19-mm (0.75-in) inside diameter and is 1.57 mm (0.062 in) thick. The polyurethane has a 15.9-mm (0.625-in) outside diameter and a wall thickness of 1.57 mm (0.062 in). After the voltage tap wires are pulled through the tubing, the polyurethane tubing is bonded to G-10CR wire runs. The braided glass sleeving and tubing are routed through the piccolo, tunnel, and stub stack. The glass sleeving is pulled tight and will shrink to a tight fit on the tubing. Epoxy, Epon 815 and Versamid 115, is brushed onto the glass sleeving. Plastic sheet with a parting agent is put under the tubing before applying the epoxy. This is to prevent the epoxy accidentally being spilled into the coil. The plastic sheet is removed when the epoxy has cured. The glass sleeving and epoxy produces a rigid fiberglass tube when cured.

2.9 Coil Support System

The A2I coil is supported by the A20 coil. Figures 2-41 and 2-42 show the coil support system. There are twelve adjustable shims between the outer ring of the A2I coil and the inner ring of the A20 coil. The shims transmit vertical and side loads. The axial load adapter ring is welded to both coils and transmits axial (Z) loads.

2.9.1 Shim Assembly

The shims are made from 304L annealed stainless steel. The shim assembly consists of two pieces of tapered mating faces that provide an adjustment range of 8 mm (0.315 in) to 11.8 mm (0.465 in). Figure 2-43 shows the details of a shim assembly. The tapered portion of the shim assembly provides the bearing area for transmitting load.

After the A2I coil is aligned with the A20 coil, the shims are inserted between the coils and snugged down. Nuts are tightened on the studs to maintain the selected position. The shim next to the A20 coil is tack welded to the coil providing positive positioning of the shim.

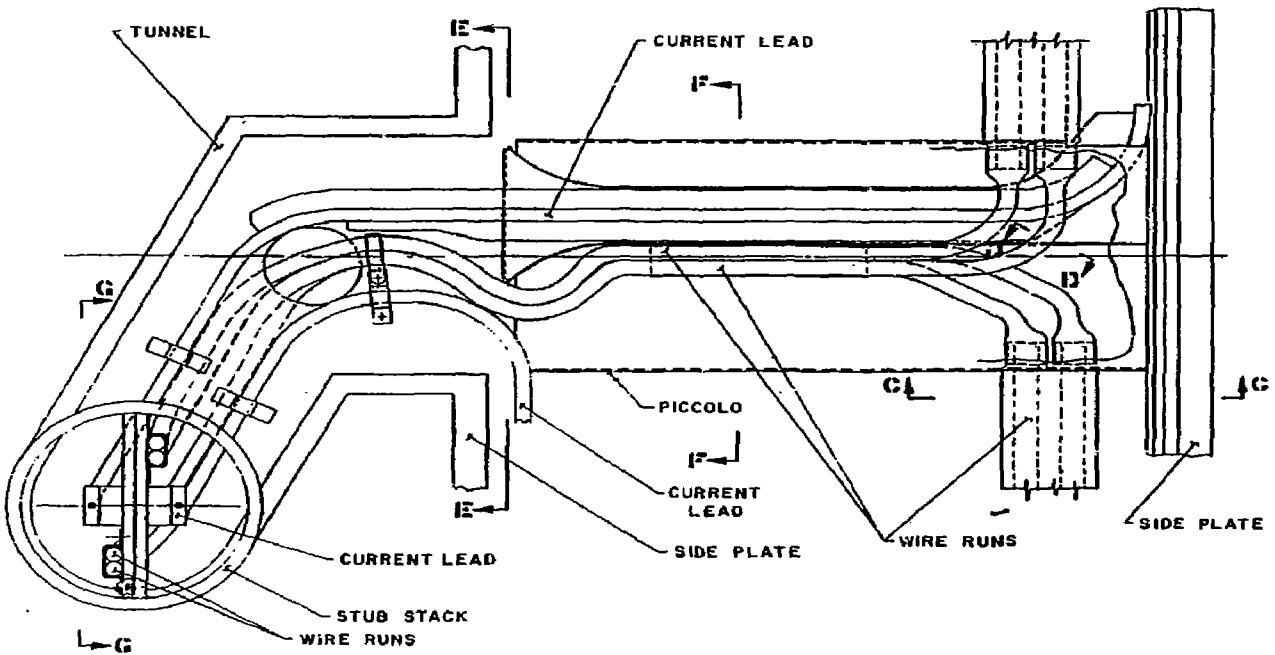

Figure 2-39. Voltage Tap Wire Runs

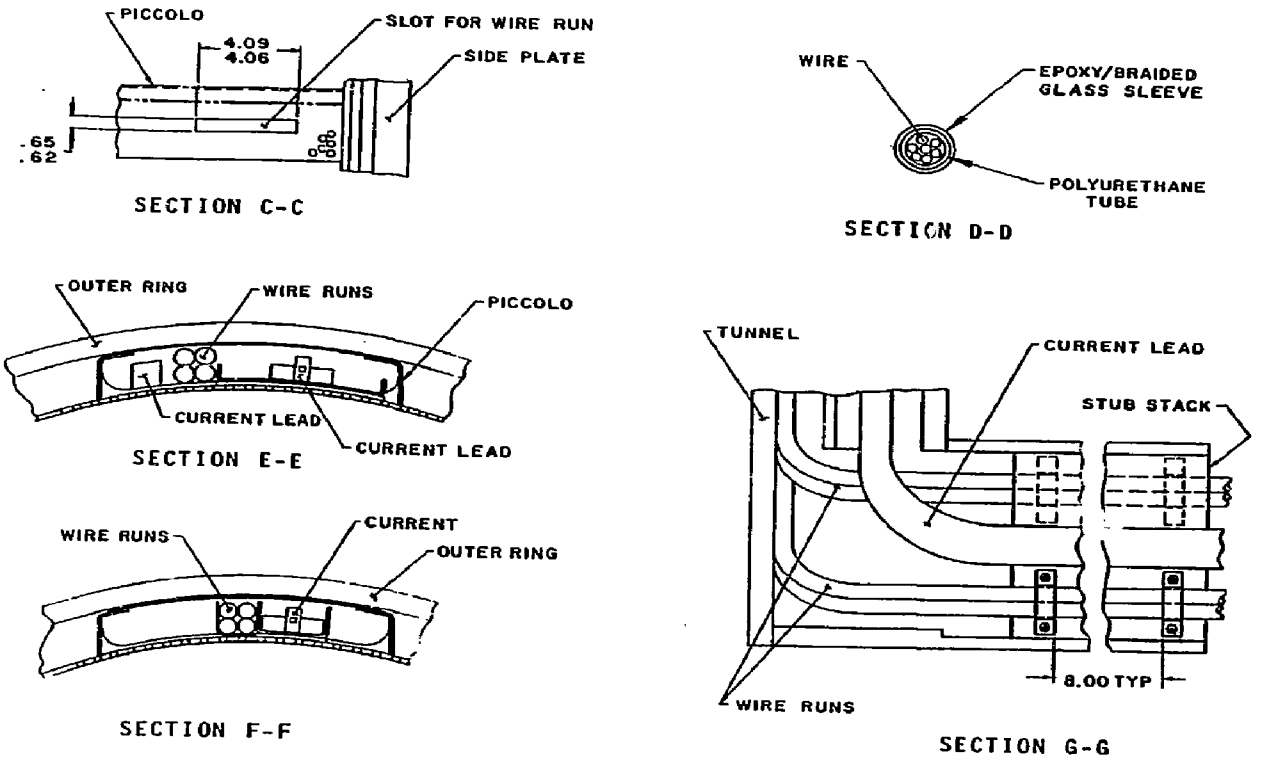

Figure 2-40. Voltage Tap Wire Runs

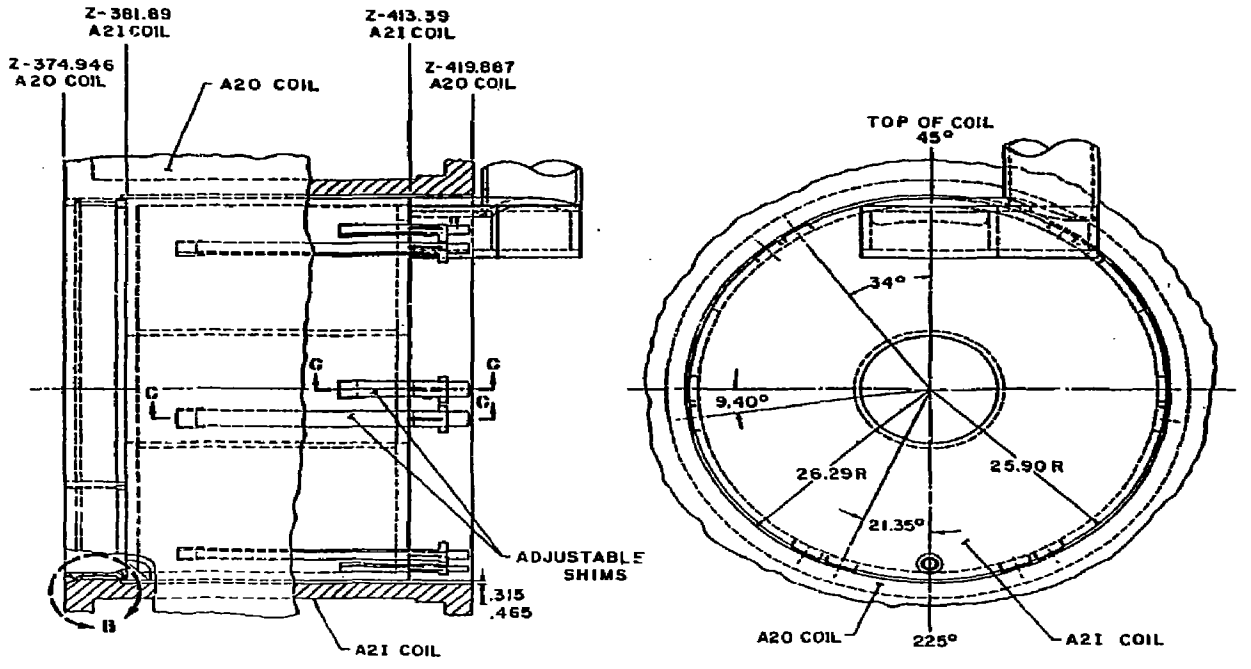

Figure 2-41. Coil Support System

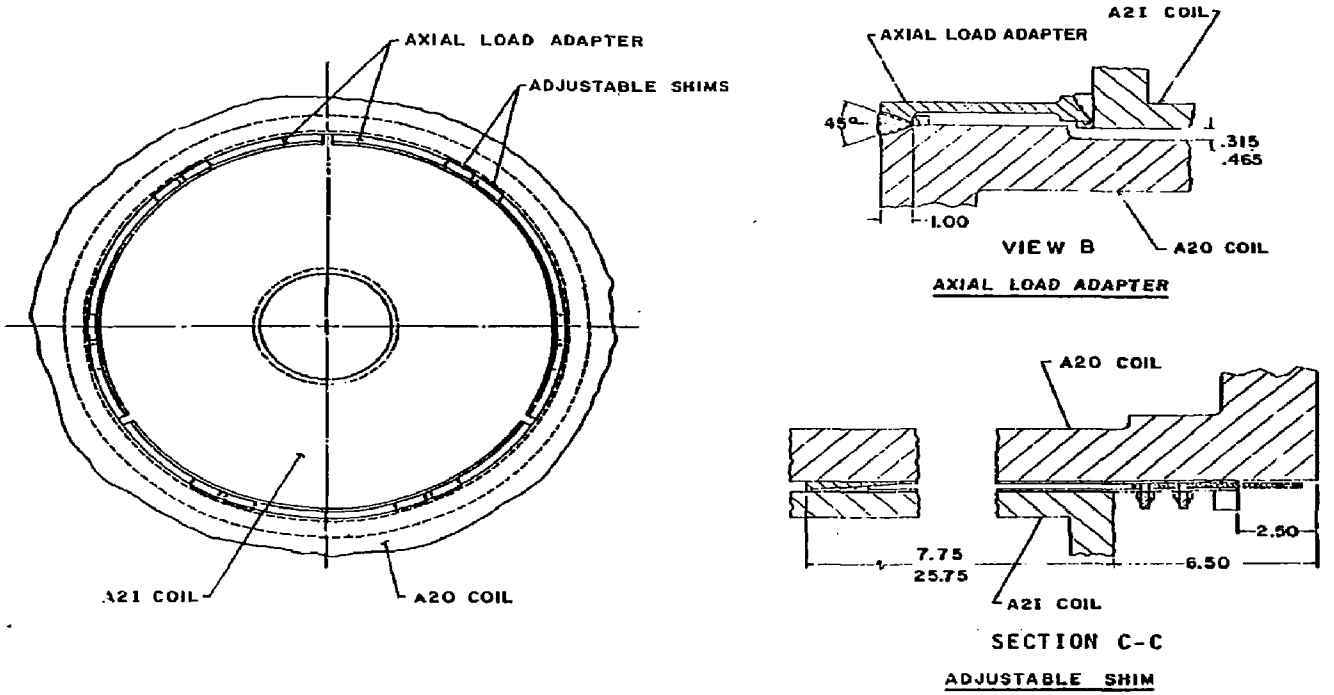

Figure 2-42. Coil Support System

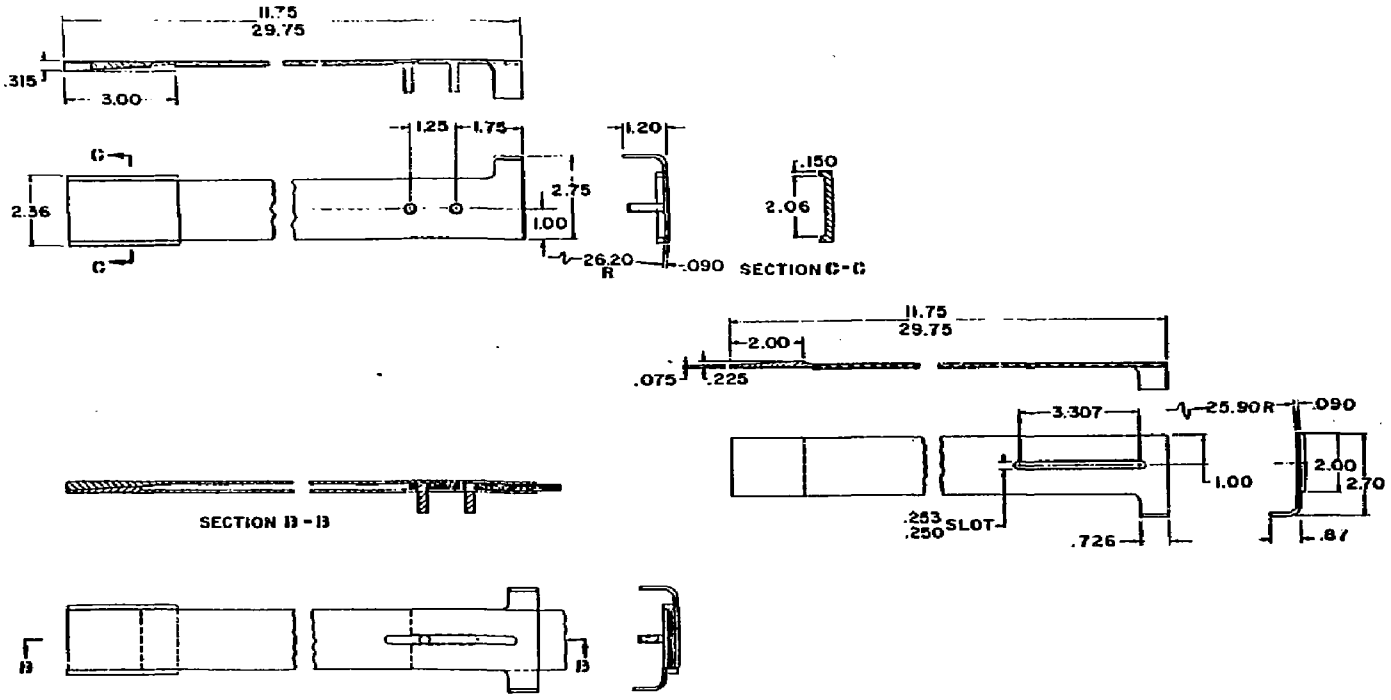

Figure 2-43. Shim Assembly

2.9.2 Axial Load Adapter

The axial load adapter is in three pieces and is 304LN annealed stainless steel. Figure 2-44 shows one of the three identical adapter segments. The adapter is welded to the A2I coil and the A2O coil after the shims are installed.

2.10 Coil Weight

The A2I high field insert coil weight is shown in Table 2-1.

2.11 Drawing Tree

The drawing tree for detail design of the MFTF Nb_3Sn high field coil is in Appendix C.

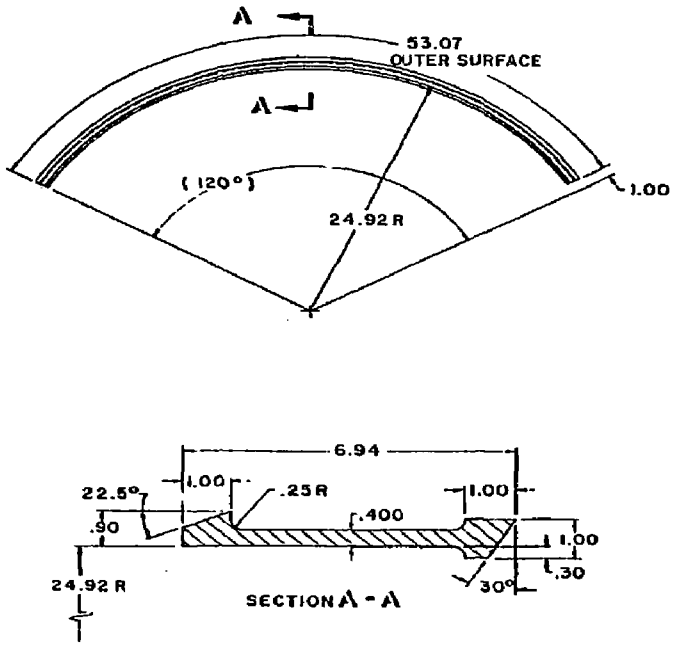

Figure 2-44. Axial Load Adapter

TABLE 1. RELATIVE ADVANTAGES/DISADVANTAGES OF THE THREE CANDIDATE CONDUCTORS HAVE BEEN IDENTIFIED:

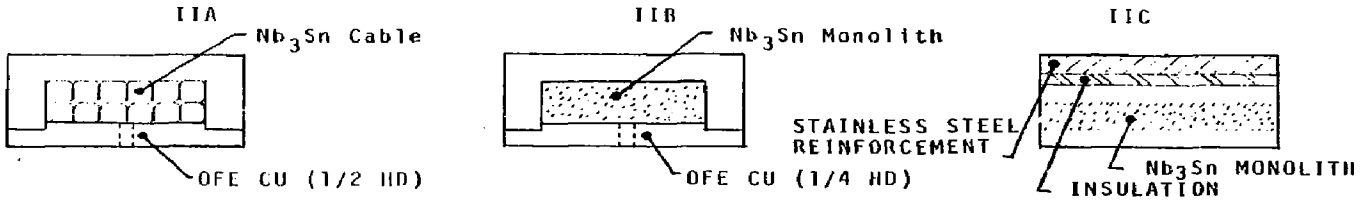

ADVANTAGES

- Cabling eliminates anisotropy.
- 1/2 hard stabilizes reacts hoop forces.
- Relatively easy to wind.

- Monolithic insert improves structural integrity.
- 1/4 hard stabilizes reacts hoop forces.
- Relatively easy to wind.

- Least risk for superconductor vendors.
- Eliminates solder operation. operation.

DISADVANTAGES

- Reacted cable is prone to damage.
- More difficult to solder than IIB.
- Soldering operations induce risk of damage.

- Difficult to solder
- Soldering operations induce risk of damage.

- Greater potential impact of A2 outer and A1 coils due to reduced current density allowable.
- Relatively more difficult to co-wind stainless-steel.
- Greater technical risk.

Table 2-1. High Field Coil Weight Summary

Item	Weight Pounds
Case Structure	3,205
Tunnel Structure	450
Conductor and Leads	8,811
Conductor Splices	202
Insulation	892
Coil Support Structure	216
Total Weight of One Coil	13,776

The vertical stack structure, stack leads, insulations, and vapor-cooled leads are not included in coil weight.

3.0

MATERIALS CONSIDERATIONS

3.1 Selection of Materials

Materials selected for various components of the high field Nb_3Sn insert coil are:

(i) 304LN stainless steel for magnet case structure. 304 stainless steel for conductor structural splice. A-286 iron-base superalloy is used for bolts, screws, nuts, and inserts. Monel is used for rivets.

(ii) Nb_3Sn (Ti-modified) monolith superconductor manufactured by Furukawa Electric Company, Japan.

(iii) C10100 OFE copper stabilizer housing for the conductor and conductor electrical splice.

(iv) 60 Sn/40 Pb solder for associating stabilizer to the superconductor monolith.

(v) G-10CR fiberglass-epoxy and multilayer Kapton for electric insulator.

(vi) The following adhesive systems for bonding electric insulators, temperature sensors, strain gages to the structure, and fiberglass to fiberglass.

(a) Epoxies

1. Micro Measurements AE-10
2. Dexter Hysol EA 934.
3. Epon 828 with hardening agent Z.

(b) Polyurethanes

1. PR 1660 L.
2. 3M 3549 A/B.

(c) Cyanoacrylates

1. Permabond 102.

The 304LN stainless steel and the Nb_3Sn monolith superconductor with copper stabilizer have been selected in close consultation with LLNL, who has also performed the verification testing of the conductor as per the requirements of the MFTF Design Requirements Document, Reference 3-1. The G-10CR fiberglass epoxy and the multilayer Kapton insulation meet the requirements of Reference 3-1. It is expected that the organic insulators and adhesive systems will maintain their mechanical and physical integrity for the life of the MFTF system.

3.2 Radiation Considerations

The radiation environment of the MFTF-B magnet system is most severe in the axicell insert coil region. The inboard case receives the maximum neutron flux and the inboard insulation the most radiation dose. For the MARS operating mode, the absorbed dose in the inboard insulation is 133 rads/plasma-second with a corresponding neutron flux of 1.6×10^{11} n/cm^2/plasma-second. The neutron flux in the inboard case region is 1.7×10^{11} n/cm^2/plasma-second. Based on an actual plasma turn-on duration of 3000 plasma-seconds per week and a 13/18 week cycle, the cummulative radiation dose in the inboard insulation over a period of 10 years would be 1.3×10^8 rads with a corresponding neutron fluence 1.7×10^{17} n/cm^2 or an approximately 2×10^{-4} dpa (displacements per atom) maximum radiation damage in the metallic material of the structure, superconductor or the stabilizer. The maximum radiation damage in metallic materials over one thirteen week period would be approximately 8×10^{-6} dpa. These radiation levels would have negligible effect on the mechanical and physical properties of the structural material.

The critical parameters of the Nb_3Sn superconductor would not be affected to any significant degree by these radiation levels. The electrical resistivity of the copper stabilizer will increase by 0.5 nano-ohm-cm maximum as a result of irradiation over one thirteen week period and 90% of it would anneal out during the subsequent warm up of the magnet system to room temperature (Ref. 3-2). The total increase in radiation related stabilizer resistivity over ten year period is not expected to exceed 1.5 nano-ohm-cm which is a very small fraction (~2%) of the unirradiated resistivity of the stabilizer. The G-10CR fiberglass epoxy is expected to retain better than 85% of the unirradiated flexure and compression strengths and almost 100% of the unirradiated dielectric properties (Ref. 3-3). The effect of radiation and the cryogenic environment on the performance of various adhesive systems is not well known and as described below, only a rough estimate of their anticipated behavior can be made at this time.

3.3 Anticipated Performance of Selected Adhesive Systems

A literature search (Ref. 3.4-6) was conducted and the following information has been compiled about the anticipated performance of the selected adhesive systems irradiated to 2×10^8 rads at liquid nitrogen or liquid helium temperatures.

3.3.1 Epoxy (Unfilled): AE-10 (Micro Measurements)

Epoxy adhesives exhibit good resistance to irradiation at 2×10^8 rads. However, their properties at cryogenic temperatures are lower than at room temperature. Therefore, unfilled epoxy adhesives should be expected to have approximately 80% strength retention after irradiation at cryogenic temperatures.

3.3.2 Epoxy (Filled): EA 934 (Dexter Hysol Co.)

Epoxy adhesives containing fillers exhibit greater resistance to damage by irradiation than unfilled systems. This adhesive being filled is expected to exhibit high property retention after irradiation at cryogenic temperatures, in excess of the 80% anticipated for unfilled epoxy.

3.3.3 Polyurethane : PR1660L (Product Research & Chemical Co.)

Based on available data on irradiation of APCO 1252 (Ref. 3- ,, polyurethanes at room temperatures as well as liquid nitrogen and liquid hydrogen temperatures, properties such as tensile shear will be higher after exposure than initial values obtained at room temperature with no irradiation.

3.3.4 Cyanoacrylates: Permabond 102 (Permabond International)

Effects of irradiation and cryogenic temperatures on this type of adhesive are unknown. Since this adhesive is of the methyl acrylate polymer family, which is degraded by irradiation, it is expected to retain approximately 50% of its initial properties after exposure. LLNL's test on Loctite-414 (a compound similar to Permabond 102), bonded G-10CR buttons did not disbond on irradiation to 3×10^8 rads at cryogenic temperatures.

3.4 Activation of Materials

The structural material (304LN stainless steel) and the superconductor (Nb_3Sn with Ti, and Nb diffusion barrier), were selected primarily to meet structural and superconductor requirements and as such have constituents that activate strongly and have products with long radioactive half-lives. Ni, Ta and Nb are some of these elements. Both Ag and Au present in the form of plating on instrumentation cables and connector pins, can get activated and contribute to the radiation dose. Au^{198} has a short half life (28 days) and Ag^{109} a half-life of 253 days. The concentration of Ag in the instrumentation cable assembly is of the order of 1-2 mg/c.c. and can result in a contact dose rate of 1-2 mr/hr at the concrete wall location (Ref. 3-7). The background radiation dose at this location is also 1-2 mr/hr, and therefore no significant concern.

REFERENCES

3-1 "MFTF Design Requirements Documents" published by Lawrence Livermore National Laboratory; dated 17 August 1982 (revised 20 May 1983).

3-2 Klabunde, C.E., & Coltman Jr., R.R. "Fission Neutron Damage Rates and Efficiencies in several metals", J. Nucl. Matls 108 & 109 1982, pp. 183-193.

3-3 Hurley, G.F. Fowler Jr., J.D., Liepins, R., Jorgensen, J., and Hammond, J. "Comparison of Neutron and Gamma Radiation Damage in Organic Insulators", DAFS Quarterly Progress Report. April - June 1982, DOE/ER-0046/10, August 1982, p. 53-73.

3-4 Goetzel, C.F., Rittenhouse, J.B., and Singletary, J.B., "Space Materials Handbook", Addison Wesley Publishing Co. (1985) pp 303-313.

3-5 Bolt, R.O., and Carroll, J.C., "Radiation Effects on Organic Materials", Academic Press (1963), Chapters 6 and 10.

3-6 Houwink, R., and Salomon, G., "Adhesion and Adhesives", Elsevier Publishing (1967) pp 33.

3-7 Muelder, S., LLNL, Private Communication.

4.0

STRESS ANALYSIS

4.1 DESIGN CRITERIA

The Design Requirements Document (DRD, Ref. 4.1) provided by LLNL, outlines basic considerations for safety factors, loads to be evaluated, and other structural requirements. The LLNL guidelines were adapted and expanded upon by General Dynamics. The MFTF design criteria was orientated to conform to the ASME Pressure Vessel Code with the intent of providing equivalent provisions for the safety of personnel and hardware. This was necessary because today's Pressure Vessel Code is not fully adaptable to the unique problems associated with designing magnets.

Safety margin calculations are divided into room temperature (RT) conditions and 4K (-452°F) conditions. The need for separate calculations is due to the enhanced 4K material strength properties which are taken advantage of in the design of magnets. In addition, electromagnetic loads are divided into normal conditions and abnormal conditions as presented in Table 4-1. Abnormal conditions are low probability electrical fault events for which reduced safety factors are utilized. The magnet is designed to survive an abnormal condition, but applied stresses may be as high as the engineering yield stress. There is also a category known as disaster conditions for which design is impossible. Events such as open/short circuits at any coil terminal or low resistance intra-turn shorts could cause runaway load increases - these conditions are prevented by good design and fabrication quality; the actual structure could never be expected to carry the resulting loads without some level of damage.

For the Nb_3Sn coil, close inductive coupling exists between A2O and A2I. Electrical fault load analysis has shown that certain unusual (low probability) events can cause excessive current peaking in the Nb_3Sn coil. These events are not designed for, but rather, redundency in the A2I protection system prevents their occurrence. The worst design condition for A2I is defined in the DRD, which limits A2I current peaking to 115 percent of normal operating current.

4.2 MATERIAL PROPERTIES

To calculate structural safety margins and to predict deflections, basic material properties are needed. For MFTF, all magnet cases are made up of 304LN stainless steel using E316L weld wire at joints. The RT and 4K properties of steel and other magnet materials are listed in Table 4-2.

Generally, these numbers represent average values and do not reflect any sort of statistical basis. One exception is the 304LN stainless steel where the material specification calls out the listed numbers as minimum requirements. Each plate used for MFTF has a 4K yield and ultimate test run to verify compliance. If the 4K yield strength is unusually high, then 4K fracture toughness tests are also run to verify compliance. The weld wire used for MFTF must qualify to minimum strength and toughness requirements. A large data base has been compiled to date, the materials selected for the magnet case generally adhere to specified strengths. Discrepant material has been dispositioned on an individual basis.

Table 4-1. Loads on the MFTF-B Magnets are Composed of a Combination of Various Effects

INDIVIDUAL LOAD CONDITIONS		
CATEGORY	LOAD CASE	LOAD CONDITION
ELECTRO-MAGNETIC	1	NORMAL OPERATION
	2	INDIVIDUAL FAULT CONDITIONS & TRANSIENTS
	3	TRIM COIL LOADS
THERMAL	4	RESIDUAL COOL-DOWN (R.T. TO 4.2K)
	5	QUENCH (PACK LOCALLY WARM)
	6	COOL-DOWN/WARM-UP (GRADIENTS)
OTHER	7	INTERNAL PRESSURE (QUENCH)
	8	GRAVITY DEAD LOAD
	9	SEISMIC EXCITATIONS
	10	WINDING LOADS

LOAD COMBINATIONS		
CATEGORY	LOAD CASE	LOAD CONDITION
4.2K OPR.	11	1 + 3 + 4 + 8
	12	2 + 3 + 4 + 8
SEISMIC	13	8 + 9 (AT ROOM TEMP)
	14	11 + 9 (AT 4.2)
	15	12 + 9 (AT 4.2)

- ELECTROMAGNETIC LOADS ARE THE PRIMARY STRUCTURAL DESIGN DRIVERS FOR THE MAGNETS
- COMBINED LOADING CONDITIONS ARE EXAMINED IN THE MANNER SHOWN.

Table 4-2. Material Properties Used for MFTF-B are Based on Test Data and are Mutually Agreed Upon by GDC/LLNL

MATERIAL	CONDITION	USAGE	MODULUS-MSI		CTE (RT-RK) 10^{-6} IN/IN/°F	YIELD-KSI		ULTIMATE-KSI		4K TOUGHNESS K_{IC} KSI $\sqrt{IN}$
			RT	4K		RT	4K	RT	4K	
304LN STAINLESS	ANNEALED	ALL MAGNET CASES CLEVII, TURN-BUCKLES	28.	30.	5.9	35.	100.	80.	170. ST 200. L LT	200. (BUT USE 120.)
WELDS E316L	AS WELDED	ALL MAGNET CASES	--	30.	--	50.	100.	70.	150.	120.
OFE COPPER	--	Nb_3Sn Stabilizer	17.	18.	6.2	31.	37.	34.	66.	--
FIBERGLASS EPOXY G-10CR	CURED	INSULATION WARP FILL NORMAL	4.3 3.9 2.0	5.0 4.8 3.2	4.5 5.1 14.0	-- -- --	-- -- --	60. 43. -61.	125. 78. -109.*	--
EPON 828 VERSAMID 115 30% 1/4" FIBERS	CURED	COIL FORM TRUE-UP	--	1.2	~29.0	--	--	--	34.*	--
EPON 815 VERSAMID 125 50% 1/32" FIBERS	CURED	COIL FORM TRUE-UP	--	1.7	~29.0.	--	--	--	-38.*	--

* COMPRESSION ONLY ALLOWABLES

Another quantity specified as minimum is the RT yield strength of the copper housing for the conductor. In the Nb_3Sn conductor specification (Reference 4-2), the 0.2 percent offset minimum RT yield strength is given as 31 ksi. Using test data generated at General Dynamics, this value is enhanced to 37 ksi when the copper is cooled to 20K. The strength characteristics of the combined conductor are developed in the verification test program (Section 8.0).

4.3 LOADS AND LOAD COMBINATIONS

Loads on superconducting magnets are made up of various effects, Table 4-3 presents basic loads plus compatible combinations of these loads for MFTF. When the facility is at room temperature, the only expected loads are dead weight combined with seismic events.

As a magnet is being slowly cooled to 4K, uneven temperatures are inevitable due to variation in plate thicknesses, materials, and accessibility to coolant. Thus it is necessary to evaluate time slices of the cool-down process to determine if maximum thermal gradients in the magnet cause excessive thermal stresses. Once fully cooled to 4K, certain residual stresses are retained due to differences in the coefficients of contraction between the primary materials of steel and copper. These residual stresses add to basic operating loads, or act as preloads which are relieved as opposing electromagnetic forces are applied. However, these residual stresses are usually very small.

After all magnets are cooled down, the electrical current is slowly applied and Lorentz forces are developed. Generally, electromagnetic loads are the major design driver. A single fault condition is based on a 15 percent current peaking factor. This value is defined in the DRD (Ref. 4-1). It is assumed that an equivalent field peaking accompanies the current increase, thus mechanical radial loads increase by a factor of $1.15^2 = 1.32$ for fault conditions.

Another condition of interest is internal pressure buildup in the coil due to a quench. Under worst conditions, dump valves fail to open, burst disks do not burst, and several magnets simultaneously quench through the same manifold system. A maximum pressure buildup is calculated by the thermal group and is superimposed on basic operating loads. For high field coils, this pressure is usually small (<102 psi) compared to electromagnetic pressure, but does design piping attached to the magnet.

Both the Kelley mode and Mars mode loading conditions are studied in this report. The axial electromagnetic loading on the coil is not symmetrical. The variation of load is primarily a result of the proximity effect of coil T1. The maximum load condition being at the location where the T1 coil is closest to the A2O/A2I coils. This highest load condition is assumed to be acting uniformly around the circumference of the magnet case for 2-D analysis purposes (conservative). A summary of the loading follows:

Table 4-3. Design Criteria Reflects LLNL Specification Requirements and General Dynamics Requirements for Proven Safety Factors

- THE DESIGN STRESS FOR STRENGTH ANALYSIS IS BASED ON:

ITEM	NORMAL OPERATION (HIGH PROBABILITY)	ABNORMAL OPERATION (LOW PROBABILITY)
Membrane stresses, σ_m	2/3 yield	100% yield
Bending stresses, σ_b	90% yield	100% yield
Membrane + Bending	$\sigma_m + 0.741\ \sigma_b \leq 2/3$ yield	$\sigma_m + \sigma_b \leq$ yield
Ultimate stress, magnets	1/2 tensile ultimate	60% ultimate
Ultimate stress, supports	33% tensile ultimate	60% ultimate
Seismic stress	120% of above allowables	100% of above allowables
Stress Cycles	At least 4 x operating cycles	

- MAXIMUM ALLOWABLE FOR CONDUCTOR STRAIN IS 0.70%. GOAL IS TO MAINTAIN A SAFETY FACTOR OF 1.75 (i.e., WOULD LIKE OPERATING STRAIN $\epsilon \leq 0.40\%$).
- FOR BUCKLING ANALYSIS, A FACTOR OF SAFETY OF 4.0 IS SELECTIVELY APPLIED TO APPROPRIATE AREAS IF END CONDITIONS, ETC. ARE NOT PRECISELY DEFINED FOR A GIVEN COMPONENT WHICH IS UNDERGOING COMPRESSION. OTHERWISE, USE BUCKLING FACTOR = 2.0.

	Kelley Mode (1)		Mars Mode (2)	
	"Worst Normal"	Abnormal	Normal	Abnormal
Axial Load, Lbs.	255,360	377,416	-238,560	-282,017
Lb/Cir in.	1,619	2,393	-1,513	-1,788

(1) Acting on side away from attachment to A20.

(2) Acting on side that is attached to A20.

4.4 STRESS ANALYSIS

4.4.1 Nb_3Sn Conductor Analysis

The Nb_3Sn coil has a pancake winding with 54 pancakes and 57 turns per pancake.

STANSOL computer program (Ref. 4-3) was used to model a single pancake (57 turns) as shown in Figure 4-1. The model included the bobbin, first layer of insulation, and 57 turn/insulation layers. The conductor pack is assumed to be self-supporting (i.e. the outer ring is ignored when evaluating conductor stresses and deflections). A radial modulus of 0.3 MSI was assumed (based on tests of the radial stiffness of the MFTF-B solenoids and yin-yang coils). An effective hoop modulus was developed considering the initial strain state (due to conductor loading) and the σ-ε curve of the copper conductor.

The conductor cross-section is also shown in Figure 4-1. A monolithic, strain-sensitive, multi-filament Nb_3Sn conductor is used. A copper housing is incorporated to enhance the cryostability and to provide structural support for the monolith. The conductor is wound such that the electromagnetic forces are reacted by the U-Section.

Table 4-4 gives a listing of various strain-inducing components on the conductor. The electromagnetic loading is a major loading condition for the conductor. The loading is a function of both the axial and radial field data. The axial field component generates radially outward Lorentz Forces from $\overline{F} = i \times \overline{B}$. The axial field in the conductor pack is maximum in the mid-pack region at the inner bore as illustrated in Figure 4-2. This figure illustrates decreasing field with increasing pack radius.

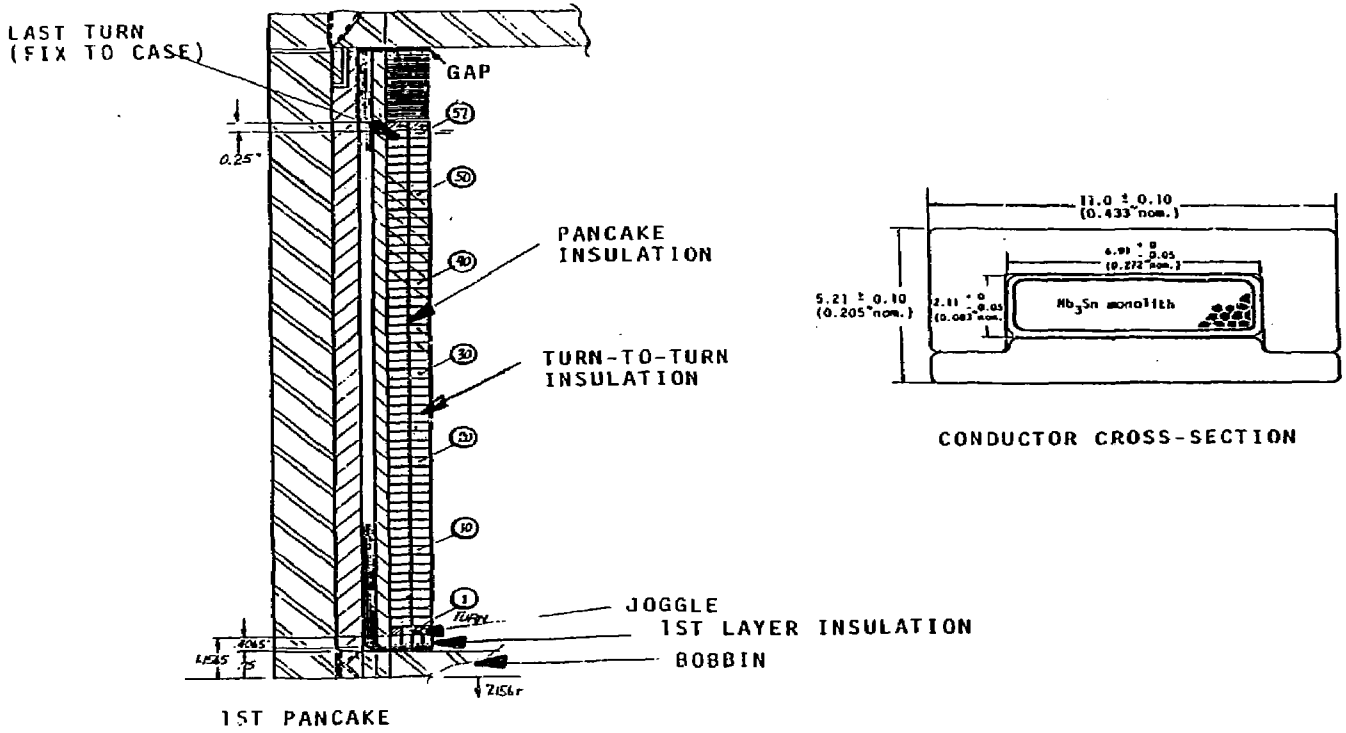

Figure 4-1. High Field Insert Coil Conductor Pack is Pancake Wound and is Designed to be Self-Supporting

Table 4-4. All Strain-Inducing Components on the Conductor Monolith must be Accounted For

*	•	ELECTROMAGNETIC LOADING (UNIAXIAL)
	•	STRAIGHTENING FROM THE REACTED DIAMETER (60, 70 AND 80 CM) (BENDING)
	•	WINDING ON BOBBIN (BENDING)
*	•	WINDING PRELOAD (300, 400, 500, AND 600 LB TENSION) (UNIAXIAL)
	•	JOGGLE BENDING (IN BOBBIN REGION)
	•	PACK MOVEMENT EFFECTS AT THE FIX T$_o$ THE CASE (FIRST AND LAST PANCAKE AT OUTER TURN) (BENDING)
*	•	COOL-DOWN EFFECTS (UNIAXIAL)

* Legend: Loading input into STANSOL model, other effects calculated by hand.

Ordinarily, a solenoid coil shows a direction change in axial field near the outer diameter of the coil. However, the data shown here (Figure 4-2) for A2I includes the background field from the outer coil, which prevents a reversal. This has the impact of maximizing conductor loads since no relieving inward loads exist (when no field direction reversals exist).

The radial axial field variation in the conductor mid-pack region is input into STANSOL to determine how the conductors in a pancake share these Lorentz forces. The hoop stress developed for normal operation, including winding tension, cool-down, and the electromagnetic loading, is illustrated in Figure 4-3. The results indicate that the developed hoop stress is a function of its radial location in the pack (turn number) and axial location (primarily because of the axial field variation throughout the pack). Figure 4-3 also illustrates a difference in conductor hoop stress of 1000-2000 psi from mid-pack (maximum location) to magnet side wall. The conductor hoop stress distribution changes as a function of winding tension also as illustrated in Figure 4-4.

The applied strain to the conductor is important in that the critical current capability is highly dependent upon it. Conductor critical current is maximized when the internal strain (prestrain resulting from the manufacturing technique of the conductor is exactly cancelled by an externally applied strain. Maximizing current carrying capability is difficult because the operating strains and manufacturing strains inherently vary with conductor pack radius. In addition, bending effects do not cancel the residual filament compression uniformly across the conductor cross-section.

A flow diagram is used in Figure 4-5 to describe the combined strain condition of the monolith.

The conductor pack strains are a result of the following:

1) Straighten after reaction.

2) Winding and unwinding from the shipping spool (assume no effect).

3) Winding on bobbin (bending strain).

4) Miscellaneous effects:

   a) Joggle bending strain (at bobbin).

   b) First and last turn - fix to case (bending strain at outer turn).

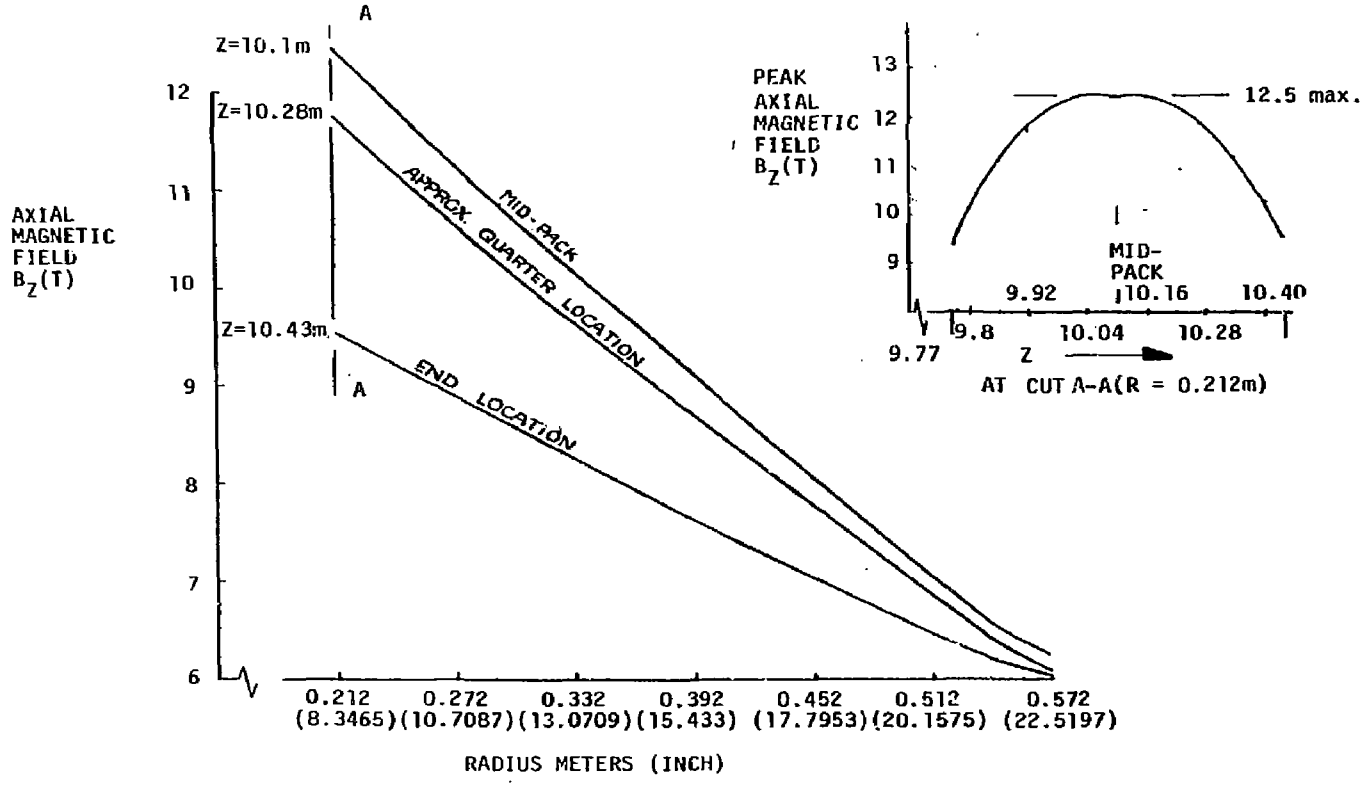

Figure 4-2. Axial Magnetic Field in the Conductor Pack is Maximum at Mid-Pack.

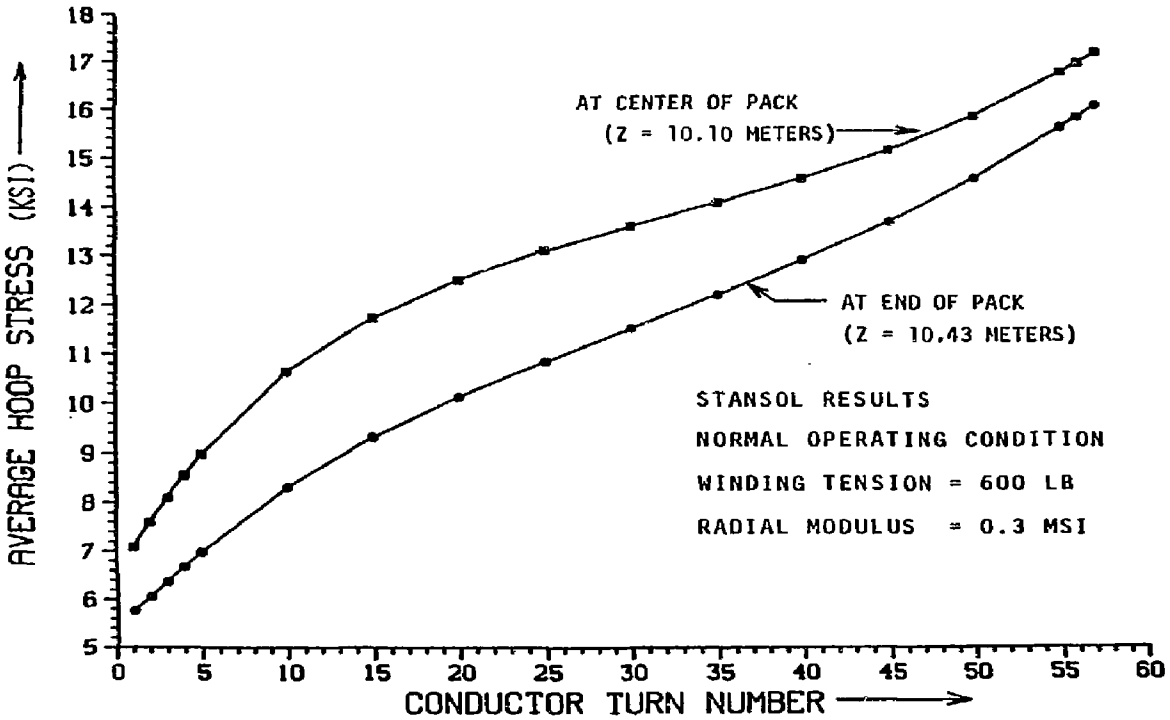

Figure 4-3. Effects of the Axial Magnetic Field Variation on Conductor Hoop Stress

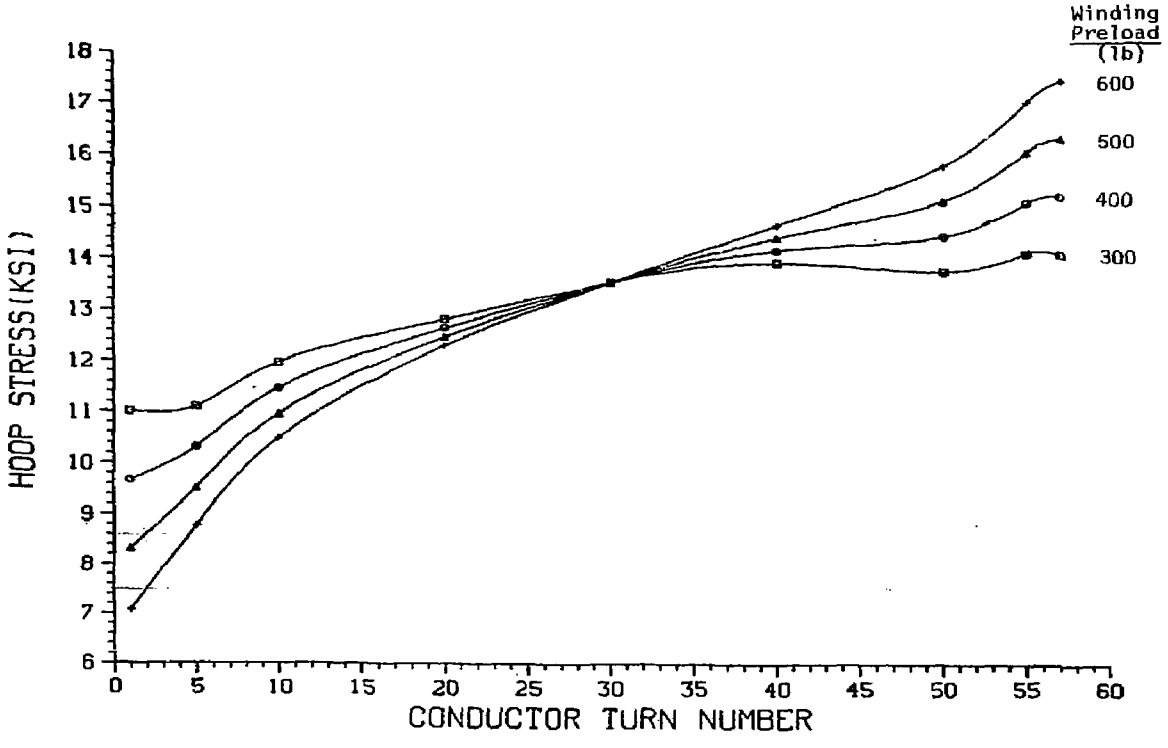

Figure 4-4. Conductor Hoop Stress vs. Winding Preload *for Normal Operation (at Mid-pack)*

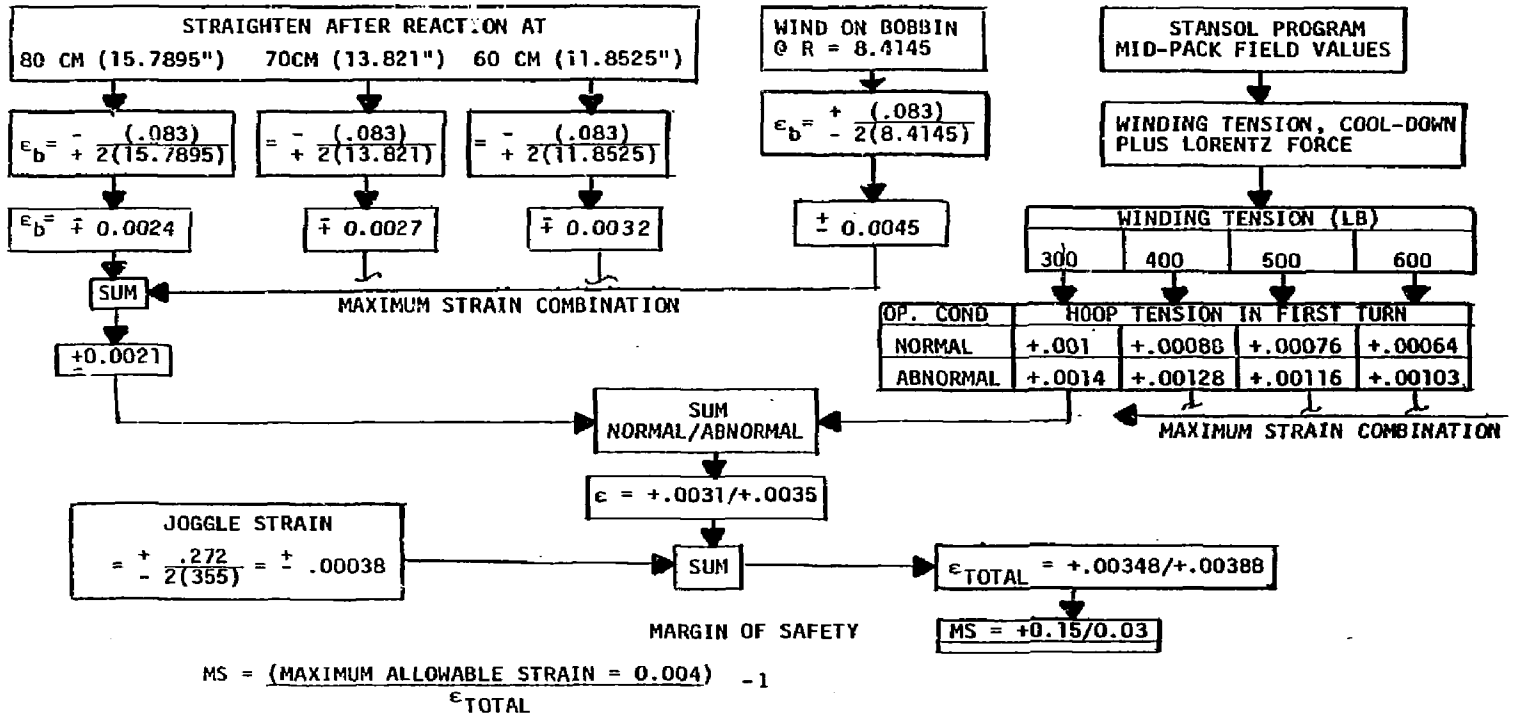

Figure 4-5. Monolith Strain Condition at Bobbin (Including Joggle) are Within Acceptable Limits

5) Winding tension.

6) Operational effects.

   a) Cool-down.

   b) Lorentz forces.

From a strength standpoint, bending strains are added directly to uniaxial strains for comparison to the +0.4 percent allowable working strain. As shown in Figure 4-5, a worst case of strain accumulation shows acceptable safety margins. Note that more than half of the strain is due to winding.

Figure 4-6 depicts the same kind of data for the outer turn.

Another source of loading that should be included in developing the total stress state for the conductor is the "crush force" (in the axial direction). Self-constricting forces within the pack are due to the presence of a radial field component. This radial component is zero at the pack centerline and maximum at the pack sides (positive on one side - negative on the other) as shown in Figue 4-7.

The bearing stress on the conductor varies throughout the pack (because of B_r field variations). The resulting stress is relatively low with the maximum developed values of 3.7 ksi (normal operation) and 4.9 ksi (abnormal operation), thus inducing only a small Poisson effect in the Nb_3Sn monolith. The effect on the copper stabilizer is negligible.

In order to establish the structural integrity of the conductor, the von Mises stress criteria was incorporated. The hoop stress component was developed using the STANSOL model (at the given winding tension) and the maximum developed axial stress (due to the "crush force") was conservatively assumed to be acting throughout the pack. The radial stress component was taken to be zero (<50 psi).

The minimum normal operating margin of safety is +0.28 and +0.56 for normal and abnormal operating conditions respectively (winding tension = 600 lb, outer turn) as shown in Figure 4-8. The margins are based on a σ_{ys} = 37 ksi @ 4K which represents the yield strength of the copper housing alone (see Table 4-2). This value was used in lieu of the composite conductor that is scheduled to be developed in the verification test program being conducted at LLNL. Indications are that the composite conductor yield strength will be smaller (approximately 34-37 ksi @ 4K), however, the margin of safety values are expected to remain positive even for the highest loaded condition (600-lb winding tension).

Figure 4-9 illustrates the conductor pack radial deflection as a function of applied loading condition.

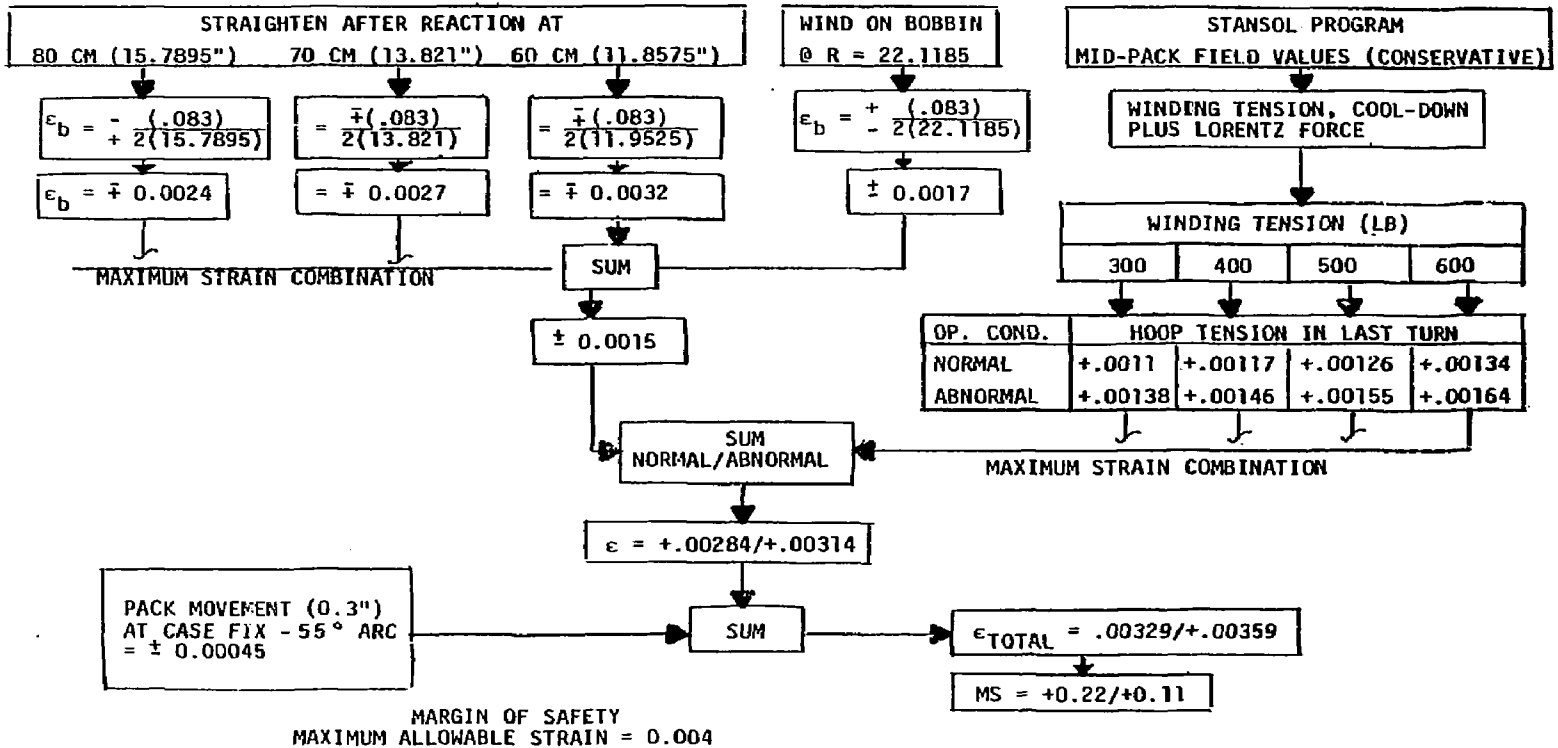

Figure 4-6. Monolith Strain Condition at Last Turn (Including Pack Movement) is also Within Allowable

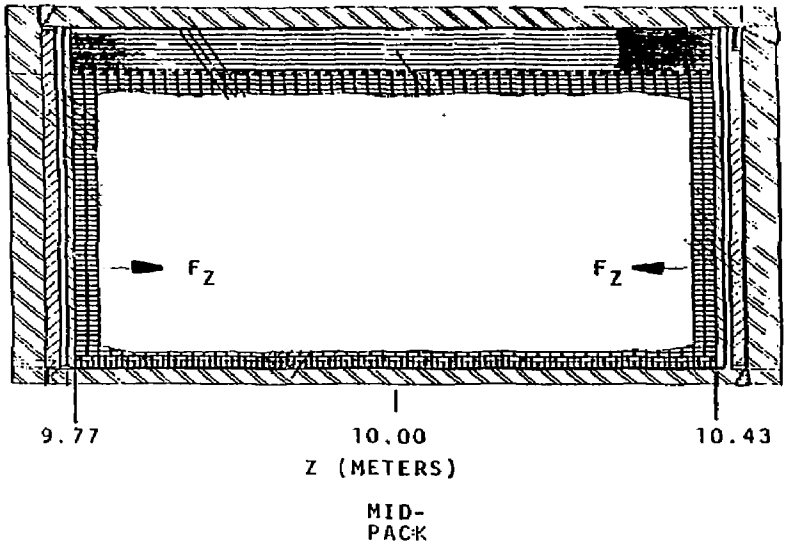

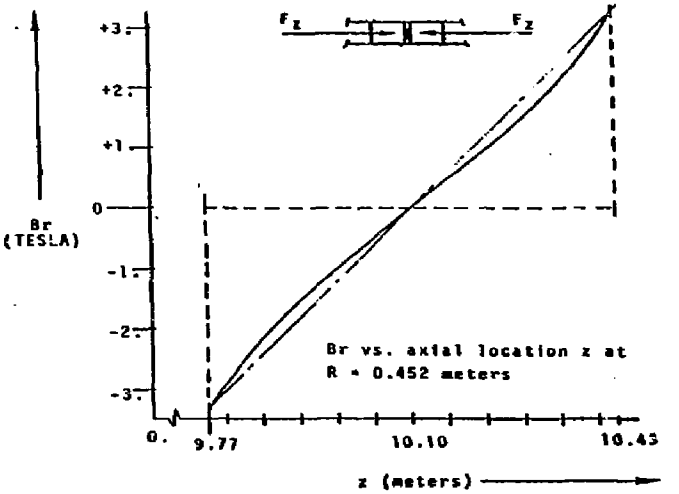

$$\sigma_{brg} = \frac{F_z}{(\text{cell height})(\text{\% brg area})}$$

where:

$$F_z = \frac{i \times \Sigma Br}{175.1} \left(\frac{lbf}{in}\right)$$

$$\Sigma Br = \frac{\text{Area under curve}}{\text{cell width}}$$

% brg area = .5 for pancake insulation

σ_{brg} = 3.71 ksi (conservative)

Figure 4-7. Conductor Pack Radial Field Distribution is Used in Development of the Pack Crush Force

Nb_3Sn CONDUCTOR LOADING

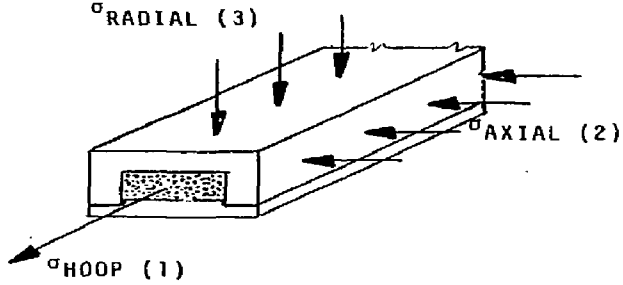

MEMBRANE STRESS ONLY

$$\sigma_{VON\ MISES} = \frac{1}{\sqrt{2}} \left[(\sigma_1-\sigma_2)^2+(\sigma_2-\sigma_3)^2+(\sigma_3-\sigma_1)^2\right]^{1/2}$$

where: $\sigma_3 \sim \phi$

MID PACK LOCATION - NORMAL/ABNORMAL MARGIN OF SAFETY

PACK RADIUS	WINDING PRELOAD, LB 300	400	500	600
8.455"	+1.0 / +1.17	+1.25 / +1.35	+1.56 / +1.56	+1.93 / +1.82
17.795"	+0.54 / +0.76	+0.51 / +0.73	+0.49 / +0.71	+0.47 / +0.70
22.119"	+0.55 / +0.82	+0.45 / +0.72	+0.36 / +0.66	+0.28 / +0.56

where: NORMAL MS $= \dfrac{2/3\ \sigma_{ys}}{\sigma_{VON\ MISES}} - 1$

ABNORMAL MS $= \dfrac{\sigma_{ys}}{\sigma_{VON\ MISES}} - 1$

and: σ_{ys} = 37000 psi @ 4°K

Figure 4-8. Margin of Safety in Conductor Housing is Positive for all Loading Conditions

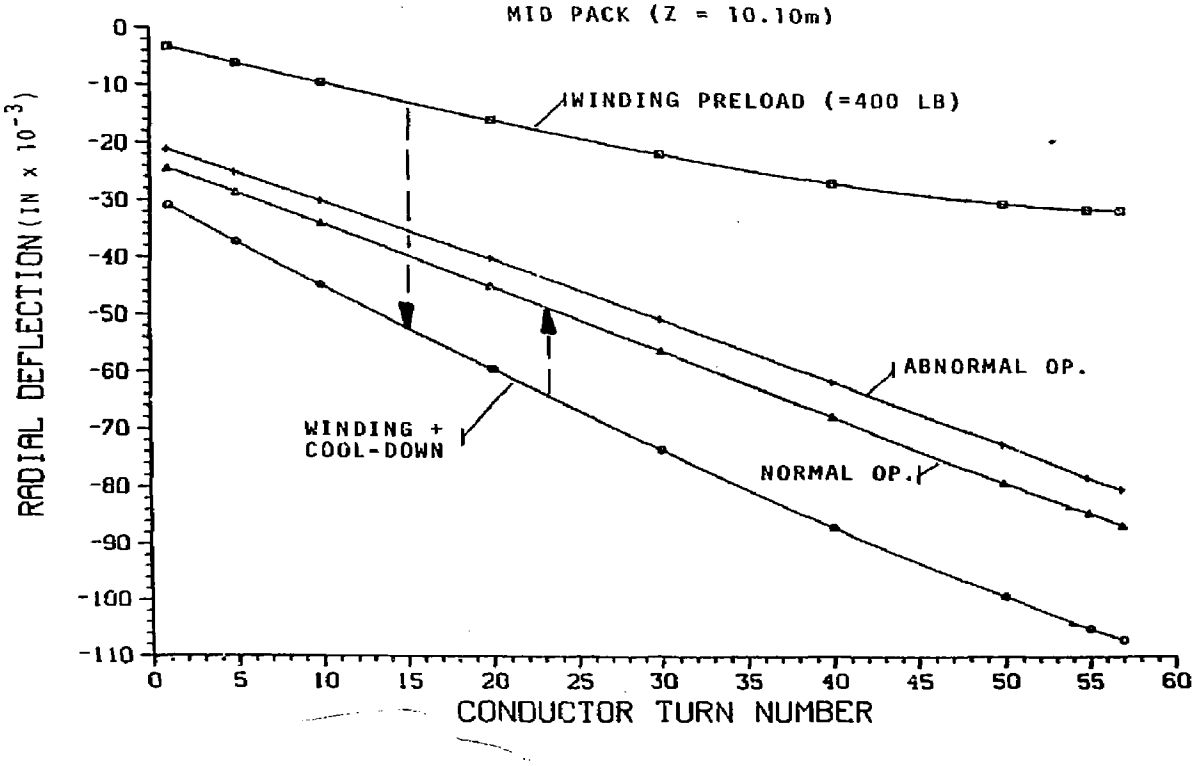

Figure 4-9. Conductor Pack Radial Deflection as a Function of Loading Condition

The sequence of loading follows:

- o Winding preload.
  - Produces an inward radial deflection.
- o Cool-down.
  - Increases the inward radial movement (thermal contraction).
- o Normal operation (or abnormal).
  - Produces outward radial deflection.

4.4.2 Magnet Case Analysis

In-plane electromagnetic forces on the conductor pack are primarily determined by self forces and the background influence of the outer A20 coil. As mentioned, this loading is reacted by the hoop capacity of the conductor pack. The self-constricting forces within the pack are due to the presence of a radial field component. This component is zero at the pack centerline and maximum at the pack sides.

When neighboring coils are turned on, a slight imbalance in the coil A2I crush force is imposed due to cancellation effects on the radial field components. In other words, coil A2I is attracted towards a neighbor coil that has been activated. A good example would be the condition of coils A2I and T1 fully charged with all other coils off. This imposes a running axial force on A2I, the distribution being determined by the geometry of coil T1 (where the T1 "C" shape comes closest to A2I, the axial attraction is maximized). These out-of-plane loads are design drivers for the magnet case and support system.

a. Magnet Case

The SOLID SAP (SOLIDSP) 2-D computer program (Ref. 4-4) was used for this analysis. The quadrilateral axisymmetric element was incorporated. The two coils (A2O/A2I) were included in the model to provide the boundary condition requirements on the welded attachment fixture. The shims between the two coils were not included in the model (conservative). The model is shown in Figue 4-10 along with the Kelley mode normal and abnormal loading conditions. The displacement profile for the abnormal loading case is also shown in Figure 4-10, overlaid on the model. The pack pressure against the case side wall results in large in-plane moments that are the primary stress contributors. The corner peaking of the bending stress as shown in Figure 4-11 is

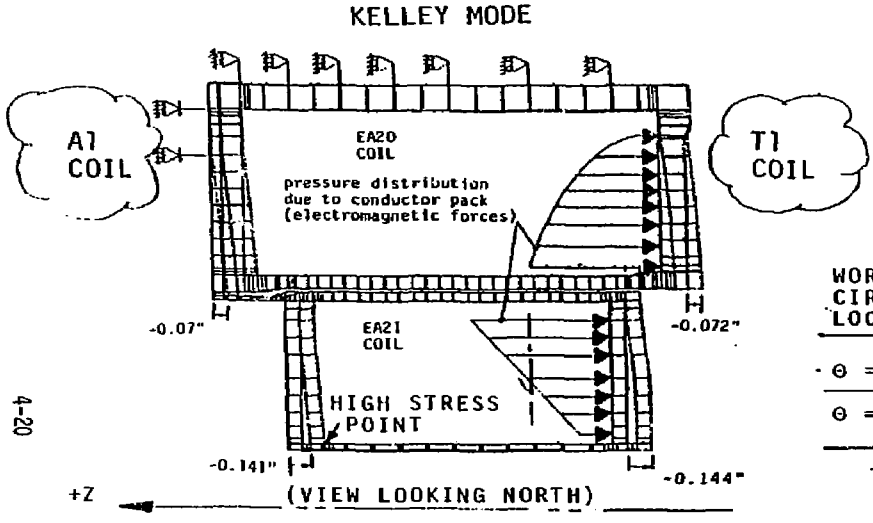

DISPLACEMENT PROFILE

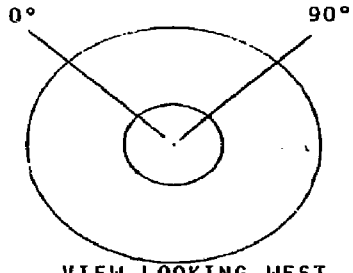

VIEW LOOKING WEST

WORST NORM. CIRCUM. LOCATION	F_{AXIAL} (LB)	COND. PACK PRESS (PSI)	COMMENTS
$\Theta = 0°$	180,280	135	P_{AVG} = 163 PSI
$\Theta = 90°$	225,360	191*	

ABNORMAL CIRCUM. LOCATION	F_{AXIAL} (LB)	COND. PACK PRESS (PSI)	COMMENTS
$\Theta = 0°$	267,440	200	P_{AVG} = 241 PSI
$\Theta = 90°$	377,416	282*	

* USED IN ANALYSIS

Figure 4-10. The Axial Load Developed in the Conductor Pack is Reacted by the Magnet Case

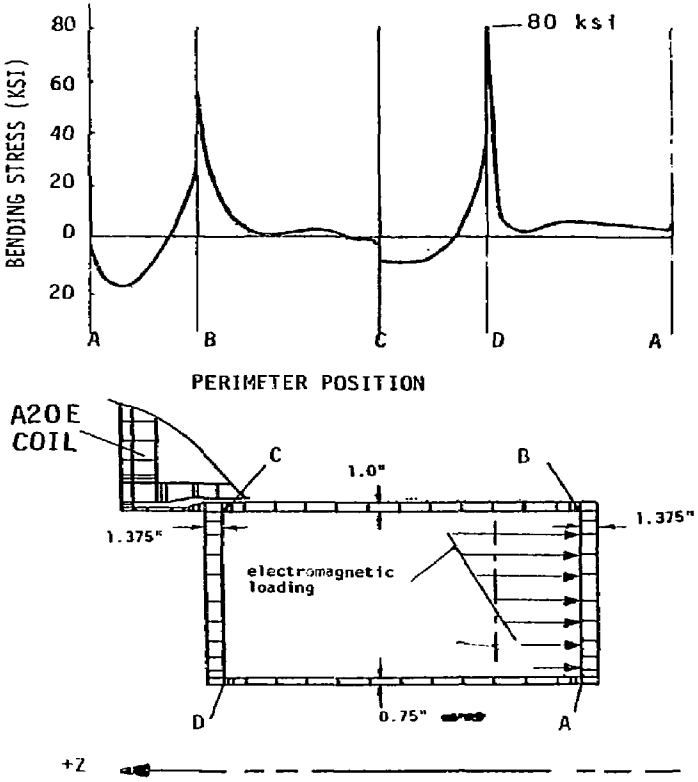

KELLEY MODE

- MAXIMUM STRESS CONDITION OCCURS IN CORNER D (NEARLY PURE MERIDIONAL BENDING):

  - NORMAL OPERATION

    @ D $\sigma_{BENDING}$ = 40 KSI (NOT ILLUSTRATED)

    $$MS = \frac{90}{40} - 1 = \boxed{+1.25 = MS}$$

  - ABNORMAL LOADING INCLUDING +150 PSI QUENCH PRESSURE

    @ D $\sigma_{BENDING}$ = 80 KSI (DISTRIBUTION SHOWN)

    $$MS = \frac{100}{80} - 1 = \boxed{+ 0.25 = MS}$$

Figure 4-11. In-plane Moments are Primary Stress Contributors

characteristic of the load reaction method used on the magnet case (fixed at one corner). The discontinuities in stress at the corners is a result of the change in section (wall thickness). Figures 4-12 and 4-13 show a similar presentation for the Mars mode. The developed margins are larger for this loading case.

b) Fracture Mechanics Analysis

The case corner closeout fracture mechanics analysis was performed under the following conditions using 1-inch thick plate stock.

1) 500 normal operating cycles par one life at normal operating stress is shown in Figure 4-14.

2) 10 abnormal cycles using 0 to 100 ksi to represent the abnormal loading condition (conservative because of the 80 ksi stress developed for the worst case loading condition for the insert magnet).

The above loading represents one lifetime of loading. The allowable initial defect size is developed by using four lifetimes. The allowable defect size from Figure 4-14, for the 40 ksi developed normal operating stress condition (Kelley mode, Figure 4-11), is approximately 0.19". This developed initial crack size is much larger than the NDE threshold value of 0.078, therefore, NDE should not be a design driver for this magnet case.

c) Coil Support Structure

Axial support for the A2I coil is offered by the nearly continuous welded attachment fixed to the A20 coil (3 pieces approximately 120° segments) as shown in Figure 4-15. Radial support is provided by shims (2 shims, 6 places) between the A20 and A2I coils (not shown in Figure 4-15). Both coils (A20 and A2I) were used in the computer model (Figure 4-10) primarily to provide the boundary condition on the welded attachment. The high stress location is at point A as shown in Figure 4-15. The radius was not included in the model, therefore, making the stress values (primarily bending) somewhat conservative. The Kelley mode developed the maximum stress condition as illustrated in Figure 4-15.

d) Thermal Stress Analysis

The same Solid SAP computer axisymmetric model that was used to develop the stress under the mechanical loading condition was used for the thermal stress analysis. The model simulated the temperature condition of the case by assuming constant component temperatures (no transition gradients from component to component). The temperature condition imposed was the cool-down cycle at about 30 hours into the transient.

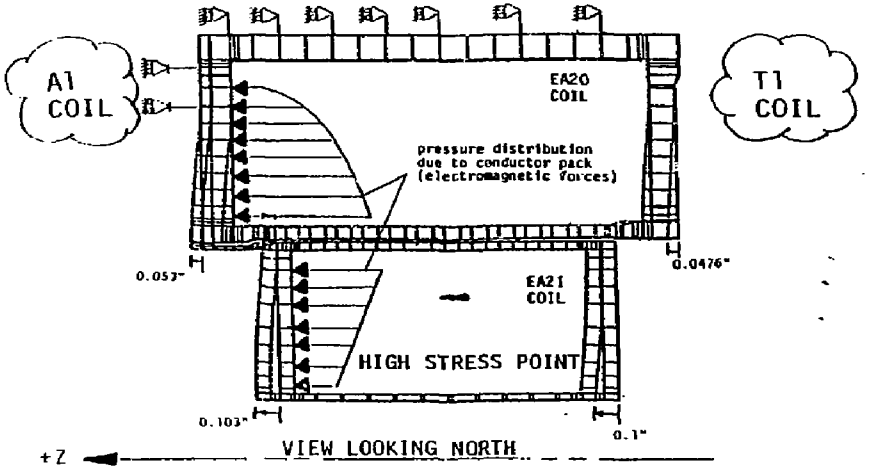

DISPLACEMENT PROFILE

NORMAL

CIRCUM. LOCATION	F_{AXIAL} (LB)	COND PACK PRESS. (PSI)
UNIFORM LOAD. 0 - 360°	238,560	178

ABNORMAL

CIRCUM. LOCATION	F_{AXIAL} (LB)	COND PACK PRESS. (PSI)
UNIFORM LOAD. 0 - 360°	282,017	211

Figure 4-12. Mars Mode - A2I Coil Axial Loading

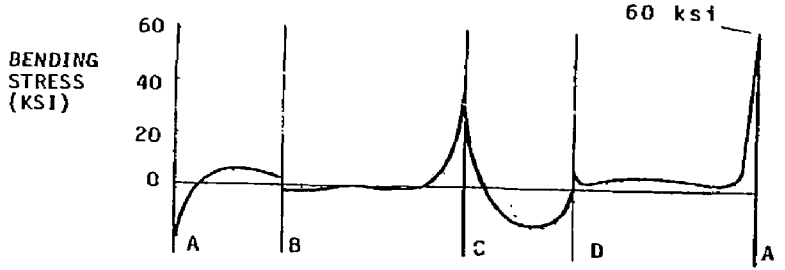

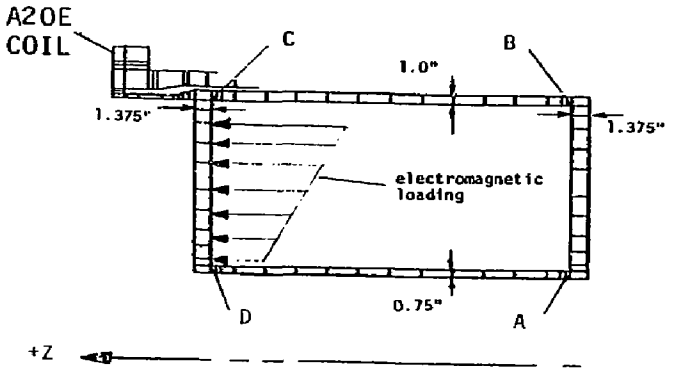

- MAXIMUM STRESS CONDITION OCCURS IN CORNER A (NEARLY PURE MERIDIONAL BENDING):
  - ABNORMAL LOADING INCLUDING +150 PSI QUENCH PRESSURE

    @ A $\sigma_{BENDING}$ = 60 KSI (DISTRIBUTION SHOWN)

    $MS = \frac{100}{60} - 1 =$ **+ 0.67 = MS**

Figure 4-13. Bending Stress in A2I Case, Mars Mode

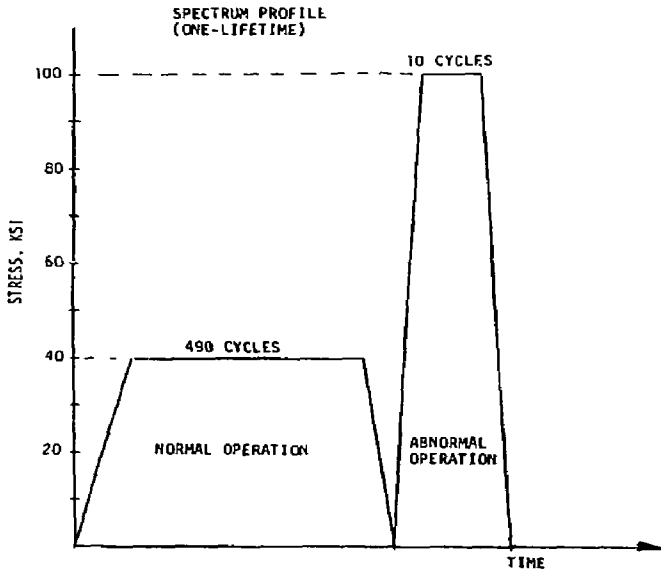

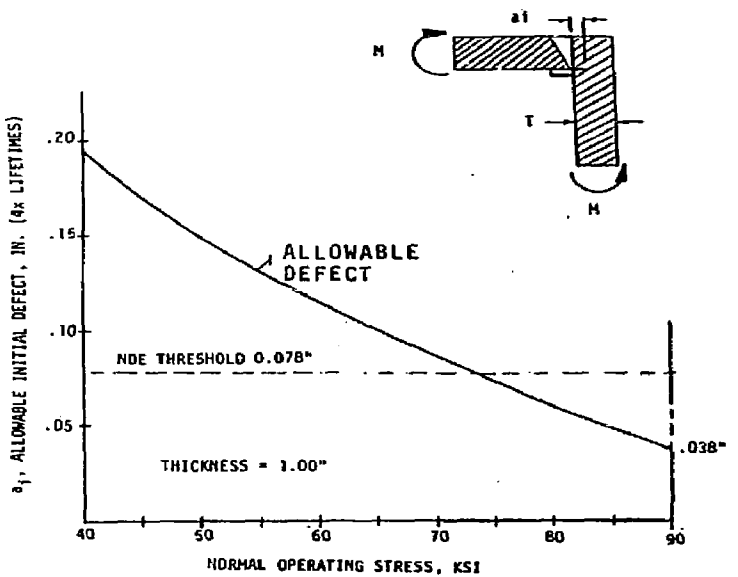

- WHERE THE FLAT BOTTOM HOLE (0.078ø) IS EQUIVALENT TO THE SIGNAL PRODUCED WITH THE 1/8" SIDE WALL DRILLED CALIBRATION BLOCK USED BY CBI.

Figure 4-14. The Fracture Mechanics Analysis for the Closeout Welds Predicts an Initial Flaw Size over the NDE Requirement

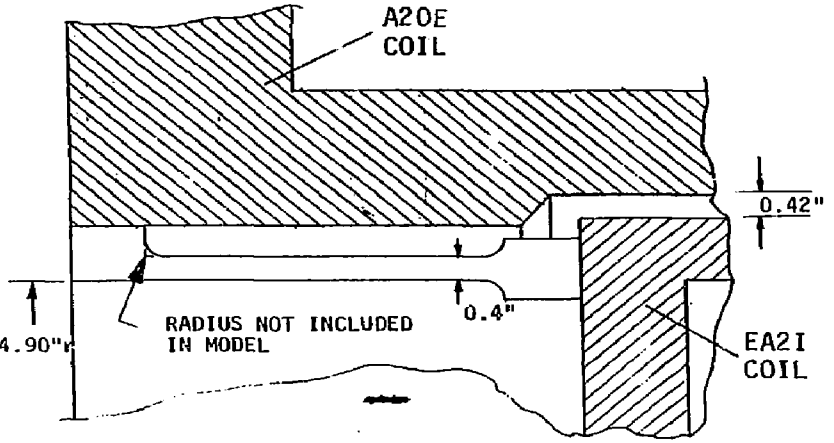

KELLEY MODE

- NORMAL OPERATION

  σ_{TOTAL} = 47 KSI (MEMBRANE+BENDING)

  σ_{MEM} + 0.741 σ_{BEND} = 4 + (.741)(43) = 36 KSI

  $MS = \frac{66.7}{36} - 1 =$ **+0.85 MS**

- ABNORMAL + 150 QUENCH PRESSURE

  σ_{TOTAL} = 70 KSI (MEMBRANE+BENDING)

  σ_{MEM} + 0.741 σ_{BEND} = 6 + (.741)(64) = 53.4 KSI

  $MS = \frac{100}{53.4} - 1 =$ **+0.87 = MS**

(MARS MODE, ABNORMAL, **MS =+1.56**)

- COOL-DOWN CYCLE:

  MAXIMUM BENDING STRESS OCCURS AT ~30 HOURS

  $\sigma_{BEND} = \pm$ 30 KSI **MS = +0.53**

  ASSUMPTIONS:

  - ΔT BETWEEN COILS OF 40°F
  - NO SHIMS

Figure 4-15. The A2I Coil is Attached to the A20 Coil by a Welded Attachment

The A2I coil has a relatively large cross-section and short conductor and helium flow path. Therefore, the temperature spread between components is relatively low with the thick (1.375-inch) side wells being somewhat warmer than the other components. The assumed temperature condition and corresponding developed stresses are presented in Figure 4-16.

A maximum delta temperature condition between A20/A2I coils was analyzed using the following loading assumptions:

I) A20 is colder than A2I (A2I warmer)

II) A2I is colder than A20 (A20 warmer)

with the following assumptions:

1) That the shims are operative for loading assumption I.

2) That the welded attachment resists an opening condition (loading assumption II).

The maximum delta temperature condition between the two coils based on the design criteria listed in table 4-1 is illustrated in Figure 4-17. The opening mode develops a bending stress in the welded attachment and the closing mode produces bending stress in the outer ring of the A20 coil (assuming no gap between the shims). The corresponding temperature condition of the individual coils are developed using the data presented in Figure 4-17 and illustrated in Figure 4-18. Included in Figure 4-18 is the expected temperature condition of the coils using design flow rates.

e) Bobbin Stability

The inelastic buckling equation shown in Figure 4-19 was used to predict the buckling characteristics of the magnet case inner ring (bobbin). This approach is considered to be a very conservative approach for the following reasons:

1) The secondary nature of the load (i.e. the load relaxes when the bobbin deflects away from the pack).

2) The self-supporting characteristics of the pack on the bobbin (i.e. the bobbin can only buckle inward, thus producing a much higher buckle mode than predicted by the equation.

The factor of safety values developed are over the required value of 2.0 for all but the highest winding tension (600 lb) as shown in Figure 4-19. The winding tension to be used has yet to be established by LLNL, however, it is not expected to be higher than 400 lb.

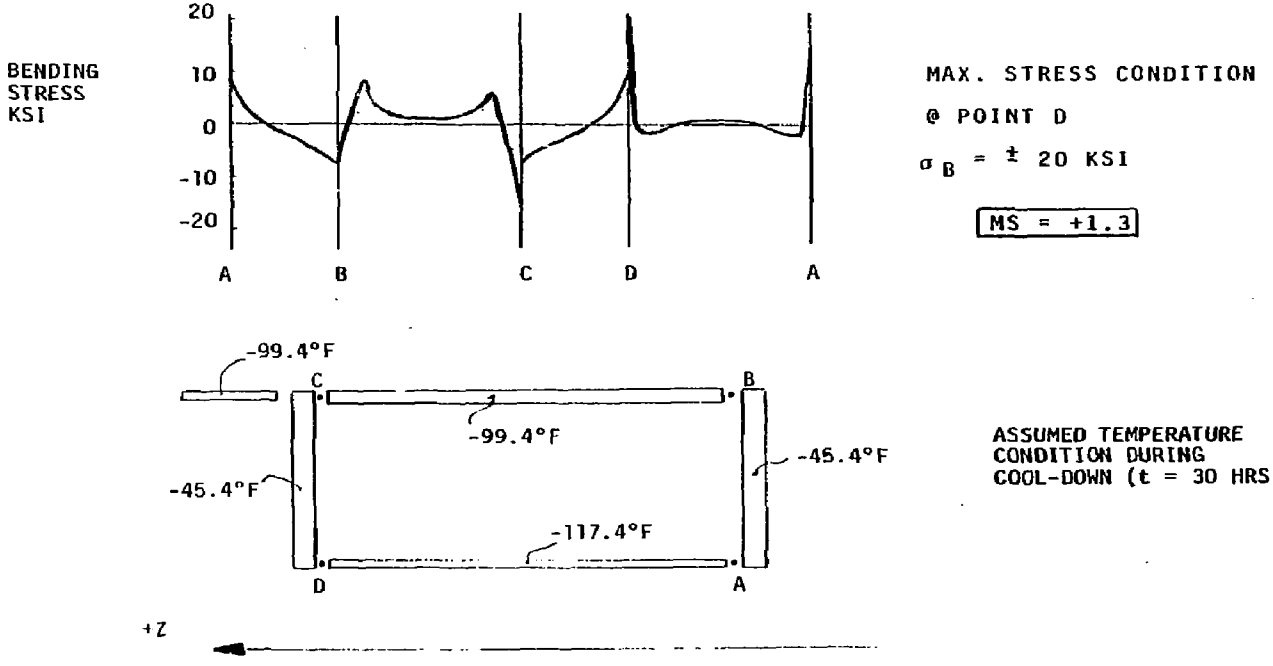

Figure 4-16. Thermal Stress Developed During Cool-down Condition

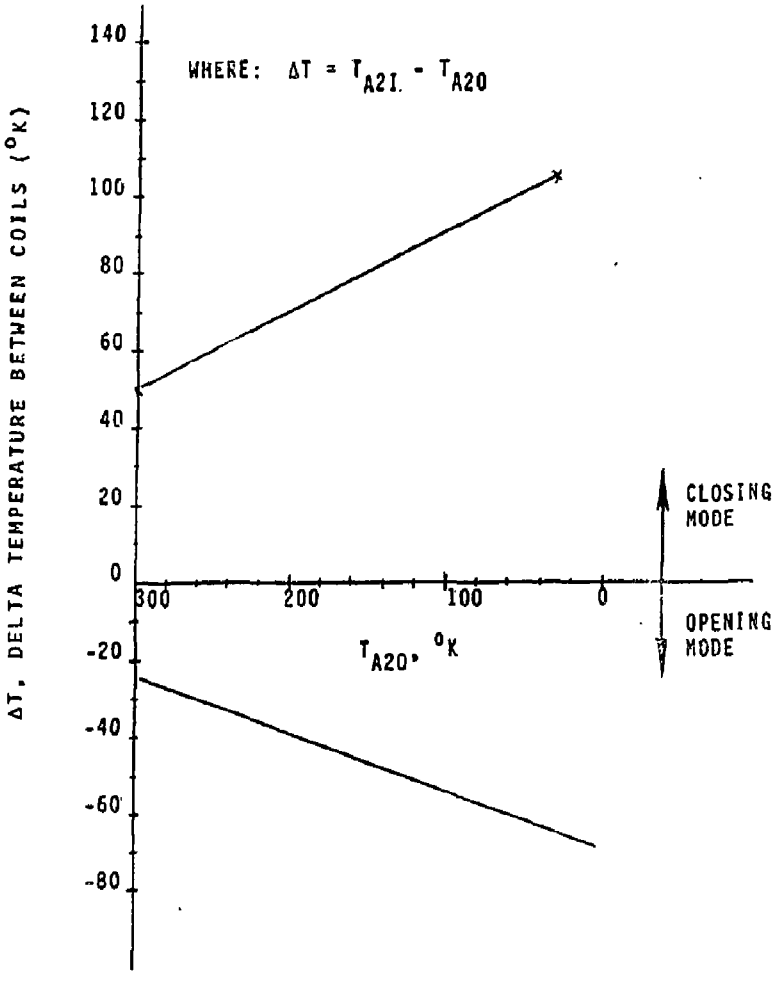

Figure 4-17. Delta-Temperature Control Requirements for the A20/A2I Coils

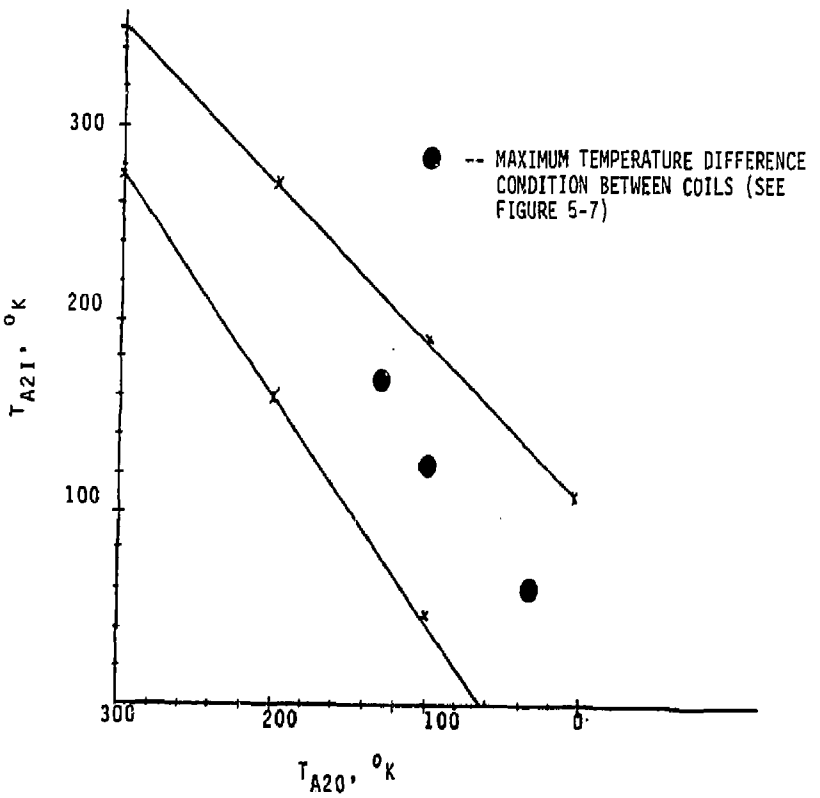

Figure 4-18. Allowable Temperature Difference Between A20/A2I Coils Based on MFTF Design Criteria

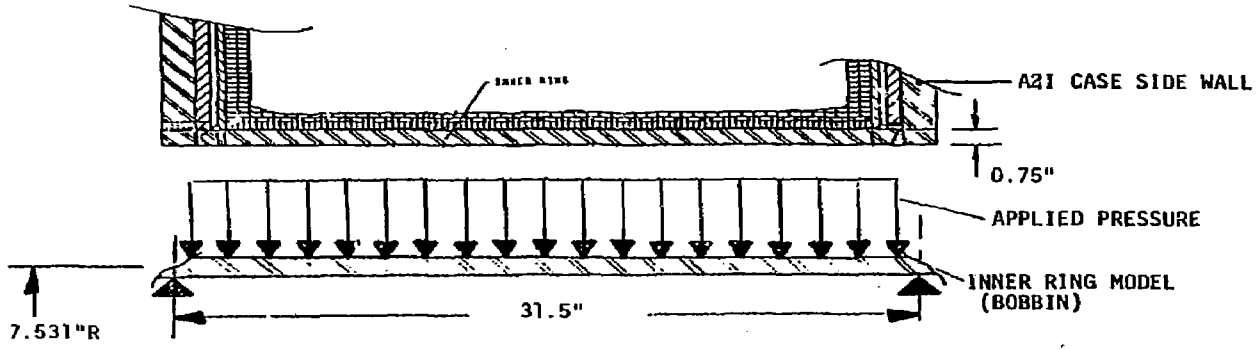

- INELASTIC BUCKLING EQUATION FOR A CYLINDER UNDER EXTERNAL PRESSURE:

$$P_{cr} = 0.926 \frac{n\,E\,\sqrt{\gamma}}{(r/t)^{2.5}(\ell/r)}$$ (EDGES SIMPLY SUPPORTED, REF. EQ. 5, NASA REPORT NO. SP-8007)

$$P_{cr} = 3246 \text{ PSI}$$

	WINDING PRELOAD (LB)			
	300	400	500	600
HOOP STRESS (PSI) RAD. PRESS. (PSI)	-8415 838	-11219 1117	-14024 1397	-16829 1676
FACTOR OF SAFETY AGAINST BUCKLING $FS = \frac{3246}{\text{RAD. PRESS.}}$	3.87	2.9	2.32	1.94

Figure 4-19. Bobbin Buckling Characteristics

f) Local Stress Concentrations

A 3-D NASTRAN (Ref. 4-5) model was used to develop the potential stress concentration effect around the opening in the side wall in the conductor lead port region. The model is shown in Figure 4-20 and represents a one-quarter section of the magnet case. The loading condition used on the model was a representation of the Kelley mode faulted loading condition. The developed margin of safety values produced were all positive as presented in Figure 4-20. The Mars mode loading condition applies the electromagnetic loading on the opposite end plate (side away from the port opening) and, therefore, produced a relatively low stress condition in the port region.

4.4.3 Insulation and Current Lead Analysis

Many different insulation types and configurations are used in and around the conductor pack. The insulation material used is G-10CR. The insulation configurations that are under a potential loading condition are listed below.

- turn insulation
- side wall channel insulation
- conductor joggle insulation
- conductur turn insulation
- ventiltated insulation
- sidewall ground insulation
- riser-grid insulation
- pancake insulation
- riser/vent insulation at splice
- plenum insulation

The different types of insulation configurations are illustrated in Figure 4-21. The maximum-stressed condition occurs when wrapping on the bobbin producing a positive margin shown in Figure 4-21. Miscellaneous geometries also included in the case are the upper and lower piccolo tube. The mechanically-induced loads on the piccolo tube are small.

The Nb_3Sn insert coil is positioned inside the A20 coil requiring a relatively complex current lead out tunnel geometry as shown in Figure 4-22. The tunnel is also complicated because of the proximity of the I1 coil. The EFFI field data for the tunnel region was obtained from LLNL. The resulting conductor loading from that field data was relatively low. Therefore, permitting the mechanical restraints to be placed such that maximum freedom of the current leads is possible reducing the thermal restraint effects to a minimum. The resulting stresses are low.

STRESS CONDITION AT LOCATION A

- LOADING CONDITION:

  KELLEY MODE

  ABNORMAL + 150 PSI QUENCH PRESSURE

  SIDE WALL

  $\sigma_{BENDING}$ = 58 KSI

  $MS = \frac{100}{58} - 1 =$ +0.72 = MS

  OUTER RING:

  $\sigma_{BENDING}$ = 80 KSI

  $MS = \frac{100}{80} - 1 =$ +0.25 = MS

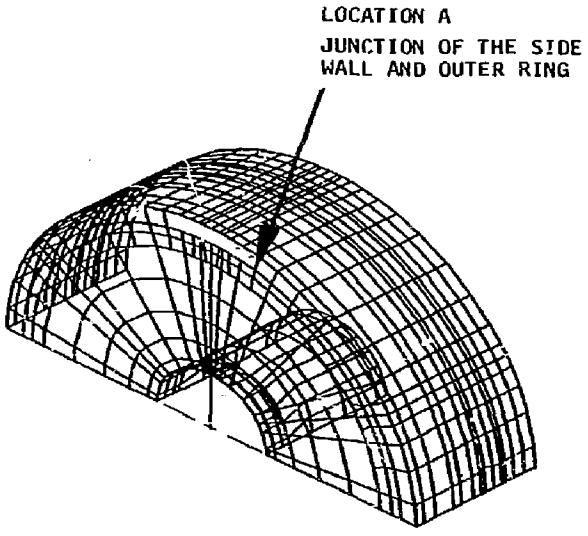

Figure 4-20. Model Used to Develop the Stress Concentration Potential Around the Conductor Lead Opening

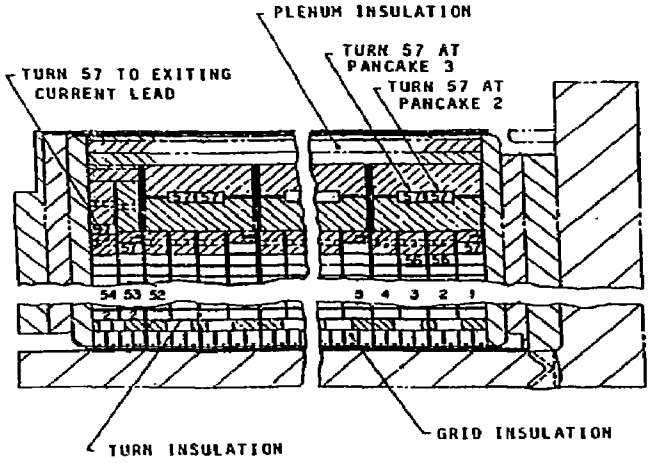

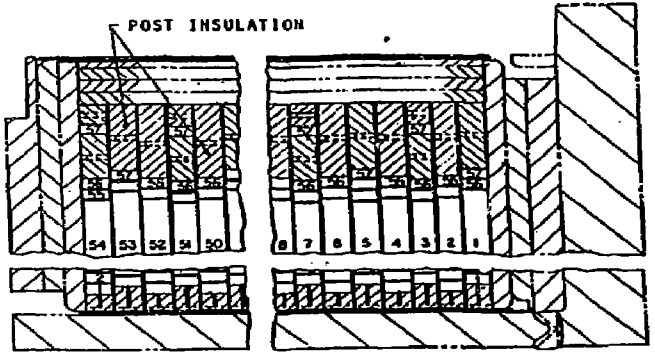

- INSULATION MATERIAL; G-10CR
- THE HIGHEST STRESS IS DEVELOPED DUE TO BENDING ON THE INNER RING

MS = + 2.1 @ R.T.

Figure 4-21. Many Different Shapes and Forms of Insulation are Used Throughout the Conductor Pack

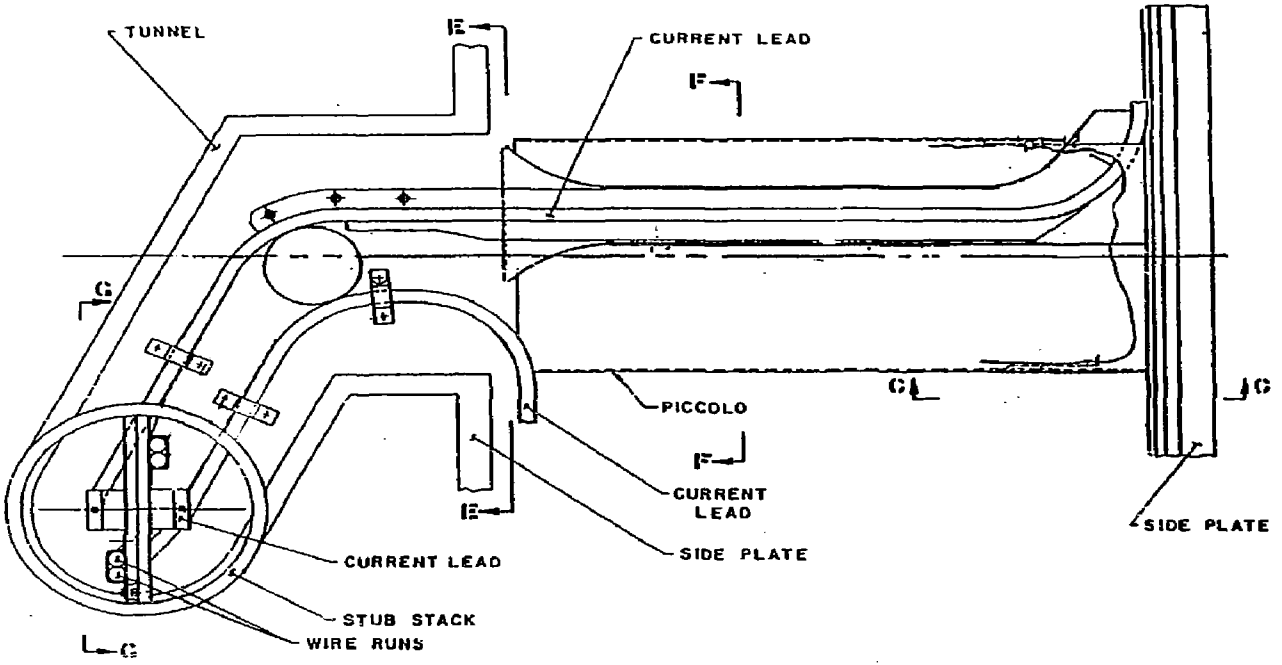

- CONDUCTOR LOADING IS RELATIVELY SMALL (< 45 lb/in.)
- THE RESULTING STRESSES ARE LOW

Figure 4-22. The Design Provides the Required Mechanical Restraints While Minimizing Thermal Restraint Effects

4.4.4 Stress Summary

The stress and corresponding margins of safety values presented in this document are taken from the stress reports listed in Appendix D and documented in reference 4-6. Table 4-5 relates the particular stress document to the corresponding component.

4.5 Verification Test Results

The tests for the insert coil conductor verification test program have not been completed at the time of this writing. The overall results received thus far, however, indicate that the conductor produced by Furukawa is a very good product which should have the capability of meeting all specification requirements. The more important results from the tests received thus far as follows:

1) Conductor Splice Test - 6.4.6

The test specimen used was a simplified representation of the prototype in that only one mechanical splice was used, along with only one conductor. The specimen was also made straight for ease of testing where the prototype is curved to match the radius of the conductor pack. The bolts were torqued to 37 in-lb in both the electrical and mechanical splice. The test on the specimen was performed in three phases.

Phase I - Thermal Cycling(RT - 80°K, 12 cycles)

Results - no apparent torque relaxation in the bolts was recorded.

Phase II - Fatigue Test

Results - no damages reported during 4X lifetime spectrum of loading (including normal and abnormal loading).

Phase III - Monotonic Tensile Test (4°K)

Results - the tensile test provided a good margin over the operating loading condition as illustrated in Figure 4-23.

The LLNL test report concluded that the bolt torque should be increased in the specimen. A hand analysis was performed on the tested configuration illustrating that there was sufficient clamping force in the electrical splice (at a bolt torque of 37 in-lb).. The equation used to develop the remaining preload (after cool-down is:

Table 4-5. Stress Summary of Both the Nb_3Sn Conductor and Stainless Steel Case

Stress Report*	Component	Result Summarized in Figure	Minimum Margin ** Condition (Normal/Abnormal)
A-1, -2 -3, & -4	Nb_3Sn Monolith and Composite Conductor	4-5 (1st turn) 4-6 (last turn & fix) 4-8 (composite conductor)	+0.15/+0.03 +0.22/+0.11 +0.55/+0.82
A-5	Current Leads Splice Joints. Splice and fix to case.	4-22	Low Stresses
A-6	Insulation	4-21	+2.1 & R.T.
B-1	Kelley Mode Case Wall Welded Attachment ΔT Between Coils	 4-11 4-15 4-15 (ΔT = 40°F)	 +1.25/+0.25 +0.85/+0.87 +0.53
	Mars Mode Case Wall Welded Attachment	 4-13 4-15	 +0.54/+0.67 +0.53/+1.56
B-2	Bobbin Stability	4-19	+1.94
B-3	Kelley Mode - Stress Concentration Around Lead Port Opening	4-20 (Side Wall) (Outer Ring)	--- /+0.72 --- /+0.25
B-4	Lead Tunnel and Attach. to Side Wall	---	Low Stresses
B-5, -6	Case Thermal Stress	4-16 (@t = 30 hrs into cool-down)	+1.3

* See Appendix D.

** A function of: a) winding tension,
b) reacted diameter, for the conductor.

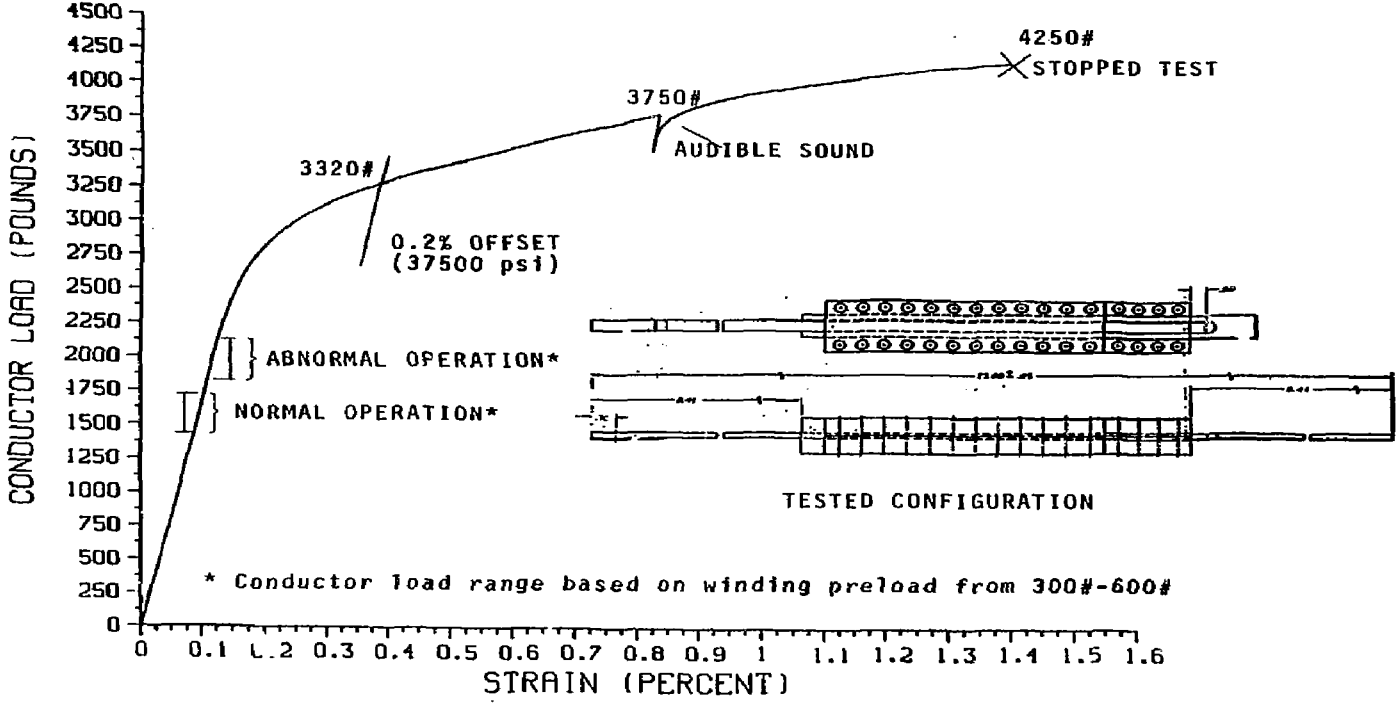

4-23. The Conductor Spiice Test Illustrates Load Capability Well Above Operating Conditions

$$P = \frac{T}{\mu d} - \frac{T(\alpha_{bolt} - \alpha_{clamp})}{\frac{L_B}{A_B E_B} + \frac{L_{clamp}}{E_{clamp} E_{clamp}}} \qquad \text{Eq. 4-1}$$

where: P = remaining preload in-bolt after cool-down.

μ = .25

ΔT = 532°

$L_B = L_{clamp}$ = 1"

α = coefficient of thermal expansion

The test specimen was assembled using a bolt torque of 37 in-lb which produces (according to Eq. 1) a clamping force at 4°K of 10,300 lb for the electrical splice (24 bolts) and 5,400 lb for the mechanical splice (8 bolts). A clamping force of 17,200 lb is developed in the electrical splice when a 50 in-lb torque is used. As mentioned, both torque values provide sufficient clamping force to restrain the 2,250-lb potential abnormal operating force (Figure 4-23). The bolt torque used in the design was 50 in-lb in both the electrical and mechanical splices.

2) Critical current vs. Conductor Insert Bend Radius Test - 6.4.4

The insert was reacted in four configurations (straight, R = 40 cm, 20 cm, and 10 cm). The curved reacted specimens were straightened and all specimens tested. The results, as shown in Figure 4-24 indicated an enhancement in current carrying capability at the prototype strain condition (approximately .002 bending strain). The bending strain induced into the specimens (from straightening) did not show any I_c degradation (from the straight specimens) for up to approximately 2X the prototype bending strain operating condition, or approximately .0048 bending strain. The relatively small I_c enhancement due to bending strain can be attributed to a minor neutral axis shift effect.

3) Conductor Damage Tolerance as a Function of Bending Strain Test 6.4.15

Conductors with inserts reacted at 70 cm were bent both in the "right direction" (decreasing reaction diameter) and in the "wrong direction" (opposite direction from the reacted shape), thus producing a bending strain in the insert. The I_c again (as in test 6.4.4) showed, as in Figure 4-25, an increase in critical current carrying capability up to a bending strain condition of approximately 0.008 (for both the right and wrong way bending) which has been defined as ε_{IRREV}. The tensile vs. I_c tests (6.4.5) have yet to be performed to confirm this ε_{IRREV} value. The

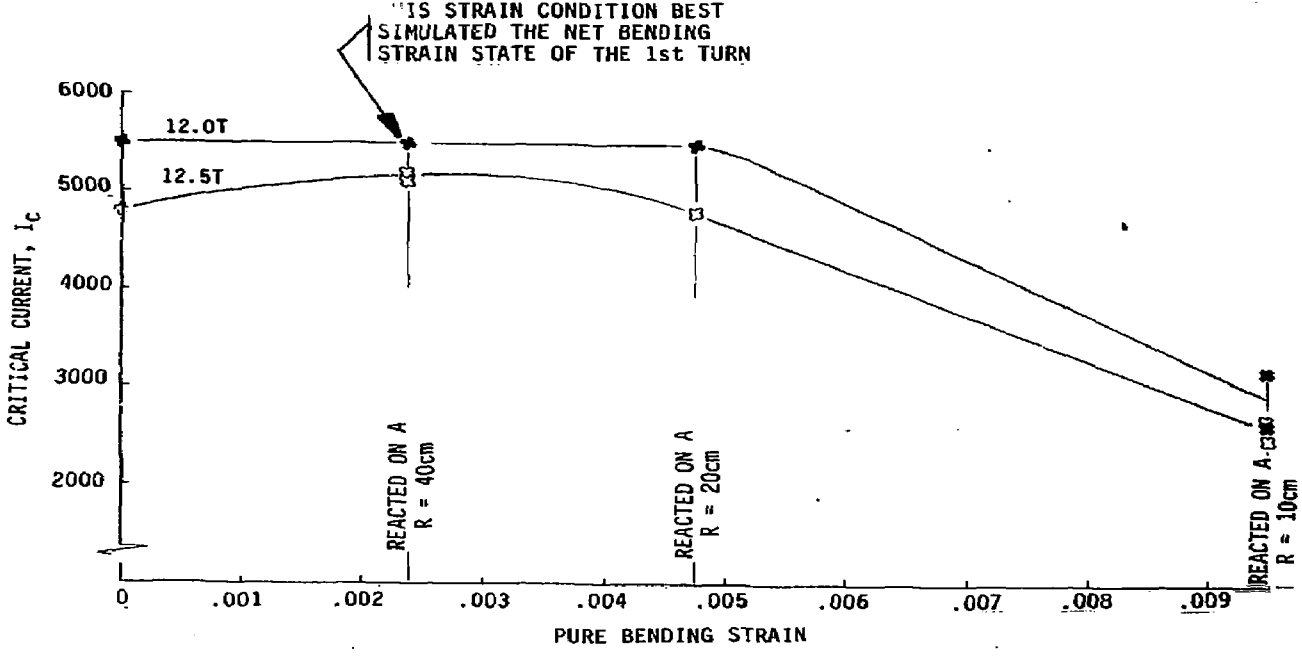

Figure 4-24. Verification Test 6.4.4 - Sensitivity of Conductor Critical Current-to-Conductor Insert Bend Radius

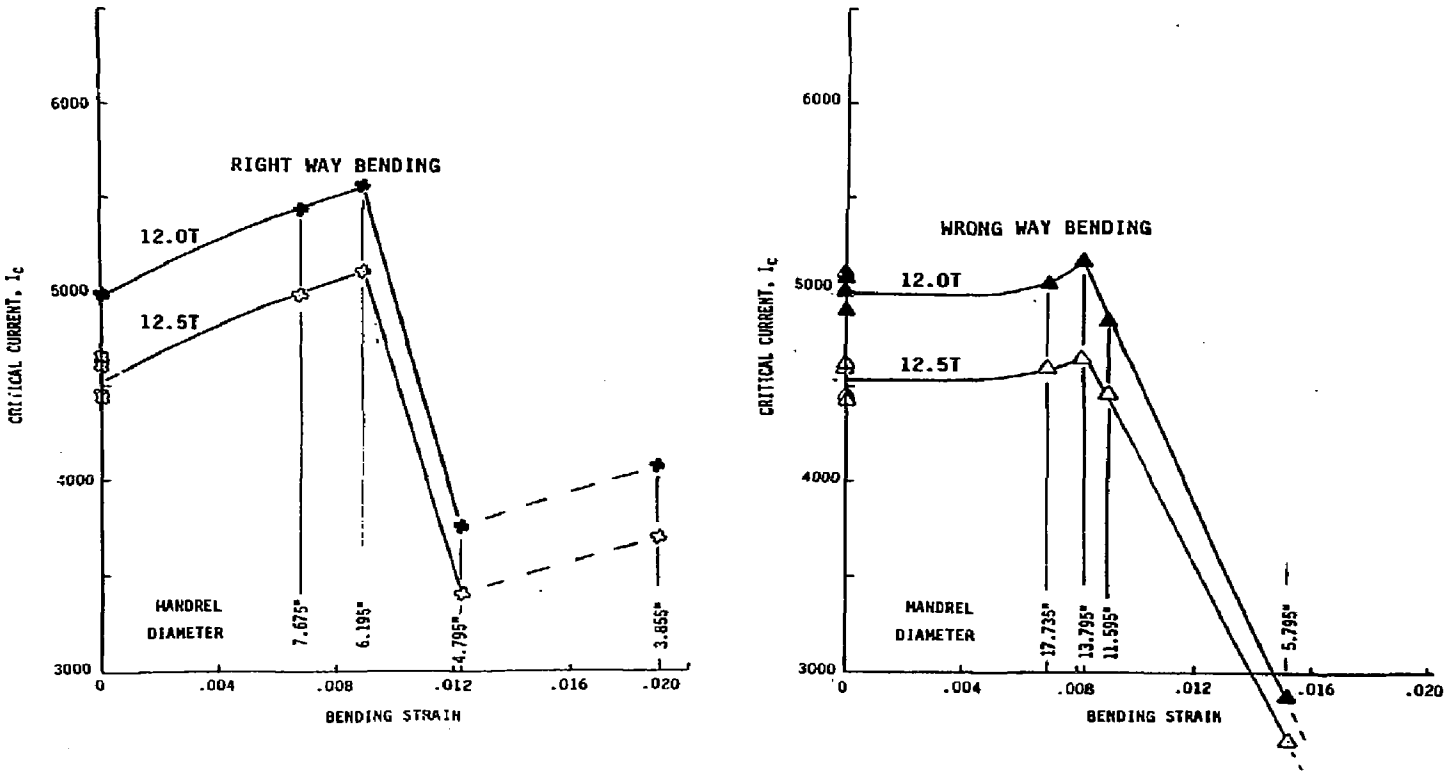

Figure 4-25. Verification Test 6.4.15 - Conductor Damage Tolerance as a Function of Net Bending Strain

ε_{IRREV} = 0.008 was used to develop minimum radius conditions for a right/wrong way bending tolerance that could be used during fabrication of the magnet. This tolerance condition is illustrated in Figure 4-26. The radius values presented represent bending in that direction only (not a possible combined directional bending condition).

4) Mechanical Properties of Insert and Conductor Tests - 6.4.1 and 6.4.2

The room temperature and the 4.2K tensile test results of the conductor and insert that have been performed are presented in Section 8.0. The purpose of these tests is to determine the relative strength characteristics of the composite conductor and the individual components. The Cu housing yield strength is developed by the rule of mixtures using the developed strength values of the composite conductor and insert with their appropriate area ratios. The Cu housing strength is important because it is presently a specification requirement (31 ksi minimum at RT). It was not obtained directly because it was thought that the insert would be an easier configuration to test. Testing of the insert, however, has been difficult primarily because of gripping problems. Testing is continuing, however, the Cu housing strength developed (using available data) indicate a strength greater than the specified minimum (>31 ksi @ RT) as shown in Table 4-6.

The I_c vs. bending results in both the insert and conductor illustrated an increase in current carrying capability before degradation begins (Figures 4-24 and 4-25). This increase in I_c vs. bending strain has been contributed to a neutral axis shift condition in the conductor. The neutral axis shift condition has the potential of increasing the strain condition of the conductor. An analytical technique was developed to estimate this potential strain source.

Typical Nb_3Sn conductor current carrying characteristics are shown schematically with respect to intrinsic strain (Nb_3Sn fiber uniaxial strain) in Figure 4-27, as shown. The curve can be represented by an empirically-developed equation. The constants used to represent the typical Nb_3Sn characteristics (from J. Ekin, Reference 4-7) are taken at B = 12.5T and T = 4.2K. The effect of bending strain on the critical current can be estimated by integrating within the limits of the applied bending strain.

The state of prestrain (ε_i) in the matrix is important in considering the bending strain effects because it influences the position of the neutral axis during bending. To obtain the overall current carried by the conductor under a bending condition, $J_c(\varepsilon)$ is integrated over the different tensile and compressive regions of the conductor (averaging over the uniaxial strain curve). The changes in J_c without a shift in the neutral axis are nearly symmetrical about point A (Figure 4-27) and the net changes in J_c will be slight.

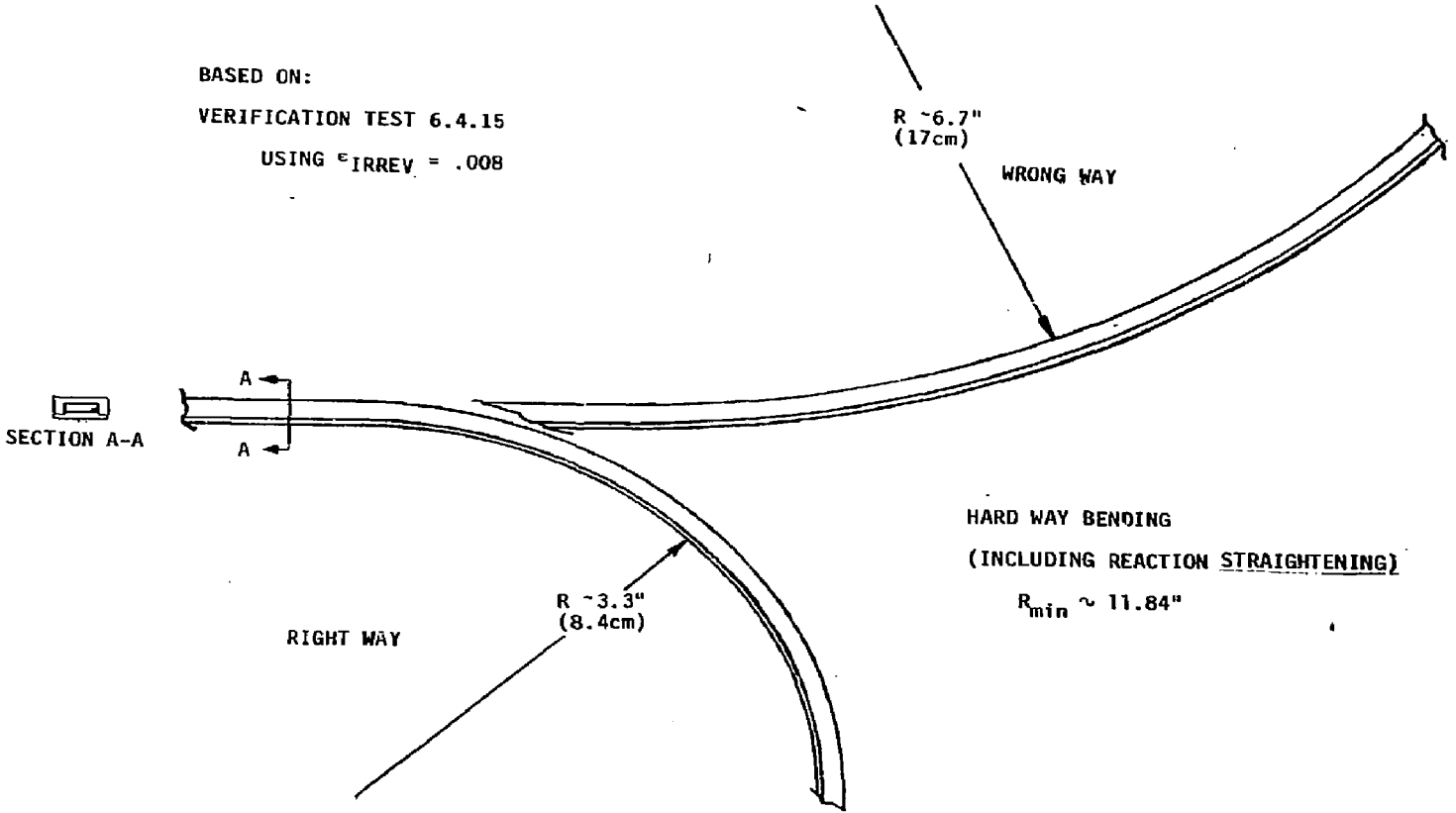

Figure 4-26. Bending Radius at Which Current Degradation Begins

Table 4-6. Mechanical Properties of Composite Conductor, Insert, and Housing (Section 8.0, Table 8-2)

Composite Conductor*

Test Temperature (K)	Yield Strength (ksi)
293	31.3
4.2	34.3

Superconductor Insert*

293	26.6
4.2	29.9

* Using minimum values from Table 8-2.

Using the rule of mixtures to develop the housing strength:

$$A_c\sigma_c = A_h\sigma_h + A_m\sigma_m$$

where: c - composite
h - housing
m - insert

@ 293K $.0888(31.3) = (.0662)\sigma_h + (.0226)(26.6)$

$\sigma_h = \underline{32.9 \text{ ksi}}$ (>31 ksi)

@ 4.2K $.0888(34.3) = (.0662)\sigma_h + (.0226)(29.4)$

$\sigma_h = \underline{35.97 \text{ ksi}}$

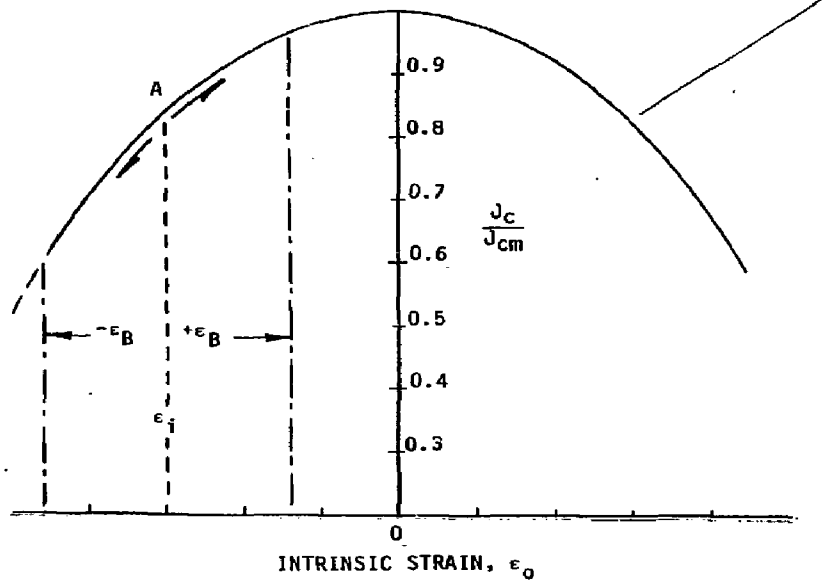

USING DEVELOPED SCALING LAWS (EKIN)

$$\frac{J_c(\varepsilon_i + x)}{J_{cm}} = \left[\frac{B^*_{c2}(\varepsilon_i + x)}{B^*_{c2m}}\right]^{n-p}\left[\frac{1 - \frac{B}{B^*_{c2}(\varepsilon_i + x)}}{1 - \frac{B}{B^*_{c2m}}}\right]^{g}$$

WHERE:

$$\frac{B^*_{c2}(\varepsilon_i + x)}{B^*_{c2m}} = (1 - a|\varepsilon + x|^u)$$

USING:

$a = 900$ ($\varepsilon_o < 0$)

$B = 12.5T$

$B^*_{c2m} = 21T$ (upper critical field)—

$n = 1$, $P = 0.5$, $g = 2.0$, $u = 1.7$ (for Nb_3Sn @ 4.2K)

THE EFFECT OF BENDING STRAIN ON THE CRITICAL CURRENT CAN BE ESTIMATED USING:

$$\frac{I_c}{I_{cm}} = \frac{1}{2\varepsilon_B}\int_{-\varepsilon_B}^{\varepsilon_B}\frac{J_c(\varepsilon_i + x)}{J_{cm}}\,dx$$

Figure 4-27. Schematic Diagram of the Effect of Bending Strain on the Critical Current

A large prestress condition influences the position of the neutral axis during bending (shifts the neutral axis from the center of the conductor toward the center of curvature). Under this condition, the changes in J_c (about point A) will no longer be symmetrical. A larger portion of the superconductor will experience an applied tensile strain and the net Jc value will, therefore, increase initially during bending. By knowing the amount of J_c increase and the initial prestress of the matrix (both developed from tests), an estimate of the additional strain (over the simple bending relationship, $\varepsilon_B = d/D$) due to the neutral axis shift can be developed. This technique is illustrated in Figure 4-28, showing both the bending test results (test no. 6.4.15) and the developed ε_B vs. Additional Strain curve. The assumptions used in developing the curves were:

1) The Furukawa conductor can be represented by typical Nb_3Sn conductor characteristics.

2) A prestress condition of -0.6 percent was assumed. This was necessary because test no. 6.4.5 that develops this value has not been performed as of this writing. A maximum compressive state was assumed in order to exaggerate the neutral shift effect.

The conclusions from the curve are:

1) There is a neutral axis shift in the prototype conductor.

2) The effect of the neutral axis shift is small in terms of additional strain (<.0005).

3) In fact, that the neutral axis shift produces an enhancement in critical current carrying capability at the prototype bending strain condition.

4.6 CONCLUSIONS

Tension preload values on the conductor pack of 300, 400, 500, and 600 pounds were included in this study. The results indicate that the 600-lb tension preload produced the optimum margin condition. It was also apparent that the margin of safety variation between the different preload values was relatively small with the 300-lb value approaching zero (MS = 0.03, Figure 4-5). It is recognized that the 600-lb preload value is relatively high with respect to past winding experience. Therefore, it is recommended that a range of preload values (300 lb $\geq$ WP $\leq$ 600 lb) be used in the trial winding and the maximum acceptable pre-load value (based on observed response) be used in the coil. The above allowable was developed based on the Nb_3Sn strain limitation established from a literature review. The planned verification test to develop the actual strain limitation for the Furukawa conductor has yet to be

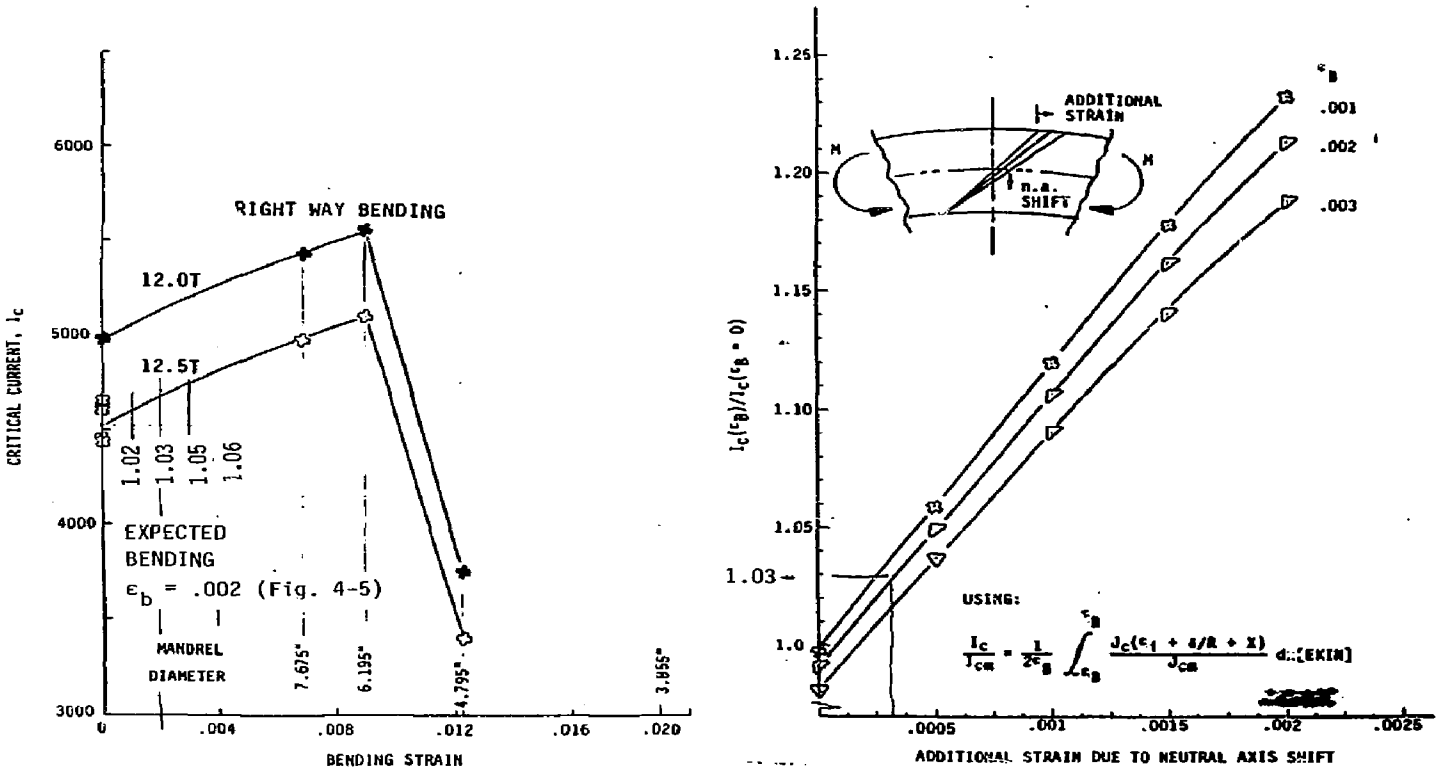

Figure 4-28. An Estimate of the Additional Strain due to Neutral Axis Shift can be Developed Using These Figures

performed. However, the bending test results on the prototype conductor in the verification test program have produced data which shows that the irreversable strain values match and/or exceed the initial design estimate (Table 4-1), and the fabrication specification requirement (Refrence 4-2).

Furukawa, in order to meet production dates, incorporated three reaction diameters in the manufacturing of the prototype conductor. The diameters used were 60, 70, and 80 cm. This causes conductor bending strain variation throughout the conductor pack as illustrated in Figures 4-5 and 4-6.

Conductor pack axial motion was included as a possible strain source in the conductor bending strain at the outer radius position at the fix to the magnet case. The potential axial pack movement (developed from "worst case" assumptions from all sources) indicated that a pack precompression be employed during fabrication to limit such motion. The resulting bending strain condition (using maximum predicted motion) is shown in Figure 4-6. It should be noted that the margin of safety for this particular area can be increased by specifying the 80-cm reacted conductor for the first and last double pancake.

The 2-D model used to represent the magnet case included both the A2O and the insert coil. The A2O case was included to provide the boundary condition on the welded attachment between the two coils. The Kelley and Mars mode loading condition were imposed on the model. Both normal and abnormal loading conditions were incorporated. The abnormal condition is a low probability electrical fault event for which reduced safety factors are utilized. There is also a category known as disaster conditions for which design is improbable. Events such as open/short circuits at any coil terminal could cause runaway load increases - these conditions are prevented by proper design of the power and protection system which is an LLNL responsibility. If such an event should occur, the insert coil could not be expected to carry the resulting loads without some level of damage. The worst design condition for the A2I case is defined in the DRD, which limits A2I current peaking to 15 percent of normal operating current. This design condition is classified as a single fault condition. It is assumed that an equivalent field peaking accompanies the current increase, thus mechanical radial loads increase by a factor of 1.15^2 for the fault (abnormal) condition. The resulting margins of safety for both the normal and abnormal loading conditions for the magnet case were positive (Figures 4-11 and 4-13). The stress level and design cyclic condition produced an initial flaw size in the fracture mechanics analysis that can be economically detected. In addition, buckling is not a design consideration for the bobbin (inner ring of the case), and the stress concentration around the port opening in the case side wall is within allowable.

The thermally-developed stresses in the magnet case are low because of the relatively low thermal gradients from wall to wall. There is a controlled condition that is to be followed during the cool-down/warm-up transients. This temperature control between the two coils is required in order to limit the bending stress in the welded attachment (opening mode between coils) and in the outer ring of A2I under the shims (for the closing mode). The relative temperature limits for the coils is presented in Figure 4-17.

A summary of the conclusions are:

- The margins of the monolith and copper housing are a function of the winding tension.

  Monolith, MS = +0.15/+0.03, normal/abnormal at W.T. = 300 lb (Figure 4-5).

  Cu Housing, MS = +0.28/+0.56, normal/abnormal at W.T. = 600 lb (Figure 4-8).

- The winding tension (between 300-600 lb) shall be selected by LLNL.

- The splice test illustrated load capability well above the operating conditions.

- The maximum magnet case stress condition produced a positive margin.

  Kelley Mode, abnormal, MS = +0.25 (Figure 4-11)

  Mars Mode, abnormal, MS = +0.67 (Figure 4-13)

- Fracture mechanics predicts an initial flaw size that can be economically detectible.

- Welded attachment, MS = +0.04, Kelley mode, normal (Figure 4-15).

- Stress concentration around tunnel port, abnormal, MS = +0.25 (Figure 4-19).

- Thermal stress in magnet case - cool-down, MS = +1.30 (Figure 4-20).

- Grid insulation wrapped on bobbin, MS = +2.1 @ R.T. (Figure 4-21).

- The verification test results on the Furukawa conductor illustrated bending strain capability of approximately 2X design strain conditions before any recorded current carrying degradation.

4.7 REFERENCES

4-1 "MFTF Design Requirements Document," published by Lawrence Livermore National Laboratory, dated 17 August 1982 (Revised 20 May 1983).

4-2 Baldi, R. W., "MFTF Magnet System Program Specification for High Field Nb_3Sn Coil Conductor," Specification No. 71E0034, Rev. B, dated 12 December 1983.

4-3 "STANSOL II" - Structural Analysis of Non-Homogeneous Solenoids, Mechanics Research Inc., September 1975.

4-4 Cronk, M. J., "Solid SAP (GDSAP) User's Manual," General Dynamics Convair, CASH-CIH-74-008 dated October, 1977.

4-5 McCormick, C. W., "MSC/NASTRAN User's Manual, MacNeil-Schwendler Corp., Los Angeles, CA, February, 1978.

4-6 Pickering, J. L. & Baxter, W. F., "Final Stress Report for the High Field Nb_3Sn Coil," Volume IX, dated February 1984.

4-7 Foner, S. and Schwartz, B., Superconductor Materials Science, Chapter 7, "Mechanical Properties and Strain Effects in Superconductors," by Ekin, J. W., Plenum Press, New York, NY, 1981.

5.0

THERMAL ANALYSIS

5.1 Objectives/Requirements

The Design Requirements Document (DRD), Reference 5-1, sets forth the requirements and criteria to guide the design/analysis of the magnets, interfaces, and the system level considerations influenced by the magnets. Thermodynamically related requirements which are relevant to the A2I coil design/analysis are shown in Table 5-1. The requirements are categorized under the four major thermodynamic task headings: cryostability, thermal conditioning, helium heat load, and magnet/lead safety.

The DRD paragraph or auxiliary reference is indicated for each requirement except the 5 atm. burst disc pressure setting for quench protection, which has been an accepted practice during previous analyses.

5.2 Cryostability

The cryostability of the conductor, based on the current sharing criteria for the high field Nb_3Sn coil, requires unconditional recovery at 115 percent of the operating current and the operating field or at the operating current and 107.5 percent of the operating field. Out of the two conditions, the one with higher current is more critical and it is at this condition the cryostability of the conductor is evaluated.

The cryostability evaluation requires cooling capability at the surface of the conductor in the helium bath and joule heating of the conductor when all the current is in the copper portion of the conductor. Both the cooling capability and joule heating are generally expressed in terms of heat flux at the conductor surface vs. conductor temperature for easy comparison. The unconditional recovery requirement means that the joule heat flux should be less than the cooling heat flux at all conductor temperatures. The helium cooling heat flux is sensitive to the conductor orientation and geometry, insulation gap and openness, and conductor location in the winding. The joule heating depends on the resistivity and cross-sectional area of the copper in the conductor, and wet surface area.

The cryostability margins of various conductor locations/splices were compared in order to find a "worst" location. The "worst" location was found at the first layer of the conductor pack where the peak field is 12.52 tesla. Figure 5-1 shows the cryostability mapping of the regular conductor at the worst location.

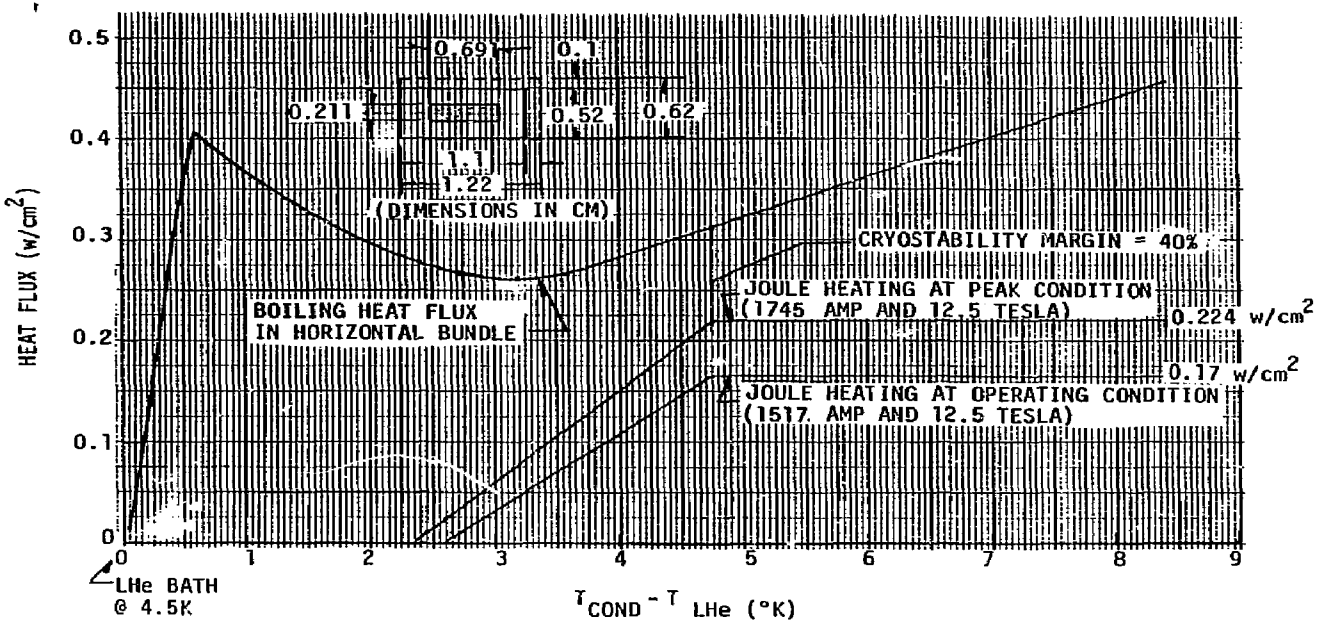

Figure 5-1. A2I Coil Conductor is Unconditionally Cryostable with Required Margin

Table 5-1
Design Requirement Study

	DRD Paragraph
Cryostability	
o Conductor Temperature Less than Superconductor Critical Temperature with Design Current in Copper	2.2.4
o Minimum Superconducting Margins Critical Current (%) : 100.0 Cryostable Field (%) : 7.5 Cryostable Current (%) : 15.0	2.4.6
Thermal Conditioning	
o Capable of Cool-down/Warm-up in 120 Hours (Specify Flow Rate)	2.4.7
o Inlet Helium Temperature Schedules	Letters JHV to JWW JWW to JHV

Cool-down		Warm-up	
Time (Hr)	Temp (K)	Time (Hr)	Temp (K)
0	220	0	80
35	95	>65	300
55	95		
>80	5		

o Temperature Gradients not Exceeding Stress Limits	2.4.7
LHe Heat Load	
o LN Liners Conduction and Radiation: <0.80 w/m^2	2.8.2
o Max. Allowable Heat Load (Non-neutron): 40 watts (2 magnets)	2.7.5
o Max. Helium Quality at Exit of Coil: 2.5% by weight	2.7.5
Lead/Magnet Safety	
o Thermal Inertia Design of Lead for 10-Minute Uncooled Operation	2.7.13.4
o Coolant Helium: 0.11G/sec/KA/pair	2.7.5
o Burst Disc Pressure: 5 atm.	

The highest operating current occurs in the Kelley Mode operation (1504 amp). This, however, has been increased to 1517 amps to reflect the loss of turns in first layer joggle. The first layer has only one half as many turns as other layers. The cooling heat flux curve is constructed using a correlation by E. Christensen (Reference 5-2). General Dynamics has conducted heat transfer tests for various conductor/insulation/orientation combinations and these test results along with others in the literature have been used to construct the correlation equation.

A cryostability margin of 40 percent over the requirement was developed. In addition to the high cryostability margin, this conductor has a high temperature margin. The current sharing temperature of 7K (or 2.5K over the bath temperature) results because of the high current margin of 100 percent (or more). The high field Nb_3Sn conductor is very cryostable and will not experience a quench easily.

5.3 Thermal Conditioning

The thermal conditioning operations are required in any magnet system which has to operate at cryogenic temperatures. These operations include cool-down, warm-up, and regeneration. A magnet experiences rapid temperature changes during the thermal conditioning. A carefully designed thermal conditioning operation is necessary for the safety of the magnet.

5.3.1 Cool-down/Warm-up

The Design Requirements Document stipulates that the cool-down and warm-up be completed within 120 hours without generating excessive thermal stress in and between magnet components. The analysis is directed to find the helium flow rates which optimally accomplish these thermal conditioning operations. The analysis also identifies any interface problems between magnets that might arise during these operations.

The flow rate requirement and cool-down/warm-up performances are sensitive to the helium inlet temperature schedule. The present helium inlet temperature schedules have been developed jointly by LLNL and General Dynamics (Reference 5-3) based on the experience acquired from the Yin-Yang Tech. Demo. experiment.

A half-symmetric computer model with 345 nodes and 805 resistors is constructed according to the format of a computer code called Convair Thermal Analyzer (Reference 5-4). The heat transfer characteristic in the conductor pack is noticeably different from those at the peripheral components like grid insulation and plenum. The magnet cross-section thus is divided into five sections, each with a helium flow. The cross-section and node distribution is shown in Figure 5-2.

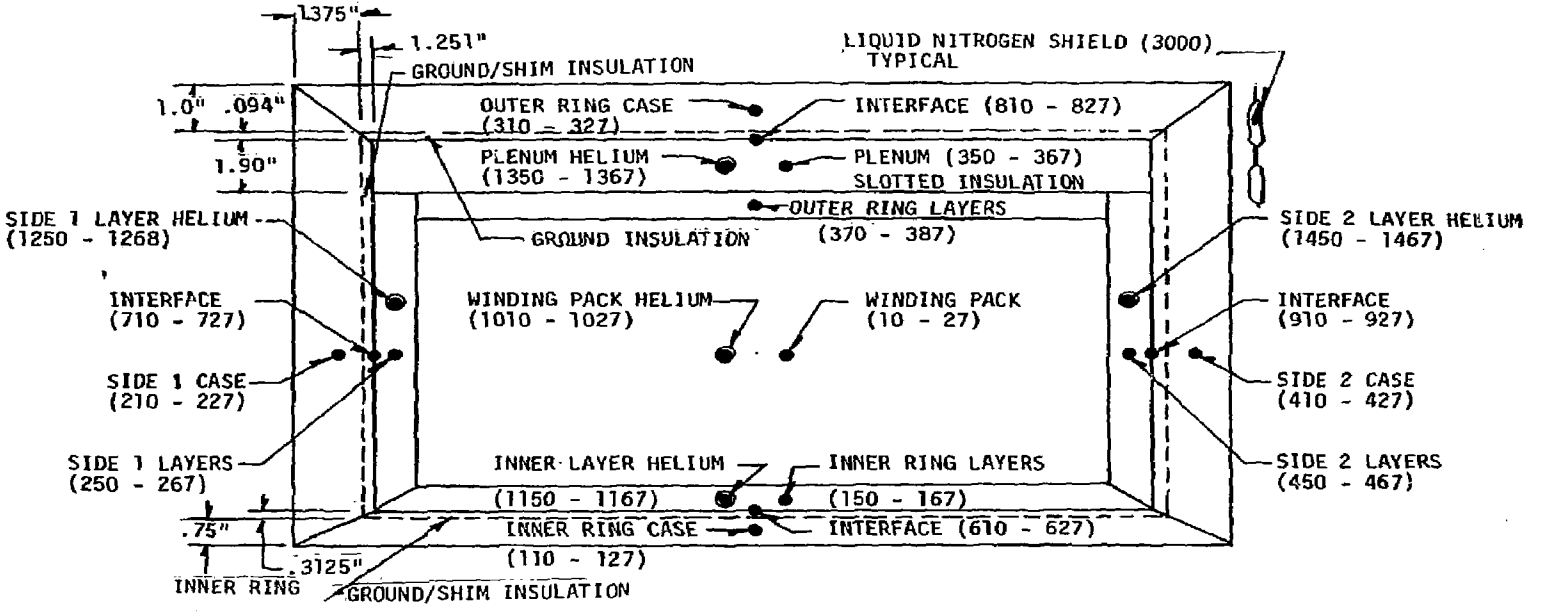

5-2. A2I Coil Cool-down/Warm-up Model Cross-Sectional Node Distribution

Both transient and steady-state solutions are obtained. The transient solutions give time-dependent temperature of the nodes in the model during the cool-down or warm-up operation and the steady-state solution finds the temperature condition during the operation as well as heat loads from the LN_2 liners. The cool-down is assumed completed when the slowest cooling component reaches within 2-3K of its steady-state temperature. The warm-up is assumed completed when the coldest spot in the magnet reaches 278K (500R). The vacuum system can be opened for service at this temperature without causing water vapor condensation. The temperature histories of the magnet components at the cross-section of helium exit is used to determine the cool-down/warm-up times and the flow rates. Figure 5-3 shows the cool-down histories at the helium exit for a recommended flow rate of 4.0 g/sec.

The temperature histories show a very uniform cool-down of all of the magnet components. The cool-down is completed by 95 hours. The flow rate recommendation of 4.0 g/sec is not made entirely as a result of the cool-down history. A flow rate of 3.4 g/sec meets the cool-down time requirement with an adequate margin. The flow rate, however, has been increased to avoid the excessive temperature difference between the two nested coils, A2I and A2O.

The temperature gradients within the magnet case are not a serious concern during the cool-down or warm-up operation of this coil. The coil has a very high cross-sectional area-to-length ratio. The strong conductive heat transfer in the magnet components effectively reduce the temperature gradients in the components. The temperature profiles of various A2I coil components during the cool-down are shown in Figure 5-4. The warm-up temperature histories of the magnet components at the helium exit are shown in Figure 5-5 illustrating very uniform warm-up results. The warm-up is completed by 102 hours. The temperature profiles of the magnet components during a warm-up are shown in Figure 5-6. Small longitudinal temperature gradients are found at all the magnet components as they were during a cool-down.

5.3.2 Temperature Difference Between Two Nested Coils

The temperature difference between two nested coils has been investigated. A maximum temperature difference of 22.8°K was predicted and presented at the Preliminary Design Review (PDR). The prediction was based on the cool-down flow rates of 3.4 g/sec and 21.0 g/sec for A2I and A2O, respectively. The design changes of the A2O coil support structure, since the PDR, required an increase of cool-down flow rate to 24.0 g/sec in the A2O coil. The faster cool-down in the A2O coil resulted in a maximum temperature difference of 45.1°K. This temperature difference was determined to be too high for a fault condition that might develop at time of maximum temperature difference. The worst fault condition results if the helium flow to a warmer coil is completely

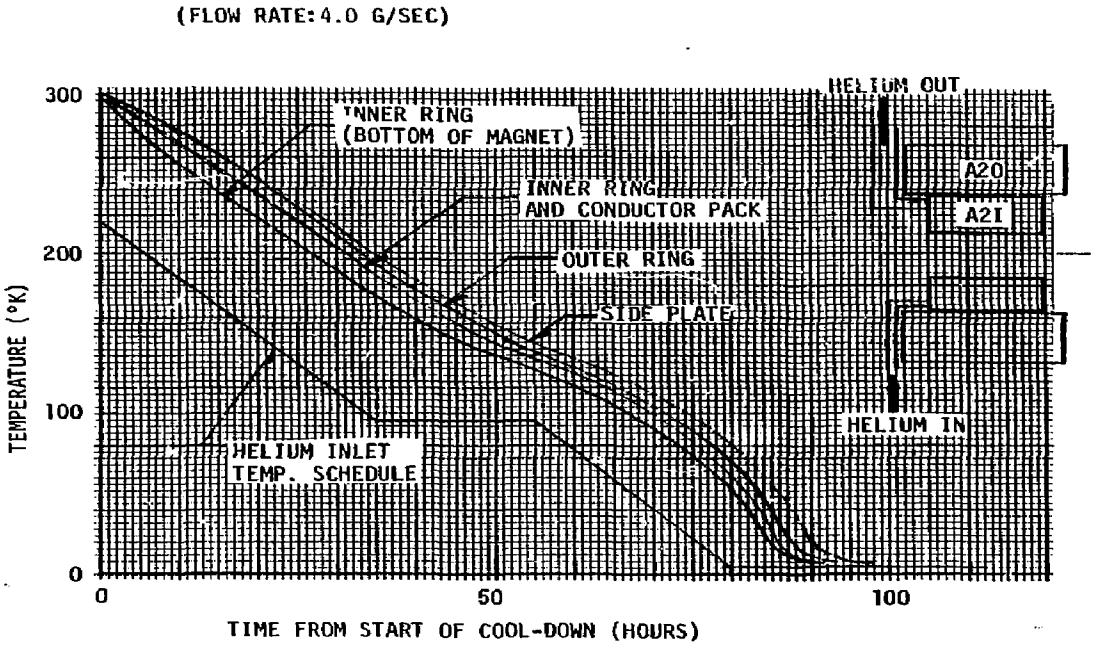

Figure 5-3. Temperature at the Top of the A2I Magnet Indicates the A2I Coil Can be Cooled in the Allotted Time

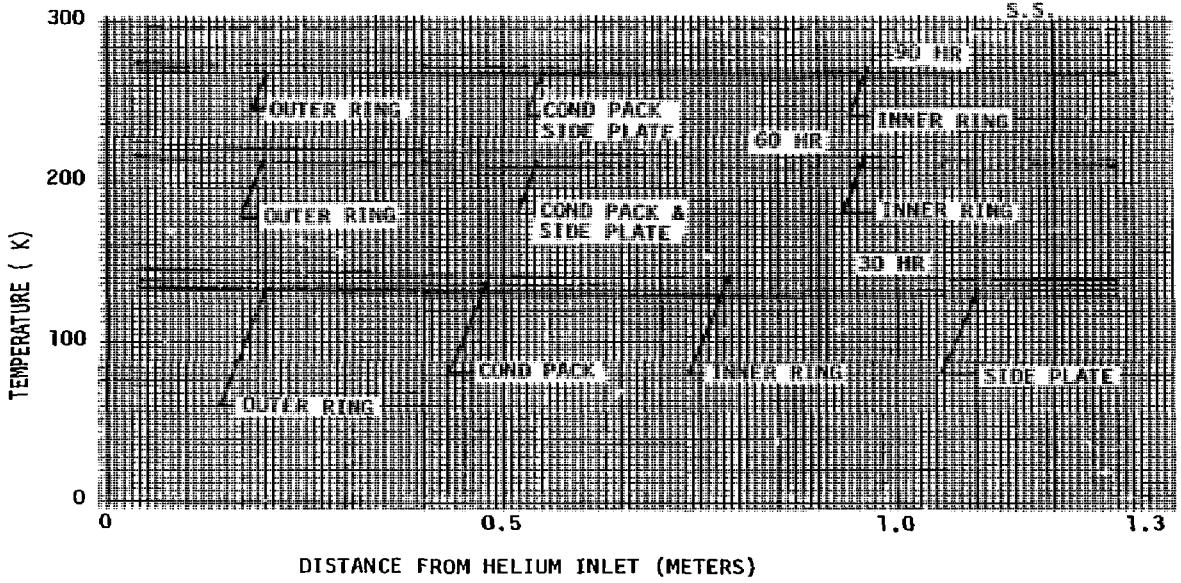

Figure 5-4. High Field Coil Temperature Gradients During the 120-Hour Warm-up are Small

blocked. A new cool-down flow rate of 4.0 g/sec in A2I resulted in a maximum temperature difference of 27.6°K. Typical temperature profiles of the two nested coils for the temperature difference are shown in Figure 5-7 along with the history of the average temperature difference.

The series of studies illustrated the sensitiveness of the temperature difference to the cool-down flow rate combination and strongly suggests separate flow control to these two nested magnets. The following table summarizes the result of three cases of flow combination.

Flow Rate (g/sec)			
A2I	A2O	ΔT (°K)	Time (Hr)
3.4	21.0	22.8	80
3.4	24.0	45.7	80
4.0	24.0	27.6	40

The temperature difference during a warm-up is presented in Figure 5-8. The temperature differences are small and, except for a short period around 50 hours, the A2I coil is cooler than the A2O coil.

The stress analysis (presented in Section 4.0) developed allowable temperature limits between coils as presented in Figure 5-9. This figure illustrates the two temperature difference boundaries, one for A2I warmer case and the other for A2I colder case. When A2I coil is warmer, the two coils are engaged and kept separated only by the shims. The peak stress is in the coil case under the shims. When the A2I coil is colder, the two coils tend to separate and the peak stress is found in the welded attachment.

The most desirable cool-down/warm-up operation, from the temperature difference standpoint, is when the temperature difference is along the middle of the two boundaries (Figure 5-9). The present cool-down operation "X" resulted in temperature differences near the middle of the two boundaries. The warm-up temperature differences "O" are found closer to the lower boundary.

Thermal instrumentation of the axicell coils, using CLTS (Cryogenic Linear Temperature Sensor) will allow monitoring of the case temperatures during cool-down/warm-up. All the nested magnets (A2IE, A2IW, A2OE, and A2OW) are instrumented for temperature monitoring. The temperature sensors at the outer case of the A2I coil and inner case of the A2O coil will be used for ΔT monitoring.

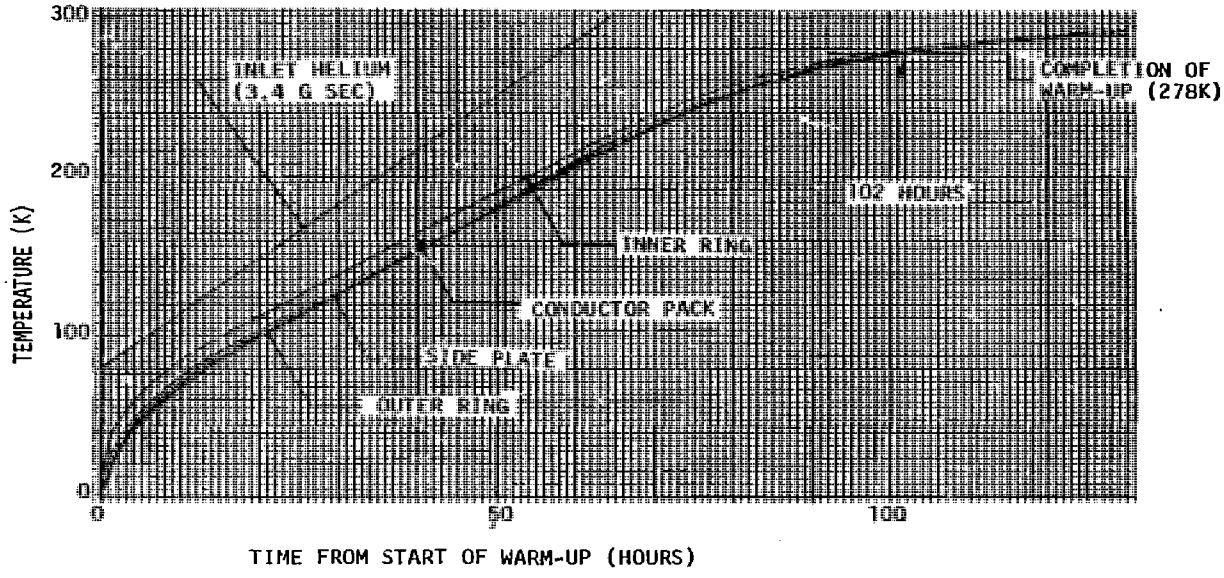

Figure 5-5. The Temperatures at the Top of the Magnet Indicate that the A20 Coil will be Warmed Up Within 120 hours

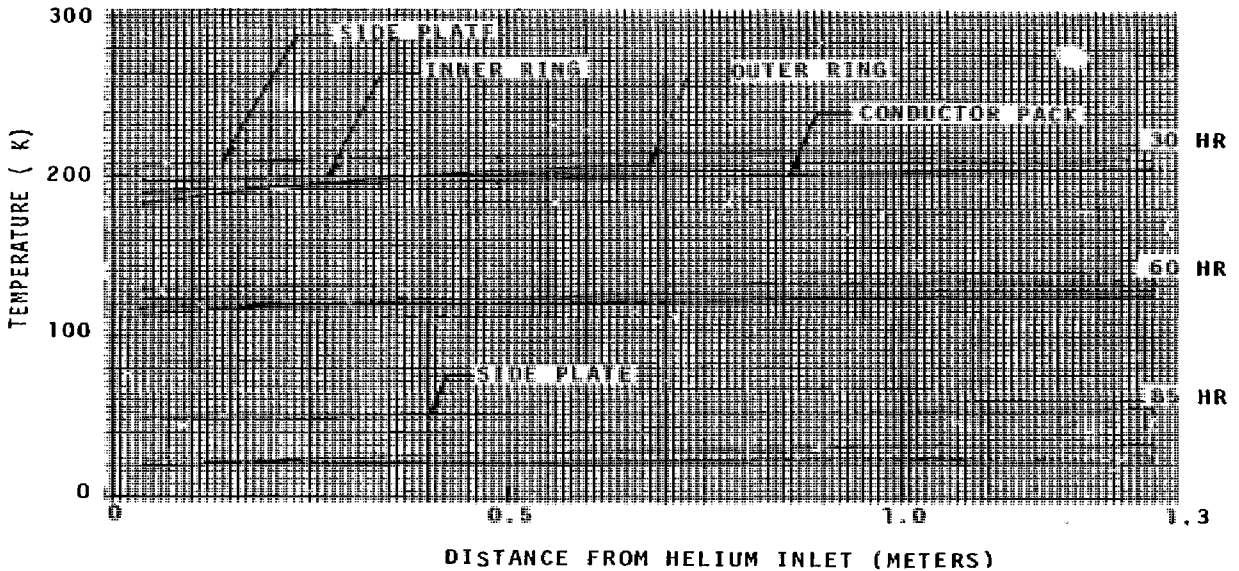

Figure 5-6. Large Cross-Section and Short Helium Path Resulted in Small Temperature Gradients In and Between the Magnet Components During the Cool-down

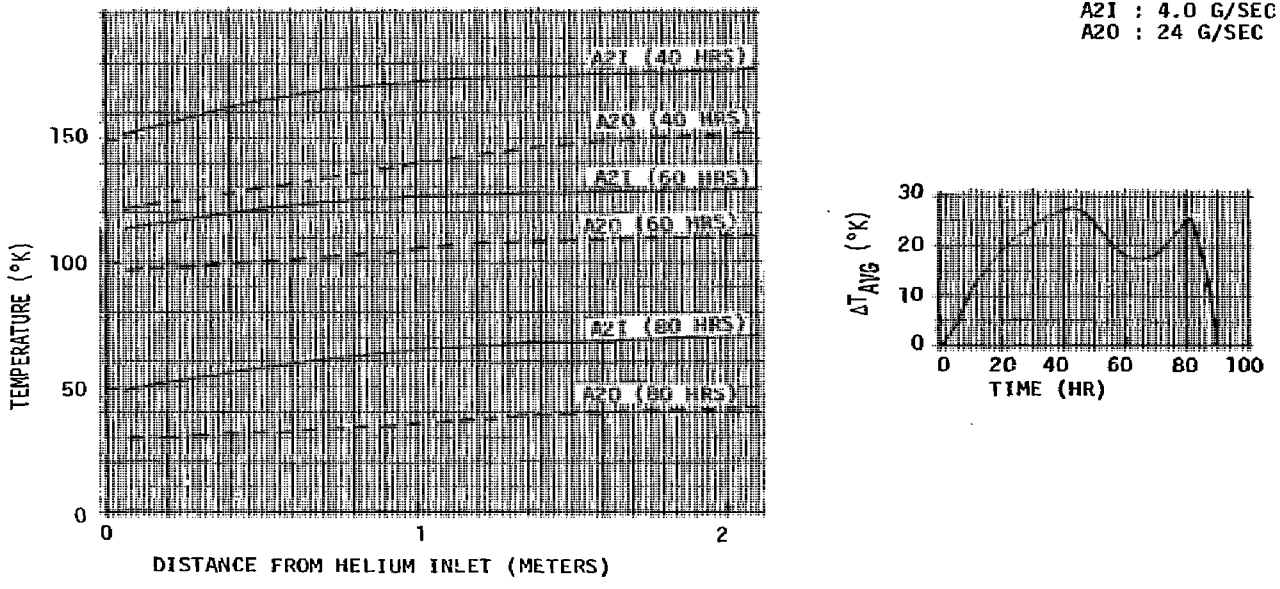

Figure 5-7, Temperature Profiles of the A2O Inner Ring and A2I Outer Ring Show a Maximum Temperature Difference of 27.6°K at 40 Hours

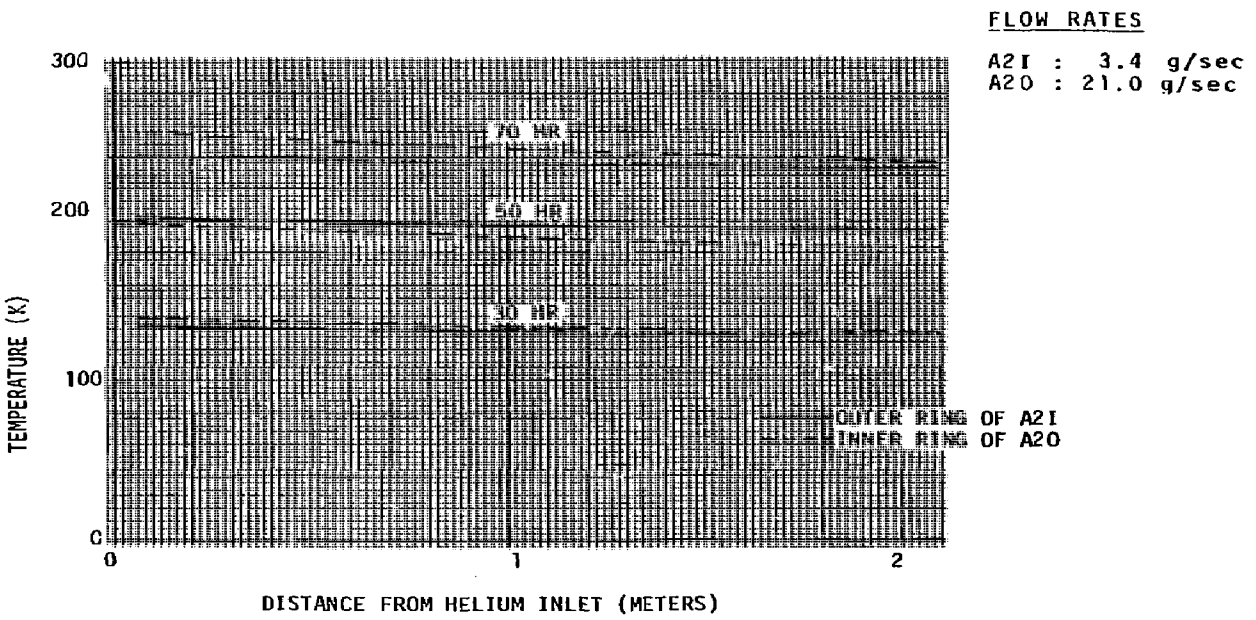

Figure 5-8. Temperature Profiles Show that the A2I Outer Ring is Slightly Cooler than the A2O Inner Ring During Most of the Warm-up Period

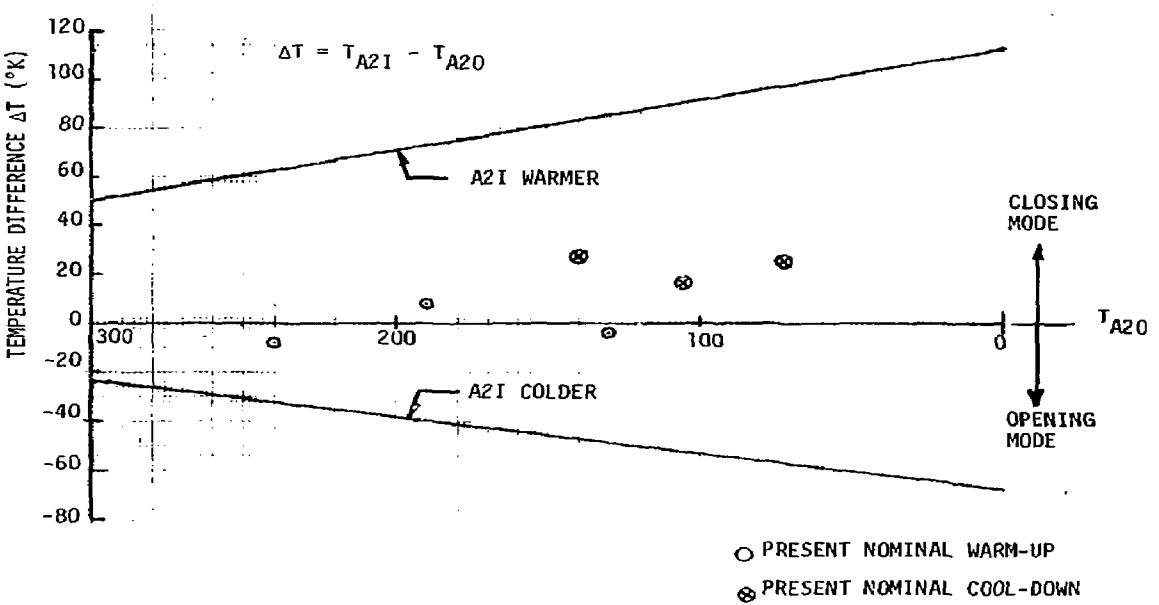

Figure 5-9. Temperature Difference Control Boundaries and Nominal Cool-down/Warm-up Predictions

Another operating parameter is the reaction time required if flow should stop in one of the nested magnets. The reaction time is determined from the minimum allowable temperature differential excursion divided by the maximum time rate of temperature change. The reaction times for the "worst" fault conditions are 25 hours during the cool-down and 10 hours during the warm-up. The "worst" fault condition occurs if the helium flow to the warmer magnet stops during the cool-down or the helium flow to the colder magnet stops during the warm-up.

5.4 Helium Heat Load

The DRD sets a helium heat load ceiling of 20 watts for an A2I coil. The 20 watts includes only the non-neutron, steady-state heating. The periodic neutron heating is accounted separately. The total helium heat load is made of several components. Some of these components are from internal sources and others are from external sources. The heat loads from coil splices and lead splices are internal whereas the radiation on the magnet case and fluid lines, heat loads from external instrumentation, stack and vapor-cooled leads are external. This coil is supported by the inner ring of the A20 coil and, thus, the support heat load is not to be considered. The steady-state heat loads are shown in Table 5-2.

The heat load from the coil splices is calculated based on 3×10^{-8} ohm resistance. The radiation heat loads on the coil case and fluid lines depend on the thermal shield design. The latest design of the thermal shields and their supports call for 1.1 watts/m^2 for the coil case and 0.8 watts/m^2 for the fluid lines.

The higher heat flux on the coil case is due to higher conduction heat load through the shield support. The stack and vapor-cooled lead requires special attention because of its unique design requirements and severe temperature variation within the components. A multi-node finite difference computer model is used for the detailed analysis. The stack heat load has been increased substantially from the PDR prediction (Reference 5-5). The main reason for this increase is because of the uniform design philosophy which uses the same size stack for all the magnets and same overall lead geometry designed for the higher current solenoid leads. The heat load contributed by the stack to the overall vapor cooled lead cooling requirement, therefore, is proportionally higher for this low current coil than for the other coils. A helium specific flow rate of 0.14 g/sec/KA/pair is recommended.

The higher heat load from the stack, however, does not affect the performance or safety of the magnet. It only increases the helium liquefaction load.

The total helium heat load exceeds the DRD limits. Every effort has been made to optimize, whenever it was possible, the design of the components that affect the heat load. The high helium heat load, however, will not affect safety or performance of the magnet.

Table 5-2.
High Field Insert Coil Steady-State Helium Heat Load

	Heat Load (Watts)/Coil
Radiation from LN_2 Shield	3.88
Coil Splices (27/coil)	1.82
o 6.25 tesla field o 8.5" overlap o 60/40 solder o 3 solder surfaces o 2 Nb barriers	
Lead Splices (5/coil)	0.25
Fluid Lines (0.8 w/m^2)	3.86
o Supply (1-1/4ø x 312") o Return (2"ø x 100") o Stack (10"ø x 130") o Tunnel and Transition (6 ft^2)	
External Instrumentation	1.00
Vapor-cooled Lead and Stack	11.00*
o 0.14 g/sec/kA/Pr** o Tube RRR = 30, bus RRR = 90 o 14 tubes 3.5" x .75" x section (common to solenoid 3kA lead) o Unwetted bus = 47 inches long	
S.S. Heating Total	21.81
S.S. Heating Target	20.00
Neutron Heating/Coil	49.20

* Add liquefaction load for coolant vapor 0.21 g/sec.

** Specific coolant flow requirement established by detail stack analysis and higher than DRD because of commonality decisions on stack, VCL, and transition bus sizes.

5.5 Quench Pressure and Venting

The conditions that maximize pressure in the magnets during a quench correspond to the most rapid propagation of the normal zone possible and maximum heat deposition in the helium contained within the magnet cryostat. This heat vaporizes the helium which causes the pressure to rise until the pressure relief burst disc opens, and thereafter the pressure response is determined by the balance between the vent system restriction to the helium flow and the energy and mass balances within the magnet.

The quench pressure and venting is analyzed with a computer code called "MAGPRS" (Reference 5-6). This analysis requires a heating scenario which gives the time history of the magnet heating during the quench. The scenario assumes that the normal zone initiates with vacuum failure and air condensation on the magnet case and helium inlet pipe. The vapor generated at the inlet pipe rises into the high field zone of the winding, normalizes the conductor and eventually permits the normal zone propagation. The results from the three-dimensional propagation analysis (Reference 5-7) for MFTF conductor and/or equations developed for maximum propagation velocities are used to predict the maximum normal zone growth rate and heating for the heating scenario. In the computer analysis, this heat rate is assumed deposited in the LHe to drive the energy and flow balance to predict the thermodynamic process in the dewar and vent system. The analysis finds the helium in the dewar, pressure, and temperature as a function of time.

The return lines of three axicell coils are plumbed together such that a simultaneous quench of these coils is considered. The results are shown in Figure 5-10. The helium mass (M), pressure (P), and temperature (T) are shown as a function of time along with the heating scenario (Q) in solid lines. The main concern of this analysis is the pressure history and the second pressure peak after rupture of the burst disc (5 atm or 73.5 psia). A secondary pressure peak of 60 psia is predicted. A limiting pressure of 102 psia is used to guide the magnet and plumbing design. The pressure trace during an isolated quench of the A2I coil alone is shown by the dotted line. For this case, a peak pressure of 30 psia is predicted. This low pressure indicates that the 2-inch return line is adequte.

The highest possible pressure condition is when all the MFTF magnets quench simultaneously and the 16-inch and 22-inch quench manifolds are saturated due to the simultaneous quench of all the magnets. For this operationally conservative case, a peak pressure of 7 atm (102 psia) is predicted. Therefore, the magnet pressure boundary should be designed for 7 atm pressure differential.

5.6 Thermosiphon Helium Flow and Vapor Quality

Supply of liquid helium to the magnet during the operation of the system is achieved through a natural convection circulation. This condition is called thermosiphon helium flow, which develops in a loop made up of the helium dewar, magnet, and piping. The thermosiphon helium flow schematic is shown in Figure 5-11.

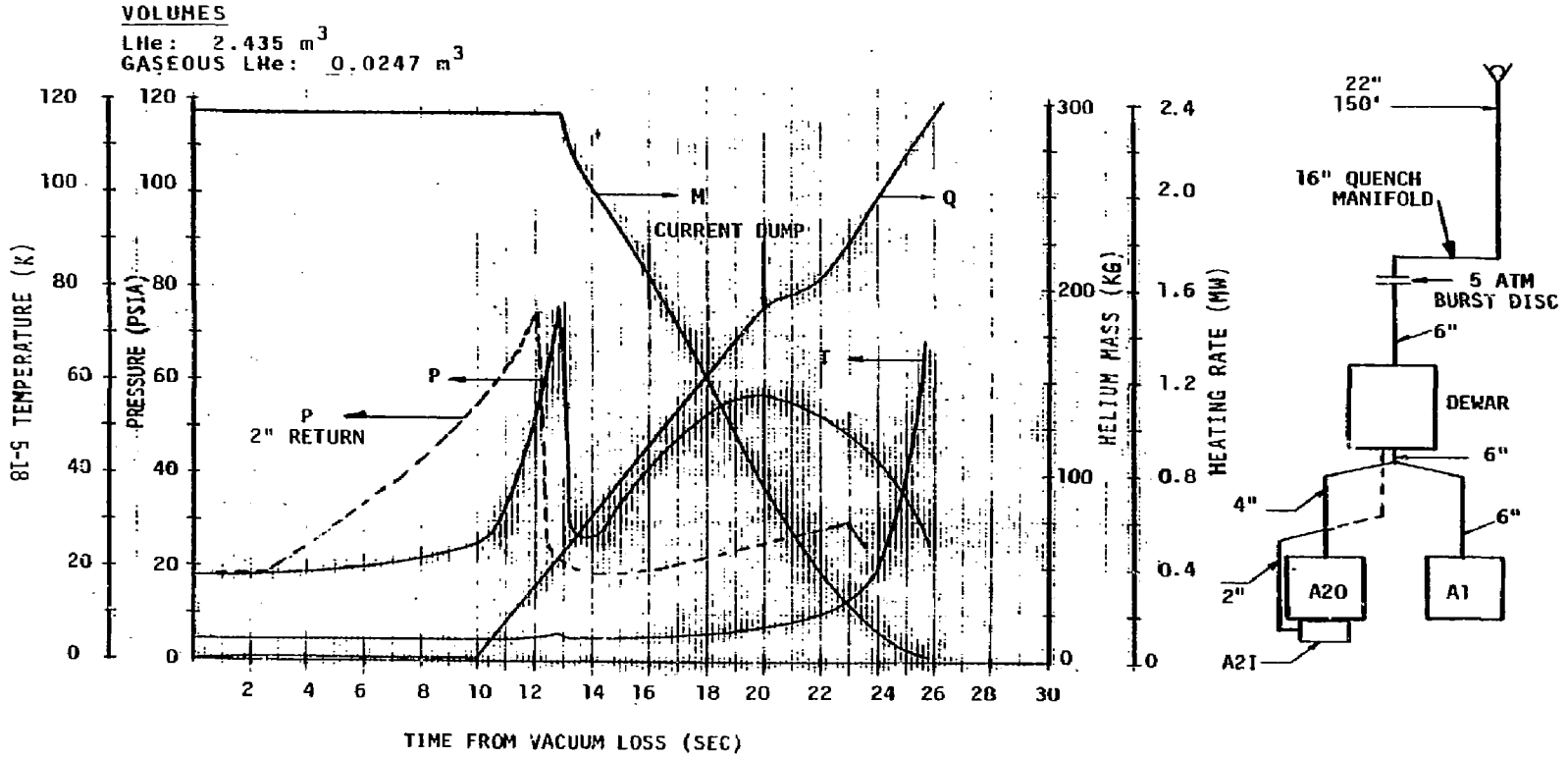

Figures 5-10. A 6-inch line and burst disc is required for Quench Venting of Axicell (A1, A2O, A2I) Coils

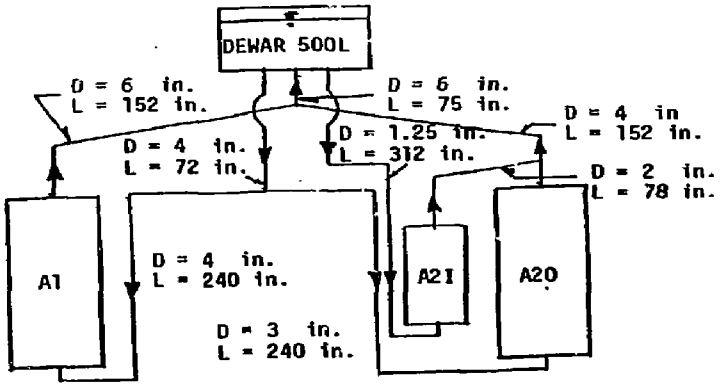

Figure 5-11. Axicell Final Configuration System (Nominal Line Sizes)

The major driver of the helium flow is heating in the magnet which induces a buoyancy force in the loop. The helium circulation is greatly accelerated when the heating generates bubbles. The bubble, however, can cause problems in a magnet when too high a vapor quality results in the winding, or bubble accumulation generates a local dry spot in the winding or around the leads. The DRD limits the maximum helum quality at the exit of each coil to 2.5 percent by weight. The exit quality can be controlled if the flow resistance is controlled. The total flow resistance in the loop is most easily controlled with variation of inlet pipe size since exit (return) lines are inherently large because of the quench venting requirements.

The available tool to analyze the thermosiphon helium flow at GDC is a computer program designed for steady-state heating operations (Reference 5-8). With all the flow resistances properly accounted for, this computer analysis finds a steady-state helium flow which simulates the real helium flow at the end of the 30-second neutron heating if an equivalent heating can be determined. The equivalent heating may be obtained by iterative process if we know:

1) Net helium heating during the 30 seconds.

2) Helium condition of the cryostat at the beginning of the neutron heating.

The estimated temperature rise of the conductor during the neutron heating without helium cooling suggests that most of the neutron heating to the conductor pack will be deposited to the helium immediately. A similar calculation for the case heating showed only 20 percent will contribute to the helium heating and circulation during the 30-second pulse. This heating scenario finds the net helium heating during the 30 seconds amounts to steady-state heating plus 85 percent of the neutron heating. The thermosiphon helium flow computer analysis with steady-state heating only, showed that most of the helium in the cryostat is slightly subcooled. The subcooled state of the helium is assumed to be that of the cryostat at the beginning of neutron heating. This is a reasonable assumption because the cryostat helium will be replaced approximately twice with the subcooled helium during the 5-minute cycle.

During the neutron heating, the cryostat helium temperature rises and bubbles will be generated when it reaches the saturation temperature. In the analysis, it was assumed that another equilibrium is reached at the end of the 30-second neutron heating and this state can be found with the equivalent heating in the computer analysis. The equivalent heating, and thus the second steady-state, can be obtained after several iterations starting with an assumed heating state. The computer analysis with the assumed heating finds a helium flow and enthalpy of helium in the cryostat. The enthalpy change between the beginning and end of the 30-second heating is subtracted from the net helium heating

to find the heat input for the next iteration. This analysis usually required 4 to 5 iterations until heat inputs of two consecutive computer runs during the iteration become identical. The final computer run gives the second steady-state which simulates the peak vapor quality flow at the end of the 30-second neutron heating. The flow parameters at the beginning and end of the heat pulse is shown as follows:

	Supply Line (in)	Heating Mode	Heating Rate	Flow Rate (g/sec)	Exit Quality (wt %)
Beginning	1.25	S.S.	8.0	98	0
End	1.25	Equivalent	152	241	2.10

A peak vapor quality of 2.1 percent by weight is found.

5.7 Conclusion

The high field Nb_3Sn coil is a very cryostable and safe magnet with a cryostability margin better than 40 percent and a temperature margin better than 2.5°K.

This magnet can be cooled down or warmed up within 120 hours without excessive thermal stress. A flow rate of 4.0 g/sec is recommended. The temperature difference between the two nested coils will be within the allowable limits during the nominal thermal conditioning operations. An excessive temperature during a fault condition can be avoided with separate flow control between the inner and outer coils. The reaction times for the "worst" fault conditions are 25 hours during the cool-down and 10 hours during the warm-up, thus allowing sufficient time for detection and correction.

The peak pressure during the simultaneous quench of three axicell coils is 65 psia. A design pressure of 102 psia (7 atm) is recommended for plumbing and facility design. The Stress group has verified that this magnet is safe at 150 psia.

5.8 References

5-1 MFTF Design Requirements Document, Lawrence Livermore National Laboratory, dated 17 August 1982, Revised 20 May 1983.

5-2 Christensen, E. H., "Pool Boiling Helium Heat Transfer from Magnet Conductor Surfaces," AIChE 1982 Annual Meeting, 4th Intersociety Cryogenic Symposium, Los Angeles, CA, November, 1982.

5-3 Christensen, E. H. and J. W. Wohlwend, "Design Helium Inlet Temperature Schedule for MFTF-B Axicell Magnet Cooldown and Warmup Analysis, MFTF-5220/6220-M-454-JWW, 5 January 1983.

5-4 O'Neil, R. F., et al, "Convair Thermal Analyzer Computer Program No. P4560D," 696-0-T-80-737, 30 June 1980.

5-5 Preliminary Design Review for the Axicell and Transition Coils for the Mirror Fusion Test Facility-B (MFTF-B) Axicell Configuration, April, 1983.

5-6 Christensen, E. H., et al, "Superconducting Magnet Thermodynamic Design Analysis Programs and Large Conductor/Insulation Systems Heat Transfer Test," GDC-ERR-80-075, December, 1980.

5-7 O'Loughlin, J. M. and E. H. Christensen, "Finite Difference Prediction of Superconductor Multidimensional Quench Propagation and Conductor Tempeature Rise," 10th Symposium on Fusion Engineering, Philadelphia, PA, December, 1983.

5-8 Johnson, K. R., "THERMOSIPHON - GDC Computer Code," GDC Report No. MFTF-M-833-KRJ, November, 1983.

6.0

ELECTROMAGNETIC ANALYSIS

6.1 Objectives

The electromagnetic analysis for the high field insert coil was limited to three areas: (1) Adiabatic conductor temperature rise during an emergency fast dump of the coil, (2) Current peaking in the coil due to quench and fast dump of neighboring coils, (3) Lorentz forces on the current leads.

6.2 Adiabatic Conductor Temperature Rise

The Design Requirements Document (DRD) (Reference 6-1) in paragraph 2.7.13.1 specifies that during magnet quench and subsequent fast dump, the calculated hot spot temperature rise of the conductor based on a two-dimensional coil heat conduction model shall be 200K or less at the end of a fast dump. Further, this limit shall apply for a delay time of 10 seconds from the start of a normal zone to initiation of the fast dump.

An adiabatic conductor temperature rise during dump of the insert coil is used to represent the requirement condition. This is a conservative approach in developing the temperature rise because of the absence of heat conduction out of the normal zone. The temperature rise of the conductor was calculated using the computer program, SUPERQ, developed at General Dynamics/Convair (Reference 6-2). Very briefly, this program calculates the time and temperature evolution of system parameters by numerically integrating the basic equations governing the power balance and voltages during a quench condition. The actual integration is performed using temperature steps, calculating the current from the temperature and the time from the current. The magnetic field varies with the current.

The data used in the calculation are shown in Table 6-1. A dump voltage of 750V was used which results in a discharge time constant of 7.5 seconds. The results are shown in Figure 6-1. The maximum temperature is only 47K, well below the allowed maximum of 200K.

6.3 Current Peaking Analysis

In the normal charge, discharge, and fast dump of the MFTF-B magnet system, all 26 magnets will be brought up or down in current simultaneously, but not with necessarily the same time constant for each magnet. This results in essentially no increase in current in any of the magnets. Induced currents will occur, however, during fault conditions. A study of worst-case conditions for current peaking in the high field insert coil was performed.

Table 6-1. Input Data for MFTF A2I

MAGNET INDUCTANCE =	3.77	(HENRIES)
OPERATING CURRENT =	1584.	(AMPS)
MAXIMUM DISCHARGE VOLTAGE =	750.	(VOLTS)
OVERALL CURRENT DENSITY =	1985.	(AMPS/SQ. CM)
MAGNETIC ENERGY =	11.6	(MEGAJOULES)
CRITICAL TEMPERATURE =	5.0	(DEG K)
NORMAL ZONE LENGTH =	100.	(CM)
NORMAL ZONE TRIGGER VOLTAGE =	.00100	(VOLTS)
DELAY =	10.00	(SEC)
SELF FIELD =	12.70	(TESLA)
BACKGROUND FIELD =	0.00	(TESLA)
BACKGROUND FIELD ANGLE =	0.00	(DEGREES)
CU/SC RATIO =	4.70	
PACKING FRACTION =	.756	
INSULATION VOID FRACTION =	.420	
RRR =	102.0	

AREA OF UNIT CELL =	.75168	(SQ. CM)
AREA OF CONDUCTOR =	.57311	(SQ. CM)
AREA OF COPPER =	.47257	(SQ. CM)
DUMP RESISTANCE =	.49867	(OHMS)

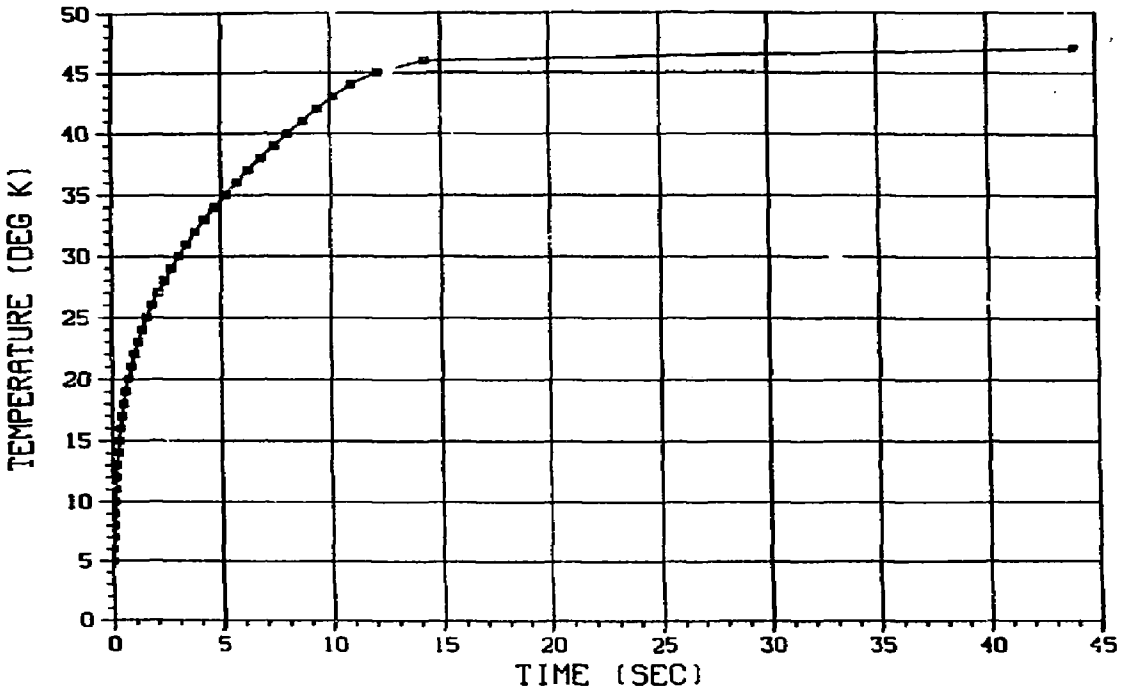

Figure 6-1. Temperature vs. Time for MFTF A2I

Calculations were made for two abnormal conditions, fault and fault-fault. A fault condition signifies the occurrence of a quench in one or more magnets, and the entire magnet system dumps 10 seconds after quench initiation. A fault-fault condition denotes the situation where a quench detector fails to detect the quench, and the magnet power supplies continue to operate. The fault-fault condition is by far the worst of the two. The power and protection system is an LLNL responsibility and LLNL has determined that a fault-fault will occur perhaps less than once in 10^6 hours of operation (Reference 6-3). Therefore, the magnets and their support systems are not designed for this contingency.

The current peaking analysis was performed using a commercially available computer program called SYSCAP. SYSCAP is a system of circuit analysis programs that perform static/dynamic and linear/nonlinear nodal analyses of electronic circuits. A complete description of the method of modeling the magnets and how the calculations are performed is given in Reference 6-4.

Figure 6-2 shows the behavior of the current in A2I as a function of time after quench initiation, using a fault condition. The magnets that were assumed to quench were the three magnets most closely coupled to A2I, namely A1, A2O, and T1. These magnets quenching should result in the maximum induced current in the high field coil. Dumping of all magnets began 10 seconds after quench initiation. The peak shown in Figure 6-2 represents a 3.3 percent increase over the normal operating current.

Figure 6-3 gives the behavior of the current in A2I as a function of time after quench initiation, during a fault-fault condition. The magnets assumed to quench were the same three as in the fault condition above. However, in the fault-fault condition, the magnet power supplies are not turned off and, as a consequence, the current in A2I increases to the large value shown. This peak is a 233 percent increase over the normal operating current.

This curve is included only for the sake of completeness. The magnet system and support structure are not designed to handle such large currents. One further comment should be made. Once the current in A2I reaches the critical current value, the magnet will quench and the current will begin to decay because of the rapid increase in magnet resistance. Realistically, therefore, the current will not atain this high value.

The high field insert coil was designed to withstand a 15 percent overcurrent as specified in Reference 6-1. The 3.3 percent peak current is thus well within this requirement.

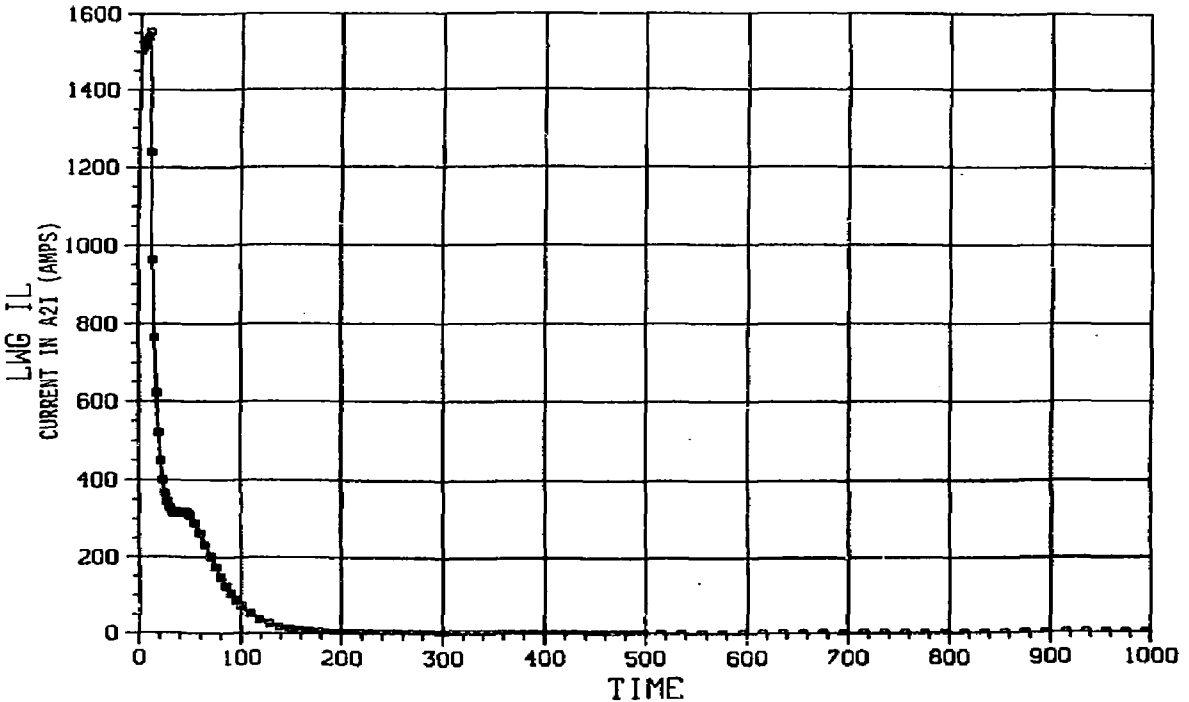

Figure 6-2. MFTF Induced Current in A2I as a Result of Quenching T1, A2O, and A1 with Dumping of Magnet System After 10 Seconds

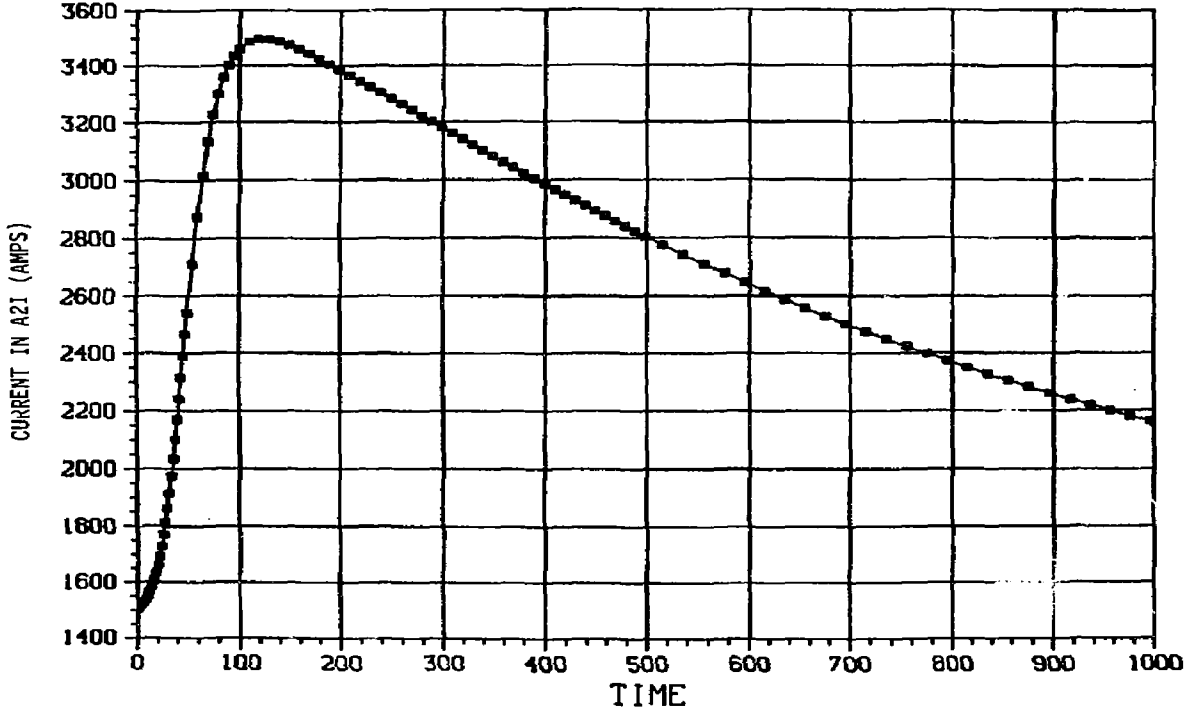

Figure 6-3. MFTF Induced Current in A2I as a Result of Quenching T1, A20, and A1 (Power Supplies Left On).

6.4 Lorentz Forces on Current Leads

The Lorentz forces on the current leads of the high field insert coil were developed. LLNL provided magnetic field data at various positions along the current leads from which the forces were calculated. The resulting forces are shown in Table 6-2. As shown, the maximum force is 52.1 lb/in.

The direction of the forces given in the table corresponds to the lead carrying the return current. For the input current, the forces will have the same magnitude, but will be reversed in direction.

6.5 Conclusions

With respect to the design requirements addressed in this section, the high field coil design has met or exceeded all specifications as listed in the MFTF-B DRD.

Electrical integrity of the coil in insured by the coice of gaps and insulation thicknesses within the magnet. In an emergency fast dump, the maximum conductor-to-ground voltage is 375V. A minimum gap distance of 3 inches has been maintained between the conductor and the ground, well beyond what is required to prevent breakdown in He gas at this voltage.

Pancake-to-ground voltage in a fast dump is 27.8. Pancake-to-pancake insulation is 0.047 inches. This provides a substantial margin of safety against insulation breakdown. Similarly, the turn-to-turn insulation thickness o 0.039 inch will easily withstand the maximum turn-to-turn voltage of 0.24V. hence, the A2I coil design guarantees electrical integrity of the coil.

6-6 References

6-1 "MFTF Design Requirements Document," published by Lawrence Livermore National Laboratory, dated 17 August 1982 (revised 20 May 1983).

6-2 Preliminary Design Review of the High Field Nb_3Sn Axicell Insert Coils for the Mirror Fusion Test Facility-B (MFTF-B) Axicell Configuration, 11 May 1983.

6-3 MFTF-B Magnet Power Supply Preliminary Design Review, 10 May 1983.

6-4 Final Design Review for the Axicell and Transition Coils for the Mirror Fusion Test Facility-B (MFTF-B) Axicell Configuration, 30 November and 1 December 1983.

Table 6-2. Lorentz Forces on the Current Leads

x(m)	y(m)	z(m)	F_x(lb/in)	F_y(lb/in)	F_z(lb/in)	F_{TOT}(lb/in)
0.412	0.412	9.77	36.2	-36.2	- 0.182	51.2
0.427	0.427	9.77	36.8	-36.8	- 0.182	52.1
0.427	0.427	10.17	- 2.81	3.34	0.0	4.36
0.427	0.427	10.37	-12.6	13.4	0.0	18.4
0.427	0.427	10.57	-15.3	16.2	0.0	22.3
0.427	0.427	10.68	-13.0	13.9	0.0	19.0
0.302	0.571	10.77	-17.9	23.6	-12.8	32.3
0.212	0.679	10.83	19.6	18.3	- 8.92	28.2
0.353	0.819	10.83	10.6	-10.7	1.38	15.1
0.495	0.962	10.83	3.53	- 3.50	0.679	5.02
0.636	1.103	10.83	0.372	- 0.372	0.334	0.622
0.778	1.245	10.83	- 0.482	0.482	0.0182	0.679
0.919	1.386	10.83	- 0.550	0.550	0.109	0.788

7.0

INSTRUMENTATION DESIGN

7.1 Instrumentation Plan

The MFTF-B instrumentation includes a combination of temperature, voltage, and liquid helium level measurements distributed over selected points on the high field magnet.

The two high field magnets included 10 temperature sensors on A2IE, 10 temperature sensors on A2IW, 34 voltage taps on A2IE, 34 voltage taps on A2IW, 1 liquid helium level sensor in A2IE, and 1 liquid helium level sensor in A2IW for a total of 90 instrumentation channels.

A measurement code number list was prepared which assigns measurement numbers to each of the 90 channels. Additionally, vacuum vessel feedthru connector assignments have been made for those cables that must go through the vacuum vessel ports. This data is summarized in Appendix E.

The temperature sensors are located for monitoring cool-down/warm-up temperatures.

Liquid helium level sensors are installed in the stack of each magnet. The active level sensing length of NbTi superconductor will extend from the G-10CR feedthru plate in each stack to approximately twelve inches below the liquid helium bypass line. The installation of one sensor in each magnet stack will provide liquid level monitoring and impending low helium level data in case of helium fill line blockages or accidents.

Voltage taps are located on coil windings, entering and exiting warm and cold lead buses for normal zone monitoring and quench detection circuit inputs.

Temperature sensors used for cool-down/warm-up operations are nickel manganin resistance sensors which provide excellent linear outputs over the wide temperature range of interest, i.e. 300K to 4.2K.

Liquid helium level sensors are NbTi superconductor wire installed in a perforated fiberglass tube.

Instrumentation cables selected include single conductor and four conductor cable configurations. All cables are Kapton insulated, shielded, and jacketed designs rated for continuous operation at 1000 volts. Single conductor cables are 30 AWG and are used for voltage taps. Four conductor cables are 26 AWG and are used for temperature sensors.

The temperature measurement instrumentation wiring inside the vacuum vessel will pass through the vacuum vessel ports via a double-ended hermetic feedthru designed to meet MIL-C-26482, Series 1. The feedthru has a jam nut mounting with a silicone rubber seal. The design leakage requirement is 10^{-8} std. cc/sec of helium.

All voltage tap and level sensor wiring exit through the magnet stack through conax fittings which allow for continuous cables run to the exterior of the vacuum vessel.

Appendix E contains the instrumentation measurement code summary with convective assignments.

Appendix F contains the instrumentation drawing tree.

7.2 Temperature Measurements

Temperature instrumentation sensors have been located for cool-down/warm-up transient operations.

a) Overall cool-down/warm-up progression so that helium flow rates can be varied to meet cool-down/warm-up requirements.

b) Bottom-to-top temperature profiles in the magnets.

c) Cross-section differentials at various lengths up the leg of the magnet.

d) Temperature differentials between legs of the magnets.

e) Abnormal cross-sectional or longitudinal distribution of helium flow.

High field coils A2IE and A2IW each have eight external case temperature sensor locations. The eight sensors on each coil are distributed as follows:

Two sensors are 90 degrees apart on the inner ring; two sensors are 90 degrees apart on the outer rings; three sensors, each 90 degrees apart, are on the side plate which faces the A1 coil and one sensor is on the side plate which faces the solendoid coils.

Each coil helium supply line and helium return line is instrumented with one temperature sensor (total of 4) for long-term magnet operation monitoring.

Table 7-1 is a summary of temperature sensor quantities and locations. Figure 7-1 depicts the coil case temperature sensor locations and measurement numbers. Figure 7-2 shows a typical CLTS temperature sensor installation. The sensor and its electrical terminals are bonded to the

Table 7-1. Temperature Sensors Have Been Located on High Field Coils for Cooldown/Warmup Operations

SUBSYSTEM	COIL	QTY.	COIL	QTY.	TOTAL
Outer Coil Case	A2IE	8	A2IW	8	16
Conductor Bus Htrs	A2IE	2	A2IW	2	4
LHe Supply Line	A2IE	1	A2IW	1	2
LHe Return Line	A2IE	1	A2IW	1	2
					24

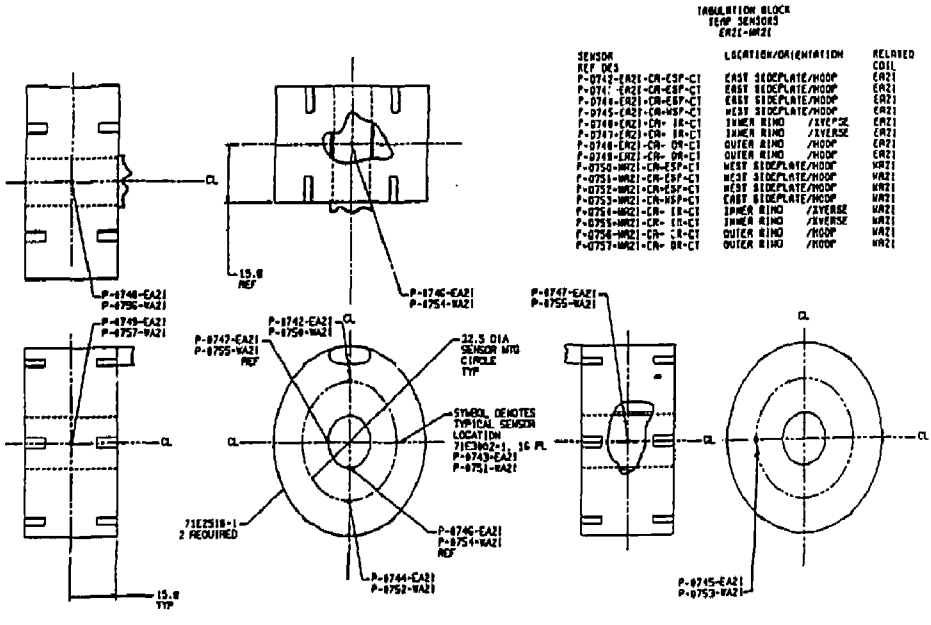

Figure 7-1. High Field Coil Case Temperature Sensor Locations

structure with the cryogenic bonding adhesive, AE-10. The sensor and wiring is finally covered with aluminum foil which is bonded down with EA934 epoxy to provide a moisture protected environment for the sensor installation. The aluminum foil is provided over a 26.7-cm (10.5-in) length to minimize thermal radiation errors in the temperature measurement.

7.3 Voltage Measurements

Voltage taps are installed on each magnet winding to provide for normal zone and quench detection circuit inputs. Voltage taps are additionally installed on the cold helium side of each vapor-cooled lead to provide protection against inadequate cooling.

Each of the two high field coils have a voltage tap installed on the splice joint for each double pancake for a total of twenty-six (26) joint taps.

Additionally, two cold bus lead-in taps, two cold bus exit taps, and two warm bus lead taps on each warm bus lead are installed for a total of eight taps in these locations for each magnet.

Table 7-2 summarizes the voltage tap locations for each coil. Table 7-3 itemizes the conductor splice joint measurement code numbers. Figure 7-3 shows the typical splice joint voltage tap installation for 13 taps on one side of the A2IE coil. Figure 7-4 shows entering and exiting cold bus lead voltage tap installations and their associated measurement code numbers. Warm bus lead voltage tap installations and measurement numbers are shown in Figure 7-5.

7.4 Liquid Helium Level Measurements

NbTi superconducting helium level sensors are installed in the stack of each magnet. The active level sensing length will extend from the GlOCR feedthru plate in each stack to approximately 12 inches below the liquid helium bypass line. The sensors are insensitive to magnetic fields up to 10 tesla. The 70-milliampere current carried by the NbTi assures resistive operation in helium gas and superconducting operation in liquid helium. The installation of one sensor in each magnet stack will provide liquid helium level monitoring and impending low helium level data in case of helium fill line blockages or accidents.

The high field coil liquid helium level sensor is shown in Figure 7-6.

7.5 Sensor Descriptions

The high field coil measurement sensors are described in Table 7-4.

The CLTS-2 temperature sensors were procured by General Dynamics and sent to a calibration laboratory for calibration. Each sensor will have a resistance vs. temperature calibration point recorded at 273.15K, 77.37K, 27.1K, and 4.2K, with an accuracy of $\pm$ 0.15K.

Table 7-2. Voltage Taps for the High Field Coil have been Distributed on Conductors and Buses for Fault Isolation and Protection C :uit Inputs

Subsystem	Coil	Qty.	Coil	Qty.	Total
Conductors - Each Double Pancake Splice	A2IE	26	A2IW	26	52
Bus Lead In	A2IE	2	A2IW	2	4
Bus Exit	A2IE	2	A2IW	2	4
Warm Bus Leads	A2IE	4	A2IW	4	8
					68

34 Total taps per high field coil.

1 redundant tap on each warm and cold bus lead.

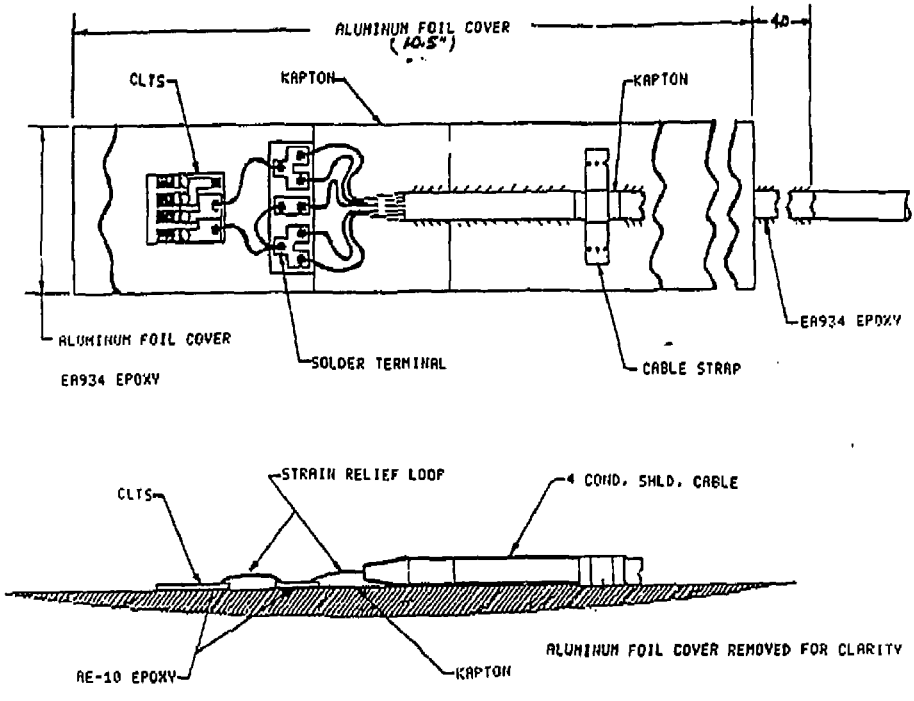

Figure 7-2. Typical CLTS Temperature Sensor Installation

Table 7-3 High Field Coil Pancake Splice Joint Voltage Tap Measurement Numbers and Locations.

TABULATION BLOCK VOLTAGE TAPS EA21		TABULATION BLOCK VOLTAGE TAPS WA21	
MEAS. NO.	DESCRIPTION/LOCATION	MEAS. NO.	DESCRIPTION/LOCATION
P-1705-EA21-CO-PC 2-TS7-VT	SPLICE BETWEEN PANCAKE 24 3	P-1739-WA21-CO-PC 2-TS7-VT	SPLICE BETWEEN PANCAKE 24 3
P-1706-EA21-CO-PC 4-TS7-VT	SPLICE BETWEEN PANCAKE 44 5	P-1740-WA21-CO-PC 4-TS7-VT	SPLICE BETWEEN PANCAKE 44 5
P-1707-EA21-CO-PC 6-TS7-VT	SPLICE BETWEEN PANCAKE 64 7	P-1741-WA21-CO-PC 6-TS7-VT	SPLICE BETWEEN PANCAKE 64 7
P-1708-EA21-CO-PC 8-TS7-VT	SPLICE BETWEEN PANCAKE 84 9	P-1742-WA21-CO-PC 8-TS7-VT	SPLICE BETWEEN PANCAKE 84 9
P-1709-EA21-CO-PC10-TS7-VT	SPLICE BETWEEN PANCAKE 10411	P-1743-WA21-CO-PC10-TS7-VT	SPLICE BETWEEN PANCAKE 10411
P-1710-EA21-CO-PC12-TS7-VT	SPLICE BETWEEN PANCAKE 12413	P-1744-WA21-CO-PC12-TS7-VT	SPLICE BETWEEN PANCAKE 12413
P-1711-EA21-CO-PC14-TS7-VT	SPLICE BETWEEN PANCAKE 14415	P-1745-WA21-CO-PC14-TS7-VT	SPLICE BETWEEN PANCAKE 14415
P-1712-EA21-CO-PC16-TS7-VT	SPLICE BETWEEN PANCAKE 16417	P-1746-WA21-CO-PC16-TS7-VT	SPLICE BETWEEN PANCAKE 16417
P-1713-EA21-CO-PC18-TS7-VT	SPLICE BETWEEN PANCAKE 18419	P-1747-WA21-CO-PC18-TS7-VT	SPLICE BETWEEN PANCAKE 18419
P-1714-EA21-CO-PC20-TS7-VT	SPLICE BETWEEN PANCAKE 20421	P-1748-WA21-CO-PC20-TS7-VT	SPLICE BETWEEN PANCAKE 20421
P-1715-EA21-CO-PC22-TS7-VT	SPLICE BETWEEN PANCAKE 22423	P-1749-WA21-CO-PC22-TS7-VT	SPLICE BETWEEN PANCAKE 22423
P-1716-EA21-CO-PC24-TS7-VT	SPLICE BETWEEN PANCAKE 24425	P-1750-WA21-CO-PC24-TS7-VT	SPLICE BETWEEN PANCAKE 24425
P-1717-EA21-CO-PC26-TS7-VT	SPLICE BETWEEN PANCAKE 26427	P-1751-WA21-CO-PC26-TS7-VT	SPLICE BETWEEN PANCAKE 26427
P-1718-EA21-CO-PC28-TS7-VT	SPLICE BETWEEN PANCAKE 28429	P-1752-WA21-CO-PC28-TS7-VT	SPLICE BETWEEN PANCAKE 28429
P-1719-EA21-CO-PC30-TS7-VT	SPLICE BETWEEN PANCAKE 30431	P-1753-WA21-CO-PC30-TS7-VT	SPLICE BETWEEN PANCAKE 30431
P-1720-EA21-CO-PC32-TS7-VT	SPLICE BETWEEN PANCAKE 32433	P-1754-WA21-CO-PC32-TS7-VT	SPLICE BETWEEN PANCAKE 32433
P-1721-EA21-CO-PC34-TS7-V.	SPLICE BETWEEN PANCAKE 34435	P-1755-WA21-CO-PC34-TS7-VT	SPLICE BETWEEN PANCAK. 34435
P-1722-EA21-CO-PC36-TS7-VT	SPLICE BETWEEN PANCAKE 36437	P-1756-WA21-CO-PC36-TS7-VT	SPLICE BETWEEN PANCAKE 36437
P-1723-EA21-CO-PC38-TS7-VT	SPLICE BETWEEN PANCAKE 38439	P-1757-WA21-CO-PC38-TS7-VT	SPLICE BETWEEN PANCAKE 38439
P-1724-EA21-CO-PC40-TS7-VT	SPLICE BETWEEN PANCAKE 40441	P-1758-WA21-CO-PC40-TS7-VT	SPLICE BETWEEN PANCAKE 40441
P-1725-EA21-CO-PC42-TS7-VT	SPLICE BETWEEN PANCAKE 42443	P-1759-WA21-CO-PC42-TS7-VT	SPLICE BETWEEN PANCAKE 42443
P-1726-EA21-CO-PC44-TS7-VT	SPLICE BETWEEN PANCAKE 44445	P-1760-WA21-CO-PC44-TS7-VT	SPLICE BETWEEN PANCAKE 44445
P-1727-EA21-CO-PC46-TS7-VT	SPLICE BETWEEN PANCAKE 46447	P-1761-WA21-CO-PC46-TS7-VT	SPLICE BETWEEN PANCAKE 46447
P-1728-EA21-CO-PC48-TS7-VT	SPLICE BETWEEN PANCAKE 48449	P-1762-WA21-CO-PC48-TS7-VT	SPLICE BETWEEN PANCAKE 48449
P-1729-EA21-CO-PC50-TS7-VT	SPLICE BETWEEN PANCAKE 50451	P-1763-WA21-CO-PC50-TS7-VT	SPLICE BETWEEN PANCAKE 50451
P-1730-EA21-CO-PC52-TS7-VT	SPLICE BETWEEN PANCAKE 52453	P-1764-WA21-CO-PC52-TS7-VT	SPLICE BETWEEN PANCAKE 52453

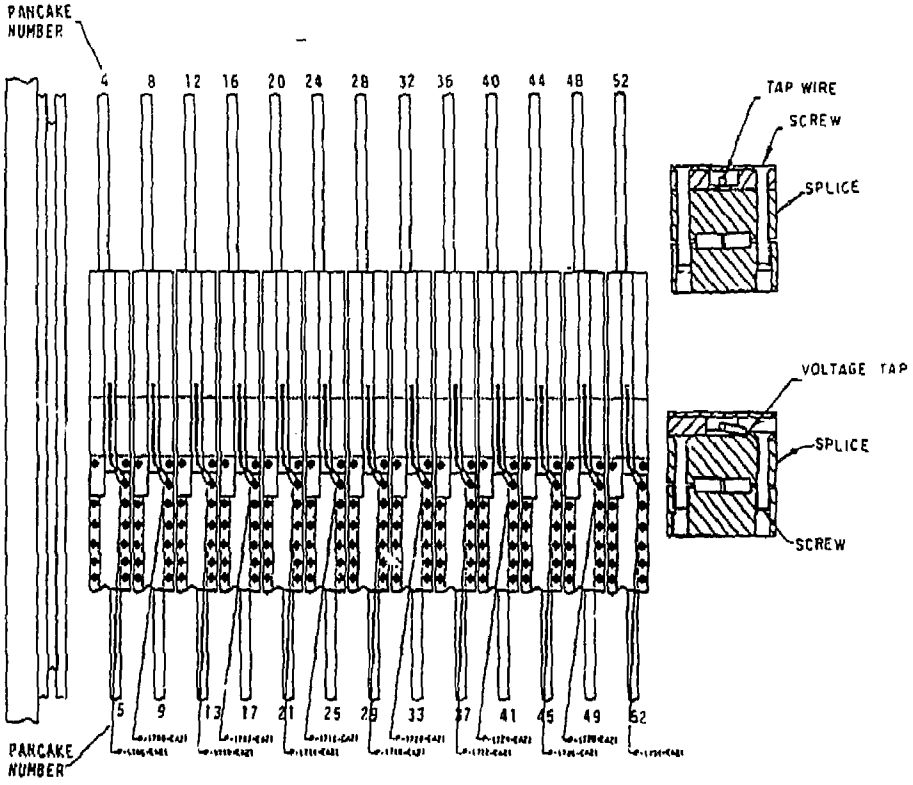

Figure 7-3 Typical High Field Coil Pancake Splice Voltage Tap Installation.

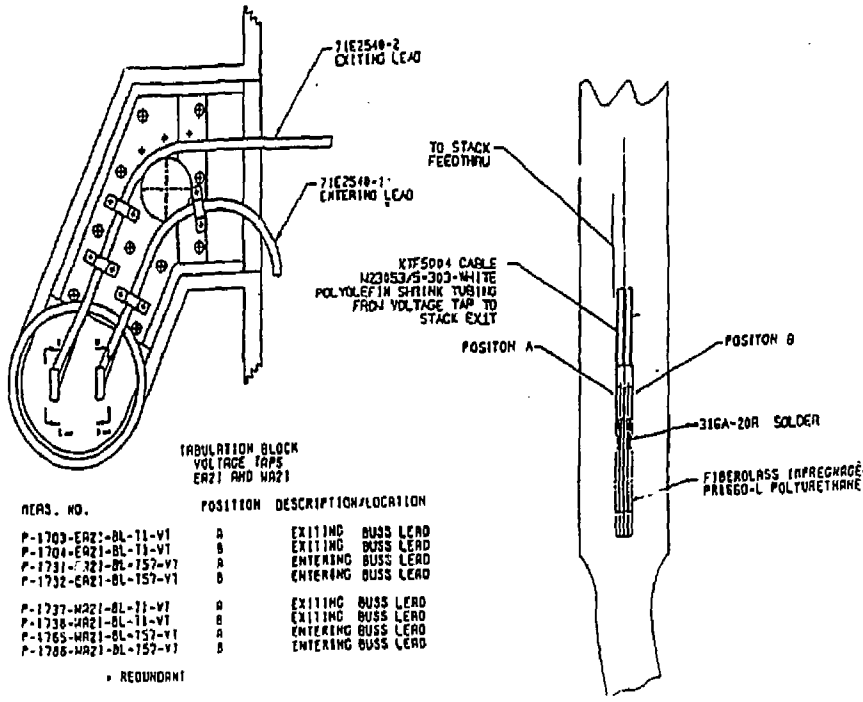

Figure 7-4. Entering and Exiting Bus Lead Voltage Tap Installation

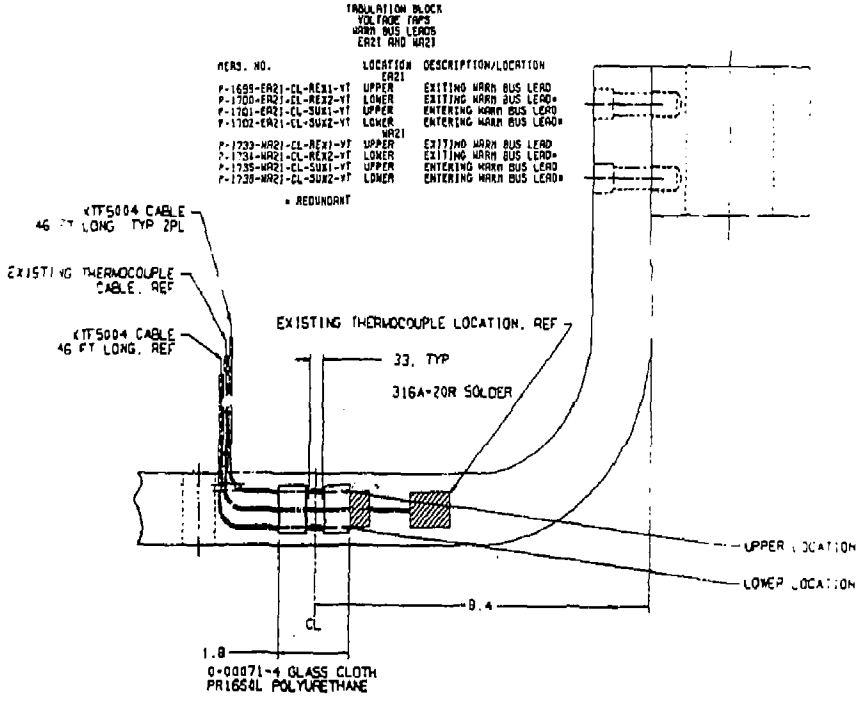

Figure 7-5. Warm Bus Lead Voltage Tap Installation

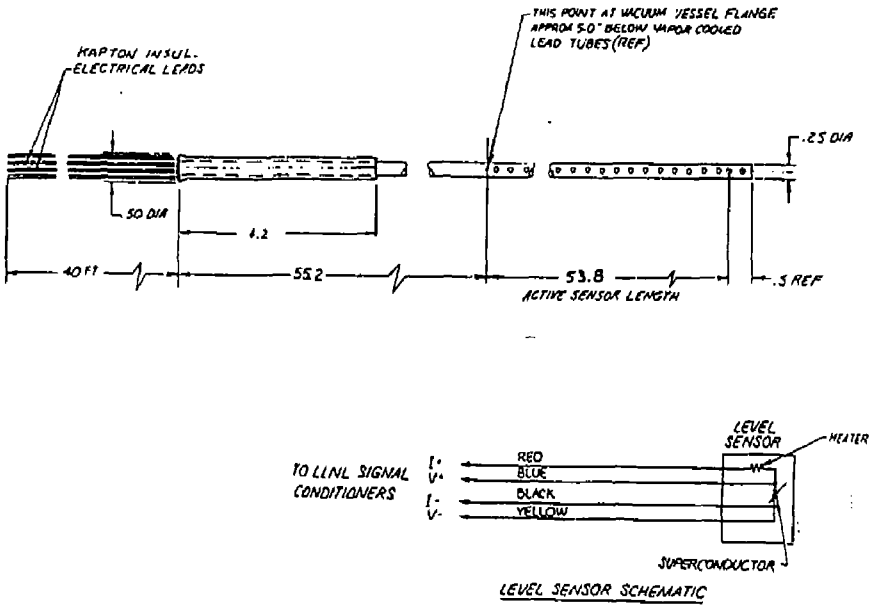

Figure 7-6 High Field Coil Liquid Helium Level Sensor

Table 7-4. Instrumentation Sensor Descriptions

Temperature Sensors

Part No.:	CLTS-2
Construction:	Thin foil sensing grids of nickel and manganin laminated into glass fiber reinforced epoxy resin matrix with integral Cu-printed crkt terminals.
Size:	0.430" long x 0.310" wide x 0.004" thick.
Resistance:	296.9K = 290 ohms + 0.5% 4.1K = 220 ohms (nominal)
Range:	300K to 4.2K
Manufacturer:	Micromeasurements

Liquid Helium Level Sensors

Construction;	NbTi superconductor element housed in a perforated epoxy fiberglass tube with four 28-AWG lead wire exits for signal conditioning.
Size:	0.25" OD fiberglass tube x magnet stack length required.
Resistance:	Nominal 5.3 ohms per cm active length @ 300K. Nominal 4.5 ohms per cm active length @ 20K.
Range:	Active sensing length is 53.8 inches.
Manufacturer:	American Magnetics, Inc.

The liquid helium level sensors will be procured and tested by LLNL. No calibration is required since the sensor is superconducting in liquid and normal above 10K in gaseous helium.

7.6 Electrical Wiring and Connectors

The instrumentation and control wiring will be of three configurations: single conductor, three conductor, and four conductor.

Single conductor 30 AWG wire is used for voltage taps and multiconductor 26 AWG wire is used for the remaining sensor types. All wires are silver plated copper.

All cables are insulated with Kapton insulation for wires and jackets. Kapton insulation .010-inch thick over each conductor and .010-inch thick for jackets.

All cables are shielded. The single conductor cable has a silver plated copper served wire shield for added mechanical protection and excellent flexibility properties. The multiconductor cables have silver plated copper copper foil with a 26 AWG drain wire.

All cables have a voltage rating of 1000 volts rms and will be sample tested by the supplier at 2000 volts from conductor-to-conductor and conductor-to-shield.

The cable usages, descriptions, and part numbers are summarized in Table 7-5.

The four cable termination categories are summarized below:

A) Vacuum Vessel Penetrations

All instrumentation wiring inside the vacuum vessel and sensors mounted on magnet and support system surfaces will pass through the vacuum vessel double-ended through bulkhead connectors.

B) Liquid Level Sensor Cables

All liquid level sensor cables will extend approximately 40 feet beyond each magnet stack and will be terminated by LLNL.

C) Voltage Tap Cables

All voltage tap cables exit each magnet stack through conax fittings which allow for one continuous cable for each voltage tap. These cables will extend approximately 40 feet beyond each stack exit point and will be terminated by LLNL at selected protection circuit inputs.

Table 7-5. Electrical Wire Summary

Function	Part Description		Part Number
Cable for Voltage Taps	One Conductor - Shielded and Jacketed		KTF 5004
	Conductor:	30 AWG, Ag Plated Cu	
	Insulation:	.010 wall Kapton	
	Shield:	Ag plated Cu served wire	
	Jacket:	.010 wall Kapton	
	Voltage Rating:	1000 VRMS	
Cable for Temp Sensors	Four Conductor - Shielded and Jacketed		KTF 5003
	All other properties same as above.		

D) High Current Lead Heater Thermocouple Cables

All high current lead temperature control thermocouple cables (Type E, chromel constantan wiring) will extend as one continuous length from the thermocouple installation on the high current lead to the LLNL heater power supply circuits.

The vacuum vessel electric feedthru connectors were procured from Kyle Technology Corporation, and meet the LLNL requirements summarized below:

- o Hermetic double-ended feedthru.
- o Per MIL-C-262482, Series 1, bayonet coupling.
- o Jam nut mounting with silicone rubber seal.
- o 61 contacts of gold-plated inconel.
- o Insert material - ceramic devoid of organics.
- o Radiation environment - 10^6 rads neutron radiation.
- o Vacuum environment - 10^{-8} torr.
- o Leakage requirement - 10^{-8} std. cc/sec helium.
- o Straight plugs for mating with above feedthru per MIL-C-26482, Series 1.

7.7 Conclusions

All instrumentation drawings have been completed and released with the exception of sensor cable routing which is pending completion of thermal shield designs. All drawings and wiring diagrams utilize a standardized instrumentation channel measurement numbering system in accordance with LLNL guidelines. Additionally, a standardized electrical feedthru pin assignment system has been incorporated on all wiring diagrams per LLNL guidelines.

Electrical wiring and connectors including grounding, shielding, and insulating properties have been incorporated per DRD requirments. Sensor selections and placements follow DRD and LLNL supplemental requirements. Sensor installation testing for long term moisture protection is still progressing at LLNL and LLNL procedure MEL-78-001435 will be updated at LLNL to include the finalized materials and methods used in sensor installations.

Only LHe supply and return line temperature measurements are required for long term operation of the magnets. Redundancy for these sensor installations is not required since more than one magnet is supplid by the same helium dewar and all magnets are instrumented with LHe supply and return line temperature sensors. The remaining temperature sensors on this coil will be used primarily for acceptance testing, cool-down/ warm-up, and demonstration of the magnet cryogenic system.

Procurement orders were placed by General Dynamics for all CLTS temperature sensors, including calibration, all electrical wiring, and all electrical connectors. Remaining instrumentation sensors and materials will be ordered by LLNL.

8.0

VERIFICATION TESTING

8.1 Requirements and Objectives

The verification tests described in this section were designed to meet the following requirements: (1) assess the ability of Furukawa Electric Co. to meet the Nb_3Sn conductor specifications listed in Appendix A, and (2) provide engineering data for comparisons with the materials property assumptions made in the design phase. A key feature of this program was the procurement of a prototype length of conductor from Furukawa. In fabricating this conductor, Furukawa used raw material (Nb, bronze, and Cu) and production equipment that was intended for use in the actual prototype production. Hence the prototype should be representative of the production material. The verification tests performed on this prototype length are listed in Table 8-1. In addition to these tests, additional measurements were made in order to evaluate the effects of cladding on the critical current and the degree of critical current anisotrophy resulting from the flattening of the Nb_3Sn elements.

8.2 Evaluation of Preliminary Design Assumptions

In order to complete the conductor design, several assumptions were made with regard to degradation in critical current expected due to (1) the addition of a copper housing for stabilizaton, and (2) aspecting the conductor in order to accommodate the bending of the conductor around the small diameter. The values used in the preliminary design were supplied by Furukawa based on their experience with a similar conductor (the Cluster Background Coil conductor supplied to the Japan Atomic Energy Research Institute). It was anticipated that in the worst case the additional precompression of the Nb_3Sn due to the application of the cold-worked Cu stabilizer could result in a 33 to 40 percent decrease in the critical current. However, Furukawa made two changes which were expected to reduce this degradation. First, they introduced a ternary alloying addition (Ti) which had been shown to decrease the strain sensitivity of Nb_3Sn. Second, they improved their cladding line so that the cold-worked Cu sheath could be soldered to the Nb_3Sn and cooled slowly in order to reduce the precompressive strain applied to the Nb_3Sn. Critical current measurements were made on the core alone and on the core after cladding. The degradation measured for the prototype conductor due to cladding was between 6 and 10 percent, indicating that the steps taken by Furukawa were effective.

When an Nb_3Sn superconductor is flattened, or aspected, the critical current becomes anisotropic with respect to the magnetic field orientation. The critical current is higher when the field is perpendicular to the wide side of the conductor and lower when the field is parallel

Table 8-1. Verification Test Summary
High Field Coil

Test Number	Title		Status or Estimated Completion Date
6.4.1	Mechanical Properties of Insert	(Proto)	Complete
6.4.2	Mechanical Properties of Conductor	(Proto)	Complete
6.4.3	CTE of Conductor	(Repre)	Complete
6.4.4	Ic vs. Insert Bend Radius	(Proto)	Complete
6.4.5	Ic vs. Conductor Loading	(Proto)	1/18/84
6.4.6	Conductor Splice Tests	(Proto)	Complete
6.4.7	V.C. Lead Operation	(Prod.)	TBD
6.4.8	RRR of Conductor in High Field	(Proto)	Complete
6.4.9	Conductor Insert Exam.	(Proto)	Complete
6.4.10	Conductor Visual Exam.	(Proto)	Complete
6.4.11	Conductor Solder Bond Verification	(Proto)	Partially Complete
6.4.12	Mechanical Properties of Conductor	(Repre)	Complete
6.4.13	Ic vs. Conductor Loading	(Repre)	Complete
6.4.14	Conductor Delamination Test	(Proto)	1/13/84
6.4.15	Damage Tolerance Test	(Proto)	Complete
6.4.16	Insert Critical Current Verification	(Proto)	Complete

to the wide side. The field in the axicell coils is parallel to the wide side of the conductor. From information supplied by Furukawa, an estimate of ± 10 percent for the current anisotropy was derived. The actual value measured on the prototype conductor was somewhat higher at ±13 percent.

8.3 Verification Test Results

The detailed justification and procedures for the tests listed in Table 8-1 are documented in References 8-1 and 8-2. Tests 6.4.1 and 6.4.2 provide the mechanical property data necessary to verify the coil design and to verify that the conductor meets the specification. The results of these tests are summarized in Table 8-2. The results were generally consistent with the values used in the coil design and incorporated in the specification. The specification requires that the 0.2 percent offset tensile yield strength of the housing at 300K be equal or greater than 31,000 psi; in practice it was not possible to perform a valid test on the housing alone. Consistent yield strength data were obtained for the composite (superconductor core and housing, see Table 8-2). In addition, it was not possible to obtain a valid mechanical test on the full cross-section of the core due to specimen failures on the outside of the gage. Several tests were completed on reduced cross-sections of the core and these results appear reasonable (see samples 9 and 10 in Table 8-2). In view of these testing difficulties, and since the important property is the composite yield strength, it is recommended that the specification be revised to require the composite yield strength to be equal or greater than 31,000 psi. The prototype conductor met the remainder of the specification requirements, as shown in Table 8-3.

An important consideration in utilizing a reacted Nb_3Sn conductor is its tolerance to bending. Consequently, bend tests were performed on both the core alone and on the composite conductor. Core samples were reacted to form Nb_3Sn while bent around 100, 200, and 400 mm radii. The samples were then straightened and critical current measurements were made; the results are shown in Table 8-4. The core could be bent to a strain of greater than ± .48 percent strain (200-mm radius) without any degradation in critical current, and the critical current is 73 percent above the operating value at a strain of ± .95 percent (100-mm bend radius).

Additional bend results were obtained for the composite samples by bending the samples to various diameters, straightening, and measuring the critical current; the results are compiled in Table 8-5. Degradation in critical current did not appear at a diameter of 15.7 cm (6.195 inches) which should be compared with a minimum coil winding diameter of about 38 cm (15 inches). In addition, the conductor could be bent in the opposite direction to 35 cm (13.8 inches) diameter without degradation (the core was reacted to a 70-cm diameter mandrel; hence "right way" refers to a bend in the original mandrel direction). Additional discussion of the bending behavior is contained in Section 4.0.

Table 8-2. Mechanical Properties of Composite Conductor and Superconductor

Sample	Test Temperature (K)	Yield Strength (ksi)	Ultimate Strength (ksi)
1A	293	31.5	34.6
1B	293	31.6	35.8
2	293	31.3	35.2
3	293	31.3	34.6
4 (Lead)	4.2	38.9	45.1
5 (Lag)	4.2	36.0	45.4
6 (Lag)	4.2	34.3	43.9
7 (Lag)	4.2	35.1	43.6
	Results for Test 6.4.1		
	Mechanical Properties of Superconductor Insert		
8	293	26.6	39.7
9*	4.2	30.2	58.5
10*	4.2	29.4	45.1

* Cross section reduced to 0.128" x 0.0824".

Table 8-3. Conductor Specification Requirements and Comparison to Test Results

Property	Specification	Measurements
Critical Current		
at 12.7, 4.2K	3200A	4300A
Copper RRR		
0 Field	120	139
12 T		27
Critical Current		
0.7% Strain and Release	3200A	

Table 8-4. Results for Tests 6.4.4 - Effect of Bending (Core Only) on I_c

Sample	Bend Radius	Critical Current 12.0T	Critical Current 12.5T	Remarks
F18A	Straight	5500	>4800	1
F18B	Straight	5500	>4800	1
F15A	400 mm	5500	5100	1
T15B	400 mm	>5450	>5200	1
F16A	200 mm	>5500	>4800	1
F16B	200 mm	>5500	>4800	1
F17A	100 mm	~2650	~2500	2
F17B	100 mm	~3200	~2700	2

1) These samples of Core Only contain only 20 percent Cu and, as a consequence, usually quench with the slightest sample motion. If sample could not be "trained" in three attempts, I_c is reported as "greater than the quench value."

2) Damage resulting from bending produces a V-I curve without a well-defined I_c value.

Table 8-5. Results for Test 6.4.15 - Critical Current vs. Bend Diameter

Sample	Mandrel Diameter (Inches)	Critical Current 12.0T	12.5T	Remarks
F21	7.675	5425	4975	Right Way, 90° Bend
F22	6.195	5550	5100	Right Way, 90° Bend
F23	4.975	3750	3400	Right Way, 90° Bend
F24	3.855	4075	3700	Right Way, 90° Bend
F26	1.795	0	0	Right Way, 90° Bend
F27	17.735	5000	4600	Wrong Way, 90° Bend
F28	13.795	5175	4650	Wrong Way, 90° Bend
F29	11.595	4850	4475	Wrong Way, 90° Bend
F30	5.795	2875	2650	Wrong Way, 90° Bend
F31	5.495	2575	2650	Wrong Way, 90° Bend
F32	3.795	1950	1775	Wrong Way, 90° Bend
F33	2.795	600	500	Wrong Way, 90° Bend
F19	Straight	4900	4425	Lead
F20	Straight	4875	4425	Lag
F26A	Straight	5075	4650	
F31A	Straight	5100	4600	
F32A	Straight	5000	4600	
F33A	Straight	4950	4450	

8.4 References

8-1 "Revised Specification for High Field Coil Conductor," General Dynamics memo MFTF-7100-M-553-RWB, to M. R. Byrd from R. W. Baldi, dated 29 April 1983.

8-2 "Test Plans for Verification Testing," General Dynamics, Memo MFTF-7100-M-742-REB, to T. A. Kozman from R. E. Bailey, dated 16 September 1983.

9.0

IN-PROCESS/ACCEPTANCE TEST

9.1 Test Objectives

The proposed testing program outlined in the following section was developed using the test technique and philosophy that proved successful during the MFTF-B solenoid coil fabrication. This philosophy includes testing at intervals designed to reveal problems before these problems became difficult and expensive to correct. This progressive testing program will insure that the completed coil is free from defects and that the coil closeout activities do not induce any defects. The periodic voltage gradient test is an example of this type of approach.

The final acceptance test program repeats many of the in-process tests performed during coil fabrication and subjects the coil to other tests designed to prove compliance to the DRD. These tests include high potential testing in helium gas and leak testing of the coil case welds. This program will insure a defect-free coil capable of meeting its performance requirements.

9.2 Test Procedures

This report lists the specific requirements to be verified during the testing operations. Detailed descriptions of similar testing procedures can be found in Reference 9-1.

9.2.1 Coil Parameters to be Verified Prior to Winding Start

a) Coil Case Subassembly Leak Tests.
These tests verify that the helium inlet and outlet vent pipe stub welds are leak-tight prior to the final coil assembly operations. The proposed method uses special tools designed to be clamped over the open portions of the vent pipe structure allowing a leak test to be made of the stub pipe to case welds.

b) Coil Ground Plane Insulation Verification.
Prior to the start of coil windings, the quality of the ground plane insulation at the side plate-inner ring joint should be confirmed. The "helium probe" technique, previously demonstrated to LLNL personnel, should be used to prove that there are no faults in the area of the insulation. In addition, the probe can be used to verify ground insulation in the helium vent area and at other similar places within the coil structure. This technique uses an insulated metal tube, about 12.7 cm (5 in) by 1.27 cm (.5 in) dia. which is connected to the high potential tester and also coupled to a source of helium gas. In operation, the

insulated part under test (coil case after kapton installation, for example) is connected to the High Potential Tester and 3-3.5K volts applied. In use, the helium is allowed to flow through the tube onto the insulation surface. In the case of a defect in the insulation film, an arc will develop between the tube and the port as the helium penetrates the insulation defect. This technique has proved very effective on other programs.

9.2.2 Coil Parameters to be Verified During Winding

a) Turn-to-Turn Voltage Tests.
At specified points during the winding of each pancake (5th, 10th, 15th turn, for example), a power supply will be attached between the pancake beginning, or at the entering lead termination, and the current stopping place on the pancake, and a known current flowed through the winding. A voltmeter will be used to measure the pancake starting voltage and each turn-to-turn voltage. These values will be compared with predicted or previously measured values to verify that no faults exist in the winding to that point.

b) Double Pancake Completion Tests.
Following completion of a double pancake (prior to the pancake splice) and following completion of the tests of part (a) above, a high potential test, pancake to remainder of winding, at a potential of 3000 Vdc will be performed. A high potential test, completed double pancake to coil case will be performed at a test voltage of 5000 Vdc, in air.
Note: If the completed double pancake is the first one, the test of 9.2.2. (c) will be performed.

c) Double Pancake Completion Tests, First Double Pancake.
Following completion of the tests of part (a) above, a high potential test, pancake-to-coil case, will be performed at a test voltage of 3000 Vdc, in helium gas. The suggested method of attaining the helium gas environment is to bag the case/completed pancake and purge it with helium gas at high flow rates.

d) Double Pancake Completion Test, Following Splice Installation.
Following installation of the conductor splice, double pancake to remainder of coil, arrange the test circuitry as described in (a) above. Measure the entering lead voltage, the voltage at all splice fittings, or at the associated voltage taps, and the voltage at the end of the last double pancake. These values will be compared to predicted or previously measured value to verify that there are no faults in the coil. This test is referred to as the "Voltage Gradient Test." Any turn-to-turn or pancake-to-pancake short, depending upon values of the short and its location, can be determined by analysis of this data.

Typically, the expected straight line plot of voltage vs. conductor length will show an offset beginning at the site of the suspected short. Examples of this procedure and accompanying plots can be found in Reference 9-1 for solenoid ES-5 (S/N 10).

9.2.3 Coil Parameters to be Verified Following Completion of all Winding.

a) The voltage gradient tests of 9.2.2 (d) will be performed following coil insulation closeout and coil exiting lead installation. The high potential test in air, coil to case, described in 9.2.2 (b) will also be performed.

9.2.4 Voltage Tap Tests

a) Following completion of fabrication of each voltage tap wire (including the poly olifin tubing installation), a resistance measurement will be made between lead wire and shield, between lead wire and splice fitting terminal, and between shield wire and splice fitting terminal. These measurements must use a 4-wire ohmmeter hookup. A voltage tap lead wire insulation test will be made using the helium probe technique described in Para. 9.2.1 (b).

b) Following installation of each voltage tap, a resistance test will be performed from the entering lead terminal to the voltage tap lead wire and between the entering lead terminal and the voltage tap shield wire. These measurements must also use a 4-wire measurement technique.

9.3 Final Acceptance Tests

Following completion of the coil case closeout, the following tests will be performed.

a) The voltage gradient test of 9.2.2 (d) will be repeated.

b) The resistance measurement for installed voltage tapes of 9.2.4 (b) will be repeated.

c) The coil cavity will be evacuated and backfilled with helium gas for at least three times. Following this, the high potential test of 9.2.2 (b) coil-to-coil case, will be performed with the coil in a helium atmosphere. The test voltage will be 2000 Vdc.

d) Coil Case Final Leak Test.
Following completion of the tests of 9.3 (c), the coil exterior welds, inner ring to side plates, and outer ring to side plates, and ring transverse welds will be tested as described below.

Using a test tool concept similar to that used to perform the final leak tests of the solenoid coils, the high field coil case welds will be checked for leaks. The test tools will be applied to the coil case exterior, the tool edges sealed to the coil case, and the space between the tool and the coil case evacuated to a pressure sufficiently low to achieve a helium leak rate sensitivity of 2×10^{-10} scc/sec. Following a determination of the leak rate for this portion of the coil, the test tool will be moved to the next adjacent portion of the coil and the process repeated until all of welded areas have been tested.

9.4 Conductor Testing

9.4.1 Conductor Tests Performed on Each Length.

The following tests or examinations will be performed on each length of production conductor.

a) Critical Current Testing
One lead and one lag sample per length.
Note: Since three winding lengths are manufactured as one continuous production length, there need be only five total samples cut per production length to meet the intent of this sample requirement.

b) Conductor Resistivity Ratio Testing.
One lead and one lag sample per length.
Note: The same samples as were used for critical current testing will be used for these tests.

c) Insert Examination.
One lead and one lag sample per length.
Note: A small portion of the samples used for 9.4.1 (a) can be used to perform this examination. The examination will be used to determine insert uniformity, evidence of excessive filament distortion, and evidence of excessive folding at the periphery of the insert.

9.4.2 Conductor Tests Performed on Selected Production Conductor Lengths.

The following tests will be performed on these winding lengths: (1, 4, 7, 10,...54). These tests will verify that each production length (three winding lengths) will have been tested as described in the following sections.

a) All of the tests of 9.4.1 will be performed.

b) The samples will be subjected to tensile testing at 300K to a 0.7% peak filament strain.
Note: Use the following table to determine the test strain.

10.0

MANUFACTURING/PRODUCIBILITY

10.1 Objectives/Requirements

Manufacturing Engineering has provided continuous surveillance and producibility analyses since the start of the design phase for the MFTF-B high field Nb_3Sn insert coils (A2 Inner). It has also been their responsibility to make sure that the drawings produced are accurate and comprehensive for shop use as well as producible with today's technology. Concurrent with this activity, they developed the tooling concepts, Manufacturing Assembly Sequence and Flow Plan, as shown in Figure 10-1. This plan defines all major operations with tooling requirements to manufacture the coils. It was updated to reflect design changes as they occurred during the program and served as an excellent tool to evaluate design aspects.

Manufacture of the two insert coils will be accomplished through the combined skills and experience of Chicago Bridge & Iron Company (CBI) in heavy metal cutting and welding and Lawrence Livermore National Laboratory (LLNL) in coil winding, assembly, and installation into the vacuum chamber. Structural components consisting of the winding form, closeout ring segments with lead tunnel, side plate, support fittings, stack tube, and axial support adapter will be fabricated by CBI's Birmingham, Alabama, facility. Coil insulation, splice details, helium inlet, and strut assembly hardware will be fabricated by other vendors. The coil's niobium tin conductor will be fabricated by Furukawa Electric Company, Japan.

The Manufacturing Sequence and Flow plan is divided into four (4) sections: Prep for Winding; Coil Winding; Closeout & Weld, and Mate & Assembly. Throughout this report, these sections are reviewed in detail, along with the manufacturing producibility accomplishments and improvements for this program.

10.2 Winding Line

Manufacture of the insert coils was originally planned for General Dynamics Convair. The use of existing solenoid coil winding equipment would be a manufacturing risk, since the conveyor-type tensioner could cause damage holding the conductor the hard way. In addition, the solenoid winders were already dedicated for winding the other MFTF-B axicell coils. Therefore, the Livermore High Field Test Facility (HFTF) coil winder and tensioning system was arranged to be used. The use of this equipment would reduce equipment procurement time, minimize development costs of new winding equipment, and enable the use of proven hardware and techniques already developed in winding a niobium tin coil.

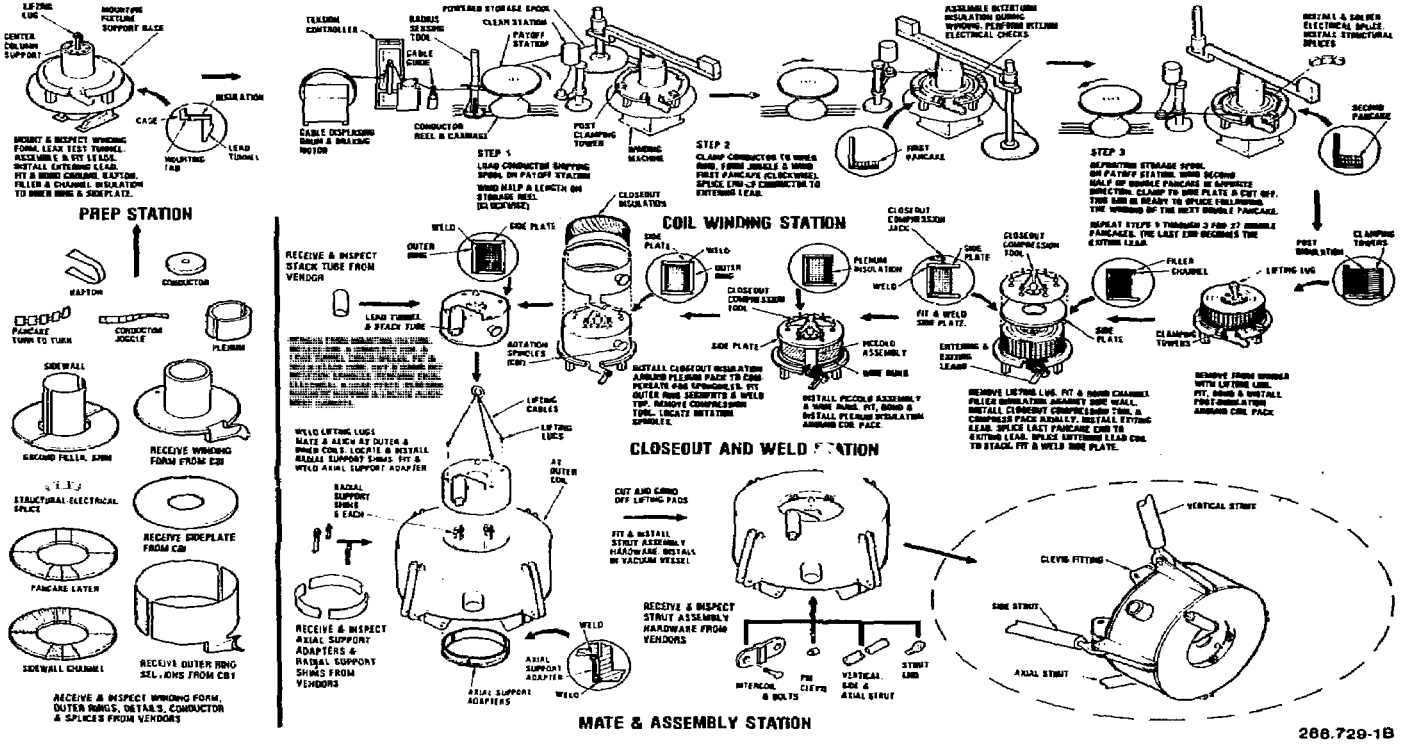

Figure 10-1. Manufacturing Assembly Sequence and Flow

10.2.1 HFTF Tension System

The HFTF tension system is shown in Figure 10-2. The winding line equipment was partially installed at General Dynamics prior to the decision that the coils would be wound at LLNL. The system includes the tension control with Dillon tensiometer, a braking motor with cable take-up drum, the conductor carriage (on tracks) with cable dispensing drum (payoff station), and cable guide. The HFTF turntable was replaced with General Dynamics' prep station turntable.

The distance between the payoff station and winder was precisely determined so a minimum length of conductor could be procured for winding a double pancake. This dimension, along with the recommended spacing for this equipment is shown in the layout of Figure 10-2. Assuming maximum tolerance buildup, there is sufficient conductor length, 19.56 cm (7.7 in), on each end so the conductor can be clamped to both shipping and orbiting storage reel. The conductor manufacturer, Furukawa Electric Company, has been requested to secure each shipping spool for a load of 400 lb tension, as well as to identify the midpoint of each length.

Also depicted in the floor layout (Figure 10-2) is the largest storage reel which will fit between the payoff station and the coil winder. Operational strains are well within conductor design limits for this spool size (O.D. 137.2 cm [54.0 in], I.D. 91.4 cm [36.0 in]).

10.2.2 HFTF Coil Winder

The HFTF coil winder is shown in Figue 10-3 and will be used to wind the coils at LLNL. If the coils were wound at General Dynamics, we would have utilized the solenoid coil prep station turntable as was shown in figure 10-2. General Dynamics' turntable is a new machine and less likely to have mechanical problems. Also, since this turntable is identical to the other winders, the control system design was essentially complete. Only the interface circuitry for the HFTF tensioner system would be required. Due to the insert coil configuration with the lead tunnel, it was advantageous to use the General Dynamics turntable since it could be installed lower to the ground. The turntable support base (Figure 10-2) can be altered with minimal installation costs to provide a more favorable work height.

Table 10-1. Proposed Tool List and Function

DESCRIPTION	FUNCTION
WINDING LINE EQUIPMENT	
• WINDING FORM SUPPORT BASE, MCAC (SK-072)	• MOUNTS WINDING FORM ON WINDER WITH CLEARANCE FOR LEAD TUNNEL
• CLAMPING TOWER & SUPPORT PLATE, MCAC (SK-080)	• PROVIDES NINE (9) COMPACTION CLAMPS FOR WINDING
• ORBITING SPOOL & SUPPORT ARM, MCAC (SK-082)	• SUPPORTS ORBITING CONDUCTOR STORAGE SPOOL & SHAFT WITH MOTORIZED DRIVE
• VERTICAL COLUMN SUPPORT & LIFTING LUG, MCAC (SK-089)	• PREVENTS BUCKLING OF INNER RING AND PROVIDES MOUNTING SURFACE FOR ACCESSORIES
• VARIABLE TENSION CONTROL & SUPPORT STAND, MCAC (SK-090)	• PROVIDES CONSTANT WINDING TENSION CONTROL & READ-OUT
• SHIPPING REEL CARRIAGE EXTENSION, MCAC (SK-091)	• EXTENDS CONDUCTOR REEL ON CARRIAGE TO ACCOMMODATE LARGER WINDING PACK
• PROTECTIVE TENT, PRCR (SK-092)	• PROVIDES A DUST FREE ENVIRONMENT
• FREON CLEAN STATION, MCAC (SK-095)	• REMOVES DUST OBTAINED IN SHIPPING AND STORAGE
WINDING TOOLS	
• WINDER WORK STANDS, MAID (SK-093)	• PROVIDES WORKABLE HEIGHT FOR WINDING
• LEAD FORM MANDRELS, FMMD (SK-094)	• BENDS AND FORMS ENTERING & EXITING LEADS PRIOR TO INSTALLATION
• CONDUCTOR PROTECTOR GUIDE, HDTO (SK-097)	• PROVIDES GUARD FOR EXPOSED CONDUCTOR BETWEEN ORBITING SPOOL AND COIL
• CONDUCTOR JOGGLE TOOL, JGDI (SK-098)	• PREVENTS STRAIN DURING FORMING PANCAKE-TO-PANCAKE JOGGLE
• CONDUCTOR RING CLAMP, HDTO (SK-099)	• PROVIDES CLAMPING AT INNER RING FOR WINDING
• CONDUCTOR SPLICE SOLDERING TOOL, WLFX (SK-100)	• PROVIDES UNIFORM HEAT CONTROL FOR SOLDERING SPLICE CLAMP PLATES
CLOSEOUT TOOLS	
• WINDING FORM (LEAD TUNNEL, HELIUM FILL & STACK) LEAK TEST TOOLS, HDTO (SK-096)	• VERIFIES INTEGRITY OF WELDS
• SIDE PLATE WELD & ASSEMBLY FIXTURE, WLFX (SK-112)	• ELIMINATES UNCERTAINTIES IN TOLERANCE BUILDUP OF WINDING PACK
• CLOSEOUT WELD LEAK TEST FIXTURE, HDTO (SK-113)	• VERIFIES INTEGRITY OF WELDS

266.729-31

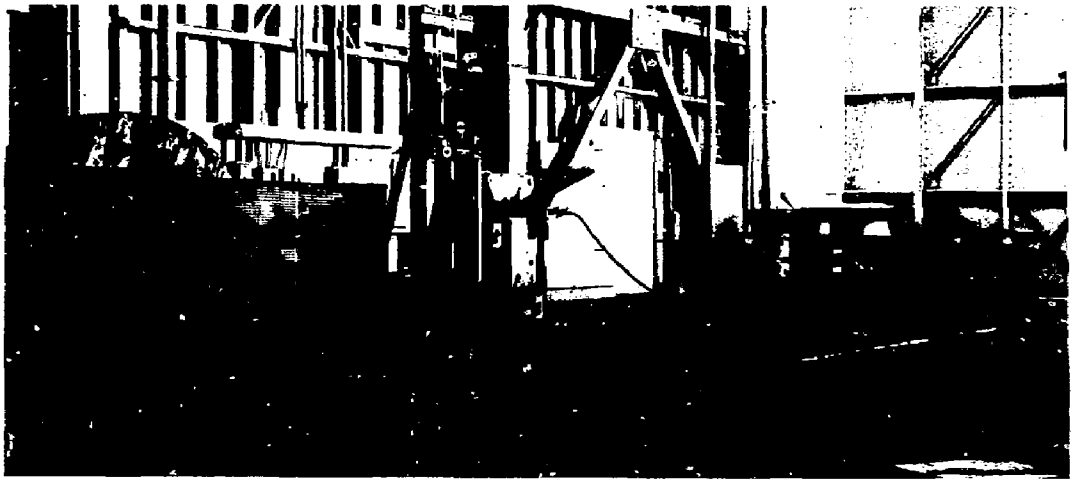

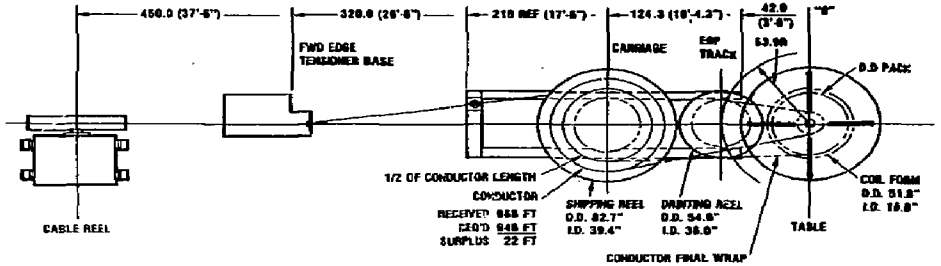

266.729-38

Figure 10-2. HFTF Tensioning System and Floor Layout

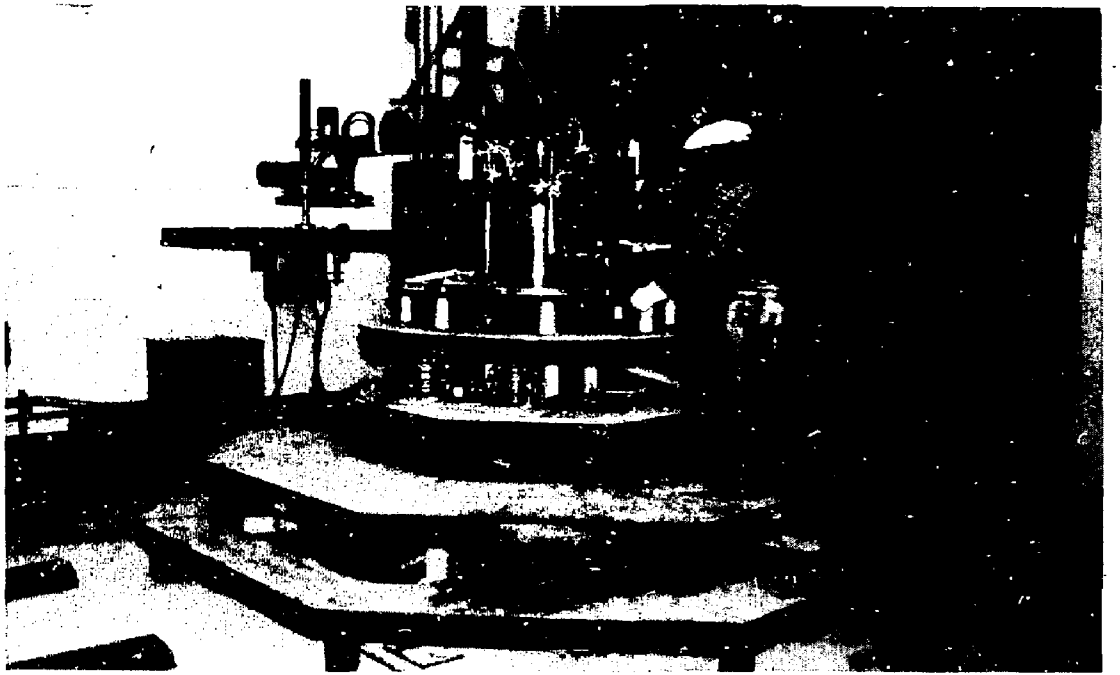

Figure 10-3. HFTF Coil Winder

266.729-39

10.2.3 Equipment Torque Requirements

Shown below are the torque requirements for the winding line equipment:

Turntable Capability (in lb)		Tensioner Capability	Required Torque at Tension (in lb)	
GDC	LLNL	(LLNL)	300 lb	600 lb
480,000	45,536	18,648	8,100	16,200

Even though the General Dynamics turntable has a larger capacity, both units are acceptable. However, the LLNL tensioner has little operating margin of safety if winding tension is 600 lb. The tension system braking motor will stall out at the higher tension values.

10.3 Proposed Tooling Plan

The conceptual layout of the winding line and tooling requirements are shown in Figure 10-4. The winding line consists of a coil winder with orbiting storage reel, conductor payoff station, and tensioning system. Based on a study of pancake winding concepts, the orbiting spool is more favorable than a concentric spool to minimize the risk in conductor strain during manufacturing. The concentric spool concept would virtually be impossible to prevent damaging strains due to the large cross section (54 pancakes) of the insert coil configuration.

Winding tension is provided by a cable wound around the dispensing drum (Figure 10-4). The torque (braking) motor applies tension by unwinding this cable on the take-up drum. Tension is controlled by the pneumatic dancer and monitored by the tensiometer. Since the amount of conductor on the shipping reel varies, the dancer must be changed continously to maintain constant winding tension.

The complete tooling list along with the function planned for each tool is shown in Table 10-1. The plan is divided into winding line equipment, winding tools, and closeout tools. Additional comments regarding the tooling design concepts are discussed in the following paragraphs.

10.3.1 Winding Line Equipment

These are the major tools used continuously during the coil winding operation (Figure 10-4). They consist of the winding form support base, clamping tower and support plate, orbiting spool and support arm, vertical column support and lifting lug, variable tension control and support stand, and the shipping reel carriage extension. The protective tent which covers the winding line and the freon clean station for the conductor (Figure 10-4) are General Dynamics Quality Assurance requirements for contamination control and may not be applicable at LLNL.

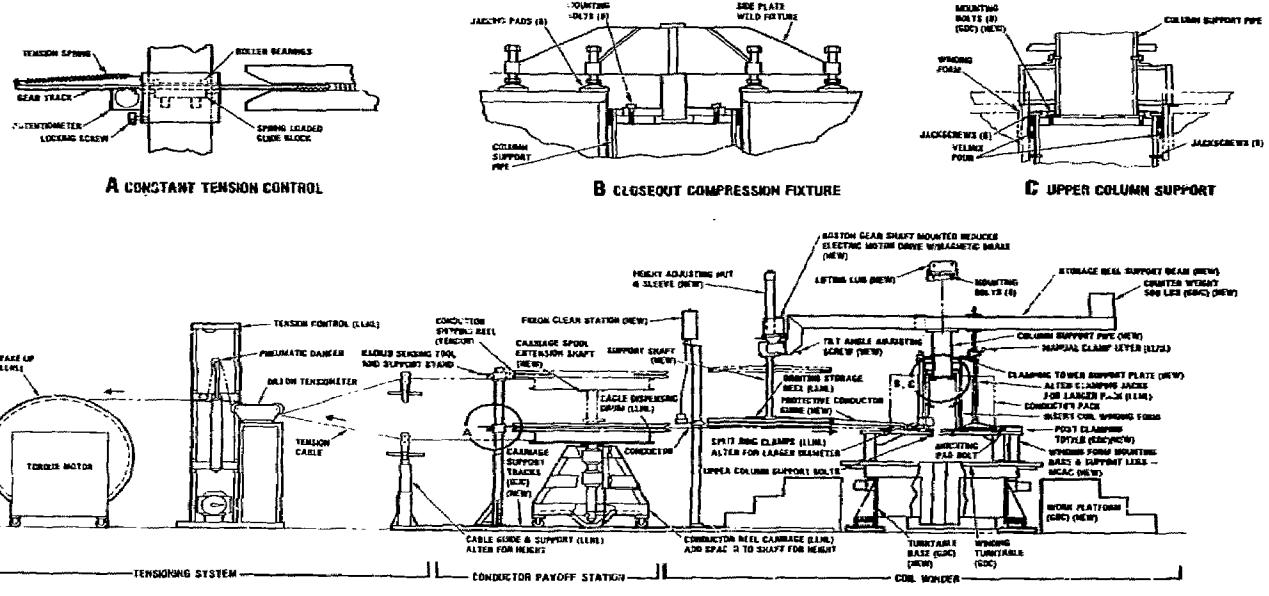

Figure 10-4. Winding Line Conceptual Layout and Tooling Requirements

266.729-8A

a) Winding Form Support Base

A cutout access must be provided in the support base for the lead tunnel and installation of leads. Also, an access must be provided for the helium fill tube. These access areas will also provide clearance for the leak test tools required to check the welds between the lead tunnel, helium fill tube, and winding form.

Also, clamping towers similar to the HFTF configuration should be incorporated in this design. The clamping towers mount to the base and are required for post-insulation installation, as well as to hold tension on the ends of each double pancake prior to splicing.

b) Clamping Tower and Support Plate

The LLNL pneumatic clamps have been replaced with manual clamps to simplify this operation and to eliminate the installation costs of a separately regulated air system. Clamp extensions are also required for the larger pack.

c) Orbiting Spool and Support Arm

General Dynamics could not use the LLNL hardware since it was supported by an overhead cable. GDC's concept incorporates a counterweight to balance the orbiting spool (500 lb). Also, for transferring one half of the conductor length from the shipping reel onto the storage reel, the orbiting spool shift is motorized. This will eliminate a handling operation that was required during winding of the HFTF coil. A recommendation is to use a Boston Gear Model SFWA332-900 shaft-mounted worm gear flanged reductor with a positive lock keyway and a 1/4 HP 115V AC motor. This motor, reversable with magnetic brake, can be be plugged in when required, and will wind 152.4 m (500 ft) of conductor in 15 minutes. The orbiting spool shaft should have both a tilt angle and height adjustment (Figure 10-4) to minimize the conductor strains in the joggle area of each double pancake.

d) Vertical Column Support and Lifting Lug

The center column support (Section View C, Figure 10-4), is a thick, walled pipe with mounting flanges which is installed inside the inner ring. The bottom flange mounts to the support base and the top flange supports the clamping tower, orbiting spool and support arm, or lifting lug as required. Jack screws are used at the top to prevent buckling of the inner ring during winding. The pipe should also extend high enough on the winding pack for installation of the split ring clamp.

e) Variable Tension Control and Support Stand

A major improvement to the winding line was the addition of a constant tension control system. This system incorporates a conductor reel radius sensing device with stand (Section View A, Figure 10-4) which automatically varies the pneumatic dancer for constant tension control. Details of the electronic control circuit are included in Appendix G. Besides a visual display of tension at the control panel, provisions for a strip chart recorder are included if a permanent record of tension is desired. This data is useful for evaluation and disposition of conductor damage in the event of an accident.

f) Shipping Reel Carriage Extension

The LLNL carriage support has a mechanical height adjustment. A shaft extension is installed when required.

The conductor carriage can be moved on tracks and positioned vertically to facilitate handling of the storage reel. This will eliminate the requirement of an "A" frame hoist in repositioning the orbiting storage spool to the payoff station.

10.3.2 Winding Tools

These are hand tools and manufacturing aids required for winding. They consist of the HFTF work stands, lead form mandrels, conductor protector guide, conductor joggle tools, conductor ring clamp, and conductor splice soldering tool. The work stands (Figure 10-3) will be modified as required.

a) Lead Form Mandrels

General Dynamics' tooling concept for the entering and exiting lead from mandrels is shown in Figure 10-5. The leads are fabricated using the A-Cell superconductor. The lead stabilizer pieces are received machined in a straight configuration. After soldering, the leads can be formed to fit in the lead tunnel using the four steps shown in Figure 10-5. The tool compensates for springback and includes dimension feelers for inspection purposes.

b) Conductor Protector Guide

The removable guide is an aluminum channel (Figure 10-4) secured to both the orbiting spool and ring clamp with pull pins. The guide will prevent possible reverse bends in the exposed conductor between orbiting spool and winder.

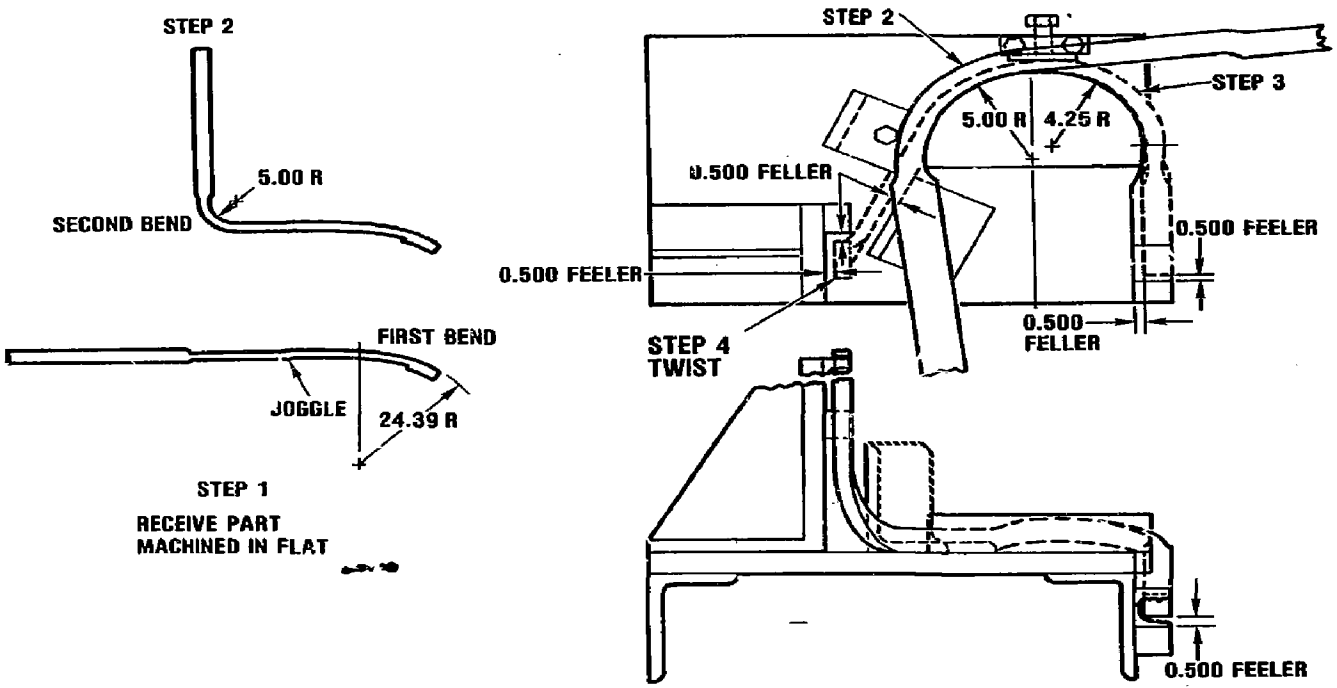

Figure 10-5. Entering/Exiting Lead Form Mandrels

c) Conductor Joggle Tool

General Dynamics' tooling concept for the conductor joggle fixture is shown in Figure 10-6. It is recommended that a tool be utilized for this operation. Any attempt to produce the offset without a tool may result in conductor damage. The tool is a die with clamping surfaces contoured for the double radii of the joggle. During development of the tool, the contoured surface pieces are removable. Analytical radii are located in the flat pieces and then rolled to the radius of the winding form.

The first step in producing the conductor joggle is to wind the conductor under tension around the inner ring (Figure 10-5). Then, with tension off, an aluminum strap is secured around the conductor (Figure 10-5) and the conductor is pulled back. The strap will prevent overstraining the conductor. The orbiting spool is raised approximately one half inch for the second pancake height and tilted down towards the inner ring. The joggle tool is then installed and the offset in the conductor is formed as the bolts are equally tightened. The bolts can be tightened from either end.

d) Conductor Ring Clamp

The split ring clamp is shown in Figure 10-4. General Dynamics planned on utilizing the HFTF design concept, redesigned for larger pack diameter. The clamp fits around the inner ring of the winding form, and is repositioned after winding each pancake. The conductor is held at the inner ring by a movable tapered block wedged against the conductor. The wedge action tightens as winding tension is applied. Adjustable dog legs extending from the perimeter of the ring clamp hold the joggle tight circumferentially.

e) Conductor Splice Soldering Tool

General Dynamics' concept is presented in Section 10.5. Coil Winding.

10.3.3 Closeout Tools

These are tools and manufacturing aids required for operations other than winding. They consist of winding form leak test tools (lead tunnel, helium fill, and stack), side plate weld and assembly fixture, and closeout weld leak fixture.

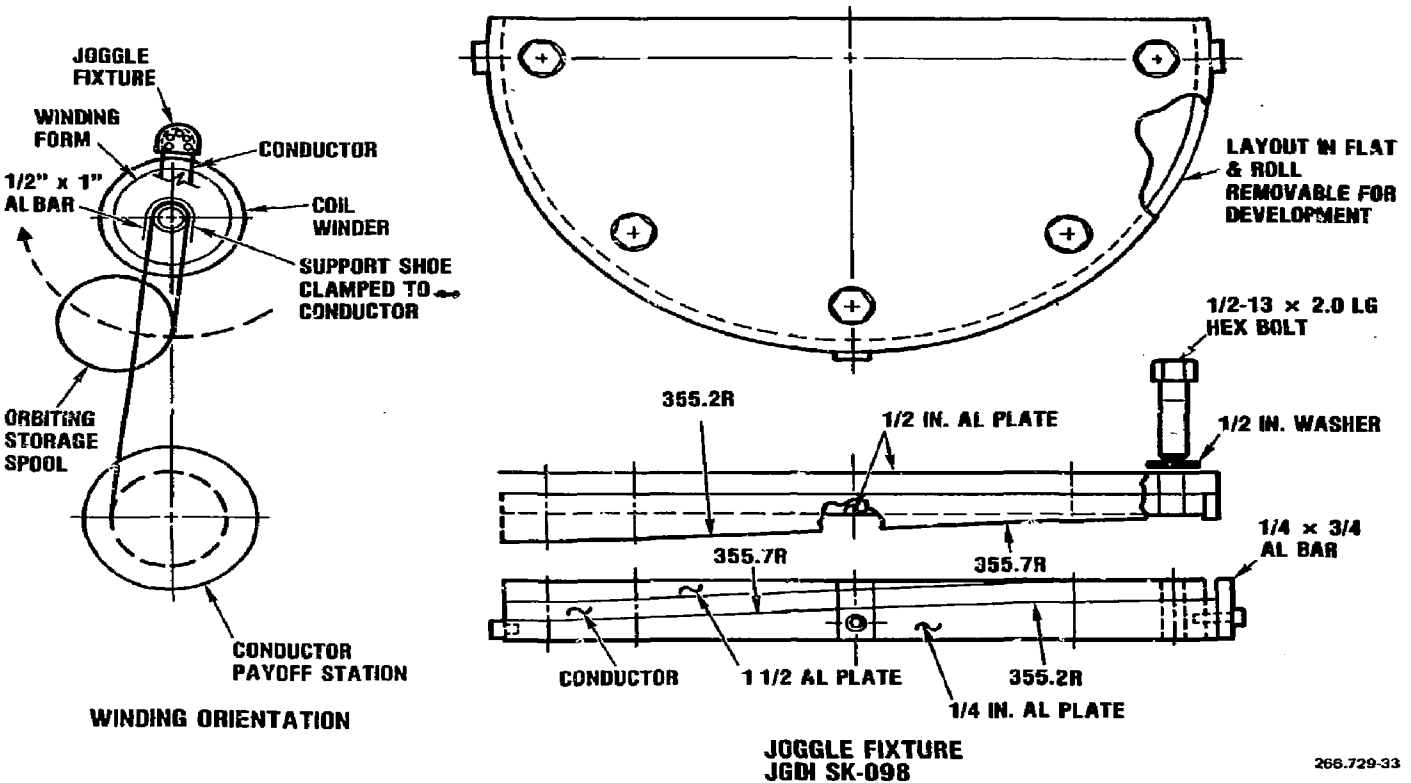

Figure 10-6. Conductor Joggle Tool

a) Winding Form Leak Test Tools

General Dynamics recommends a leak test of the lead tunnel as well as the helium fill tube prior to winding. The inner ring welds are a lower risk and will be checked after closeout. A shoe-type tool can be utilized for the tunnel welds. The other tools are similar to those used on the solenoid coils.

b) Side Plate Weld and Assembly Fixture

This fixture (Section View B, Figure 10-4) consists of six legs with jack pads that can be torqued against the side plate to eliminate potential gaps in the winding pack. The fixture mounts directly to the center column support and can provide a compression load of up to 50,000 lb.

c) Closeout Weld Leak Test Fixture

A test tool is required for both the inner ring welds as well as the other ring. The shroud concept used on the solenoid coils can be utilized for the insert coils.

10.4 Prep for Winding

The prep for winding section of the manufacturing assembly sequence and flow plan, shown in Figure 10-7, starts with receipt of the L-shaped winding form, outer ring (case) segments, and side plate from CBI. The helium fill tube, a portion of the lead tunnel, and mounting tabs are received welded to the winding form.

The first operation is to mount the winding form and support base on the prep station (coil winder if available). The winding form mounts to the base and is held in position by the machined tables provided (Figure 10-7). As a producibility item, these tabs were added to the winding form design. The turntable is then rotated to determine optimum location for flatness of the side wall and concentricity of the inner ring. Shims can be added if required to the support base legs. The turntable must be leveled prior to installing the winding form. After proper alignment is obtained, the support base is attached to the turntable. The center column support is then installed and bolted to the base (Figure 10-4). The inner ring is supported at the top by jack screws and a liquid shim (Velmix) poured to hold the winding form in a rigid position. This fixture will stay with the coil until closeout welds are complete.

A cutout access area is provided in the support base (Figure 10-7) for installation of leads and leak tests. The lead tunnel and helium fill tube welds are then helium leak tested. The inner ring/side plate welds are checked after closeout. The mounted winding form is now ready for installation of leads, insulation, and Kapton.

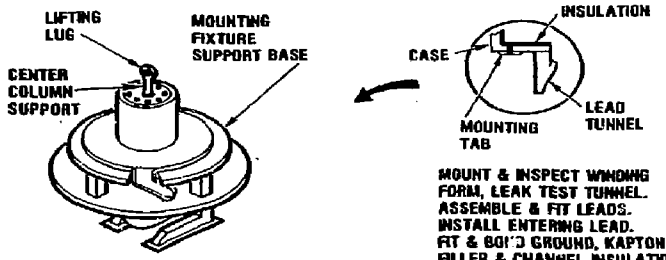

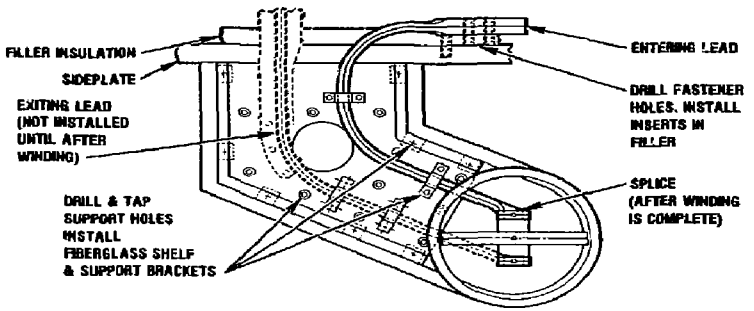

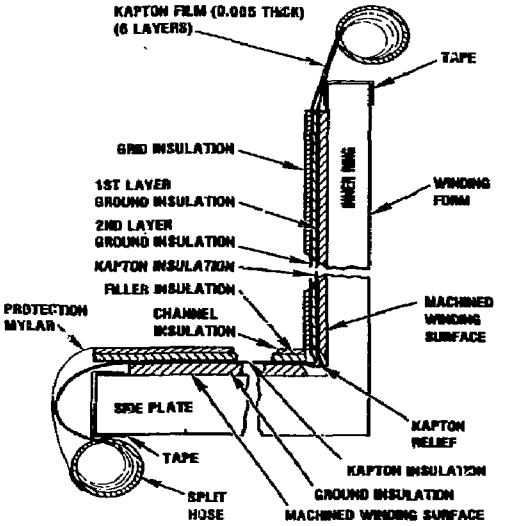

266.729-4A

Figure 10-7. Prep for Winding

10.4.1 Installation of Entering Lead

The next operation is the installation of the entering lead (Figure 10-7). Both the entering and exiting leads are fabricated using A-Cell superconductor. The copper stabilizer half sections are received machined in a straight configuration and soldered. The leads are bent utilizing the form mandrels and fitted in the tunnel.

The lead support brackets and tunnel shelf mounting holes are drilled and tapped. The fiberglass shelf and entering lead are then installed. The exiting lead is installed after winding since it is formed across the pack. Also, since the entering lead extends some three feet beyond the tunnel, it would interfere with the winding personnel. Therefore, as a producibility item, a coil-to-stack splice will be incorporated in the design to eliminate this problem. The entering lead will be spliced to the first pancake winding.

10.4.2 Installation of Insulation and Kapton

The winding form is now ready for insulation and Kapton. As shown in Figure 10-7, ground insulation is bonded to both side plate and inner ring. Six layers of Kapton are applied followed by the installation of grid insulation on the inner ring and filler and channel insulation on the side plate.

The entering lead is then located (Figure 10-7) to the side wall. Mounting holes are drilled and tapped in the side wall and inserts installed in the back side of the filler insulation.

10.5 Coil Winding

The insulated winding form with entering lead is moved (if required) to the coil winding station. A lifting lug which attaches to the center column support should be used for lifting. The orbiting storage spool support arm is then installed. Winding is divided into three steps as shown in Figure 10-8.

Step one in the winding process starts by loading the conductor shipping spool directly onto the payoff station. The conductor reacted on 80-cm spool are specified for the first and last pancakes. The end of the conductor length is inserted in a slot provided in the storage spool and secured. One half of a conductor length is then transferred onto the orbiting storage spool (clockwise) as shown in Figure 10-8. The storage spool orbits around the winding machine as the winder turns. The storage spool is then positioned as shown and rotated clockwise with the shift drive motor to the center of the conductor length as specified by the vendor.

10.5.1 Winding First Half of Double Pancake

The orbiting storage spool is then repositioned for winding the first pancake. Step two starts with the installation of the joggle at the first turn where the conductor joggles from one pancake to another. (Refer to conductor pack cross-section in Figure 10-8). The joggle tool is used to produce the offset in the conductor at the center length. The conductor joggle is then secured against the inner ring by the split ring clamp. With tension applied, the first half of the double pancake is wound. A winding tension of between 300-600 lb shall be selected by LLNL. The actual value will be determined by observation during practice winding. Turn-to-turn insulation, provided on a reel, will be inserted simultaneously between each turn of conductor. Nine (9) compaction clamps as shown in Figure 10-8 will be utilized to insure a tight pack. The end from the first pancake is then spliced and soldered to the entering lead and fastened, under tension, to the side plate with the splice anchor support fitting. Tension is provided by a portable weight stand.

10.5.2 Winding Second Half of the Double Pancake

Upon completion of the 57 turns of the first pancake, dimensional inspections and electrical tests are performed. The dimensional inspections are described in Section 10.9, Inspection Plan. The electrical tests were already discussed in Section 9.0. Pancake insulation is installed over the first pancake.

The conductor storage spool is then removed and repositioned on the payoff station (Figure 10-8). The payoff station carriage can be moved on tracks as described earlier to facilitate handling of the conductor. The second pancake is wound in the opposite direction as shown in Figure 10-8. The conductor is clamped to the side plate with the clamping tower and cut off. This end of conductor is ready to splice to another pancake following the winding of the next double pancake. This process is repeated until twenty-seven double pancakes have been wound. The last end is then splied to the exiting lead and fastened to the side plate during closeout.

10.5.3 Pancake-to-Pancake Splice

The conductor pancake-to-pancake splice assembly and conceptual design of the soldering tool are shown in Figure 10-9. The splice is made in three sections. Soldered copper clamp plates are used in the middle for the electrical splice and stainless steel clamp plates are used on both sides for the structural splice. The splices are four pancakes wide and alternate from the left side to the right side of the coil for a total of 26 splices. The clamp plates are received contoured and machined with slots for the two conductor ends as shown. At alternate ends of each structural splice, a recessed area is provided so only one conductor end is clamped.

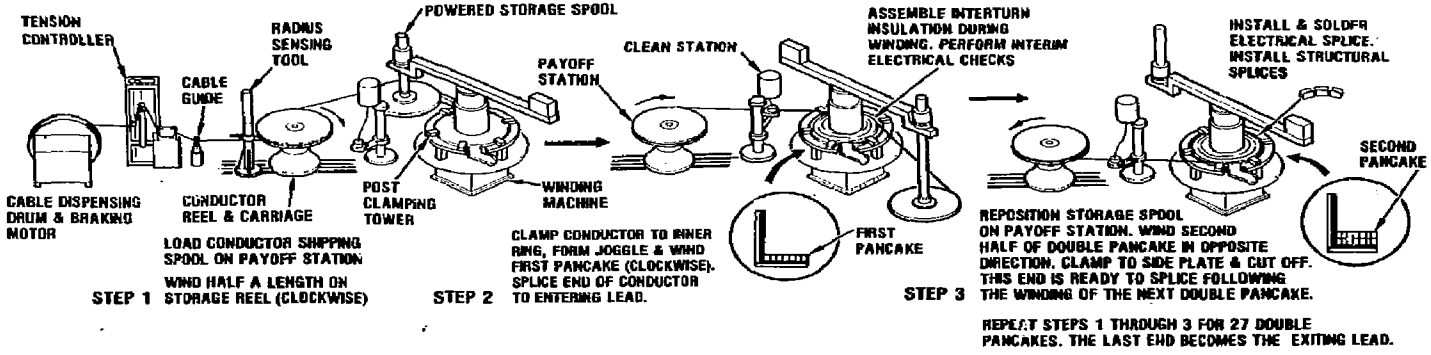

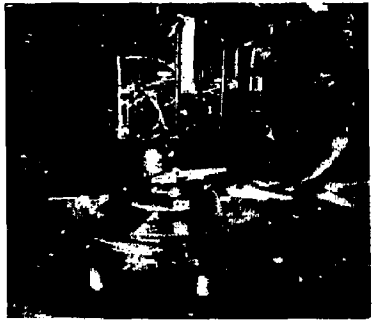

WIND HALF LENGTH OF CONDUCTOR ON STORAGE REEL

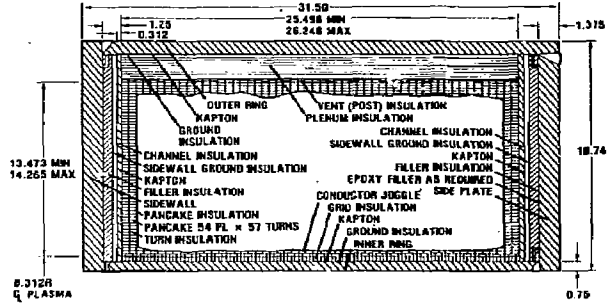

WINDING PACK

COMPACTION CLAMPS & POST CLAMPING TOWERS

266.729-3A

Figure 10-8. Coil Winding

For soldering, two 300-watt soldering irons are threaded in an aluminum heat conduction block, contoured to the copper clamp plates. During operation, six of the splice fasteners will be used to hold the tool in place. The remaining fasteners are torqued as the solder is melted. Temperature is controlled by a dimmer switch and monitored by a surface pyrometer (Figure 10-9) and thermocouples attached to the splice fitting if desired. Each conductor end is tensioned with portable weight stands before clamping towers are removed. The structural splice plates are installed with the fasteners and torqued prior to soldering. General Dynamics had planned on making a practice splice for development and proofing of this tool. However, the design was never completed, and budget for this task was returned to LLNL.

10.6 Closeout and Weld (Side Plate)

The coil is now ready for closeout and welding on the side plate, Figure 10-10. The coil is removed from the winder with the mounting fixture and positioned on the floor. The orbiting spool support arm is replaced with the lifting lug.

The next operation is the installation of channel, filler, and ground insulation for the side wall (Figure 10-10). Kapton is wrapped between the channel and ground insulation. The side plate is then fitted and the closeout compression fixture installed (Figure 10-10). Based on torque versus deflection values, the six jacking pads are equally loaded to eliminate any gaps in the winding pack. Since movement in the pack is expected, caution should be taken to avoid hitting the weld backup bar. A thicker piece of filler may be required prior to loading.

10.6.1 Installation of Exiting Lead

The exiting lead is then installed in the lead tunnel (Figure 10-10). The mounting holes are located in the side wall and drilled and tapped The compression fixture, along with the side plate and filler insulation, are disassembled for installation of the inserts in the filler.

10.6.2 Installation of Side Plate

The side plate and compression fixture are then reinstalled and load applied. After proper weld gaps are obtained, the side plate is welded by CBI. A high temperature fabric (Hitco) tape shall be used to seal and protect the coil edge prior to welding. The jacking pads should be backed-off during welding to allow for weld shrinkage. The last pancake is then spliced and soldered to the exiting lead and fastened, under tension, to the side plate with the splice anchor support fitting (Figure 10-10). Tension is provided by a portable weight stand. The entering lead coil-to-stack splice is then installed.

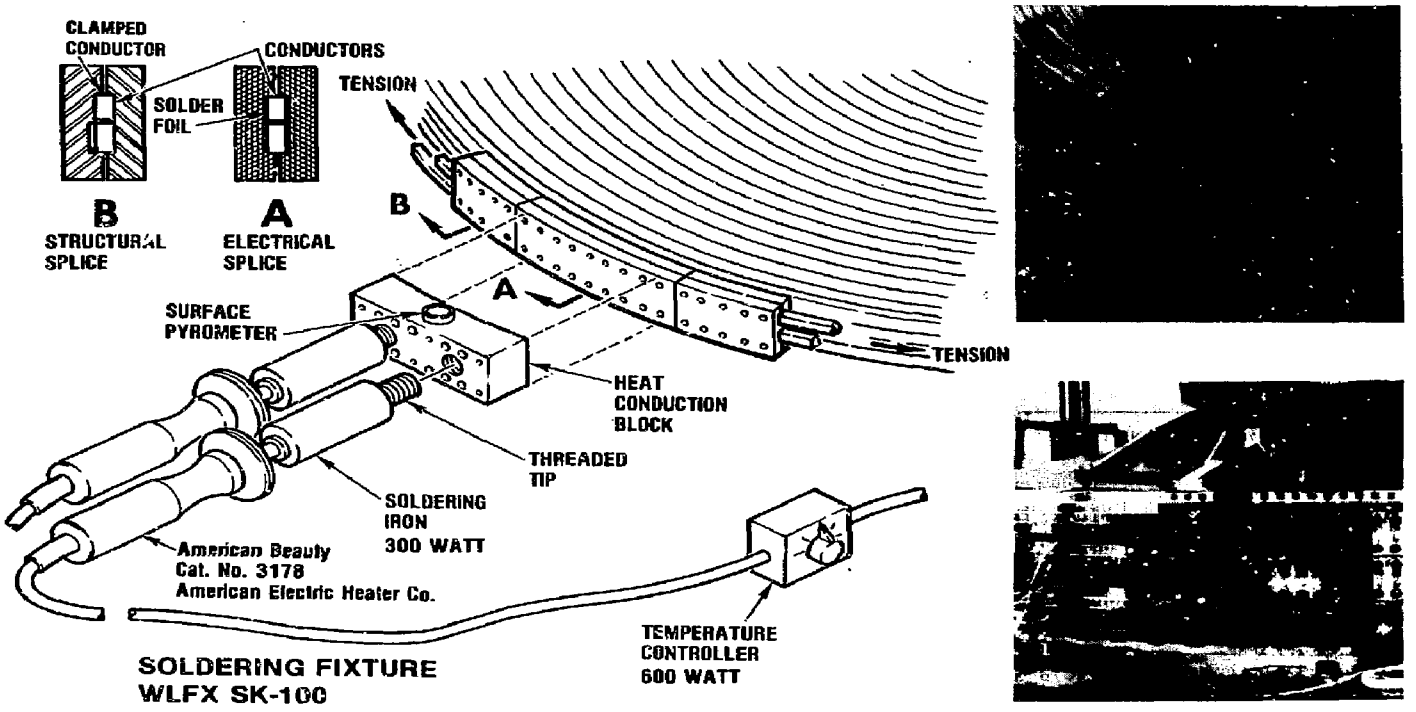

Figure 10-9. Conductor Splice Assembly and Soldering Tool

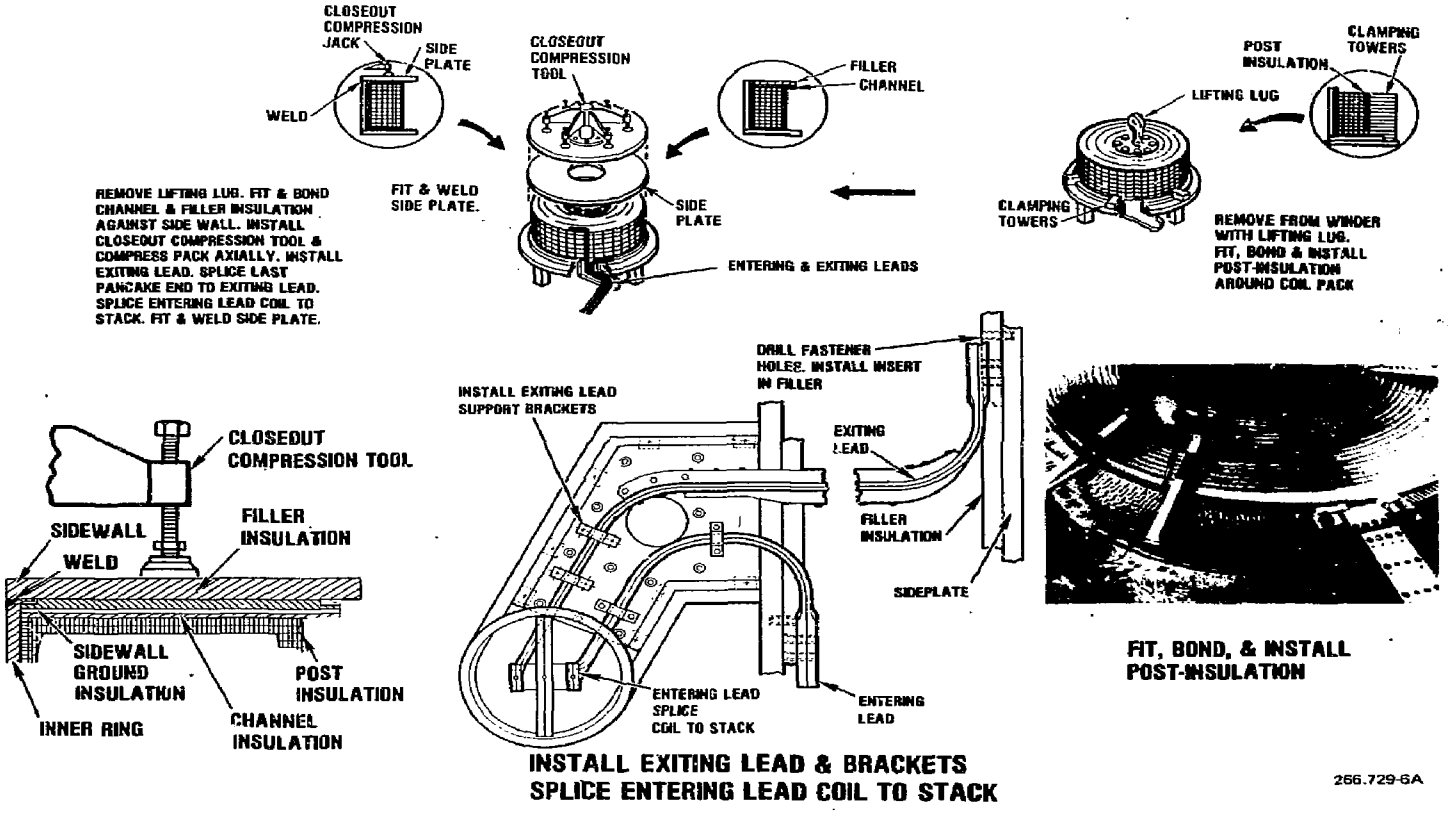

Figure 10-10. Closeout and Weld (Side Plate)

10.7 Closeout and Weld (Outer Ring)

The coil is now ready for closeout and welding of the outer ring and final verification tests as shown in Figure 10-11. Closeout continues with the installation of plenum and wire-run insulation. Voltage tap wires are routed to the lead tunnel area and insulation covers installed. The wires run through the tunnel in polyurethane tubing covered with braided glass sleeving and epoxy. The piccolo assembly and helium fill tube vent are then installed along with the fiberglass tunnel covers, shoulder bushing, polyurethane corner insulation, and Kapton insulation for the tunnel area. The coil's six layers of Kapton insulation are then trimmed and wrapped around the outside of the coil. Closeout is completed by installing insulation covers and closeout insulation over the Kapton (Figure 10-11).

10.7.1 Installation of Closeout Insulation

The insulation covers and closeout insulation are cut away to provide clearances in the coil open areas. The open areas are for the outer ring vertical weld backup bars, piccolo and vent assemblies, and wire-run insulation. Under operating conditions, the conductor loads are fully self-reacted. Therefore, the outer ring should not be installed to form hard regions in these open areas which would support the conductor.

After insulation covers are installed, it is recommended that the plenum insulation be snugged down against the pack using nylon straps with rachet buckles. These straps will eliminate plenum gaps without inducing radial loads to the conductor. The pack can then be held in place with fiberglass tape (Figure 10-11). With the straps removed, however, some sponginess will remain. Closeout insulation is then installed, if required, to compensate for this sponginess. Closeout insulation is a solid fiberglass sheet (Figure 10-11) with thickness accurately determined as shown in Figure 10-12.

The amount of closeout insulation required is a function of the compressed dimension (Figure 10-12) and weld gaps established by CBI. Based on certain weld gaps, the amount of closeout insulation may be negligible and not required. An average compression value can be determined by checking the coil at several radial locations. Closeout insulation should be installed in increments of .8 mm (1/32 in) for gaps in excess of 1.5 mm (0.060 in). Allow at least .76 mm (0.030 in) between the pack and outer ring for any uncertainties.

10.7.2 Installation of Outer Ring

The two outer ring segments are then fitted to the side plates by CBI. With the aid of large "C" clamps, the outer ring is located as shown in Figure 10-11. After the proper weld gaps have been obtained (Figure 10-12), the vertical welds and closeout welds on

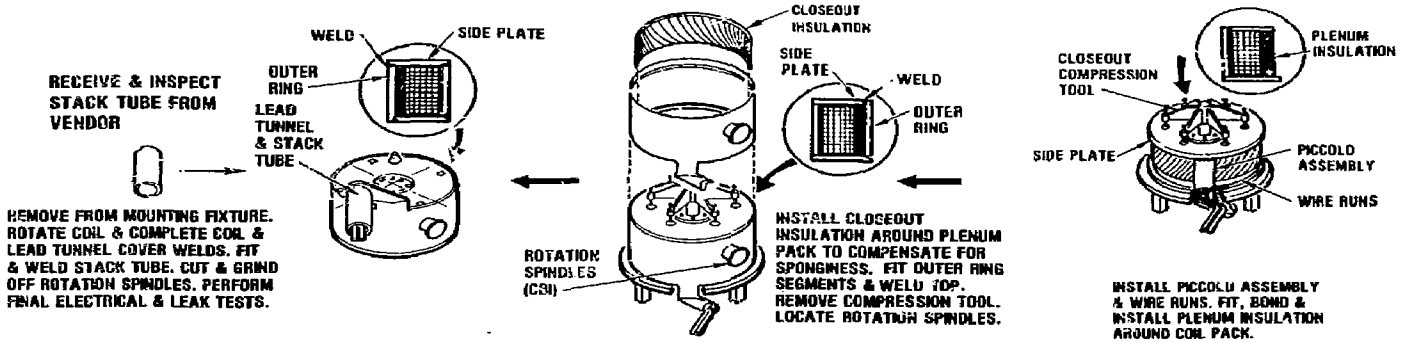

PERFORM FINAL ELECTRICAL & LEAK TESTS.

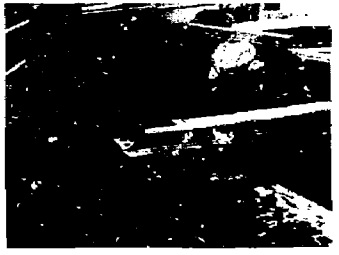

FIT OUTER RINGS TO SIDE PLATES LOCATE OUTER RINGS IN POSITION WITH 'C' CLAMPS & WELD (CBI)

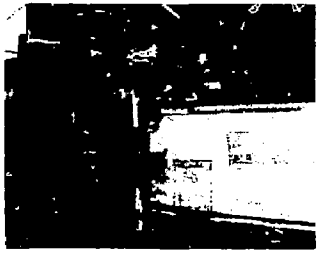

COMPLETE CLOSEOUT, WRAP KAPTON, INSTALL INSULATION COVERS. CLOSEOUT INSULATION

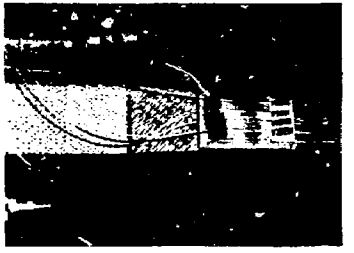

INSTALL PLENUM & WIRE RUN INSULATION

266.729-32

Figure 10-11. Closeout and Weld (Outer Ring)

PLENUM INSULATION
EXCEEDS CASE

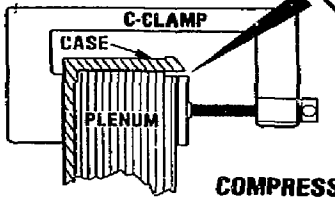

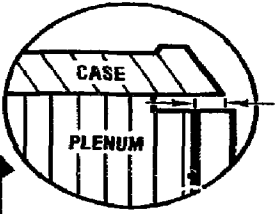

COMPRESS PACK TO DETERMINE
COMPRESSION VALUE

COMPRESS OUTER RINGS FOR
DESIRED WELD GAP

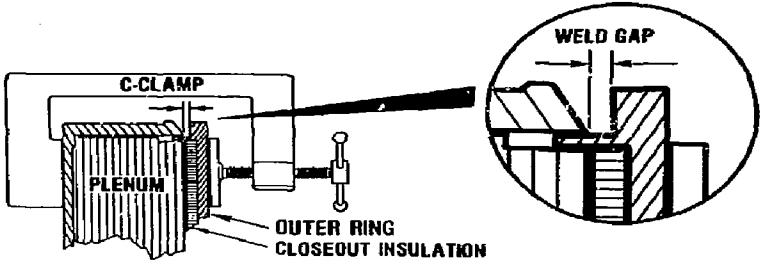

$$\text{COMPRESSION DIMENSION} + \frac{\text{WELD GAP}}{2} = \text{CLOSEOUT INSULATION DIMENSION}$$

266.647-37

Figure 10-12. Compress [illegible]

one side are completed. A high temperature fabric (Hitco) tape shall be used to seal and protect the coil edge prior to welding. Rotation spindles (Figure 10-11) are then installed by CBI. The coil mounting fixture and closeout compression tool are removed. The coil is rotated to complete the closeout welds.

The tunnel cover, which is part of the outer ring, is then welded, along with the the stack tube. It is also recommended that the helium fill tube adapter required during the plumbing installation, be welded here. These areas are not accessible after the insert coil has been aligned inside the outer axicell coil. After welding is complete, the rotation spindles are cut off and ground flush.

10.7.3 Final Verification Tests

The coil is now ready for final electrical and leak tests, and magnetic axis determination. The electrical tests were already discussed in Section 9.0. After the case closeout welds are completed, the entire coil is tested for leaks along the welded seams. Special test shoes (shrouds) matched to either the inner and outer ring radius will be used to isolate each seam area for leak testing. Additional tools are provided for testing case seam leaks in the vicinity of the lead tunnel. Some of these shoes should contain calibrated leak fittings so the sensitivity of the leak detector equipment can be checked.

The magnetic mapping test for determination of the magnetic axis may not be required. If required, LLNL shall determine the method of performing the test. It is recommended, however, that a mechanical center be used in lieu of a magnetic axis, and that the mechanical center be located geometrically. Centerlines will be required during the mating and installation operations. The geometric centerlines of the coil can be very accurately located since the critical dimensions on the coil case are closely machined. An inspection tool, indexed off the inner ring inner surface of the winding form, shall be used to establish the centerlines prior to winding. Centerlines should be established for both ends of the coil and identified by punch marks. The case markings should also indicate the top of the coil as well as the true horizontal orientation.

10.8 Mate and Assembly

The completed insert coil (A2 Inner) is now ready to be mated with the axicell coil (A2 Outer) and installed in the vacuum vessel as shown in Figure 10-13. Originally, these coils were to be mated in a horizontal position at General Dynamics Convair. This two-coil assembly will now be mated by CBI at LLNL utilizing a vertical assembly concept (Figure 10-13). This new approach was a major improvement to eliminate the requirement for expensive horizontal mating fixtures.

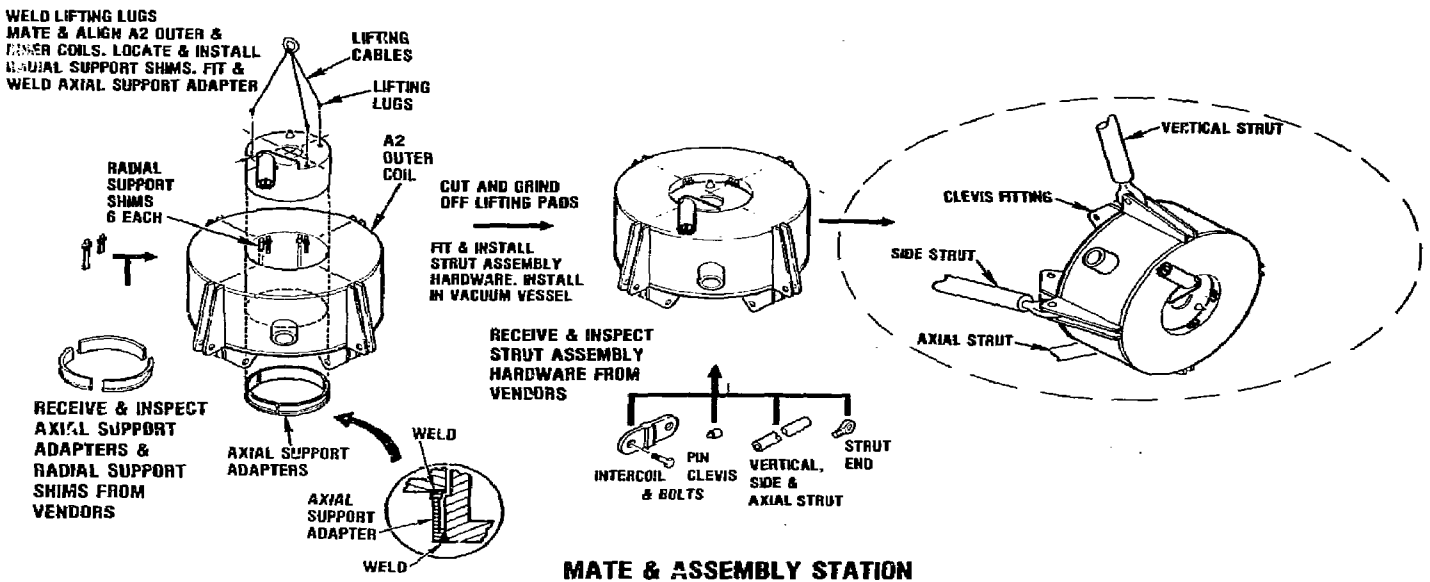

Figure 10-13. Mate and Assembly

266.729-7A

Prior to mating, exterior surfaces of the coils, lead tunnel, and stacks are to be cleaned. It is recommended that scale, rust, and oxides be removed by grinding and sandblasting. These surfaces shall then be wiped clean with freon.

The Mate and Assembly section of the Manufacturing Sequence and Flow plan starts by welding lugs to three of the four mounting pads (Figure 10-13). The A20 coil is then positioned on blocks and shimmed with mechanical axes level. The A2I coil is lowered into position by lifting cables (Figure 10-13). Temporary wooden wedges will be used to obtain radial position. The three-piece axial support adapter (Figure 10-13) is then fitted for proper axial location. Wooden blocks are then used under the A2I coil for support and shimmed as required to align the mechanical centers. Inspection tools indexed off the machined inner ring inner surfaces of each coil can provide accurate alignment measurements at both ends of the coil.

After proper alignment and positioning of the two coils, the wooden wedges are removed, one at a time, and the six sets of radial support shims installed (Figure 10-13). After all twelve shims are installed, the shim adjustment studs are torqued, locking them into position; and the sides of each shim are tack-welded to the A20 coil preventing movement during operation. It is recommended that alignment measurements be checked several times during this assembly. The axial support adapter pieces are then welded. Welding should not create significant distortion. It is recommended that all three adapter pieces be tack welded in place. Then a weld pass would be done on first one, then the next and the next, thereby applying the weld metal build-up to all three uniformly. The axial load adapter does not control misalignment since it is installed after the shims are in place and snug.

The lifting lugs and mounting pads are then cut off and ground flush. The mounting pads would interfere with the thermal liner installation. Finally, the mated assembly is now ready for installation in the vacuum vessel.

10.9 Inspection Plan

The proposed inspection plan is shown in Table 10-2. It is recommended that data sheets, logs, and checklists, similar to those used during the solenoid coil manufacturing process, be developed for the Nb_3Sn coil (Reference 10-1). To achieve adequate overall quality these detailed documentation requirements must be implemented. After each pancake is wound, a review of all inspection data is recommended. At completion of coil winding and mating, final acceptance is recorded and provided on the inspection acceptance sheet (Reference 10-1). The plan is divided into three groups - dimensional inspections, in-process inspections, and visual inspections.

10.9.1 Dimensional Inspections

On receipt of the winding form, the winding form should be dimensionally inspected and the measurements checked against those given on a receiving inspection form (Reference 10-1). Compaction

Table 10-2. Proposed Inspection Plan

DIMENSIONAL INSPECTIONS

- WINDING FORM RECEIVING MEASUREMENTS
- TURN COMPACTION MEASUREMENTS
- PANCAKE COMPACTION MEASUREMENTS
- MATING ALIGNMENT MEASURMENTS

IN-PROCESS INSPECTIONS

- WINDING
  - TURN-TO-TURN GAP (<0.002 INCH)
  - TURN FLATNESS (<0.002 INCH)
- SPLICING
  - ULTRASONIC OF SOLDER BOND
  - SCREW TORQUE VERIFICATION
- WELDING
  - DYE PENETRANT
  - ULTRASONIC

VISUAL INSPECTIONS

- *SUPERCONDUCTOR*
- TURN INSULATION
- VOLTAGE TAPS AND INSTRUMENTATION LEADS
- CLEANINESS/DEBRIS
- PANCAKE FLATNESS (<0.005 INCH)

266.729-36

measurements are required for both turn and pancake buildup as shown in Figure 10-14. A check gage, similar to the one used on the solenoid coils, could be fabricated, but would have to be removed when winding to prevent interference with the orbiting storage reel. Therefore, the recommendation is to use optical equipment as shown in Figure 10-14. Instructions on how to set up this equipment for compaction measurements are included in the following paragraphs. Also, alignment measurements are required for mating of the A2I and A20 coils A table should be prepared for measurements which align the mechanical centers of the two coils. Data should be recorded before and after final assembly and checked aginst those in the table.

Turn (Radial) Compaction Measurements -- The recommended turn compaction record sheet is shown in table 10-3. To check radial buildup of the pack, locate two (2) tooling buttons on the floor to establish line-of-sight. The buttons should be approximately four feet from the center of the turntable. Set up a jig transit to the buttons on the floor for the line-of-sight (Figure 10-14). Prior to winding, take a scale reading at each radial position (0°, 90°, 180°, and 270°) from the inner ring to the line-of-sight and record these base dimensions. During winding, repeat the scale readings for the turns specified (Table 10-3) to the line-of-sight for each pancake. The difference between these dimensions and the base values is the pack radial buildup.

Pancake (Axial) Compaction Measurements

The recommended pancake compaction record sheet is shown in Table 10-4. To check axial buildup of the pancakes, set up an optical level as close to the coil winder as practical. The level line-of-sight must be above the top of the last pancake (Figure 10-14). Using the top of the coil winder as a reference plane, take a scale reading at each radial position (0°, 90°, 180°, and 270°) to the line-of-sight and record these base dimensions. Next repeat the measurements from the top of the insulated winding form to the line-of-sight, prior to winding the first pancake. The difference between these dimensions and the base values is the distance from the bottom of the pack to the top of the winder. Record these reference measurements. During winding, repeat the scale readings for the turns specified (Table 10-4) to the line-of-sight for each pancake. The difference between these dimensions and the base values gives the distance from the top of the pack to the top of the winder. Subtracting this difference from the reference dimensions tabulated earlier is the pack axial buildup.

10.9.2 In-Process Inspections

In-process inspections are to be made and recorded on log sheets on a continuous basis during manufacture. Any noted deviation from the tolerance limits require immediate halting of the operation until a correction is made. The in-process inspections are divided into winding, splicing, and welding.

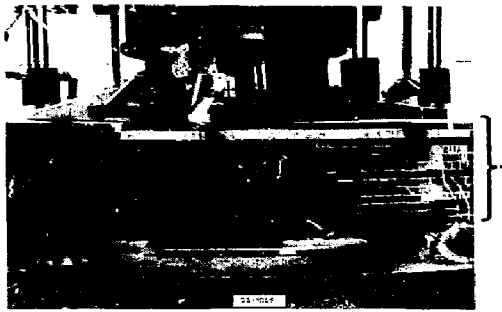

PANCAKE (AXIAL)
COMPACTION

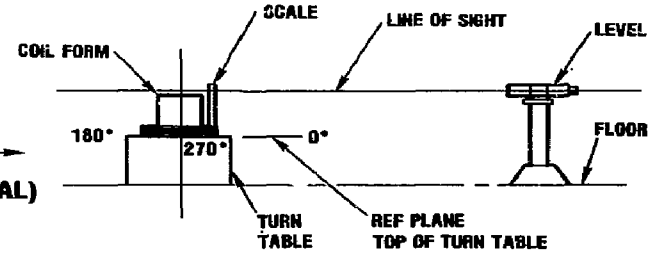

TURNS 1, 57
FOR 0°, 90°, 180°, 270°

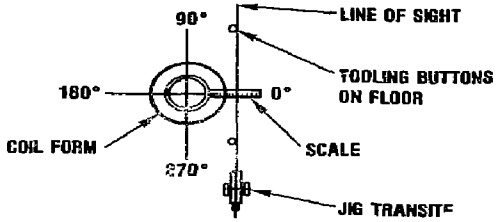

TURNS 1, 14, 29, 43, 57
FOR 0°, 90°, 180°, 270°,

TURN (RADIAL)
COMPACTION

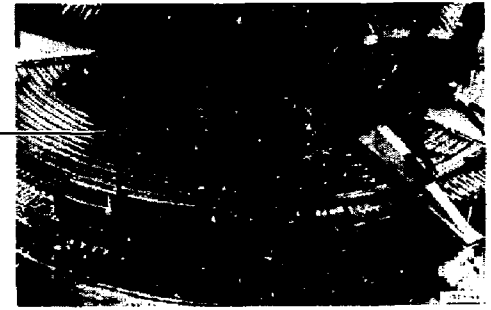

Figure 10-14. Optical Compaction Measurements

266.729-37

Table 10-3 (Turn (Radial) Compaction Record

Coil No. ____

	TURN																				
	1				4				29				48				57				
	POSITION				POSITION				POSITION				POSITION				POSITION				
PANCAKE NO.	0°	90°	180°	270°	0°	90°	180°	270°	0°	90°	180°	270°	0°	90°	180°	270°	0°	90°	180°	270°	
1																					
2																					
3																					
4																					
5																					
6																					
7																					
8																					
9																					
53																					
54																					

Table 10-4. Pancake (Axial) Compaction Record

	POSITION							
	0° TURN		90° TURN		180° TURN		270° TURN	
PANCAKE NO.	1	57	1	57	1	57	1	57
1								
2								
3								
4								
5								
6								
7								
8								
⋮								
53								
54								

Reaction Mandrel

Diameter, cm	80	70	60
Test Strain, %	.46	.43	.38

These listed strains will result in a total applied fiber strain of 0.7 percent considering the bending strain induced from straightening from the reacted shape.

c) Repeat the critical current tests of 9.4.1 (a).

Note: If these tests (a, b, and c above) consistently produce results that show no evidence of degradation, a savings in cost and schedule could be realized by eliminating the initial critical current tests.

9.5 High Field Coil Sensor Tests

9.5.1 Sensor Tests Following Sensor Installation

a) Following the CLTS temperature sensor installation on the coil case, coil supports and coil helium supply and return links, the sensor resistance will be measured and the insulation resistance (sensor to coil case) at a low (50 Vdc) voltage will be measured.

b) Following installation of the liquid level sensor, the tests defined by the sensor manufacturer will be performed.

9.5.2 Sensor Tests Following Sensor Lead Wire Installation

a) Prior to and following termination of the CLTS temperature sensor lead wires in the vacuum chamber internal connectors, the tests of 9.5.1 (a) will be performed. These tests will be repeated following mating of these connectors with the appropriate vacuum chamber feedthrough receptacles.

b) Following the connection of the liquid level sensor lead wires to the sensor, and the routing of these lead wires through the coil stack assembly, the tests of 9.5.1 (b) will be repeated.

9.6 References

9-1. "In-Process and Final Verification Test Procedure for MFTF-B Solenoid Coil," Document No. 71E0011.

For winding, turn-to-turn gaps and turn-to-pancake gaps are monitored to ensure that the winding tolerances are maintained throughout the coil. The maximum allowable gap between winding turns and the turn insulation shall be less than .05 mm (0.002 in). It shall not be possible to insert a .05-mm (0.002-in) feeler gage between them. Also, the bottom surface of each turn must be against the pancake insulation, and it shall not be possible to insert a .05-mm (0.002-in) feeler gage between them.

For splicing, an ultrasonic inspection of the solder bond is required. Also, a screw torque verification is required during soldering as well as after the splice has cooled. The heads of each fastener will be marked for verification purposes with an acceptable ink pen. Inspection torque paint is not acceptable for coil use.

For welding, both the root pass and final pass are dye-penetrant inspected. Also, an ultrasonic inspection is performed at completion of closeout welds, with repairs made as required.

10.9.3 Visual Inspections

A series of visual checks are required to complete our proposed inspection plan. These inspections are monitored by a checklist. Visual inspections insure that there is no damage to either the conductor or instrumentation leads. These inspections insure that the voltage taps are installed correctly, that the turn insulation is not protruding above the surface of the conductor, and that the coil is clean and free of debris. Finally, each completed pancake is checked, using a .13-mm (0.005-in) feeler gage and a straight edge, to assure that the flatness is within .13 mm (0.005 in).

10.10 Conclusions

There is a high level of confidence that the Nb_3Sn insert coils can and will be produced within the current manufacturing and tooling state-of-the-art. General Dynamics is confident in the design and the plan for manufacturing, not only based on past experience on other Energy Systems' programs, but that LLNL with their management and experience on the HFTF coil will successfully wind the Nb_3Sn coils.

Risks of damaging the superconductor have been minimized through the suggested tooling concepts. The plan reduces the number of handling operations as well as provides special safety featues to avoid damaging strains. The tooling concepts assure strains are kept well within conductor design limits. A viable plan to successfully manufacture the two Nb_3Sn insert coils has been presented.

10.11 References

10-1 "MFTF-B Solenoid Coil Winding Procedure," General Dynamics Specification No. 71E0021, Revision A, dated 28 September 1982.

11.0

CONCLUSION

The high field coil described in this report fully meets the design requirements defined in LLNL's Design Requirements Document. Design parameters have been selected to ensure reliable operation of the A2I insert coils. Critical current specification for the conductor is a minimum of 3200 amperes at 12.7 tesla and 4.2K (for a zero applied strain). This design provides 100 percent critical current margins, since the operating current is 1517 amperes. The design operating life is 10 years, considering irradiation degradation effects.

The case structure is fabricated from 304LN annealed stainless steel plate. The conductor consists of an Nb_3Sn monolith superconductor soldered into a copper stabilizer housing. The conductor is manufactured by the Furukawa Electric Company, Ltd. of Japan. Various forms and shapes of the insulation material G-10CR were used throughout the conductor pack. All materials used will maintain their mechanical and physical integrity for the life of the MFTF system.

Tension preload values on the conductor pack of 300, 400, 500, and 600 pounds were included in the stress analysis. The final winding preload shall be selected by LLNL after a trial winding. Furukawa, in order to meet production dates, incorporated three reaction diameters in the manufacturing of the prototype conductor. The diameters used were 60, 70, and 80 cm (23.6, 27.6, and 31.5 inches). This causes conductor bending strain variation throughout the conductor pack. The resulting margins, considering both the different winding pretension values and reaction diameters, were positive with the highest stressed region being in the joggle (1st turn) and at the outer pack radius where the conductor is fixed to the case (1st and last pancakes).

A 2-D finite-element model was used to represent the magnet case incorporating both the A2O and insert coil (A2I). The A2O case was included to provide the boundary conditions on the welded attachment between the two coils. The Kelley mode and Mars mode loading conditions were imposed on the model. Both the normal and abnormal loading conditions were incorporated; the abnormal condition being a low probability electrical fault event for which reduced safety factors are used. The worst design condition for the A2I case is defined in the DRD which limits A2I current peaking to 15 percent of the I_c (critical current). The resulting margins of safety for both the normal and abnormal loading conditions for the magnet case were positive. The stress level and design cyclic condition produced an initial flaw size in the fracture mechanics analysis that can be economically detected.

The high field Nb_3Sn coil is a very cryostable and safe magnet thermally, with a cryostability margin of better than 40 percent and a temperature margin of better than 2.5°K. The thermally-developed stresses in the magnet case are low because the coil has a very high cross-sectional area-to-length ratio. The strong conductive heat transfer in the magnet components effectively reduces the temperature gradients in the components. A flow rate of 4

g/sec for the cool-down/warm-up cycles is recommended. This flow rate will reach design conditions within the 120-hour requirement. There is a temperature controlled condition that is to be monitored during the cool-down/warm-up transient conditions. The temperature control is between the two nested coils. It is required in order to limit the bending stress in the welded attachment (opening mode between the two coils) and in the outer ring of coil A2I under the shims (for the closing mode). This control can best be achieved with a separate flow control on each coil. This would introduce another operating parameter, that being the reaction time required if flow should stop in one of the nested magnets. The reaction time was determined from the minimum allowable temperature differential excursion divided by the maximum time rate of temperature change. The reaction times for the "worst" abnormal conditions are 25 hours during the cool-down, and 10 hours during the warm-up. The "worst" abnormal condition occurs if the helium flow to the colder magnet stops during the warm-up.

The peak pressure of 65 psia is developed during a simultaneous quench of three axicell coils. A design pressure condition of 7 atm (102 psia) was recommended. (Note that 150 psia was used for the stress analysis of the magnet case.) A peak helium quality at the exit of the coil is calculated to be 2.1 percent by weight which is within the DRD limit of 2.5 percent.

The instrumentation on the high field coil includes a combination of temperature, voltage, and liquid helium level measurements distributed over selected points. A total of 90 instrumentation channels are allocated. All instrumentation (selection and placement) follow the DRD and LLNL supplemental requirements. Only the LHe supply and return line temperature measurements are required for long-term operation of the magnet. The remaining temperature sensors on this coil will be used primarily for acceptance testing, cool-down/warm-up, and demonstration of the magnet cryogenic system.

A verification test program was structured to assess the Nb_3Sn conductor and provide engineering data to support the design phase. It was anticipated during the initial design phase that, in the worst case, the additional precompression of the Nb_3Sn due to the application of the cold-worked Cu stabilizer could result in a 33 to 40 percent decrease in the critical current. However, Furukawa made two changes which were expected to reduce this degradation. First, they introduced a ternary alloying addition (Ti) which had been shown to decrease the strain sensitivity of Nb_3Sn. Second, they improved their cladding line so that the cold-worked Cu sheath could be soldered to the Nb_3Sn and cooled slowly in order to reduce the precompressive strain applied to the Nb_3Sn. Critical current measurements were made on the core alone and on the core after cladding. The degradation measured for the prototype conductor due to cladding was between 6 and 10 percent, indicating that the steps taken by Furukawa were effective. The high aspected shape of the conductor was also a concern because of potential anisotropic behavior with respect to the magnet field orientation. The measured effect on the prototype conductor was approximately $\pm$ 13 percent.

The results of the mechanical property tests were generally consistent with the values used in the coil design and incorporated in the specification. The specification requires that the 0.2 percent offset tensile yield strength of the housing at 300K be equal or greater than 31,000 psi; in practice, it

was not possible to perform a valid test on the housing alone. Consistent yield strength data were obtained for the composite (superconductor core and housing). In addition, it was not possible to obtain a valid mechanical test on the full cross section of the core due to specimen failures outside the gage length. Several tests were completed on reduced cross sections of the core, and these results appear reasonable. In view of these testing difficulties, and since the important property is the composite yield strength, it is recommended that the specification be revised to require the composite yield strength to be equal or greater than 31,000 psi.

Bend tests were performed on both the core alone and on the composite conductor in order to develop the tolerance to bending. The core could be bent to a strain of greater than $\pm$ 0.48 percent bending strain without any degradation in critical current, and the critical current was 7% percent above the operating value at a strain of $\pm$ 0.95 percent. Bending tests performed on the composite conductor illustrated that degradation in critical current did not appear at a diameter of 16.4 cm (6.6 inches). In addition, the conductor could be bent in the opposite direction to a 35-cm (13.8-inch) diameter without degradation.

Included in this report is a comprehensive testing program to insure that the completed coil is free from defects and that the coil closeout activities do not induce any defects. The final acceptance test program repeats many of the in-process tests performed during coil fabrication and subjects the coil to other tests designed to prove compliance to the DRD. This testing program will insure a defect-free coil capable of meeting its performance requirements.

There is a high level of confidence that the Nb_3Sn insert coils can and will be produced within the current manufacturing and tooling state-of-the-art. General Dynamics is confident that in the design and the plan for manufacturing, not only based on past experience on other energy Systems' programs, but that LLNL with its management and experience on the HFTF coil, will successfully wind the Nb_3Sn coils.

Risks of damaging the superconductor have been minimized through the suggested tooling concepts. The plan reduces the number of handling operations, as well provides special safety features to avoid damaging strains. The tooling conepts assure that manufacturing strains are kept well within conductor design limits.

General Dynamics believes it has developed a viable plan for the successful manufacture of the two Nb_3Sn insert coils.

APPENDIX A

MFTF MAGNET SYSTEM PROGRAM SPECIFICATION

FOR HIGH FIELD Nb_3Sn COIL CONDUCTOR

GENERAL DYNAMICS
Convair Division
CODE IDENT NO.
14170

SPECIFICATION NO.	REV
71E0034	B
DATE: 27 January 1983	PAGE: 1 OF 16
CONTRACT NO.: 9590309	

MFTF MAGNET SYSTEM PROGRAM
SPECIFICATION FOR
HIGH FIELD Nb_3Sn COIL CONDUCTOR

PREPARED BY R. W. Baldi

APPROVED BY R. E. Iatro

CHECKED BY _____

APPROVED BY W. D. Johnston
Quality Assurance Manager
System Safety

SPECIFICATION CHANGE NOTICES—INCORPORATED IN SPEC REVISIONS

SCN NO(S)	INCORP BY	CHECK BY	APPROVED BY	DATE	SPEC REV	REVISION PACKAGE NO.	RELEASE
				4/25/83	A		
				12/10/83	B		

INITIAL PACKAGE NO.	RELEASE	DOC TYPE	DISTR CODE

SUMMARY OF REVISION A CHANGES

PARAGRAPH	CHANGE
2.2	Added "to below 3200A." to last sentence.
2.7	Revised paragraph to clarify length requirements.
2.8, 2.10	Revised reaction spool diameter to 70.0 cm.
2.16	Revised solder composition to 60 w/o Sn - 40 w/o Pb.
2.17	Add initial sentence: "The orientation of the reacted core with respect to the copper stabilizer shall be as shown in figure 2."
2.20	Added sentences: "The final surface finish shall be the arithmetic average roughness, Ra = 63 microinches (1.6 micrometers)." and "The complete exterior surface of the stabilizer may be covered with an anodic oxidized CuO film to facilitate soldering.
5.4	Added reference to attachment B and deleted item 8 from shipment marking instructions.
Attachment A	Accelerated delivery dates of the short sample by two (2) weeks.
Attachment B	Added Attachment B defining conductor serial numbers and defining total length requirements.

SUMMARY OF REVISION B CHANGES

2.8	Replaced single reaction spool with three concentric spools.
2.9	Revised maximum applied strain allowance from (±0.3) to (+0.4 to -0.6) percent.
2.10	Revised minimum bend radius from 70.0 cm to 60.0 cm.
5.2	Added clarification regarding conductor orientation on shipping spool.
5.4.2	Added requirement to mark serial number and reaction mandrel diameter on each length of conductor.

1.0 SCOPE

1.1 Purpose

This specification describes the requirements for a cryostable Nb_3Sn Conductor to be developed for the MFTF-B magnets at the Lawrence Livermore National Laboratory (LLNL). The magnets are DC superconducting magnets with a charging time constant of 4 hours and a fast dump time constant of 6.8 sec.

1.2 Scope of Work

The Nb_3Sn conductor shall be in multifilamentary form. It shall be cryostable with C10100 Oxygen-Free copper per specification ASTM B152-77 as stabilizer. The cross-sectional dimensions are shown in Figure 1.

The Seller shall furnish all materials, fabricate and test as required and deliver the superconductor as specified herein. The Seller shall be responsible for developing all fabrication processes which are not specified in this specification. The Seller shall submit his manufacturing plan, quality control plan, test plan to Buyer for review.

These plans and documents shall include step-by-step fabrication processes and the verification tests that Seller shall perform at each important fabrication stage.

2.0 Technical Requirements

2.1 Superconducting Composite Configuration

The superconducting composite shall be multifilametary Nb_3Sn in a bronze matrix which is stabilized by oxygen-free copper. A diffusion barrier must be provided to protect oxygen-free copper from tin diffusion.

2.2 Current Carrying Capacity

The Seller shall guarantee that the superconductor shall have a critical current of no less than 3200 A at 4.2K and at zero external applied strain and under a 12.7T magnetic field which is parallel to the conductor broad face but transverse to conductor longitudinal axis. The critical current shall be determined based on resistivity criterion of 3×10^{-11} ohm-cm over the non-copper area. A single application and release of externally applied tensile strain of 0.7 percent (applied either at 4.2K or 300K) shall not degrade the critical current (at 12.7T and 4.2K with zero external applied strain) to below 3200A.

2.3 Copper Resistivity in the Superconducting Composite

The copper used for the superconducting composite insert shall have a residual resistivity ratio, RRR greater than or equal to 120 at zero magnetic field. The zero field resistivity ratio is defined as:

$$RRR = \frac{\text{Resistivity of Copper at 295K}}{\text{Resistivity of Copper at 20K}}$$

2.4 Nb_3Sn Filament Uniformity

The total cross-sectional area of the Nb_3Sn shall not vary more than $\pm$ 20 percent along the length of each conductor.

2.5 Diffusion Barriers

The bronze matrix island shall be surrounded by a niobium diffusion barrier. The diffusion barrier shall protect oxygen-free copper stabilizer from tin diffusion.

2.6 Conductor Bonding

The conductor (superconducting composite and copper stabilizer) shall be free of cracks, voids, or other unwanted foreign materials.

2.7 Conductor Length

The quantity and continuous conductor lengths required are listed below:

Quantity	Description	Lengths
1	Initial length to proof processing	370 meters
56	Production lengths	295 meters

The length shown for the initial length of conductor includes the additional length required for verification testing as defined in paragraph 3.3.1. As described in paragraph 3.3.1, a portion of the initial length shall be provided in the unsoldered condition.

The length shown for the production lengths of conductor do not include lengths required for buyer verification tests. Additional lengths 2.0 meters long from each end of the conductor are required for acceptance testing as outlined in Attachment B.

Additional lengths required for seller verification test and inspection requirements shall be provided by the seller.

2.8 Reacting Spool

B The reacting spool shall be a steel spool, to be supplied by Seller. Three concentric spools shall be used for reacting the conductor. They shall have a winding diameter of 60.0, 70.0 and 80.0 cm. The empty spools shall be heat treated at the conductor reacting temperature for more than two hours in a high purity gas environment. The conductor shall be wound in a single layer on to each of the reacting spools. Means must be provided to prevent inter-layers from diffusion bonding during the Nb_3Sn reaction.

2.9 Maximum Strain Limit and Handling of Reacted Nb_3Sn Conductor

B Sound quality control procedures must be developed and carried out in the production line, packing, shipping, or other handling to ensure that a maximum applied strain of no greater than +0.4 to -0.6 percent is exerted on the Nb_3Sn filaments.

The frequency of the applied strain shall be kept at a minimum.

2.10 Bend direction and Minimum Bend Diameter

B The reacted conductor shall subsequently be bent or straightened only in the same direction in which the conductor was bent on the reacting spool for heat treatment. Furthermore, the minimum bend diameter shall be no less than 60.0 cm in the easy direction and 234 cm in the hard direction.

2.11 Finished Surface Condition of the Superconducting Insert

The finished surface of the superconducting insert shall be free of pores, laminations, folds, dirt, or oil contamination. Nowhere shall any part of the non-copper region be visible at the conductor surface.

2.12 Maximum Bronze-Niobium Core Size

The maximum size for the bronze-niobium core region shall be no greater than the size shown in figure 1.

2.13 Filament Twist Pitch

The Nb_3Sn filament twist pitch shall be 25 +/- 5 cm.

2.14 Copper Housing Resistivity

When conductor is in its final form, the copper housing shall have a zero field resistivity, RRR, of no less than 100.

2.15 Copper Housing Tensile Yield Strength.

The copper housing, when ready for delivery, shall have a tensile yield stress equal or greater than 31,000 psi at 300K and at 0.2 percent strain offset. (The yield strength test shall be conducted at room temperature on a full section of conductor. The superconductor mechanical behavior shall be extracted from the test results in order to determine the copper housing yield strength.)

2.16 Soldering Composition

The soft solder to be employed shall be 60 w/o Sn - 40 w/o Pb solder per specification MIL-S-6872.

2.17 Soldering Bond

The orientation of the reacted core with respect to the copper stabilizer shall be as shown in figure 2.

The maximum length of a completely unbonded zone at both wide faces shall be no longer than 0.5 cm. The partially bonded zone shall be statistically averaged and ultrasonically inspected so that the unbonded area at both wide faces shall be no more than 20 percent of total bondable area over any 10 cm of conductor length.

The solder bond shall have sufficient structural integrity to sustain winding and joggling induced strain without delamination. The winding bend radius (easy bend direction) is 21.1 cm. The joggling bend radius (hard bend direction) is 762 cm.

2.18 No Splice

There shall be no splice in either the Nb_3Sn monolithic insert or copper housing.

2.19 Approval for Soldering Assembly

The initial length of monolithic inserts shall not be soldered into copper housing until Buyer has determined that it conforms fully with the requirements of this specification.

2.20 Surface Finish of Completed Conductor

The conductor surface shall be free of splinters, dirt, oil, or any other contaminants. There shall be no folds, seams, or laminations in the surface. Nicks and gouges causing more than 3 percent loss in conductor cross-section are not permitted. The final surface finish shall be the arithmetic average roughness, Ra = 63 microinches (1.6 micrometers.) The complete exterior of the conductor may be covered with anodic oxidized CuO film to facilitate soldering.

2.21 Solderability

The conductor shall be delivered in a condition that will facilitate fabrication of an electrical joint using a commercial lead-tin solder.

3.0 SELLER'S QUALITY ASSURANCE, INSPECTION, AND TESTS

3.1 Seller Responsibility

The seller shall establish a quality assurance program that assures manufacture of a product that complies with this specification. Seller shall provide Buyer with Seller's sampling plan and inspection schedule and a description of the means whereby he will maintain control over his own and his subcontractor's manufacturing processes, inspection and testing, handling, and storage. Included shall be a means for inspecting parallelism, for identification of non-conforming material, serialized identification by lot of finished product, and procedures for the segregation of nonconforming material. Seller shall provide qualified personnel for performing ultrasonic inspections. Qualifications of selected personnel shall be subjected to Buyer approval. The Seller's record keeping system shall be such that traceability exists for all QC records and materials used in the stabilized conductor from the time raw materials are received by the Seller until the final conductor is completed.

3.2 Test Witnessing

Buyer reserves the right to witness manufacturing steps, tests, and inspections established under Seller's quality assurance program, and all other testing performed at Seller's plant and his subcontractors' plants to demonstrate compliance with this specification.

3.3 Quality Control Samples

3.3.1 The Seller shall submit the following samples to Buyer for test per paragraph 4. Tests performed on these samples are intended to supplement the Seller's test program. They do not release the Seller from the obligation to perform testing and inspection.

Core Samples

Samples from each end of the initial length of superconducting niobium-bronze-copper composite core shall be sent to Buyer for verification testing. A total length of 18 m is required. A portion of this material may require pre-bending prior to reaction to meet verification testing requirements. The individual lengths and bending requirements for these test samples shall be established by the Buyer.

Copper Housing

A sample from each end of the initial length of copper housing shall be sent to Buyer for resistivity ratio and tensile tests. Samples shall be 2 m in length.

Finished Product Samples

Samples from each end of the initial length of the completed conductor shall be sent to Buyer for verification testing. A total of 22 meters is required. A sample, 2 m long, from all other lengths of finished, stabilized conductor shall be identified and sent to Buyer for quality assurance acceptance tests. Approval based on these tests must be obtained before conductor is shipped to Buyer.

3.3.2 The Seller shall test samples of soldered conductor prior to soldering each length of deliverable conductor to ensure solder bond quality. This destructive test shall consist of positioning a sample between two 15 cm radius mandrels and banding the sample through +/- 90 degrees for at least 5 cycles. As a result of this test, there shall be no visual evidence of failure in the core and sheath bond.

3.4 Manufacturing, Quality Control, and Test Plan

An integrated plan shall be supplied which shows the proper sequencing of the significant manufacturing operations keyed to inspection or testing to be performed and organized as to provide traceability of all materials throughout the process. Detailed manufacturing procedures are not required but shall be available for review and comment. Inspection and testing methods may be referenced or described as necessary. Wherever possible, the Seller's established procedures and methodologies shall be used and either be supplied or be available for review and comment. The elements of the original plan and any subsequent changes shall be mutually agreed to by Buyer and Seller before work is performed.

3.5 Control of Nonconforming Material

The Seller shall have a system for controlling nonconforming material ensuring that it will be removed from the production area to prevent its inadvertent use. Discrepancy descriptions shall be submitted to Buyer for disposition. High quality, close-up photographs shall be included for visual discrepancies.

3.6 Records

The Seller shall maintain a set of all records pertaining to the manufacture and testing of the conductor. These records shall be available for review by the Buyer. The records shall be retained intact for a period of two years after completion of the contract. A copy of test results shall be sent to Buyer upon Buyer's request.

4.0 BUYER VERIFICATION TESTS

Buyer shall perform the following verification tests: (1) short sample test; (2) copper zero-field resistance test; (3) filament twist pitch, filament diameter, and filament number; (4) composition of conductor such as copper - non-copper ratio and bronze-niobium ratio; (5) the copper bonding; (6) soldering bonding, and (7) mechanical strength of copper housing and the superconducting composite.

5.0 PACKING AND SHIPPING REQUIREMENTS

5.1 Packing and Shipping Requirements

The Seller shall submit a packaging and shipping plan to Buyer for review prior to completion of the superconductor.

5.2 Handling and Spooling

B Handling and spooling prior to shipment shall not degrade the conductor with respect to any of the above specifications. The seller shall insure that the conductor is wound on the shipping spool such that the "U-shaped" section of the stabilizer is oriented radially outward.

5.3 Shipping Spools and Preparation for Delivery

The shipping spool will be supplied by the Seller. Both the start and finish ends shall be attached in such a manner to prevent any loosening of the conductor on the spool. The spools shall be properly cushioned and protected with sheets of protective wrapping against weather, dust, or other foreign materials.

5.4 Marking

5.4.1 The package shipment shall be marked with the following information:

"Nb_3Sn Conductor for MFTF-B Magnets."

1. Purchase Order or Contract Number.
2. Manufacturer
3. Name of Material
4. Size and Length
5. Serial Number (reference Attachment B)
6. Gross, Net, and Tare Weights
7. Q.A. Acceptance Verification

5.4.2 Every length of production conductor and test sample shall have the serial number and reaction mandrel diameter vibro-engraved on the conductor. The engraving shall be confined within 2.0 inches of the conductor ends. Minimum number height shall be 1/8 inch. The legibility of every numeral shall appear in its entirety and shall be totally and clearly visible.

5.5 Storage

All components and the final product awaiting further processing or shipment shall be handled and stored in a manner which precludes physical damage and contamination.

5.6 Packaging

All material shall be packaged in a manner to maintain cleanliness during handling and shipping and to prevent damage in transit to its destination when properly transported by any common carrier. The conductor shall be wound upon a reel of diameter not less than that specified in paragraph 2.8.

6.0 SHIPPING

After receiving approval from Buyer to ship the product, shipping shall be performed in accordance with all applicable regulations of the United States Department of Transportation. Approval for shipment shall be in accordance with the Quality Assurance Plan of paragraph 3.1 of this specification.

ATTACHMENT A

SCHEDULE - INITIAL AND PRODUCTION LENGTHS

Place Prototype Order (LLNL)	January 28, 1983
Letter of Intent from GDC	February 11, 1983
Authorization for Long Lead (1) and processing up to second stage (GDC)	May 19, 1983
Deliver Prototype FOB (LLNL)	November 15, 1983
Final Specification (LLNL)	December 15, 1983
Delivery - Production	
6 Lengths FOB LLNL	April 1, 1984 (by air)
6 Lengths	April 15, 1984 (by vessel)
11 Lengths	May 5, 1984 (by vessel)
11 Lengths	June 1, 1984 (by vessel)
11 Lengths	June 20, 1984 (by vessel)
11 Lengths	July 15, 1984 (by vessel)
56 Total Lengths	

ATTACHMENT B

CONDUCTOR SERIAL NUMBERING SYSTEM, PRODUCTION LENGTH REQUIREMENTS, AND ACCEPTANCE TEST SAMPLE LOCATIONS.

SERIAL NUMBER AND LENGTH REQUIREMENTS

LENGTH NUMBER	LENGTH TO GDC	LENGTHS TO LLNL	LENGTH FOR FURUKAWA	TOTAL LENGTH
9001	≥ 295m	2 - 2m samples	1 - 2m sample	301m
9002	"	1 - 2m samples	0	297m
9003	"	1 2m samples	0	297m
				895m
9004	≥ 295m	2 - 2m samples	1 - 2m sample	301m
9005	"	1 - 2m samples	0	297m
9006	"	1 2m samples	0	297m
				895m
9007	≥ 295m	2 - 2m samples	1 - 2m sample	301m
9008	"	1 - 2m samples	0	297m
9009	"	1 2m samples	0	297m
				895m
9010	≥ 295m	2 - 2m samples	1 - 2m sample	301m
9011	"	1 - 2m samples	0	297m
9012	"	1 2m samples	0	297m
				895m
9013	≥ 295m	2 - 2m samples	1 - 2m sample	301m
9014	"	1 - 2m samples	0	297m
9015	"	1 2m samples	0	297m
				895m
9016	≥ 295m	2 - 2m samples	1 - 2m sample	301m
9017	"	1 - 2m samples	0	297m
9018	"	1 2m samples	0	297m
				895m
9019	≥ 295m	2 - 2m samples	1 - 2m sample	301m
9020	"	1 - 2m samples	0	297m
9021	"	1 2m samples	0	297m
				895m
9022	≥ 295m	2 - 2m samples	1 - 2m sample	301m
9023	"	1 - 2m samples	0	297m
9024	"	1 2m samples	0	297m
				895m

9025	≥ 295m	2 - 2m samples	1 - 2m sample	301m
9026	"	1 - 2m samples	0	297m
9027	"	1 2m samples	0	297m
				895m
9028	≥ 295m	2 - 2m samples	1 - 2m sample	301m
9029	"	1 - 2m samples	0	297m
9030	"	1 2m samples	0	297m
				895m
9031	≥ 295m	2 - 2m samples	1 - 2m sample	301m
9032	"	1 - 2m samples	0	297m
9033	"	1 2m samples	0	297m
				895m
9034	≥ 295m	2 - 2m samples	1 - 2m sample	301m
9035	"	1 - 2m samples	0	297m
9036	"	1 2m samples	0	297m
				895m
9037	≥ 295m	2 - 2m samples	1 - 2m sample	301m
9038	"	1 - 2m samples	0	297m
9039	"	1 2m samples	0	297m
				895m
9040	≥ 295m	2 - 2m samples	1 - 2m sample	301m
9041	"	1 - 2m samples	0	297m
9042	"	1 2m samples	0	297m
				895m
9043	≥ 295m	2 - 2m samples	1 - 2m sample	301m
9044	"	1 - 2m samples	0	297m
9045	"	1 2m samples	0	297m
				895m
9046	≥ 295m	2 - 2m samples	1 - 2m sample	301m
9047	"	1 - 2m samples	0	297m
9048	"	1 2m samples	0	297m
				895m
9049	≥ 295m	2 - 2m samples	1 - 2m sample	301m
9050	"	1 - 2m samples	0	297m
9051	"	1 2m samples	0	297m
				895m

9052	≥ 295m	2 - 2m samples	1 - 2m sample	301m
9053	"	1 - 2m samples	0	297m
9054	"	1 2m samples	0	297m
				895m
9055	≥ 295m	2 - 2m samples	1 - 2m sample	301m
9056	"	1 - 2m samples	0	297m
				598m
	56 x 295	75 - 2m samples	19 - 2m samples	16,708m

ACCEPTANCE TEST SAMPLE LOCATION REQUIREMENTS

F L (A)	GDC (L) (B)	GDC (L) (B)	GDC (L) (B)
Start Length	9001	Length 9002	Length 9003
	9004	9005	9006
	9007	9008	9009
	9010	9011	9012
	9013	9014	9015
	9016	9017	9018
	9019	9020	9021
	9022	9023	9024
	9025	9026	9027
	9028	9029	9030
	9031	9032	9033
	9034	9035	9036
	9037	9038	9039
	9040	9041	9042
	9043	9044	9045
	9046	9047	9048
	9049	9050	9051
	9052	9053	9054
	9055	9056	
	LLNL	LLNL	LLNL
A	Samples B	Samples B	Samples B
Example:	9001A	9002B	9003B
	9001B		

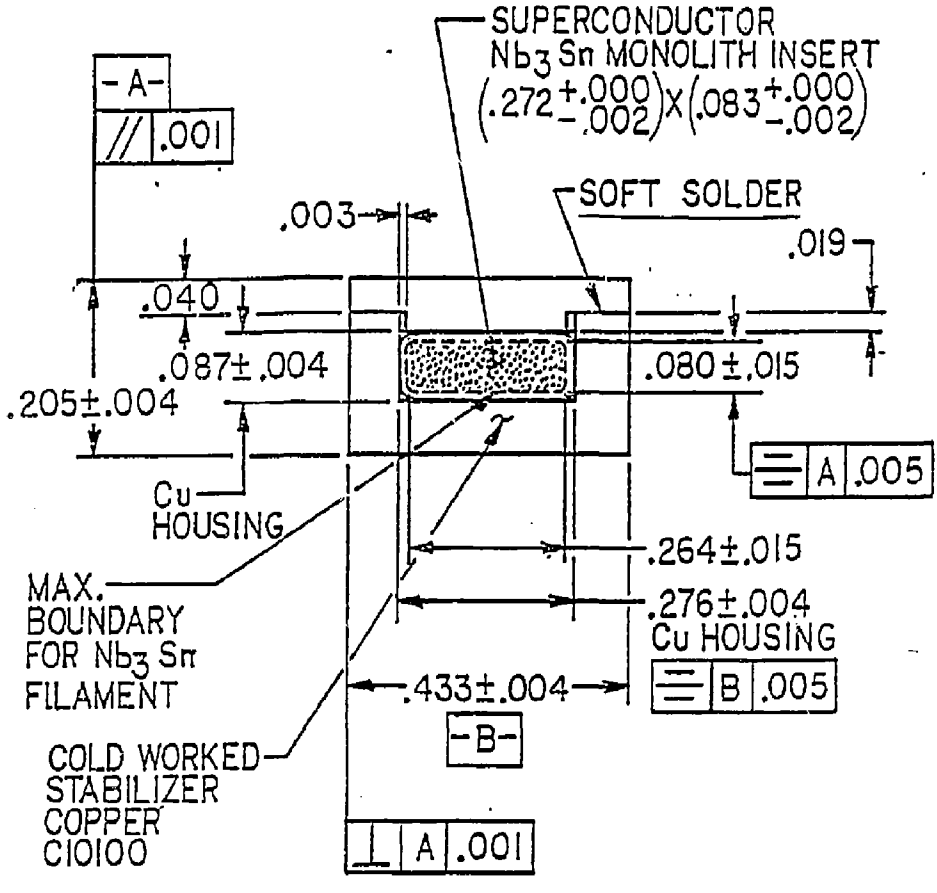

1. ALL FILLET RADII - $.010^{+.000}_{-.005}$.
2. STABILIZER CORNER RADII - .010 ± .005.
3. MONOLITH CORNER RADII - $.015^{+.000}_{-.005}$.
4. SOLDER SUPERCONDUCTOR TO STABILIZER HOUSING. SOLDER MATCHING SURFACES OF STABILIZER.
5. DIAMETER IN INCHES.
6. PARALLEL TOLERANCE: RANDON ±.004", CONSISTENT ±.001".

Figure 1. Soldered conductor with monolithic insert.

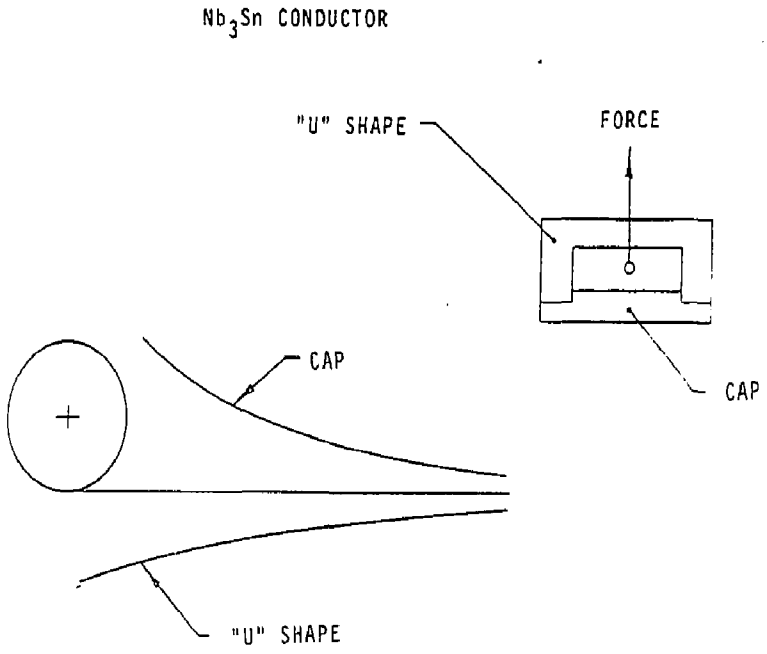

Figure 2. Orientation of reacted core with respect to copper stabilizer.

APPENDIX B

DESIGN CHARACTERISTICS SUMMARY

FOR MFTF Nb_3Sn HIGH FIELD COIL

GENERAL DYNAMICS SUPERCONDUCTING MAGNETS

PROGRAM		MFTF-B INSERT COIL	MFTF-B AXICELL A-1	MFTF-B AXICELL A-2
CUSTOMER		LLNL	LLNL	LLNL
GD PROGRAM MANAGER		R.E. TATRO	R.E. TATRO	R.E. TATRO
GD CHIEF ENGINEER		R.W. BALDI	J.W. WOHLWEND	J.W. WOHLWEND
GENERAL DATA:				
MAGNET TYPE	-	SOLENOID	SOLENOID	SOLENOIC
NUMBER OF UNITS	-	2	2	2
OVERALL SIZE	M	1.32M DIA	2.5M O.D.	2.5M O.D.
STORED ENERGY	MJ	4.25-11.6	76.8	76.8
AMPERE TURNS	MAT	4.63	9.245	9.245
INDUCTANCE	H	3.77	6.018	6.018
CHARGING TIME	MIN	240	240	240
PEAK FIELD	TESLA	12.7	7.68	7.48
CENTRAL FIELD	TESLA	12.0	6.0	6.0
UNIFORMITY REQUIREMENTS	%	N/A	N/A	N/A
UNIFORMITY REGION	M	N/A	N/A	N/A
DISCHARGE TIME CONSTANT	SEC	-	109	109
OPERATING TEMPERATURE	K	4.5	4.5	4.5
COOL DOWN TIME	HR	120	120	120
HELIUM VOLUME	L	180	724	724
CONDUCTOR COOLING MODE	-	POOL BOILING	POOL BOILING	POOL BOILING
WARM UP TIME	HR	120	120	120
CONDUCTOR DATA:				
				
GRADE	-		I II	I II
CONDUCTOR TYPE	-	MONOL SOLD STB	MONOLITH W/CU WRAP	MONOLITH W/CU WRAP
OPERATING CURRENT	AMPS	1517	4620 4620	4620 4620
S/C CURRENT DENSITY	AMPS/CM SQ	13.700	29.472 78.465	29.472 78.465
PACK CURRENT DENSITY	AMPS/CM SQ	2007	2.420 2.420	2.420 2.420
CRITICAL CURRENT	AMPS	3200@4.2K/12.7T	8.930 7.200	8.930 7.200
LENGTH	KM	7.52/MAGNET	11.67	11.67
SUPERCONDUCTING MATL	-	NB3 SN + TI	NB TI	NB TI
CU: NON-CU RATIO	-	4.3:1	6:4 18:7	6:4 18:7
CROSS SECTIONAL AREA	CM SQ	.573	1.16 1.16	1.16 1.16
COND PACKING FACTOR	-	.756	.599	.599
HE VOL TO COND VOL	-	.16	.335	.335
STABILIZER HEAT FLUX	W/CM SQ	.17	.19	.19
STABILIZER MATERIAL	-	C10100 OFE CU	OFHC CU	OFHC CU
R.R.R. STABILIZER	-	100	220	220
SOLDER MATERIAL	-	40%PB/60%SN	50%PB/50%SN	50%PB/50%SN
PROTECTION SYSTEM DATA:				
DUMP RESISTOR	OHMS	0.5	.055	.055
DUMP TRIGGER VOLTAGE	VOLTS	-	-	-
TERM PEAK VOLTAGE	VOLTS	750	254	254
FAST DUMP TIME CONST	SEC	7.5	109	109
STABILIZER PEAK TEMP	K	47	200	200
PEAK DUMP PRESSURE	PSIA	75	57	57
MATERIALS:				
WINDING SUB-STRUCTURE	-	-	N/A	N/A
WINDING SUPER-STRUCTURE	-	304LN	304LN	304LN
HELIUM VESSEL	-	304LN	304LN	304LN
TENSION BANDS	-	N/A	N/A	N/A
WINDING PACK INSULATION	-	G10 CR	G10 CR	G10 CR
COLD MASS SUPPORTS	-	304LN/304L	A286/304LN	A286/304LN
MULTI-LAYER INSULATION	-	-	-	-
VACUUM VESSEL	-	-	-	-
MAGNETIC SHIELD	-	-	-	-
RADIATION SHIELD	-	316L	-	-
DUMP RESISTOR	-	-	-	-
WEIGHTS:				
TOTAL	K LBS	13.8	61.690	64.000
COLD MASS	K LBS	13.6	55.630	55.200
CONDUCTOR	K LBS	9.0	28.970	28.970
WINDING STRUCTURE	K LBS	4.6	26.660	30.160
TENSION BANDS	K LBS	-		
N2 RADIATION SHIELD	K LBS	.16	1.790	1.790
VACUUM VESSEL	K LBS	-	-	-
MAGNETIC SHIELD	K LBS	-	-	-
COLD MASS SUPPORTS	K LBS	-	1.440	4.190
STACK & VCL'S	K LBS	-	2.830	2.830

APPENDIX C

DRAWING TREE FOR DETAIL DESIGN

OF THE

MFTF Nb_3Sn HIGH FIELD COIL

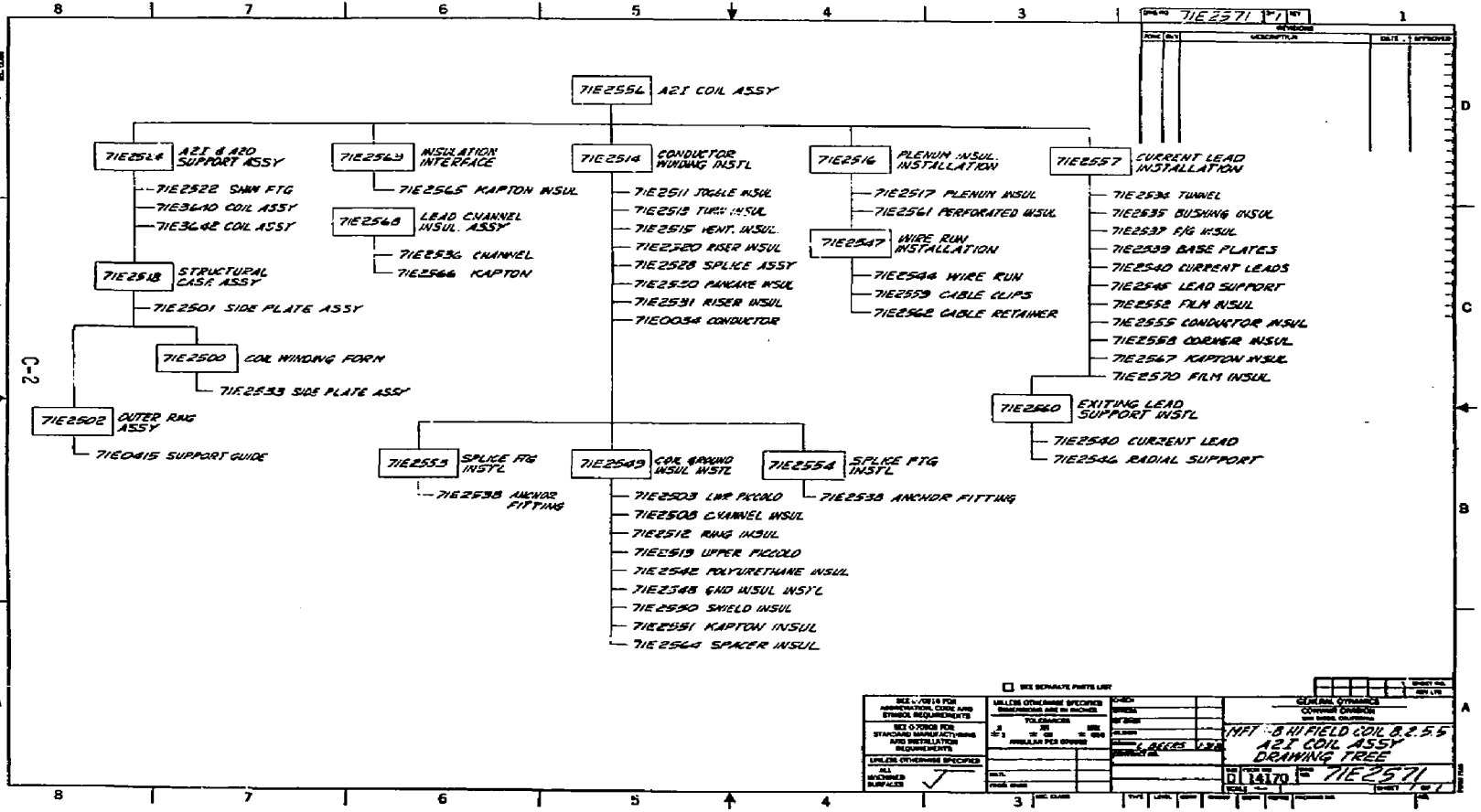
71E2571
71E2564 A2I COIL ASSY
71E2524 A2I & A20 SUPPORT ASSY
71E2522 SHIM FTG
71E3640 COIL ASSY
71E3642 COIL ASSY
71E2518 STRUCTURAL CASE ASSY
71E2501 SIDE PLATE ASSY
71E2500 COIL WINDING FORM
71E2533 SIDE PLATE ASSY
71E2502 OUTER RING ASSY
71E0415 SUPPORT GUIDE
71E2563 INSULATION INTERFACE
71E2565 KAPTON INSUL
71E2568 LEAD CHANNEL INSUL. ASSY
71E2536 CHANNEL
71E2566 KAPTON
71E2514 CONDUCTOR WINDING INSTL
71E2511 JOGGLE INSUL
71E2513 TURN INSUL
71E2515 VENT. INSUL.
71E2520 RISER INSUL
71E2528 SPLICE ASSY
71E2530 PANCAKE INSUL
71E2531 RISER INSUL
71E0034 CONDUCTOR
71E2516 PLENUM INSUL. INSTALLATION
71E2517 PLENUM INSUL
71E2561 PERFORATED INSUL
71E2547 WIRE RUN INSTALLATION
71E2544 WIRE RUN
71E2559 CABLE CLIPS
71E2562 CABLE RETAINER
71E2557 CURRENT LEAD INSTALLATION
71E2536 TUNNEL
71E2535 BUSHING INSUL
71E2537 F/G INSUL
71E2539 BASE PLATES
71E2540 CURRENT LEADS
71E2545 LEAD SUPPORT
71E2552 FILM INSUL
71E2555 CONDUCTOR INSUL
71E2558 CORNER INSUL
71E2567 KAPTON INSUL
71E2570 FILM INSUL
71E2560 EXITING LEAD SUPPORT INSTL
71E2540 CURRENT LEAD
71E2546 RADIAL SUPPORT
71E2553 SPLICE FTG INSTL
71E2538 ANCHOR FITTING
71E2549 COIL GROUND INSUL INSTL
71E2503 LWR PICCOLO
71E2508 CHANNEL INSUL
71E2512 RING INSUL
71E2519 UPPER PICCOLO
71E2542 POLYURETHANE INSUL
71E2548 END INSUL INSTL
71E2550 SHIELD INSUL
71E2551 KAPTON INSUL
71E2564 SPACER INSUL
71E2554 SPLICE FTG INSTL
71E2538 ANCHOR FITTING
GENERAL DYNAMICS
CONVAIR DIVISION
MFT - BHI FIELD COIL 82.5.5
A2I COIL ASSY
DRAWING TREE
D 14170
71E2571

APPENDIX D

LIST OF STRESS ANALYSES IN SUPPORT OF THE Nb_3Sn HIGH FIELD COIL

APPENDIX D - LIST OF STRESS ANALYSES

Reference: MFTF-A2I (Insert Coil) Final Stress Report, Volume IX, Appendices A and B.

Nb_3Sn Conductor Analyses

A-1 Baxter, B., "MBTF-B A2I Conductor Nb_3Sn Fiber Strain Calculation," 21 June 1983.

A-2 Pickering, J. L., Baxter, B., "Nb_3Sn Monolith Total Strain Summary," 14 November 1983.

A-3 Pickering, J. L., Baxter, B., "Conductor Bending Stress Due to Pack Axial Movement," 13 October 1983.

A-4 Baxter, B., Pickering, J. L., "Conductor Pack Potential Axial Movement during Operation," 12 October 1983.

A-5 Pickering, J. L., Baxter, B., "Axicell - Nb_3Sn Current Lead Stress Analysis," 10 October 1983.

A-6 Pickering, J. L., "A2I Coil Insulation Stress Analysis," 12 December 1983.

Magnet Case Analysis

B-1 Pickering, J. L., "Stress Analysis of A2I Coil Case and Attachment to A20 case (SAP Model), 29 June 1983.

B-2 Pickering, J. L., "A2I Bobbin Stability Analysis," 15 August 1983.

B-3 Pickering, J. L., "A2I Conductor Lead Port Opening Analysis, 27 July 1983.

B-4 Pickering, J. L., "Axicell-Current Lead Tunnel Stress Analysis," 22 August 1983.

B-5 Pickering, J. L., "A2I Magnet Case Thermal Analysis," 15 August 1983.

B-6 Rinker, M., "Thermal Stress Analysis of A2I Coil Case during Cool-down Cycle," 30 September 1983.

HIGH FIELD COIL TEMPERATURE MEASUREMENT NOS. AND VACUUM VESSEL FEEDTHRU CONNECTOR ASSIGNMENTS

MEASUREMENT NO.	COIL/SUBSYSTEM	TEMP SENSOR QTY.	CONN. PIN QTY.	CONN. NO.
P742 EA2I CA ESP CT THRU P749 EA2I CA OR CT	EA2I - Outer Coil Case	8	40	J53
P750 WA2I CA ESP CT THRU P757 WA2I CA OR CT	WA2I - Outer Coil Case	8	40	J55

HIGH FIELD COIL VOLTAGE TAP MEASUREMENT NUMBERS

MEASUREMENT NUMBERS	COIL/SUBSYSTEM
P1699 EA2I CL REX1 VT THRU P1702 EA2I CL SUX2 VT	EA2I - VAPOR COOLED LEADS
P1703 EA2I BL T1 VT THRU P1732 EA2I BL T57 VT	EA2I - CONDUCTORS
P1733 WA2I CL REX1 VT THRU P1736 WA2I CL SUX2 VT	WA2I - VAPOR COOLED LEADS
P1737 WA2I BL T1 VT THRU P1766 WA2I BL T57 VT	WA2I - CONDUCTORS

APPENDIX E

INSTRUMENTATION
MEASUREMENT CODE NUMBER SUMMARY
WITH CONNECTOR ASSIGNMENTS

HIGH FIELD COIL LIQUID HELIUM LEVEL SENSOR
MEASUREMENT NUMBERS

MEASUREMENT NUMBERS	COIL/SUBSYSTEM
P1321 EA2I STK HVL LL	EA2I - STACK AND PLENUM
P1322 WA2I STK HVL LL	WA2I - STACK AND PLENUM

APPENDIX F

INSTRUMENTATION

DESIGN DRAWINGS

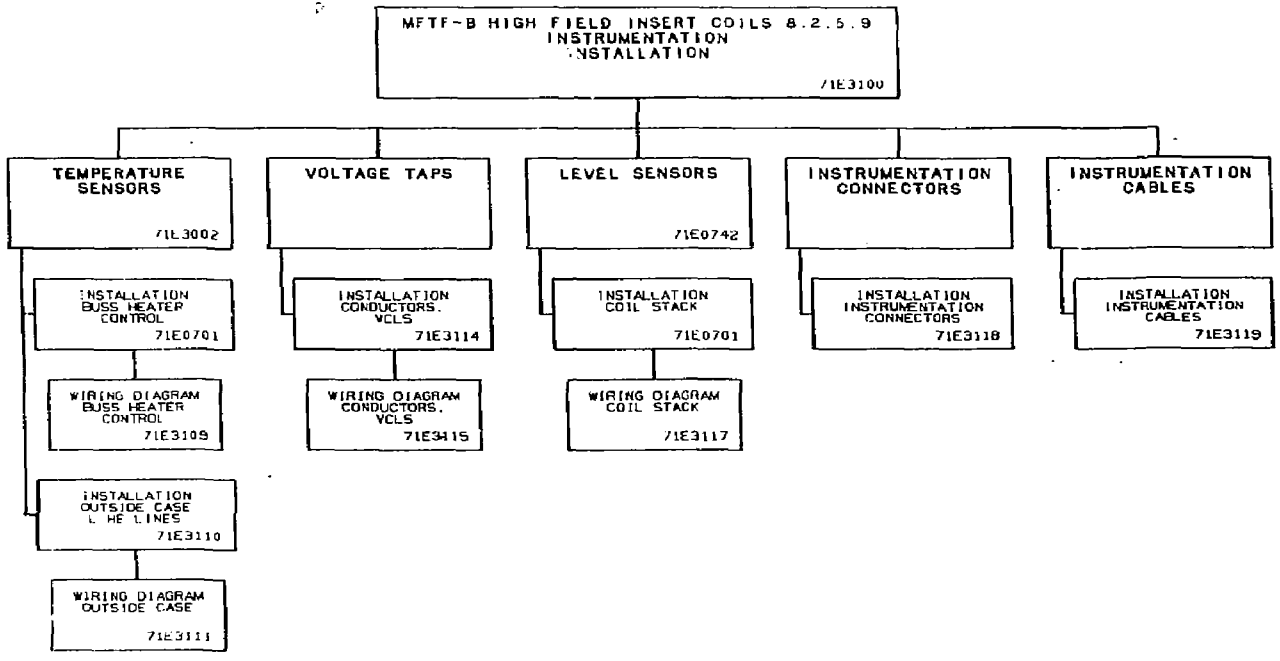
MFTF-B HIGH FIELD INSERT COILS 8.2.5.9
INSTRUMENTATION
INSTALLATION
71E3100
TEMPERATURE SENSORS
71E3002
VOLTAGE TAPS
LEVEL SENSORS
71E0742
INSTRUMENTATION CONNECTORS
INSTRUMENTATION CABLES
INSTALLATION BUSS HEATER CONTROL
71E0701
INSTALLATION CONDUCTORS, VCLS
71E3114
INSTALLATION COIL STACK
71E0701
INSTALLATION INSTRUMENTATION CONNECTORS
71E3118
INSTALLATION INSTRUMENTATION CABLES
71E3119
WIRING DIAGRAM BUSS HEATER CONTROL
71E3109
WIRING DIAGRAM CONDUCTORS, VCLS
71E3115
WIRING DIAGRAM COIL STACK
71E3117
INSTALLATION OUTSIDE CASE L HE LINES
71E3110
WIRING DIAGRAM OUTSIDE CASE
71E3111

1.0 INTRODUCTION

1.1 This appendix contains the ideas, plans, and schematics for control of the Nb_3Sn tensioner as conceived when the stop work order was given.

The work is complete enough to start fabrication of the radius sensing tool and breadboard of the electronics control.

Preliminary analysis indicates that it is very feasible to maintain a winding tension of 600 lb ± 5 percent with minimal cost and hardware impact.

2.0 PROPOSED TENSIONER CONTROL LOOP NiSn COIL

2.1 Philosophy -- the torque motor and dancer air regulator control the tension on the idler of the payout spool. If the conductor on the payout spool and the cable on the idler have the same diameter, then the tension as measured at the dancer and the coil have the same value. As the conductor is unwound though, the diameters change and, hence, the tension (see Figure 1 below).

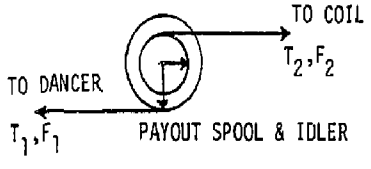

FIGURE 1

T = Torque F = Tension R = Radius

$T_1 = T_2$ R_1 is fixed

$T_1 = F_1R_1$ $T_2 = F_2R_2$

$F_1R_1 = F_2R_2$, $F_2 = \frac{F_1R_1}{R_2}$,

Let R_1 be constant, i.e., $F_2R_2 = K_1F_1$, then $F2 = \frac{K_1F_1}{R_2}$

To keep F_2 constant with R_2 being an independent variable, F_1 must be the control variable. This can be accomplished with an analog circuit as shown in Figure 2.

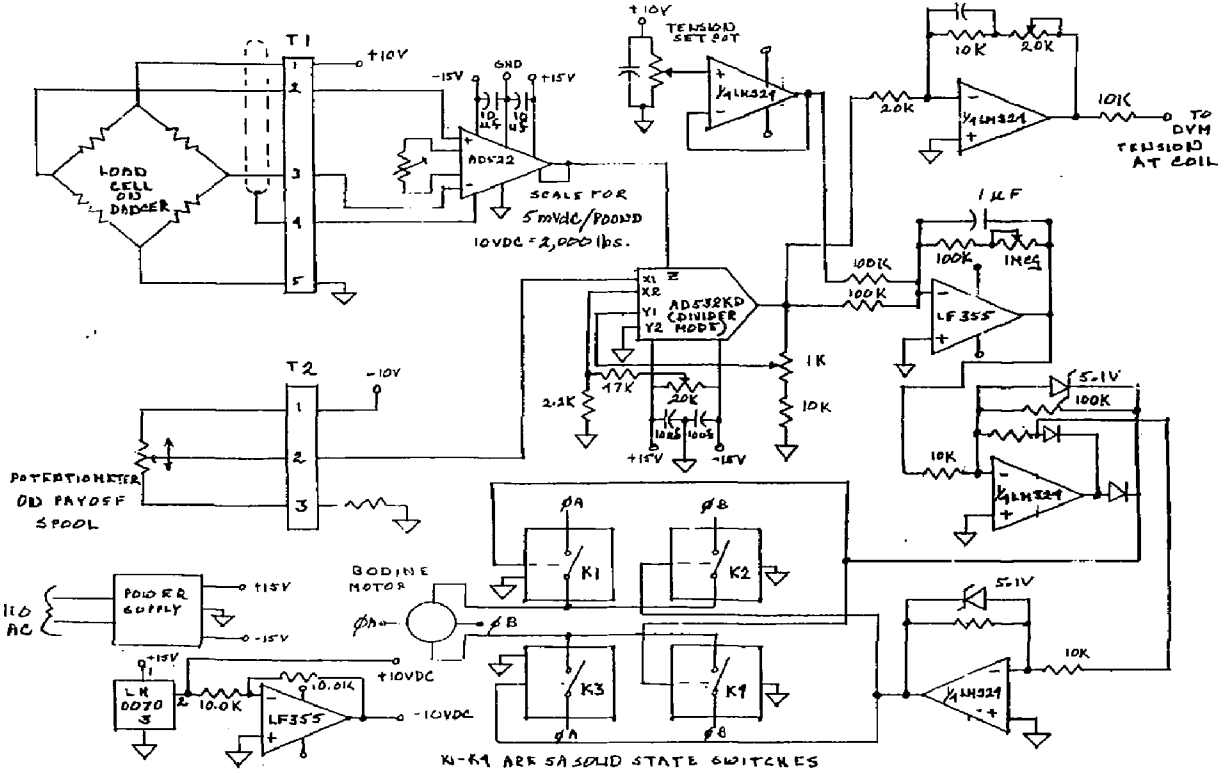
T1
+10V
LOAD CELL OR DANCER
-15V
GND
+15V
10 µF
10 µF
AD522
SCALE FOR
5mVdc/POUND
10VDC = 2,000 lbs.
+10V
TENSION SET POT
1/4 LM324
10K
2.0K
2.0K
10K
1/4 LM324
TO DVM TENSION AT COIL
1 µF
100K
100K
100K
100K
LF355
AD532KD (DIVIDER Y2 MODE)
1K
2.2K
17K
20K
10K
100pf
100pf
+15V
-15V
5.1V
100K
10K
1/4 LM324
T2
-10V
POTENTIOMETER ON PAYOFF SPOOL
ØA
ØB
K1
K2
BODINE MOTOR
110 AC
POWER SUPPLY
+15V
-15V
+15V
LM 0070
3
10.0K
10.0K
LF355
+10VDC
-10VDC
K3
K4
ØA
ØB
5.1V
10K
1/4 LM324
K1-K4 ARE SA SOLID STATE SWITCHES

FIGURE 2

3.0 SYSTEM RESPONSE ANALYSIS

3.1 An analysis of the system response to the circuit shown in Figure 2 is given below:

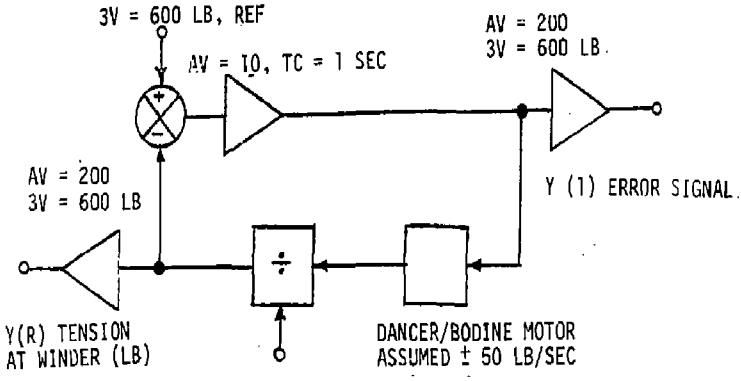

FIGURE 3

The stability and error analysis of the circuit shown in Figure 2 is based on the circuit shown in Figure 3. Assumptions: (Worst Case):

a) System scale factor - 3VDC = 600 lb.

b) Dancer regulartor and bodine motor can change pressure at ± 50 lb/sec.

c) A change in payoff spool radius of -2.75%/sec.

The data results are tabulated in Tables 1 and 2, where "x=" represents time in seconds, "y(1)" represents the rate change of tension, and "y(2)" represents absolute tension.

Table 1 shows the results of an instantanious command of 600-lb tension with no previous load. In addition, the radius change of the payoff spool is -2.75%/sec.

TYPICAL LAYOUT FOR DIAMETER SENSING UNIT

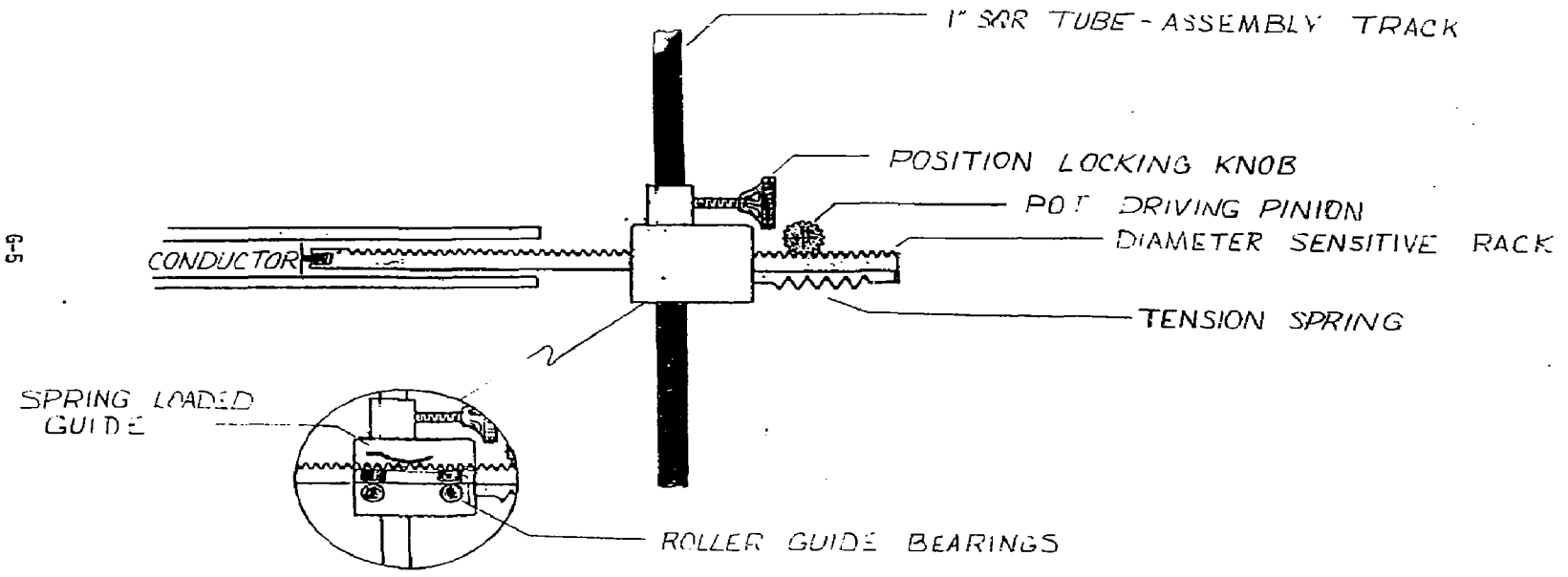

FIGURE 4

TABLE 1

X= 0

Y(1)= 0.00000E 00
Y(2)= 0.00000E 00

X= 0.5

Y(1)= 2.31519E 03
Y(2)= 2.32316E 01

X= 1

Y(1)= 3.61750E 03
Y(2)= 4.94106E 01

X= 1.5

Y(1)= 4.38377E 03
Y(2)= 7.62916E 01

X= 2

Y(1)= 4.61229E 03
Y(2)= 1.02316E 02

X= 2.5

Y(1)= 4.68328E 03
Y(2)= 1.32291E 02

X= 3

Y(1)= 4.62267E 03
Y(2)= 1.61416E 02

X= 3.5

Y(1)= 4.46687E 03
Y(2)= 1.91291E 02

X= 4

Y(1)= 4.25194E 03
Y(2)= 2.21316E 02

X= 4.5

Y(1)= 3.99997E 03
Y(2)= 2.53291E 02

X= 5

Y(1)= 3.72209E 03
Y(2)= 2.85416E 02

X= 5.5

Y(1)= 3.42555E 03
Y(2)= 3.18291E 02

X= 6

Y(1)= 3.11474E 03
Y(2)= 3.51316E 02

X= 6.5

Y(1)= 2.79232E 03
Y(2)= 3.86291E 02

X= 7

Y(1)= 2.45991E 03
Y(2)= 4.21416E 02

X= 7.5

Y(1)= 2.11849E 03
Y(2)= 4.57291E 02

X= 8

Y(1)= 1.76865E 03
Y(2)= 4.93016E 02

X= 8.5

Y(1)= 1.41076E 03
Y(2)= 5.31291E 02

X= 9

Y(1)= 1.04502E 03
Y(2)= 5.69416E 02

X= 9.5

Y(1)= 6.71597E 02
Y(2)= 6.08291E 02

X= 10

Y(1)= 2.90538E 02
Y(2)= 6.47316E 02

X= 10.5

Y(1)=-8.19404E 01
Y(2)= 6.64582E 02

X= 11

Y(1)=-2.16437E 02
Y(2)= 6.23458E 02

X= 11.5

Y(1)=-1.34682E 02
Y(2)= 5.81583E 02

X= 12

Y(1)= 6.43464E 01
Y(2)= 5.62979E 02

X= 12.5

Y(1)= 8.85878E 01
Y(2)= 6.87354E 02

X= 13

Y(1)=-5.13223E 01
Y(2)= 6.25583E 02

X= 13.5

Y(1)=-.64270E 01
Y(2)= 5.80708E 02

X= 14

Y(1)= 4.89300E 01
Y(2)= 5.99074E 02

X= 14.5

Y(1)=-2.33745E 01
Y(2)= 6.03552E 02

X= 15

Y(1)= 8.08324E 00
Y(2)= 6.07666E 02

X= 15.5

Y(1)= 5.18945E 00
Y(2)= 5.80635E 02

X= 16

Y(1)=-1.63829E 01
Y(2)= 6.02739E 02

X= 16.5

Y(1)= 1.41731E 01
Y(2)= 6.00041E 02

X= 17

Y(1)= 8.32097E 00
Y(2)= 5.82005E 02

X= 17.5

Y(1)=-1.54314E 01
Y(2)= 6.03927E 02

X= 18

Y(1)= 1.57990E 01
Y(2)= 6.00416E 02

X= 18.5

Y(1)= 9.23046E 00
Y(2)= 5.82135E 02

X= 19

Y(1)=-1.58276E 01
Y(2)= 6.04114E 02

X= 19.5

Y(1)= 1.00086E 01
Y(2)= 6.00791E 02

X= 20

Y(1)= 9.64413E 00
Y(2)= 5.81305E 02

TABLE 2

X= 0.5

Y(1)= 1.45158E 01
Y(2)= 5.97042E 02

X= 1

Y(1)=-5.88268E 00
Y(2)= 5.95572E 02

X= 1.5

Y(1)=-3.98167E 00
Y(2)= 6.01108E 02

X= 2

Y(1)= 9.82139E 00
Y(2)= 5.97754E 02

X= 2.5

Y(1)=-7.35388E 00
Y(2)= 5.95202E 02

X= 3

Y(1)=-3.80651E 00
Y(2)= 6.03858E 02

X= 3.5

Y(1)= 1.42758E 01
Y(2)= 5.97567E 02

X= 4

Y(1)=-8.12721E 00
Y(2)= 5.94827E 02

X= 4.5

Y(1)=-4.28987E 00
Y(2)= 6.10688E 02

X= 5

Y(1)= 1.09847E 01
Y(2)= 5.97370E 02

X= 5.5

Y(1)=-8.24683E 00
Y(2)= 5.94452E 02

X= 6

Y(1)=-4.58741E 00
Y(2)= 6.11358E 02

X= 6.5

Y(1)= 1.17516E 01
Y(2)= 5.97102E 02

X= 7

Y(1)=-3.33819E 00
Y(2)= 5.94827E 02

X= 7.5

Y(1)=-4.80472E 00
Y(2)= 6.12188E 02

X= 8

Y(1)= 1.25312E 01
Y(2)= 5.97804E 02

X= 8.5

Y(1)=-9.09662E 00
Y(2)= 5.93702E 02

X= 9

Y(1)=-5.13234E 00
Y(2)= 6.12858E 02

X= 9.5

Y(1)= 1.33137E 01
Y(2)= 5.98817E 02

X= 10

Y(1)=-1.04813E 01
Y(2)= 5.93827E 02

APPENDIX G

DESIGN SUMMARY FOR

CONSTANT TENSION CONTROL SYSTEM

APPENDIX H

NEUTRONIC ENVIRONMENT EVALUATION

RADIATION CONSIDERATIONS

The radiation environment is most severe in the axicell insert coil region. The inboard case receives the maximum neutron flux and the inboard insulation the maximum radiation dose. According to the magnet neutron heating analysis for L-71 (MARS) configuration (Steve Muelder's memo MF-7.1.3 dated November 1, 1982), the absorbed dose in the inboard insulation is 133.76 rads/plasma-second with a corresponding neutron flux of 1.6×10^{11} n/cm^2/plasma-second. The neutron flux in the inboard case region is 1.7×10^{11} n/cm^2/plasma-sec. The cumulative radiation dose in the inboard insulation over a ten year period, based on an actual plasma turn-on duration of 3000 plasma-seconds per week and a 13/18 week cycle, would be 1.3×10^8 rads with a corresponding neutron fluence of 1.6×10^{17} n/cm^2. The radiation dose in the insulation would be mainly due to fast neutrons.

R. R. Coltman Jr. et al (Oak Ridge National Laboratory) have conducted a study to determine effects of gamma radiation at 4.2K on mechanical and physical properties of glass-epoxy and glass-polyimide insulators. A similar study has been undertaken by G. F. Hurley et al (Los Alamos National Laboratory) for determining effects of fast neutron irradiation. Incidentally, samples of G. F. Hurley's study have been irradiated to a fast neutron fluence of 1.51×10^{17} n/cm^2, a fluence very close to 1.6×10^{17} n/cm^2 expected in the inboard insulation region over a period of ten years. Thus results of G. F. Hurley's study can be directly applied to the present situation without much interpolation or extrapolation.

G. F. Hurley's study indicates that for G-10CR, there are no significant changes in the electrical properties, but there is a small reduction in compression strength and strain to failure following neutron irradiation. The modulus of rupture is decreased about 16%. The properties of G-11 CR and polyimide-glass are affected to a lesser degree or not affected at all at this level of irradiation. These experiments are still in progress, but the results so far give us confidence in using the less expensive G-10 CR as the insulation material.

GENERAL DYNAMICS
Convair Division

INBOARD INSULATION OF A2I COIL RECEIVES THE HIGHEST RADIATION DOSE

- FOR THE L-71 (MARS) CONFIGURATION, THE MAXIMUM RADIATION DOSE IS 133.8 Rads/PLASMA-SEC, WITH THE CORRESPONDING NEUTRON FLUX 1.6×10^{11} n/cm^2 sec. (En > 0.1 Mev)

  (STEVE MUELDER, 11-1-82)

- TOTAL RADIATION DOSE OVER 10 YEAR PERIOD

  1.3×10^{8} Rads

  or 1.6×10^{17} n/cm^2

- THE RADIATION DOSE IS MAINLY DUE TO NEUTRONS

GLASS-EPOXY INSULATORS CAN HANDLE ACTUAL RADIATION DOSE OVER 10 YEAR PERIOD IN MFTF-B AXICELL SUPERCONDUCTING INSERT COIL

- G-10 CR AND G-11 CR RETAIN MOST OF THEIR PRE-IRRADIATED MECHANICAL AND PHYSICAL PROPERTIES WHEN IRRADIATED TO A NEUTRON FLUENCE OF 1.52×10^{17} n/cm^2 (En > 0.1 Mev)
  (G.F. HURLEY, LOS ALAMOS NATIONAL LAB (1982))

- MORE EXPENSIVE POLY-IMIDE - FIBERGLASS INSULATORS NOT NEEDED

- COMPRESSION STRENGTH AND MODULUS OF RUPTURE OF G-10 CR DECREASED A LITTLE FOLLOWING IRRADIATION. THOSE OF G-11 CR WERE UNAFFECTED. THE RESULTS ARE SHOWN ON NEXT PAGE.

EXPECTED NEUTRON ENVIRONMENT DOES NOT SIGNIFICANTLY AFFECT THE MECHANICAL PROPERTIES OF G-10CR OR G-11CR

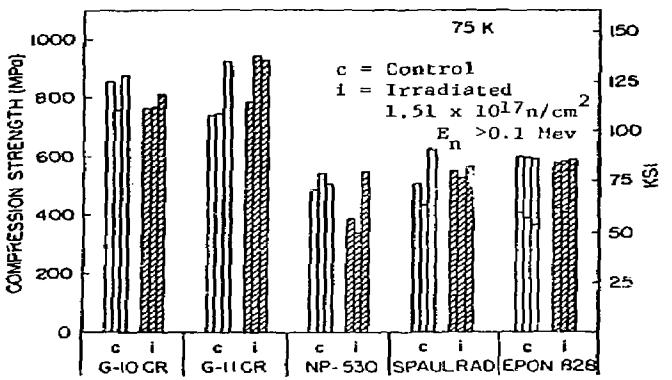

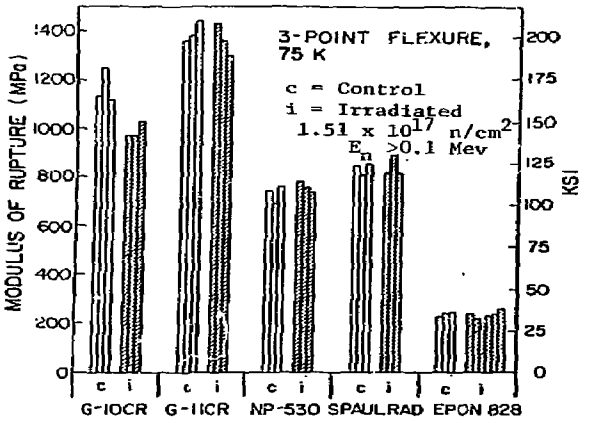

FIGURES SHOWN WERE TAKEN FROM THE DAFS (1982) REPORT PERTAINING TO "COMPARISON OF NEUTRON AND GAMMA RADIATION DAMAGE IN ORGANIC MATERIALS BY G. F. HURLEY OF LOS ALAMOS NATIONAL LAB.